Metabolic Reprogramming and Epigenetic Regulation in Renal Cell Carcinoma

by

Adam Stewart Kinnaird

A thesis submitted in partial fulfillment of the requirements for the degree of

Doctor of Philosophy

in

Experimental Medicine

Department of Medicine
University of Alberta

Abstract

Renal cell carcinoma comprises approximately 2-3% of all malignancies, with the majority, approximately 70%, being clear cell renal cell carcinoma (ccRCC). ccRCC features many cancer hallmarks such as suppressed mitochondrial glucose oxidation, apoptosis-resistance, angiogenesis, immune evasion, uninhibited proliferation, and invasion and metastasis, thought to be driven by sporadic mutations or epigenetic silencing of the tumor suppressor gene, von Hippel Lindau (VHL). VHL loss leads to up-regulation of its target protein, hypoxia inducible factor (HIF), even in normoxia. HIF controls many downstream targets in order to prepare the cell for hypoxia, with the net effect being suppression of mitochondrial glucose oxidation, up-regulation of glycolysis, angiogenesis and apoptosis-resistance. Unchecked, as in VHL-deficiency, this becomes a critical step in tumorigenesis. We show that reversing the suppression of mitochondrial glucose oxidation in ccRCC using dichloroacetate, an inhibitor of the HIF target gene mitochondrial pyruvate dehydrogenase kinase (PDK), which inhibits a major producer of acetyl-CoA, the Pyruvate Dehydrogenase Complex (PDC), results in increased production of mitochondrial acetyl-CoA via PDC, reduced proliferation and angiogenesis, and induces apoptosis in animal models. We also show that mitochondrial PDC dynamically translocates to the nucleus in multiple types of cancer cells, including ccRCC, in response to growth factor signaling, to produce acetyl-CoA in the nucleus. This local production of acetyl-CoA by nuclear PDC is used to acetylate core histones involved in S-phase progression and cellular proliferation. Next, we show that VHL, which has been

described as a multipurpose adapter protein, directly binds the tumor suppressor p53, preventing its activation, promoter binding and expression of its target genes. This process is independent of the VHL-HIF axis and results in an attenuation of p53 inducing therapies. Finally, we study Myocyte Enhancer Factor 2A (Mef2A), a transcription factor with ties to multiple hallmarks of cancer, like mitochondrial suppression, invasion and immune evasion. We show that Mef2A expression is up-regulated in patient tumors compared to adjacent normal kidney parenchyma and that nuclear Mef2A levels correlate with larger tumor size. Mef2A activity is increased in VHL-deficient ccRCC cells due to HIF-mediated growth factor signaling and it induces expression of the pro-tumor chemokine, CCL20. Inhibition of Mef2A results in reduced ccRCC tumor growth in vivo and may provide mechanistic insight into immune evasion as immune checkpoint inhibitors develop into the first line therapy in metastatic ccRCC.

Preface

Chapter 1 of this thesis has been previously published as Kinnaird, A. and Michelakis, E. Metabolic Modulation of Cancer: A new frontier with great translational potential. (2015) *Journal of Molecular Medicine* 93(2):127-42

Chapter 2 of this thesis has been previously published as Kinnaird A, Dromparis P, Saleme B, Gurtu V, Watson K, Paulin R, Zervopoulos S, Stenson T, Sutendra G, Pink DB, Carmine-Simmen K, Moore R, Lewis JD and Michelakis ED. Metabolic Modulation of Clear-cell Renal Cell Carcinoma with Dichloroacetate, an Inhibitor of Pyruvate Dehydrogenase Kinase. (2016) *European Urology* 69(4):734-44

Chapter 3 of this thesis has been previously published as Sutendra G, Kinnaird A, Dromparis P, Paulin R, Stenson TH, Haromy A, Hashimoto K, Zhang N, Flaim E and Michelakis ED. A functional nuclear pyruvate dehydrogenase complex is important for a mitochondria-independent generation of acetyl-CoA and histone acetylation. (2014) *Cell* 158(1):84-97

Chapter 4 and 5 have not yet been published but are in preparation for submission to peer-reviewed journals at this time.

Acknowledgements

First, I would like to acknowledge my supervisor, Professor Evangelos Michelakis, for his mentorship, dedication to his trainees, and creation of a 'sky is the limit' environment for exploring new ideas and hypotheses. I have learned much from his advice and look forward to continuing to work together as clinician scientists. I must also acknowledge my committee members, Dr. Ronald Moore and Dr. Jayan Nagendran, for their leadership and insight throughout my studies. Most importantly, I would like to thank my wife, Dr. Erin Bristow and my parents, Helga and David Kinnaird, for their love, support and genuine excitement for me to pursue a career in science and surgery. Furthermore, I must thank Dr. Peter Dromparis and Dr. Gopinath Sutendra for their friendship, guidance and laying the ground work from which I started this endeavor. Finally, I would like to acknowledge Dr. Vikram Gurtu, Dr. Aristeidis Boukouris, Sotirios Zervopoulos and Bruno Saleme for the laughter, the friendship and the hard work together, without which this would not have been possible.

Table of Contents

List of Abbreviations

2-HG – 2-hydroxyglutarate
ΔΨm – Mitochondrial Membrane Potential
αKG – Alpha-ketoglutarate
ACL – ATP-Citrate Lyase
AML – Acute myeloid leukemia
ADP – Adenosine diphosphate
ATP – Adenosine triphosphate
ccRCC – Clear Cell Renal Cell Carcinoma
CCL20 – Chemokine ligand 20
CCR6 – Chemokine receptor 6
CoA – Coenzyme A
CRISPR – Clustered regularly interspaced short palindromic repeats
CS – Citrate Synthase
DCA – Dichloroacetate
DNA – Deoxyribonucleic acid
EGF – Epidermal growth factor
EGFP – Enhanced Green Fluorescent Protein
EGFR – Epidermal growth factor receptor
ETC – Electron transport chain
FADH – Flavin adenine dinucleotide
FDG – Fluorinated Deoxyglucose
G6PD – Glucose-6-Phosphate Dehydrogenase
GBM – Glioblastoma multiforme
GLUT – Glucose transporter
GLY – Glycolysis
GO – Glucose Oxidation
HIF – Hypoxia Inducible Factor
HK – Hexokinase
HSF1 – Heat shock factor 1
HSP70 – Heat shock protein 70
IDH – Isocitrate Dehydrogenase
LDH – Lactate Dehydrogenase
LCSC – Lung cancer stem cell
PET – Positron Emission Tomography
PDH – Pyruvate Dehydrogenase
PDC – Pyruvate Dehydrogenase Complex
PDK – Pyruvate Dehydrogenase Kinase
PHD – Prolyl hydroxylase
PKM2 – Pyruvate Kinase isoform 2
PPP – Pentose Phosphate Pathway
MAPK – Mitogen-activated protein kinase
MDM2 – Mouse double minute 2 homolog
MEF – Mouse embryonic fibroblast
Mef2A – Myocyte Enhancer Factor 2A
MLS – Mitochondrial localization sequence
MPP – Mitochondrial processing peptidase
mROS – Mitochondrial reactive oxygen species
MnSOD – Manganese Superoxide Dismutase
NADH – Nicotinamide adenine dinucleotide

NADPH – Nicotinamide adenine dinucleotide phosphate
NFAT – Nuclear Factor of Activated T-cells
PDGF – Platelet derived growth factor
PGC1α – Peroxisome proliferator-activated receptor gamma coactivator 1 alpha
PT – Proximal Tubules
PUMA – p53 Upregulated Modulator of Apoptosis
SAEC – Small Airway Epithelial Cells
SCS – Succinyl-CoA Synthetase
SDF-1 – Stromal cell-derived factor 1
SDH – Succinate Dehydrogenase
shRNA – Short hairpin ribonucleic acid
siRNA – Short interfering ribonucleic acid
SIRT3 – Sirtuin 3
TACE – Transarterial Chemoembolization
TCGA – The Cancer Genome Atlas
TGFα – Transforming growth factor alpha
TIGAR – Tp53-induced glycolysis and apoptosis regulator
TMRM – Tetramethylrhodamine
VEGF – Vascular endothelial growth factor
VHL – von Hippel Lindau

Chapter One

Metabolic modulation of cancer: A new frontier with great translational potential

Introduction

The majority of chemotherapeutic drugs for cancer inhibit pathways fundamental to the life of all cells, leading to adverse effects on healthy tissues [1]. In addition, traditional drug development in cancer has been focusing on a single molecular pathway, following the "one gene - one drug" approach. It became apparent however that most tumors are characterized by multiple molecular abnormalities so that when the therapies are offered even in combination of 2-3 drugs, the tumor eventually relapses. It is a rather rare example to find therapies that are effective and not toxic. This requires the identification of molecular abnormalities that are not only critical for the life of cancer – but not normal cells – but are also the dominant or the only molecular abnormality within the tumor. For example, this can be seen in certain leukemias or tumors where a mutation in the majority of cancer cells not only dominates their molecular phenotype but is also critical for their survival, explaining the great success of agents such as Gleevec for Chronic Myelogenous Leukemia [2] or Herceptin for certain breast cancers [3]. Yet, most cancers, like glioblastoma for example, are characterized by several cellular phenotypes within each tumor and yet, in each of these cell types there are several genetic and molecular abnormalities [4], obviously not susceptible to a single or even a combination of 2-3 drugs. Is it possible to identify a common denominator across all of these abnormalities that is not only critical for the survival of cancer cells but is also not present in normal cells? And to push the envelop even further, is it possible that this common denominator is also present in cancer stem cells, so that if targeted, tumor relapse would be limited as well [5]? In other words, is there an Achilles' heel for such complex and molecularly plastic tumors? Recent work over the past 10 years suggests that such a common denominator, unique to cancer cells, may exist and be no other than the unique metabolism of cancer cells, first identified by Otto Warburg, more than 90 years ago [6]. Unfortunately, the work of Warburg, who was awarded the Nobel Prize for his work on metabolism, did not translate in cancer therapies for many decades as it was wrongly assumed that the unique cancer metabolism was a consequence, not a

cause or contributing factor in cancer. We now know that if not causal, like in certain examples of mutations in key metabolic enzymes, this metabolic remodeling is a strong contributing or promoting factor as it promotes proliferation, resistance to apoptosis and tumor angiogenesis, facilitating tumor growth and metastasis. Even better, tumor metabolism is typically different than that of normal cells. The development of 'metabolic modulators' over the past 10 years has already entered early-phase trials. Although it sounds 'too good to be true' that metabolism is the long-sought Achilles' heel for cancer, a new field has already opened, which includes new therapies and metabolism-based imaging such as FDG-PET. Metabolic Oncology is an exciting frontier in the battle against cancer and this review focuses on the rationale for the development of metabolic modulators, concentrating on those that hold promise or already have entered human trials.

1.1.0 Cancer's abnormal metabolism and its molecular consequences.

The cornerstone of metabolism in the cell is the mitochondrion. Traditional biochemistry taught us that mitochondria's main job is to generate heat and energy (ATP). We now know that although the most efficient means for ATP production lie within mitochondria, ATP can be adequately produced outside of mitochondria, through cytoplasmic glycolysis, at amounts enough to support the energy-hungry cancer cells. We also now know that mitochondria do much more: they produce diffusible mediators that can regulate multiple molecular pathways in the cell and even the nucleus. They can also induce apoptosis, an intriguing fact since the "provider of life" (i.e. ATP) can also be the provider of death for the cell. It was perhaps this "paradox" that did not allow mitochondria to be seen as targets for pro-apoptotic strategies until recently. Therefore, suppression of mitochondrial function can suppress apoptosis and alter cellular signaling toward a pro-proliferative phenotype as we discuss below. It is thus not a surprise that cancer cells have suppressed mitochondrial function.

Normally, cells metabolize glucose to pyruvate in the cytoplasm by glycolysis; then this is converted by pyruvate dehydrogenase (PDH) into acetyl-

CoA, which enters the mitochondrial Krebs' cycle, where it is oxidized to eventually produce the electron donors NADH and $FADH_2$. These donate electrons down a redox-gradient in the electron transport chain (ETC), while protons are pumped out of the mitochondria and mitochondria-derived reactive oxygen species (mROS; mostly the negatively charged superoxide) are generated, creating a membrane potential ($\Delta\Psi m$) across the mitochondrial inner membrane (Figure 1-1). This process uses oxygen as the final electron acceptor in Complex IV of the ETC (forming water), and uses the stored energy of the $\Delta\Psi m$ to produce and release ATP. As protons re-enter the inner membrane, they release energy used to pump ATP out in the cytoplasm and bring ADP in. A similar process is followed in the oxidation of fatty acids, forming acetyl-CoA, which is also oxidized in the Krebs' cycle producing the same electron donors. Thus mitochondria process fuel (carbohydrates, lipids, oxygen) to produce energy and have evolved to be important fuel sensors. When fuel supply is ample, the growth and differentiation of tissues can be kept under control by the coordinated induction of apoptosis, producing effective cell population control. In contrast, when fuel is limited, mitochondria suppress apoptosis in an attempt to preserve life under stressed conditions. It is here that mitochondria can be "fooled" by the cancer cells.

Let's say, for example, that oxygen is limited. This de-facto inhibits oxidative phosphorylation in the mitochondria. Immediately the mitochondria sense the lack of fuel and ignite a series of mechanisms for the cell to: a) seek alternate means of ATP production and b) suppress apoptosis since stress may be imminent:

a) The expression of glucose transporters is increased and more glucose enters the cell. This can be achieved by the activation of HIF1α directly by hypoxia but -remarkably- the mitochondrial suppression can also activate HIF1α. This is because alpha-ketoglutarate (αKG), a Krebs' product that is a required co-factor for the prolyl-hydroxylases that de-stabilize HIF1α, is decreased [7]. Independent of its stabilization, the HIF1α transcription machinery, in part driven by the redox-sensitive p53, may also be activated when the diffusible mROS

decrease (for example H_2O_2 from superoxide's dismutation from manganese superoxide dismutase) [8-11]. Activated HIF1α not only increases the expression of glucose transporters but also increases the transcription of almost all the glycolytic enzymes in the cytoplasm. Thus, with more glucose and activated glycolysis, more ATP can be produced. Normally the efficiency of glycolysis for ATP is less than that of mitochondria (each mol of glucose produces 36 mol of ATP in mitochondrial glucose oxidation but only 2 mol of ATP in glycolysis), but as glycolysis is enhanced the cell may eventually compensate for the ATP that is missing from the inhibited mitochondria.

b) The next thing that happens is that mitochondria hyperpolarize (increased ΔΨm) [12, 13]. The pro-apoptotic factors stored inside mitochondria (like cytochrome c or apoptosis inducing factor) are unable to leak out, making cancer cells resistant to mitochondria-dependent apoptosis. This is because these factors leak through the mitochondrial transition pore (MTP); a mega-channel that, being voltage- and redox-sensitive, tends to close while membrane potential is high and mROS are low [14]. The mechanism for mitochondrial hyperpolarization is not clear although it has been known since the 1980s to be a feature of most cancers [15]. One potential mechanism is that glycolysis leads to a GSK-3β-driven translocation of the cytoplasmic hexokinase II (HK2) to the outer mitochondrial membrane, where it binds and inhibits the major channel that releases negatively charged ions, i.e. the voltage-dependent anion channel (VDAC; a critical component of the MTP), leading to a build up of anions inside the mitochondria [16, 17]. (Figure 1-1) Another mechanism may be that the enhanced production of ATP in the cytoplasm due to the enhanced glycolysis, causes a decrease in the ATP/ADP gradient in the microdomains around the outer mitochondrial membrane, decreasing the function of ATP synthase and thus preventing the re-uptake of the positively charged H^+ ions back to the mitochondria [16]. Therefore, mitochondrial suppression supports a state of apoptosis-resistance, while adequate production of ATP is maintained. Interestingly, HIF1α also induces pyruvate dehydrogenase kinase (PDK), inhibiting PDH, and thus decreasing the production of acetyl-CoA entering the Krebs' cycle.

Let's now see what would happen if PDH were to be inhibited by other means, not by the hypoxia-mediated activation of HIF1α. Immediately, the mitochondria will sense a lack of fuel entering them since the supply of acetyl-CoA will decrease (despite the fact that the supply of glucose and oxygen to the cell remains normal). They will then ignite the same process described above, leading to resistance to apoptosis. One can follow the same logic and realize that inhibition of any critical enzyme used in glucose or fatty acid oxidation may have the same consequences, "fooling the mitochondria" and inhibiting oxidative phosphorylation, as if there was lack of fuel. This mechanism can be used by cancer cells to inhibit apoptosis, a *sine qua non* of cancer. At the same time, there are three additional advantages that the cancer cells gain by this "inappropriate" mitochondrial suppression:

First, the cancer cell can now use pyruvate, that is not oxidized in the Krebs' cycle, for biomass generation, as the tumor grows [18]. In other words, the unused pyruvate helps a dividing cell create the amino acids, nucleotides, and lipids needed to replicate. Specifically, unused pyruvate can be transaminated to produce amino acids. Similarly, unused pyruvate can be metabolized and shunted into the pentose phosphate pathway to produce both nucleotides and NADPH, which is required to synthesize lipids [18].

Second, as in the case of decreased production of αKG which contributes to HIF1α activation, there are other downstream signals from mitochondria, like decreased mROS, dysregulation of cytoplasmic calcium or induction of chaperones that via the retrograde pathway (a series of mechanisms that mitochondria induce under stress to send signals to the nucleus) directly or indirectly activate other pro-proliferative master transcription factors (like Nuclear Factor of Activated T-cells (NFAT) for example) [12, 19-21]. Like HIF1α, NFAT can suppress several aspects of mitochondrial function, enhancing the proliferative potential of cancer cells and driving positive reinforcing feedback loops (proliferative signals → mitochondrial suppression → proliferative signals).

Third, this mitochondrial remodeling promotes angiogenesis, not surprising since this mitochondrial remodeling "mimics" hypoxia, a well-known

driver of angiogenesis. While hypoxia and HIF1α activation induce mitochondrial suppression [22] the reverse is also true [10], establishing a powerful feedback loop that sustains angiogenesis even in the absence of hypoxia. The majority of solid tumors experience hypoxia during early tumor development as it occurs several cell layers away from capillaries (~150μm) [23]. This leads to an initial primary hypoxia-driven activation of HIF1α and angiogenic signaling to form new blood vessels to supply the growing tumor with nutrients. However, HIF1α stabilization is also regulated by several diffusible mitochondria-derived factors, like αKG and mROS as discussed above [23]. These lead to the inhibition of the degradation of HIF1α through VHL-dependent ubiquitination or activation of its transcriptional activity, respectively [24, 25]. Thus as the newly formed blood vessels bring in more oxygen, limiting hypoxia, the mitochondrial suppression that takes place in the tumor, now causes a primary normoxic activation of HIF1α, sustaining angiogenesis as the tumor continues to grow [10, 22]. Furthermore, by reducing pyruvate into lactic acid during glycolysis, cancer cells increase extracellular acidosis. This potentiates breakdown of the extracellular matrix and allows penetration of the cancer through the basement membrane, thereby driving metastasis [26].

Thus mitochondrial suppression promotes suppressed apoptosis, increased proliferation, angiogenesis and metastatic potential and so can be seen as a critical hub of cancer signaling. While hypoxia is a physiologic mechanism for global mitochondrial suppression, we will now discuss a variety of prominent cancer mechanisms that all lead to mitochondrial suppression, in a sense, mimicking hypoxia.

1.2.0 The cause of mitochondrial suppression in cancer

Mitochondria are well-known “integrators” of multiple signals [12]. Thus mitochondrial suppression can occur through four overarching mechanisms in cancer: (1) growth and transcription factor signaling or (2) off-target effects of specific oncogenes that can suppress specific enzymes or ETC complexes; (3) suppression of factors regulating mitochondrial homeostasis and (4) mutations in

key metabolic enzymes. It is important to note that more than one of these factors may be present within any given tumor.

1.2.1 Growth Factors: One of the pleiotropic effects of growth factors up-regulated in cancer, such as epidermal growth factor (EGF) and fibroblast growth factor (FGF), is the regulation of the flux of pyruvate into the mitochondria by the gate-keeping enzyme PDH. EGF and FGF increase the activity of Pyruvate Dehydrogenase Kinase (PDK) [27] which phosphorylates and inhibits PDH, thus preventing the entry of pyruvate into the Krebs' cycle and suppressing glucose oxidation (GO) [28]. Furthermore, EGF signaling has recently been show to also directly inhibit PDH function, through a PDK-independent tyrosine phosphorylation of its E1 subunit [29]. Furthermore, PDK is a target gene of HIF1α, which is up-regulated in most solid tumors [23, 30]. HIF1α works at multiple levels to shift the balance of metabolism from GO toward glycolysis, including up-regulation of glucose transporters and glycolytic enzymes. HIF1α also increases the translation of the EGF receptor, thereby suppressing mitochondrial function by both up-regulating and activating PDK [31]. There are four PDK isoenzymes with variable tissue expression and some, like PDK 4, are inducible in conditions of metabolic stress [32]. Thus it is reasonable to assume that other, not yet identified, "fuel sensing" mechanisms exist in inducing the transcription of one or more PDKs in tumors, in addition to increasing PDK activity through tyrosine kinase signaling.

1.2.2 Oncogenes: Mitochondrial function is also suppressed by many oncogenes, with p53 and c-MYC being prime examples. The Cancer Genome Atlas (TGCA) has identified p53 to be the most commonly mutated gene in cancer [33]. p53 inhibits glycolysis by inducing the expression of Tp53-induced glycolysis and apoptosis regulator (TIGAR) as well as by reducing the expression of glycolytic enzymes, like phophoglycerate mutase [34, 35]. Furthermore, p53 enhances GO by increasing the expression of cytochrome c oxidase subunits of the ETC [36]. Loss of p53 function causes up-regulation of both the glycolytic enzyme

Hexokinase II (HKII) and PDK [37, 38]. Overall, loss of p53 function suppresses mitochondria and shifts the cell to a more glycolytic phenotype. It is important to note that post-translational modifications like acetylation, a process intimately linked to mitochondrial function, are also known to regulate p53's function in cancer and in the absence of mutations [39]. Like p53, c-MYC increases the expression of multiple glycolytic enzymes including HKII, phosphofructokinase, GAPDH and Enolase A, as well as glucose transporters and Lactate Dehydrogenase (LDH) [40-42]. On top of driving glycolysis, up-regulation of LDH shifts the flux of pyruvate away from GO, thereby further suppressing mitochondrial function.

1.2.3 Regulation of factors that control mitochondrial homeostasis: Global mitochondrial function can be regulated through inhibition of mitochondria-specific factors like Sirtuin 3 (Sirt3; the main de-acetylase in the mitochondria) and Uncoupling Protein-2 (UCP-2; a putative mitochondria calcium transporter). Inhibition of Sirt3 and UCP-2 suppresses mitochondrial function by increasing protein acetylation and decreasing mitochondrial calcium, respectively. When Sirt-3 is deficient, the acetylation of the majority of proteins involved in oxidative metabolism, including Krebs' enzymes and ETC complexes, increases; this post-translational modification typically leads to the inhibition of enzymatic function [43, 44]. Overall, loss of Sirt3 activity can cause up to 50% reduction in mitochondria-derived ATP and respiration. Thus it is not surprising that loss of Sirt3 function has been shown to promote the Warburg Effect and cancer. In fact, embryonic fibroblasts lacking Sirt3 require activation of only one other oncogene to transform into cancer [45], in contrast to wild-type cells that require at least two. Moreover, mice deficient in Sirt3 spontaneously develop breast cancer, and many human cancers are deficient in Sirt3 [45-47]. These observations have led investigators to propose that Sirt3 fulfills the criteria to be an oncogene [45].

Similarly, loss of UCP-2 function, which despite its name is a weak uncoupler but good mediator of calcium entry into the mitochondria, promotes proliferation [20] in part due to a reduction in mitochondrial calcium, which

decreases activity of many calcium-dependent mitochondrial enzymes such as PDH, isocitrate dehydrogenase, and α-ketoglutarate dehydrogenase [48, 49]. Mice deficient in UCP-2 are more prone to develop colon cancer than wild-type UCP-2 littermates when exposed to a carcinogen, demonstrating a predisposition to oncogenic transformation in these glycolytic animals [50]. Similarly to Sirt3, UCP2 was recently proposed to be a tumor-suppressing factor [20].

Another way that mitochondrial function can be suppressed globally is disturbance of the way mitochondria form networks in the cell (mitochondrial fission and fusion) or the way these organelles are "recycled" (mitophagy) [51]. Since these mitochondrial properties are closely linked to cell cycle progression and cell division, it is not surprising that there is early evidence that they may be involved in carcinogenesis [52, 53]. Yet, the importance of these essential functions for many dividing healthy cells may limit their therapeutic potential.

1.2.4 Enzymatic mutations: Mutations in Krebs' cycle enzymes lead to suppressed mitochondrial function. Three examples of this are fumarase, succinate dehydrogenase (SDH) and isocitrate dehydrogenase (IDH). Mutations in fumarase have been identified in almost all cases of the tumor susceptibility syndrome, Hereditary Leiomyomatosis and renal cell carcinoma [54]. Similarly, SDH mutations have been linked to the development of pheochromocytoma, paraganglioma, and renal cell carcinoma [55, 56]. Loss of Fumarase or SDH function leads to an accumulation of intracellular fumarate or succinate, respectively. Each of these Krebs' metabolites has been shown to stabilize HIF1α by inhibiting the prolyl-hydroxylases required for HIF1α degradation [57-59]. This leads to a high level of HIF1α activity even in the presence of oxygen. As a result these tumors are very vascular. Similarly, a powerful pseudohypoxic environment is created in tumors housing IDH mutations due to gain-of-function activity. Two independent cancer genome sequencing projects found that missense mutations in patients with glioblastoma multiforme and acute myelogenous leukemia caused substitutions of a homologous arginine in the active site of the enzyme at R132 and R172 in IDH1 and IDH2, respectively [60,

61]. These mutations cause a gain-of-function, neomorphic activity, in which the mutant IDH-mediated reaction yields 2-hydroxyglutarate (2-HG) rather than the normal product, αKG [62, 63]. Nearly structurally identical to αKG, 2-HG may competitively inhibit the over 60 αKG-dependent dioxygenase enzymes in humans by binding to the αKG binding pocket in the enzyme's active site [7]. These αKG-dependent enzymes (and thus 2-HG targets) are involved in a broad range of biological processes including HIF1α degradation, collagen synthesis and histone methylation [64]. 2-HG also alters HIF1α degradation by inhibiting HIF prolyl-hydroxylases. As a result, cells producing 2-HG, due to an IDH mutation, are locked into a state of pseudohypoxia and mitochondrial suppression. Similar to renal cell carcinoma, glioblastomas are also particularly vascular tumors.

Like p53, many of the Krebs' enzymes, including those discussed above, can be (at least partially) inhibited via posttranslational modifications like acetylation, even in the absence of mutations and this has also been shown to be present in several cancers [65, 66].

1.3.0 Mitochondria-targeting cancer therapies

We will now follow the sequential metabolism of glucose in cancer cells to highlight several cancer-specific metabolic targets that have been explored (Figure 1-2), focusing on the translational potential of these discoveries.

1.3.1 Glucose Transport and Phosphorylation: Since glycolysis is up-regulated in many cancers, it may appear logical to attempt to inhibit it at its early stage. Glycolysis starts by glucose entry into the cell, through glucose transporters (GLUTs), followed immediately by phosphorylation by Hexokinase (HK), required to "trap" glucose intracellularly. Logically, pharmacological inhibition of these two proteins may make sense as both are up-regulated in many cancers in order to increase glucose uptake and glycolysis and compensate for the loss of GO. However, being so proximal in the metabolic pathway and ubiquitous in all cells, inhibition of GLUTs and HK, while effective in some pre-clinical studies,

has suffered set backs when tested in early phase human trials [67, 68]. For example, inhibition of GLUTs led to brain toxicity as neurons rely mostly on the use of carbohydrate metabolism [69]. Similarly, HK inhibition led to severe hepatic toxicity, an organ heavily involved in both catabolism and anabolism of glucose [69]. In fact, more than half of the clinical trials using the GLUT and HK inhibitors, 2-Deoxyglucose and Lonidamine, were terminated prematurely [70]. Nevertheless, the HK inhibitor, 3-bromopyruvate, which showed good effect in a xenotransplant model, was used in a patient with fibrolamellar hepatocellular carcinoma [71, 72]. While this patient survived the duration of therapy, with few reported serious systemic side effects, the drug was delivered directly to the tumor-related artery by Transarterial Chemo Embolization (TACE) [73], perhaps limiting toxicity. Inhibiting glycolysis follows a more traditional "cytotoxic" pathway as inhibition of glycolysis causes nonspecific necrosis; in fact suppressing glycolysis will unavoidably further suppress mitochondrial function as it deprives mitochondria from the primary fuel in most tissues, limiting the therapeutic potential of this strategy. This is in contrast to the metabolic modulators discussed below that target the "coupling" of glycolysis to GO, actually enhancing mitochondrial function, allowing mitochondria to operate their intrinsic apoptotic machinery (an energy consuming function) or normalize their downstream signaling. While it is easy to criticize retrospectively, the investigators of these early clinical studies should be given credit as the first that attempted to target a metabolic process in human cancer, contributing to our re-examination of Warburg's "forgotten" theory.

1.3.2 Pyruvate Kinase M2 (PKM2) Activation: Pyruvate stands at a crossroads of metabolic fates: it is the product of cytoplasmic glycolysis, the product of cytosolic malate oxidation (to make anabolic NADPH), a precursor for amino acid production through transamination, the substrate of PDH versus LDH to either make acetyl-CoA which drives the mitochondrial Krebs' cycle, or lactate and complete glycolysis, respectively [69, 74, 75]. Pyruvate kinase (PK) is the last enzymatic step in glycolysis, catalyzing the reaction of phosphoenolpyruvate to

pyruvate, and consists of four isoforms [76]. Two of these isoforms, M1 (PKM1) and M2 (PKM2), are encoded by alternative splicing of the PKM2 (15q23) gene [77, 78]. Enzymatically, PKM1 is the highly active version and is found in normal tissues requiring large amounts of glucose-derived ATP, like skeletal muscle or brain [79, 80]. In contrast, the less active PKM2 is expressed in most tissues during development and has been found in many cancer cell lines [80-82]. Indeed, preferential expression of PKM2 over PKM1 is associated with mitochondrial suppression and enhanced tumorigenesis [80, 83, 84]. The enzymatic activity of PKM2 is regulated by several factors including glycolytic intermediates, tyrosine phosphorylation and acetylation [85-87]. Therefore, even though PKM2 expression in increased in cancer, its overall activity may be decreased [80]. Furthermore, it is dynamic since in nutrient-abundant states PKM2 forms active tetramers that function similarly to the more active PKM1 [80, 88]. The importance of this dynamic regulation of PKM2 has recently been explored in cancer [89]. Israelson *et al.* found, that mice conditionally deficient in PKM2, had a more accelerated tumor growth and mortality than their wild-type littermates. Furthermore, the ratio of the inactive over active form of PKM2 was found to tip the balance towards cancer growth. In contrast to the earlier belief that it was the switch from one isozyme to the other that promotes cancer, this work showed that it is the overall suppression of PKM1/2 activity as a whole (and thus the suppressed GO) that promotes cancer (Figure 1-3A). Indeed, over-expressing PKM1 in cancer cell lines lead to reduced tumor growth in xenotransplant models [83]. Thus, while the early discovery of an isozyme "specific for cancer" would have triggered efforts to inhibit it, it appears that it is PKM2 activators that may hold promise as cancer therapies. Several small molecules have been developed, such as TEPP-46, DASA-58 and ML265, which bind PKM2 at the subunit interaction interface to promote formation of enzymatically active tetramers [90]. This leads to a constitutively active enzyme with over 200% enhanced activity [83]. *In vitro*, treatment with these small molecule activators decreased the intermediates necessary for biomass generation, reduced lactate production and lipid synthesis and lead to smaller and slower growing tumors *in vivo* [83, 91].

Despite these promising results, pharmacologic activation of PKM2 may not induce cytotoxic changes in cancer. While populations of cancer cells expressing PKM2 do not proliferate, they continue to persist in a non-proliferative, perhaps senescent state [89]. Therefore, once a tumor has been detected, treatment with PKM2 activators may only limit further growth and would need to be combined with another agent or treatment modality to debulk the tumor by increasing cytotoxicity or by inducing apoptosis.

1.3.3 Pyruvate Dehydrogenase Kinase (PDK) Inhibition: PDK phosphorylates and inhibits the E1a subunit of PDH [28]. The net result of inhibited PDH is an increase in the ratio of glycolysis over GO (Figure 1-3B), with all the subsequent downstream signaling events that were discussed earlier. It is possible that increased expression and activity of PDK (via HIF1α or tyrosine kinase signaling as discussed earlier) is enough to induce the Warburg Effect and be the dominant mechanism in certain cancers [13, 92] or other proliferative diseases, like pulmonary arterial hypertension, characterized by a proliferative vascular remodeling and mitochondrial suppression [12, 93]. For example, PDK is significantly more increased in glioblastoma tumors compared to healthy brain tissues from the same patient [94], although this has not been systematically studied in cancer yet. There is strong evidence that PDK inhibition decreases cancer growth *in vitro* and *in vivo* in a variety of tumors as discussed below.

Dichloroacetate is an orally available small molecule inhibitor of PDK (structurally resembling pyruvate) that can reach most tissues and cross the blood brain barrier. DCA inhibits PDK at concentrations of 10-250 μM, while it is more active against some of the four PDK isoforms (i.e. the ubiquitously expressed PDK2) compared to others [95, 96]. DCA's mechanism of action is quite specific as it is mimicked by molecular PDK knockdown; in addition, DCA has no additional effects in cells with effective PDK knockdown [94, 97].

Originally, DCA was pioneered by Dr. Stacpoole's group at the University of Florida to limit lactic acidosis in children with congenital mitochondrial diseases (for example, deficiencies of PDH or other mitochondrial enzymes) and

over the past 40 years it has been explored in a number of disease states associated with lactic acidosis or with a primary mitochondrial suppression, including: diabetes, malaria, pulmonary arterial hypertension, lactic acidosis, heart failure, and exercise tolerance in chronic respiratory disease [98-106]. In 2007, we described DCA's pro-apoptotic and anti-proliferative effects due to normalization of mitochondrial function in a variety or cancers (non-small cell lung cancer, breast cancer, glioblastoma) *in vitro* and in xenotransplant models *in vivo* (Figure 1-4A) [97]. DCA, a generic drug, cannot be patented, creating the potential for financial barriers in its development as a cancer treatment. Yet, a number of investigators have shown interest since and have described similar effects in a variety of tumors. Some examples include prostate cancer [107], colon cancer [108-110], gastric cancer [111], endometrial cancer [112], glioblastoma [113], neuroblastoma [114], T-cell lymphoma [115], non-Hodgin's lymphoma [116], fibrosarcoma [117], and metastatic breast cancer [118] (Table 1). In this last study, DCA reduced lung metastases by 58% in a highly metastatic breast cancer model [118].

DCA appears to not have significant effects in normal cells, perhaps because of low levels of PDK activity in healthy tissues. Generally speaking, normal cells need active mitochondria with active PDH and keep the levels of its inhibitor (PDK) low. For example, DCA normalized the high $\Delta\Psi m$ of non-small cell lung cancer, glioblastoma and breast cancer cell lines without altering the $\Delta\Psi m$ of each cancer's non-malignant tissue analogue, i.e. small airway epithelial cells, mammary epithelial cells or healthy brain tissues [10, 94, 97].

In addition to the induction of apoptosis and inhibition of proliferation DCA can exhibit effects apparent only *in vivo*, as it suppresses angiogenesis by reversing the pseudohypoxic state caused by activated PDK. By promoting the decarboxylation of pyruvate into acetyl-CoA, DCA drives the Krebs' cycle to produce αKG, as well as NADH and $FADH_2$ to be used in the ETC [10]. This leads to increased mROS, which increases activity of redox sensitive tumor suppressors like p53 [10, 13, 94, 115]. Together, increased p53 activity and increased levels of αKG prevent the stabilization of HIF1α as well as reduce

HIF1α transcriptional activity and the expression of downstream HIF1α targets [10, 119]. DCA reduces the levels of angiogenic signaling molecules such as VEGF and SDF-1 and prevents neovascularization both *in vitro* and in xenotransplant tumor models [10]. In addition, inhibition of PDK using RNA interference has recently been shown to promote oncogene-induced senescence in melanoma *in vitro* and *in vivo*, providing another mechanism through which DCA may be exerting antitumor effects [120].

DCA has had success in early-phase small clinical trials for GBM and recurrent brain tumors [94, 121]. Compared to healthy brain tissue removed during surgery for epilepsy, tumors from 49 patients with GBM exhibited significantly higher levels of PDK and hyperpolarized $\Delta\Psi m$. Treatment of 5 patients with DCA (for which brain tissue was removed at the time of debulking surgery at baseline as well as after DCA treatment, allowing direct pre-post comparisons) caused mitochondrial depolarization, increased rates of apoptosis, activated p53, reduced proliferation and inhibited HIF1α activity and tumor vascularity [94]. Despite the very advanced stage of their disease, some patients showed evidence of tumor regression whereas others remained clinically stable for >18 months (Figure 1-4B). No patient developed hematologic, hepatic, renal, or cardiac toxicity. Peripheral neuropathy developed in some patients but reversed at a lower dose of DCA. Similar results, supporting the safety of the drug and the need for phase II trials in glioblastoma, were confirmed by another Phase I trial performed by an independent group, demonstrating clinically stable disease with no significant side effects beyond peripheral neuropathy, which when it occurs is dose-dependent and reversible [121]. Recently, the University of Florida group published their experience with DCA in children that were treated with DCA in their group continuously from 9.7 to 16.5 years at a dose of 12.5mg/kg twice a day (i.e. higher or equal to the doses used in the glioblastoma trials in humans). They reported no hematological, electrolyte, renal, or hepatic toxicity, with the only toxicity being a reversible and dose-dependent peripheral neuropathy (treated with dose reduction or only temporary discontinuation of DCA) [122].

Although the initial half-life of DCA is very short (i.e. approximately 2 hours) [96], the drug inhibits its own metabolism until it reaches a plateau, and thus therapeutic concentrations can be achieved in plasma with time (for example, at a dosing regime of 6.25mg/kg twice a day for three months) [94]. Nevertheless, this may take more than 3 months. Thus DCA may not be a good choice as a monotherapy in advanced and rapidly proliferating tumors. Like the PKM2 targeting drugs, it is not cytotoxic and could be seen as a drug that "sensitizes" the tumors to apoptosis, perhaps best used as a part of a combination therapy with a more cytotoxic drug at the early stages of treatment.

Another fact that may support DCA's sustained effects in the long-term, is its ability to inhibit HIF1α. For example, the early effectiveness of VEGF inhibitors is limited by the eventual escape of the tumor, which, having sustained HIF1α activity can continue to generate alternate pro-angiogenic factors. Thus, metabolic modulators like DCA that have the ability to inhibit the normoxic activation of HIF1α, may offer much more sustained and effective inhibition of angiogenesis [10]. Indeed, synergy between DCA and VEGF inhibitors was recently shown in glioblastoma cancer models [113].

The anti-cancer efficacy of DCA increases when combined with other agents. Similar to the synergy between DCA and VEGF inhibitors or DCA and temozolomide, a combination agent, called mitaplatin, combines DCA with cisplatin [123]. This unique drug is synthesized by adding two DCA moieties (one onto each end) of a cisplatin core. Once this drug enters a cancer cell, it is reduced to release one molecule of free cisplatin and two molecules of free DCA. The result is the combined effect of DCA on mitochondria (increasing cytochrome c release and apoptosis) as well as cisplatin mediated DNA crosslinking. Mitaplatin exceeded the anticancer efficacy of cisplatin alone in a variety of cancer cell lines [123]. DCA has also been used in combination with 5-Fluorouracil (5-FU) to re-sensitize hypoxic gastric cancer cells that developed resistance to 5-FU monotherapy [111]. Similarly, the combination of DCA with tamoxifen and omeprazole exhibited more potent antitumor activity than those agents alone [117]. Furthermore, other therapeutic modalities, such as external beam radiation

have been found to be efficacious in combination with metabolic modulators. DCA sensitized prostate cancer cells (which were previously resistant due to overexpression of BCL-2), to radiation therapy [107]. Furthermore, in combination with etoposide or irradiation, DCA decreases the apoptosis resistance seen in gliomas compared to treatment with either of these agents alone [124]. These examples suggest that mitochondrial activation may be effective in combination strategies for several tumor types.

DCA's proven ability to increase the GO/glycolysis ratio in the treated tumors and its ability to decrease HIF1α activity and thus reverse the up-regulation of glucose transporters, suggest that metabolic imaging, like FDG-PET maybe used to track its effects *in vivo*, a very desirable tool in drug development (Figure 1-4C). Tumor cells, expressing a relative abundance of glucose transporters and glycolytic enzymes take up much more fluorinated deoxyglucose (a metabolite that once up-taken remains trapped intra-cellularly allowing its imaging) than surrounding non-cancerous tissue. In theory, one of the first signs of DCA's effectiveness *in vivo* maybe its ability to decrease the FDG uptake under FDG-PET imaging, a possibility that although has been documented in animal models [10], should be systematically pursued in future clinical trials.

1.3.4 Lactate Dehydrogenase A (LDHA) Inhibition: Suppressed mitochondria in cancer cells force pyruvate to be reduced to lactate in order to allow glycolysis to continue. This is achieved by Lactate Dehydrogenase (LDH), a tetrameric enzyme that facilitates the recycling of NAD+ from NADH by reducing pyruvate to lactate in the cytoplasm. There are five isoforms of LDH made from differing subunit combinations of the products from two genes, LDHB and LDHA: LDHB expresses a constitutively active form, LDH-H (heart); LDHA is a HIF1α responsive gene that transcribes a more efficient enzyme, LDH-M (muscle) [74, 125] (Figure 1-3C). In highly glycolytic tumors, the isoform made exclusively from four subunits of LDH-M, known as LDH5, predominates [126]. Similarly, tumors epigenetically silence the LDHB gene through hypermethylation of its promoter region, thereby further shifting the ratio of LDH towards LDH5 [127].

Indeed, the increased expression of this highly active tetramer is a marker of poor prognosis in multiple malignancies [126, 128, 129]. In tissues where LDH activity is enhanced, its inhibition will facilitate pyruvate's entry into the mitochondria (assuming that PDH is active), increasing GO and preventing the shift of pyruvate's metabolism into anabolic precursors.

Indeed, inhibition of LDH5 with short hairpin RNA enhanced respiration and reduced $\Delta\Psi m$. LDHA knockdown reduced cancer growth rates *in vitro* and *in vivo* in animal models [130]. This work led to the development of a small molecule inhibitor of LDH, FX11, which was shown to be effective in animal models of lymphoma and pancreatic cancer [131]. Another class of LDH5 competitive inhibitors, N-hydroxy-2-carboxy-substituted indoles, called NHI-1 and NHI-2, has been developed [132, 133]. These more specific and efficient LDH5 inhibitors decrease lactate production and reduce proliferation in multiple cancer cells lines.

Recently, ^{13}C labeled magnetic resonance spectroscopy has been adapted to follow dynamic metabolic conversions *in vivo* [134]. This imaging biomarker assesses real-time changes in intracellular metabolism such as decreased reduction of pyruvate to lactate in response to drugs like LDH inhibitors or DCA [135, 136].

1.3.5 Mutant Isocitrate Dehydrogenase (IDH) Inhibition: As discussed above, mutant IDH leads to pseudo-hypoxic signaling, due to the production of 2-HG (Figure 1-3D). Recently, pharmacological inhibition of IDH has been explored. Several small molecule inhibitors that specifically inhibit the mutant form of IDH have been developed [137, 138]. Discovered through high-throughput screening, AGI-5198 inhibits the production of 2-HG by mutant IDH1 while AGI-6780 inhibits 2-HG production by mutant IDH2. This inhibition appears highly specific for the mutant isoform as AGI-5198 impairs only the growth of IDH1 mutant but not IDH1 wild-type glioma xenotransplant tumors [138].

2-HG producing tumors cause exponentially higher levels of this metabolite in the patient's circulation [63]. Fathi *et al.* have taken advantage of

this unique cancer metabolite, to non-invasively diagnose and subsequently follow response to treatment in AML by detecting the levels of 2-HG in patients' serum and urine samples before and during therapy [139]. While IDH inhibitors have yet to be tested in humans, this powerful biomarker will facilitate IDH inhibitor development in clinical trials.

1.4.0 Cancer Stem Cells: Mitochondrial metabolism also determines stem cell fate. Temporally, a switch to glycolysis precedes expression of stem cell markers and subsequent entry into a pluripotent state [140]. Conversely, an increase in mitochondrial glucose oxidation is necessary for initiating stem cell differentiation [141]. Normal stem cells, similar to cancer cells, exhibit increased LDHA, HKII, PDK and phosphorylated PDH, compared to differentiated progeny, leading to mitochondrial suppression [142]. This mitochondrial suppression is further exacerbated in hypoxic tumor cells and cancer stem cells. For example, when lung cancer stem cells (LCSCs) are directly compared to differentiated lung cancer cells, LCSCs demonstrate lower oxygen consumption, mROS, mitochondrial numbers and ATP levels, as well as higher mitochondrial membrane potential [143]. Similarly, when studied in parallel, healthy brain tissue, glioblastoma cancer cells, and glioblastoma putative cancer stem cells exhibit a graded increase in mitochondrial suppression, with the highest levels of $\Delta\Psi m$ seen in the cancer stem cells [94]. Mechanistically, overwhelming mitochondrial suppression in cancer stem cells provides significant resistance to apoptosis, potentially contributing the cancer stem cells' resistance to apoptosis and conventional chemotherapeutics.

Activating mitochondria unlocks apoptosis resistance in cancer stem cells. For example, tumor biopsies from GBM patients treated with DCA found induction of apoptosis in glioblastoma putative cancer stem cells, particularly when used in combination with temozolomide in vivo and in vitro [94]. Similarly, DCA reduces cancer stem cell viability in embryonal cancer stem cells when the substrate for PDH, pyruvate, is available [144].

Despite the induction of apoptosis in cancer stem cells, there is evidence

that DCA exhibits specificity for cancer stem cells and not healthy stem cells. For example, patients treated with long-term (up to 16 years) DCA did not suffer any hematological side-effects, suggesting lack of effects on bone marrow stem cells [122]. Yet, it is possible that more potent mitochondrial activators may have this problem, an important issue that has to be addressed in the future with long-term studies. On the other hand, metabolic disturbances may affect the ability of stem cells to differentiate and, in the case of IDH mutations in leukemic cells, there is evidence that they may impair the ability of hematopoietic stem cells to differentiate, resulting in leukemias that mimic a difficult to treat, hematopoietic stem cell phenotype [145].

1.5.0 Glucose oxidation and histone acetylation: Histone acetylation has received a lot of attention in cancer research [146]. As the source of the acetyl group is acetyl-CoA (a prime mitochondrial product) it is possible that the mitochondria suppression discussed herein may actually also impact epigenetic mechanisms. Isolated nuclei exposed to acetyl-CoA exhibit increased histone acetylation [147]. Intriguingly, the acetyl-CoA molecule is extremely unstable and has to be used in the organelle that is produced. In other words, acetyl-CoA cannot simply leak out of mitochondria and enter the nucleus. Recent work however has shown two mechanisms by which mitochondria can regulate histone acetylation:

a) PDH activity promotes citrate production in the Krebs' cycle, which can diffuse out of the mitochondria and into the nucleus to be used as a substrate to acetylate histones by the enzyme ATP-citrate lyase, which is present both in the cytoplasm and the nucleus [148]. Thus, a primary inhibition of PDH will also result eventually in a suppression of citrate production and histone acetylation, unless citrate can be replenished by alternate pathway like the reductive glutamine pathway, which can produce citrate in the cytoplasm from the amino acid glutamine [149].

b) We recently described an alternate way of nuclear production of acetyl-CoA by showing that PDH can actually translocate into the nucleus in a cell-cycle

dependent manner [150]. Interestingly, several subunits of the PDH complex, E1a and E2, had previously been shown to be present in the nucleus of leukemic T cells, although at the time their presence was not linked to the main function of PDH, i.e. production of acetyl-CoA [151]. We found that nuclear PDH (which included all subunits of the complex), although in small amounts, is functional, providing a source of acetyl-CoA to be used to acetylate specific histone residues involved in cell-cycle progression [150]. Intriguingly, PDK does not follow PDH in the nucleus (potentially being displaced from its binding site on the E2 subunit by HSP70, which then transports a 'PDK-free' HSP70-PDH complex to the nucleus) suggesting that nuclear PDH will be immune to DCA and perhaps represent a potential "escape" mechanism to DCA treatment (Figure 1-5) [150].

The fact that translocation of such a large enzyme like PDH takes place between mitochondria and the nucleus is not as surprising as one may first think. For example, while mitochondrial PDH has been classically thought to be localized in the mitochondrial matrix, it has also been shown to move through the mitochondrial inner membranes and remain functional in the outer mitochondrial membrane [27]. This is in keeping with our finding that the chaperone HSP70 may be involved in its nuclear translocation since it may easily reach PDH on the outer mitochondrial membrane [150]. The role of nuclear PDH is not entirely clear, but suggests that it may provide a critical regulatory mechanism for gene expression by mediating a shift from heterochromatin to euchromatin thereby facilitating transcription factor binding. Identifying a mechanism by which this translocation is blocked, may represent a new means of cancer therapy, merging the fields of metabolism and epigenetic regulation therapeutics.

Table 1-1: Evidence for Dichloroacetate's benefits in multiple cancer types.

Cancer Type	Model	Outcome	Monotherapy vs. Combination	Ref.
Breast	*In vivo* lung metastasis model	Reduced number of lung metastases, increased apoptosis	Monotherapy	[118]
Breast	Xenotransplant	Reduced tumor growth and angiogenesis	Monotherapy	[10]
Colon	Xenotransplant	Reduced tumor growth and restored mitochondrial ultrastructure	Monotherapy	[108]
Colon	*In vitro*	Reduced proliferation and increased apoptosis	Monotherapy	[109]
Colon	Spontaneous colorectal adenocarcinoma	Decreased tumor grade, tumor size, and number of tumors formed	Monotherapy	[110]
Endometrial	*In vitro*	Increased apoptosis	Monotherapy	[112]
Fibrosarcoma	*In vitro*	Increased apoptosis	Combination with Tamoxifen and Omeprazole	[117]
Gastric	*In vitro*	Increased apoptosis and sensitized resistant cancer cells to 5-fluorouracil	Combination with 5-fluorouracil	[111]
Glioblastoma	*In vitro*	Increased apoptosis	Monotherapy	[97]
Glioblastoma	Xenotransplant	Reduced tumor growth	Combination with bevacizumab	[113]
Neuroblastoma	Xenotransplant	Reduced tumor growth	Monotherapy	[114]
Non-Hodgkin's Lymphoma	*In vivo*	Complete remission on PET	Monotherapy	[116]
Non-small cell lung	Xenotransplant	Reduced tumor growth and increased apoptosis in vivo	Monotherapy	[97]
Prostate	*In vitro*	Increased apoptosis	Combination with external beam radiation	[107]
T-cell lymphoma	*In vitro*	Increased apoptosis Reduced HIF1α function	Monotherapy	[115]

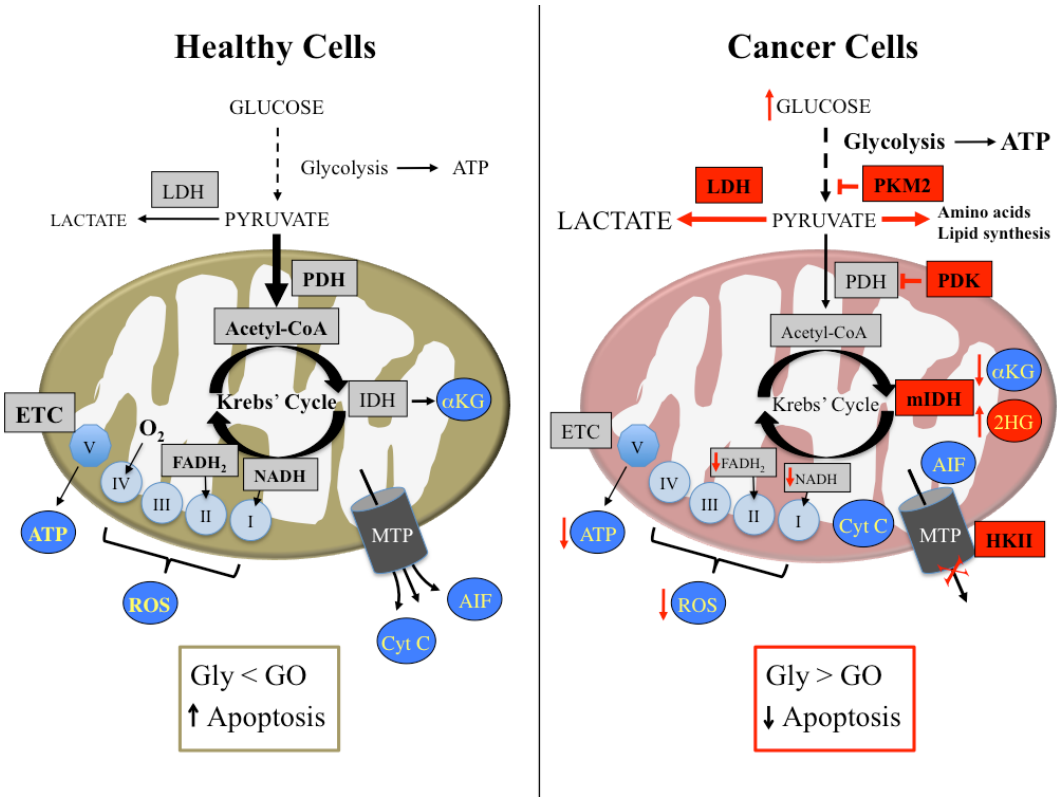

Figure 1-1. Suppressed mitochondrial function in cancer cells under normoxia (Warburg Effect).

While the mitochondrial glucose oxidation (GO) is suppressed, the cytoplasmic glycolysis (Gly) is enhanced in cancer. This is caused by a combination of inhibited mitochondrial enzymes, whether by upregulation of PDK (a PDH inhibitor), LDH5 and PKM2 (isozymes that confer increased enzymatic activity) or by mutations in IDH. All of these enzymes are induced by HIF1α. On the other hand, the effects of this remodeling include decreased production of αKG (as a result of inhibited Krebs' cycle) and increased levels of 2-HG, the product of mutated IDH. Both of which result in HIF1α stabilization, closing a powerful feedback loop. In addition, this remodeling results in mitochondrial hyperpolarization (in part of a translocation of the glycolytic enzyme HKII to the VDAC, inhibiting the function of the Mitochondrial Transition Pore, a mega channel that allows the release of pro-apoptotic factors like cytochrome c and apoptosis inducing factor, thus inhibiting mitochondria-dependent apoptosis. Pyruvate dehydrogenase kinase (PDK), Pyruvate dehydrogenase (PDH), Lactate

dehydrogenase 5 (LDH5), Pyruvate kinase M2 (PKM2), Isocitrate dehydrogenase (IDH), Hypoxia inducible factor 1α (HIF1α), Alpha-ketoglutarate (αKG), 2-hydroxyglutarate (2-HG), Hexokinase II (HKII), Voltage-dependent anion channel (VDAC).

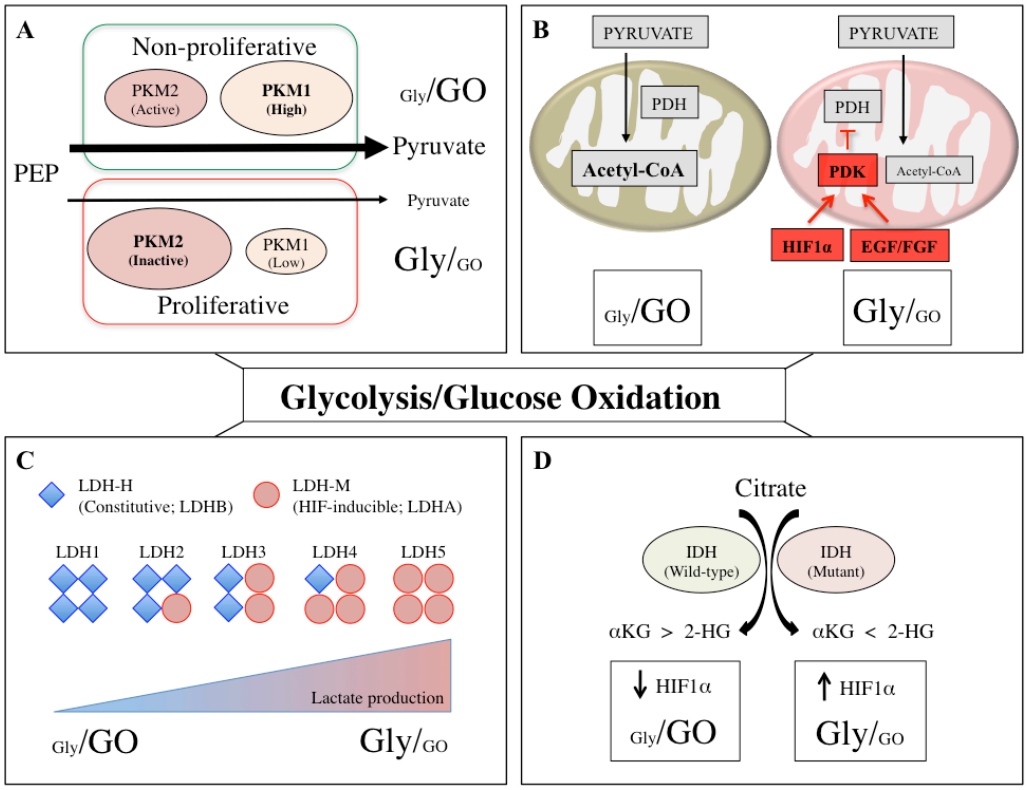

Figure 1-2. Ratio of Glycolysis to Glucose Oxidation increases in cancer due to changes in several key metabolic enzymes.

(A) Cells that express a low amount of Pyruvate kinase M1 (PKM1) and an abundance of low-activity Pyruvate kinase M2 (PKM2; which results in an overall decrease in pyruvate kinase activity) prevent the entry of pyruvate into the mitochondria, inhibiting glucose oxidation (GO).

(B) Pyruvate dehydrogenase kinase (PDK) also inhibits the entry of pyruvate into the mitochondria by phosphorylating and inhibiting pyruvate dehydrogenase (PDH).

(C) The Lactate dehydrogenase (LDH) enzyme is made from four subunits comprised of H (Heart) or M (Muscle) isoforms. Overexpression of the hypoxia-inducible factor 1α (HIF1α) inducible LDH-M creates an enzyme comprised of four M subunits resulting in increased activity, favouring the reduction of pyruvate to lactate, thereby shunting pyruvate away from GO.

(D) Mutation in isocitrate dehydrogenase (IDH) leads to the production of the oncometabolite, 2-hydroxyglutarate (2-HG), which antagonizes the normal

product, alpha-ketoglutarate (αKG), leading to suppressed GO via the stabilization and accumulation HIF1α.

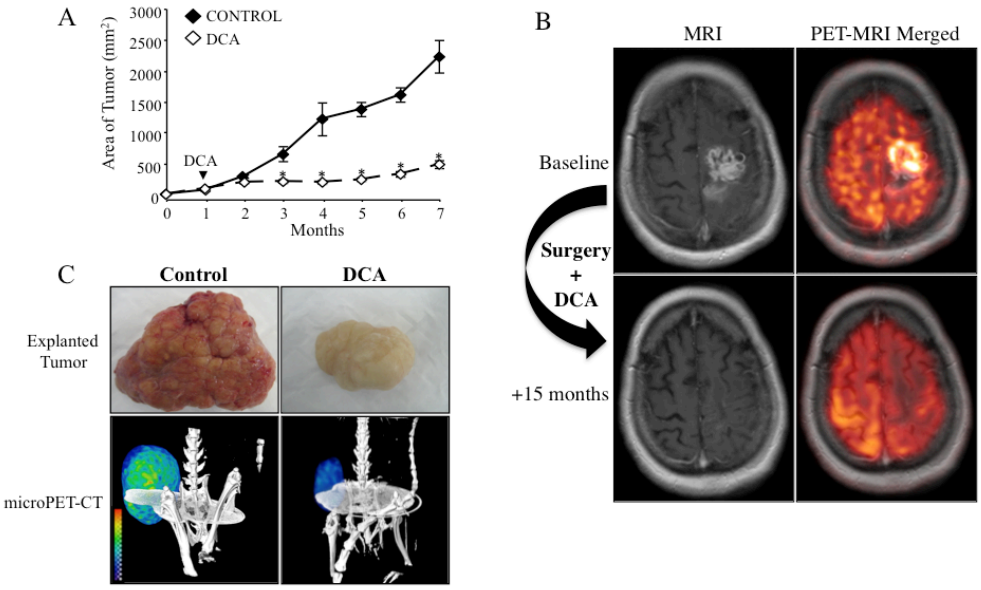

Figure 1-3. Translation of DCA from animal studies to an early phase human trial. DCA decreased tumor size (A), vascularity and FDG uptake (measured by microPET-CT (C) in a xenograft rat model with non-small cell lung cancer. In a small human glioblastoma trial, DCA normalized mitochondrial metabolism, increased apoptosis, suppressed angiogenesis and reduced tumor growth after debulking surgery for at least 18 months, in a patient that had failed all approved therapies and was otherwise destined for hospice care (B).

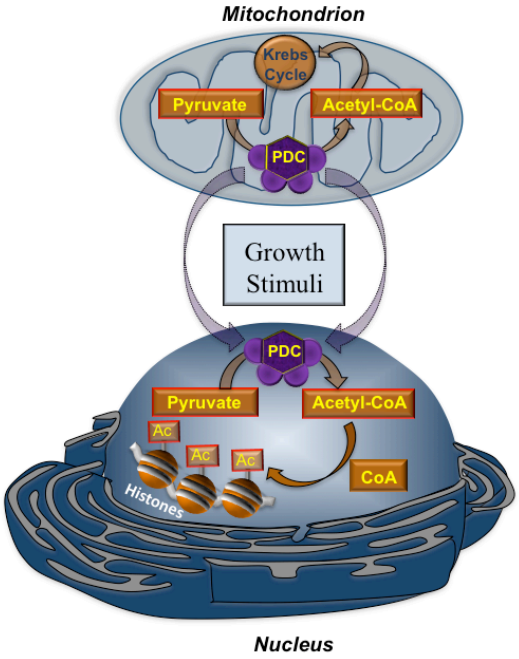

Figure 1-4. Nuclear translocation of the PDH Complex (PDC) provides Acetyl-CoA for histone acetylation. PDC dynamically translocates from the mitochondria to the nucleus in response to growth factors, like epidermal growth factor (EGF), to provide acetyl-CoA for histone acetylation and cell cycle progression.

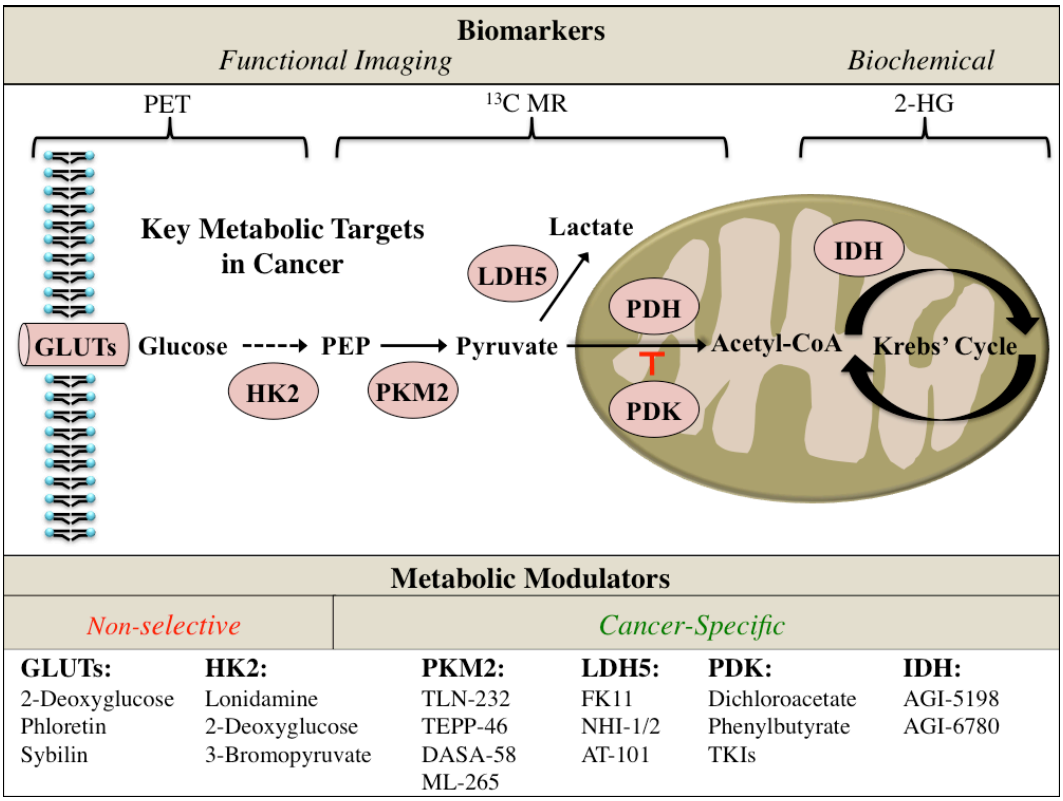

Figure 1-5. Biomarkers and metabolic modulators arising from the metabolic theory of cancer (see text). Biomarkers (top) and metabolic modulators (bottom) that have been developed for target enzymes and have been or are in preclinical or clinical trials. Glucose transporter 1 (GLUT1), Hexokinase II (HKII), M2 isoform pyruvate kinase (PKM2), Lactate dehydrogenase 5 (LDH5), Pyruvate dehydrogenase (PDH), pyruvate dehydrogenase kinase (PDK), Tyrosine Kinase Inhibitors (TKIs) Isocitrate dehydrogenase (IDH), Phosphoenolpyruvate (PEP), Positron emission tomography (PET), Magnetic resonance (MR), 2-hydroxyglutarate (2-HG).

References

1. Le Tourneau C, Lee JJ, Siu LL (2009) Dose escalation methods in phase I cancer clinical trials. J Natl Cancer Inst 101: 708-720.
2. Druker BJ, Talpaz M, Resta DJ, Peng B, Buchdunger E, Ford JM, Lydon NB, Kantarjian H, Capdeville R, Ohno-Jones S, Sawyers CL (2001) Efficacy and safety of a specific inhibitor of the BCR-ABL tyrosine kinase in chronic myeloid leukemia. N Engl J Med 344: 1031-1037.
3. Slamon DJ, Leyland-Jones B, Shak S, Fuchs H, Paton V, Bajamonde A, Fleming T, Eiermann W, Wolter J, Pegram M, Baselga J, Norton L (2001) Use of chemotherapy plus a monoclonal antibody against HER2 for metastatic breast cancer that overexpresses HER2. N Engl J Med 344: 783-792.
4. Wen PY, Kesari S (2008) Malignant gliomas in adults. N Engl J Med 359: 492-507.
5. Loureiro R, Mesquita KA, Oliveira PJ, Vega-Naredo I (2013) Mitochondria in cancer stem cells: a target for therapy. Recent Pat Endocr Metab Immune Drug Discov 7: 102-114.
6. Warburg O (1923) Metabolism of tumours. Biochem Zeitschr 142: 317-333.
7. Loenarz C, Schofield CJ (2008) Expanding chemical biology of 2-oxoglutarate oxygenases. Nat Chem Biol 4: 152-156.
8. Schmid T, Zhou J, Kohl R, Brune B (2004) p300 relieves p53-evoked transcriptional repression of hypoxia-inducible factor-1 (HIF-1). Biochem J 380: 289-295.
9. Vousden KH, Ryan KM (2009) p53 and metabolism. Nat Rev Cancer 9: 691-700.
10. Sutendra G, Dromparis P, Kinnaird A, Stenson TH, Haromy A, Parker JM, McMurtry MS, Michelakis ED (2012) Mitochondrial activation by inhibition of PDKII suppresses HIF1a signaling and angiogenesis in cancer. Oncogene 32: 1638-1650.
11. Maddocks OD, Vousden KH (2011) Metabolic regulation by p53. J Mol Med (Berl) 89: 237-245.
12. Dromparis P, Michelakis ED (2013) Mitochondria in vascular health and disease. Annu Rev Physiol 75: 95-126.
13. Sutendra G, Michelakis ED (2013) Pyruvate dehydrogenase kinase as a novel therapeutic target in oncology. Front Oncol 3: 38.
14. Zamzami N, Kroemer G (2001) The mitochondrion in apoptosis: how Pandora's box opens. Nature reviews Molecular cell biology 2: 67-71.
15. Chen LB (1988) Mitochondrial membrane potential in living cells. Annu Rev Cell Biol 4: 155-181.
16. Lemasters JJ, Holmuhamedov E (2006) Voltage-dependent anion channel (VDAC) as mitochondrial governator--thinking outside the box. Biochimica et biophysica acta 1762: 181-190.
17. Pastorino JG, Hoek JB, Shulga N (2005) Activation of glycogen synthase kinase 3beta disrupts the binding of hexokinase II to mitochondria by phosphorylating voltage-dependent anion channel and potentiates chemotherapy-induced cytotoxicity. Cancer Res 65: 10545-10554.

18. Vander Heiden MG, Cantley LC, Thompson CB (2009) Understanding the Warburg effect: the metabolic requirements of cell proliferation. Science 324: 1029-1033.
19. Butow RA, Avadhani NG (2004) Mitochondrial signaling: the retrograde response. Mol Cell 14: 1-15.
20. Esteves P, Pecqueur C, Ransy C, Esnous C, Lenoir V, Bouillaud F, Bulteau AL, Lombes A, Prip-Buus C, Ricquier D, Alves-Guerra MC (2014) Mitochondrial retrograde signaling mediated by UCP2 inhibits cancer cell proliferation and tumorigenesis. Cancer Res 74: 3971-3982.
21. Wallace DC (2012) Mitochondria and cancer. Nat Rev Cancer 12: 685-698.
22. Semenza GL (2010) HIF-1: upstream and downstream of cancer metabolism. Current opinion in genetics & development 20: 51-56.
23. Denko NC (2008) Hypoxia, HIF1 and glucose metabolism in the solid tumour. Nat Rev Cancer 8: 705-713.
24. Yu F, White SB, Zhao Q, Lee FS (2001) HIF-1alpha binding to VHL is regulated by stimulus-sensitive proline hydroxylation. Proc Natl Acad Sci U S A 98: 9630-9635.
25. Ke Q, Costa M (2006) Hypoxia-inducible factor-1 (HIF-1). Molecular pharmacology 70: 1469-1480.
26. Gatenby RA, Gillies RJ (2004) Why do cancers have high aerobic glycolysis? Nat Rev Cancer 4: 891-899.
27. Hitosugi T, Fan J, Chung TW, Lythgoe K, Wang X, Xie J, Ge Q, Gu TL, Polakiewicz RD, Roesel JL, Chen GZ, Boggon TJ, Lonial S, Fu H, Khuri FR, Kang S, Chen J (2011) Tyrosine phosphorylation of mitochondrial pyruvate dehydrogenase kinase 1 is important for cancer metabolism. Mol Cell 44: 864-877.
28. Korotchkina LG, Patel MS (2001) Probing the mechanism of inactivation of human pyruvate dehydrogenase by phosphorylation of three sites. J Biol Chem 276: 5731-5738.
29. Fan J, Kang HB, Shan C, Elf S, Lin R, Xie J, Gu TL, Aguiar M, Lonning S, Chung TW, Arellano M, Khoury HJ, Shin DM, Khuri FR, Boggon TJ, Kang S, Chen J (2014) Tyr-301 phosphorylation inhibits pyruvate dehydrogenase by blocking substrate binding and promotes the Warburg effect. J Biol Chem 289: 26533-26541.
30. Kim JW, Tchernyshyov I, Semenza GL, Dang CV (2006) HIF-1-mediated expression of pyruvate dehydrogenase kinase: a metabolic switch required for cellular adaptation to hypoxia. Cell Metab 3: 177-185.
31. Franovic A, Gunaratnam L, Smith K, Robert I, Patten D, Lee S (2007) Translational up-regulation of the EGFR by tumor hypoxia provides a nonmutational explanation for its overexpression in human cancer. Proc Natl Acad Sci U S A 104: 13092-13097.
32. Wu P, Inskeep K, Bowker-Kinley MM, Popov KM, Harris RA (1999) Mechanism responsible for inactivation of skeletal muscle pyruvate dehydrogenase complex in starvation and diabetes. Diabetes 48: 1593-1599.

33. Kandoth C, McLellan MD, Vandin F, Ye K, Niu B, Lu C, Xie M, Zhang Q, McMichael JF, Wyczalkowski MA, Leiserson MD, Miller CA, Welch JS, Walter MJ, Wendl MC, Ley TJ, Wilson RK, Raphael BJ, Ding L (2013) Mutational landscape and significance across 12 major cancer types. Nature 502: 333-339.
34. Bensaad K, Tsuruta A, Selak MA, Vidal MN, Nakano K, Bartrons R, Gottlieb E, Vousden KH (2006) TIGAR, a p53-inducible regulator of glycolysis and apoptosis. Cell 126: 107-120.
35. Kondoh H, Lleonart ME, Gil J, Wang J, Degan P, Peters G, Martinez D, Carnero A, Beach D (2005) Glycolytic enzymes can modulate cellular life span. Cancer Res 65: 177-185.
36. Matoba S, Kang JG, Patino WD, Wragg A, Boehm M, Gavrilova O, Hurley PJ, Bunz F, Hwang PM (2006) p53 regulates mitochondrial respiration. Science 312: 1650-1653.
37. Contractor T, Harris CR (2012) p53 negatively regulates transcription of the pyruvate dehydrogenase kinase Pdk2. Cancer Res 72: 560-567.
38. Mathupala SP, Heese C, Pedersen PL (1997) Glucose catabolism in cancer cells. The type II hexokinase promoter contains functionally active response elements for the tumor suppressor p53. J Biol Chem 272: 22776-22780.
39. Choudhary C, Weinert BT, Nishida Y, Verdin E, Mann M (2014) The growing landscape of lysine acetylation links metabolism and cell signalling. Nature reviews Molecular cell biology 15: 536-550.
40. Dang CV, Semenza GL (1999) Oncogenic alterations of metabolism. Trends in biochemical sciences 24: 68-72.
41. Shim H, Dolde C, Lewis BC, Wu CS, Dang G, Jungmann RA, Dalla-Favera R, Dang CV (1997) c-Myc transactivation of LDH-A: implications for tumor metabolism and growth. Proc Natl Acad Sci U S A 94: 6658-6663.
42. Kim JW, Zeller KI, Wang Y, Jegga AG, Aronow BJ, O'Donnell KA, Dang CV (2004) Evaluation of myc E-box phylogenetic footprints in glycolytic genes by chromatin immunoprecipitation assays. Mol Cell Biol 24: 5923-5936.
43. Nogueiras R, Habegger KM, Chaudhary N, Finan B, Banks AS, Dietrich MO, Horvath TL, Sinclair DA, Pfluger PT, Tschop MH (2012) Sirtuin 1 and sirtuin 3: physiological modulators of metabolism. Physiological reviews 92: 1479-1514.
44. He W, Newman JC, Wang MZ, Ho L, Verdin E (2012) Mitochondrial sirtuins: regulators of protein acylation and metabolism. Trends in endocrinology and metabolism: TEM 23: 467-476.
45. Kim HS, Patel K, Muldoon-Jacobs K, Bisht KS, Aykin-Burns N, Pennington JD, van der Meer R, Nguyen P, Savage J, Owens KM, Vassilopoulos A, Ozden O, Park SH, Singh KK, Abdulkadir SA, Spitz DR, Deng CX, Gius D (2010) SIRT3 is a mitochondria-localized tumor suppressor required for maintenance of mitochondrial integrity and metabolism during stress. Cancer Cell 17: 41-52.
46. Guarente L (2014) The Many Faces of Sirtuins: Sirtuins and the Warburg effect. Nature medicine 20: 24-25.

47. Finley LW, Carracedo A, Lee J, Souza A, Egia A, Zhang J, Teruya-Feldstein J, Moreira PI, Cardoso SM, Clish CB, Pandolfi PP, Haigis MC (2011) SIRT3 opposes reprogramming of cancer cell metabolism through HIF1alpha destabilization. Cancer Cell 19: 416-428.
48. Denton RM (2009) Regulation of mitochondrial dehydrogenases by calcium ions. Biochimica et biophysica acta 1787: 1309-1316.
49. Dromparis P, Paulin R, Sutendra G, Qi AC, Bonnet S, Michelakis ED (2013) Uncoupling protein 2 deficiency mimics the effects of hypoxia and endoplasmic reticulum stress on mitochondria and triggers pseudohypoxic pulmonary vascular remodeling and pulmonary hypertension. Circ Res 113: 126-136.
50. Derdak Z, Fulop P, Sabo E, Tavares R, Berthiaume EP, Resnick MB, Paragh G, Wands JR, Baffy G (2006) Enhanced colon tumor induction in uncoupling protein-2 deficient mice is associated with NF-kappaB activation and oxidative stress. Carcinogenesis 27: 956-961.
51. Archer SL (2013) Mitochondrial dynamics--mitochondrial fission and fusion in human diseases. N Engl J Med 369: 2236-2251.
52. Mitra K, Wunder C, Roysam B, Lin G, Lippincott-Schwartz J (2009) A hyperfused mitochondrial state achieved at G1-S regulates cyclin E buildup and entry into S phase. Proc Natl Acad Sci U S A 106: 11960-11965.
53. Rehman J, Zhang HJ, Toth PT, Zhang Y, Marsboom G, Hong Z, Salgia R, Husain AN, Wietholt C, Archer SL (2012) Inhibition of mitochondrial fission prevents cell cycle progression in lung cancer. FASEB journal : official publication of the Federation of American Societies for Experimental Biology 26: 2175-2186.
54. Tomlinson IP, Alam NA, Rowan AJ, Barclay E, Jaeger EE, Kelsell D, Leigh I, Gorman P, Lamlum H, Rahman S, Roylance RR, Olpin S, Bevan S, Barker K, Hearle N, Houlston RS, Kiuru M, Lehtonen R, Karhu A, Vilkki S, Laiho P, Eklund C, Vierimaa O, Aittomaki K, Hietala M, Sistonen P, Paetau A, Salovaara R, Herva R, Launonen V, Aaltonen LA, Multiple Leiomyoma C (2002) Germline mutations in FH predispose to dominantly inherited uterine fibroids, skin leiomyomata and papillary renal cell cancer. Nature genetics 30: 406-410.
55. Neumann HP, Pawlu C, Peczkowska M, Bausch B, McWhinney SR, Muresan M, Buchta M, Franke G, Klisch J, Bley TA, Hoegerle S, Boedeker CC, Opocher G, Schipper J, Januszewicz A, Eng C, European-American Paraganglioma Study G (2004) Distinct clinical features of paraganglioma syndromes associated with SDHB and SDHD gene mutations. Jama 292: 943-951.
56. Baysal BE (2003) On the association of succinate dehydrogenase mutations with hereditary paraganglioma. Trends in endocrinology and metabolism: TEM 14: 453-459.
57. Isaacs JS, Jung YJ, Mole DR, Lee S, Torres-Cabala C, Chung YL, Merino M, Trepel J, Zbar B, Toro J, Ratcliffe PJ, Linehan WM, Neckers L (2005) HIF overexpression correlates with biallelic loss of fumarate hydratase in renal cancer: novel role of fumarate in regulation of HIF stability. Cancer Cell 8: 143-153.

58. King A, Selak MA, Gottlieb E (2006) Succinate dehydrogenase and fumarate hydratase: linking mitochondrial dysfunction and cancer. Oncogene 25: 4675-4682.
59. Selak MA, Armour SM, MacKenzie ED, Boulahbel H, Watson DG, Mansfield KD, Pan Y, Simon MC, Thompson CB, Gottlieb E (2005) Succinate links TCA cycle dysfunction to oncogenesis by inhibiting HIF-alpha prolyl hydroxylase. Cancer Cell 7: 77-85.
60. Parsons DW, Jones S, Zhang X, Lin JC, Leary RJ, Angenendt P, Mankoo P, Carter H, Siu IM, Gallia GL, Olivi A, McLendon R, Rasheed BA, Keir S, Nikolskaya T, Nikolsky Y, Busam DA, Tekleab H, Diaz LA, Jr., Hartigan J, Smith DR, Strausberg RL, Marie SK, Shinjo SM, Yan H, Riggins GJ, Bigner DD, Karchin R, Papadopoulos N, Parmigiani G, Vogelstein B, Velculescu VE, Kinzler KW (2008) An integrated genomic analysis of human glioblastoma multiforme. Science 321: 1807-1812.
61. Mardis ER, Ding L, Dooling DJ, Larson DE, McLellan MD, Chen K, Koboldt DC, Fulton RS, Delehaunty KD, McGrath SD, Fulton LA, Locke DP, Magrini VJ, Abbott RM, Vickery TL, Reed JS, Robinson JS, Wylie T, Smith SM, Carmichael L, Eldred JM, Harris CC, Walker J, Peck JB, Du F, Dukes AF, Sanderson GE, Brummett AM, Clark E, McMichael JF, Meyer RJ, Schindler JK, Pohl CS, Wallis JW, Shi X, Lin L, Schmidt H, Tang Y, Haipek C, Wiechert ME, Ivy JV, Kalicki J, Elliott G, Ries RE, Payton JE, Westervelt P, Tomasson MH, Watson MA, Baty J, Heath S, Shannon WD, Nagarajan R, Link DC, Walter MJ, Graubert TA, DiPersio JF, Wilson RK, Ley TJ (2009) Recurring mutations found by sequencing an acute myeloid leukemia genome. N Engl J Med 361: 1058-1066.
62. Dang L, White DW, Gross S, Bennett BD, Bittinger MA, Driggers EM, Fantin VR, Jang HG, Jin S, Keenan MC, Marks KM, Prins RM, Ward PS, Yen KE, Liau LM, Rabinowitz JD, Cantley LC, Thompson CB, Vander Heiden MG, Su SM (2009) Cancer-associated IDH1 mutations produce 2-hydroxyglutarate. Nature 462: 739-744.
63. Ward PS, Patel J, Wise DR, Abdel-Wahab O, Bennett BD, Coller HA, Cross JR, Fantin VR, Hedvat CV, Perl AE, Rabinowitz JD, Carroll M, Su SM, Sharp KA, Levine RL, Thompson CB (2010) The common feature of leukemia-associated IDH1 and IDH2 mutations is a neomorphic enzyme activity converting alpha-ketoglutarate to 2-hydroxyglutarate. Cancer Cell 17: 225-234.
64. Rose NR, McDonough MA, King ON, Kawamura A, Schofield CJ (2011) Inhibition of 2-oxoglutarate dependent oxygenases. Chemical Society reviews 40: 4364-4397.
65. Guan KL, Xiong Y (2011) Regulation of intermediary metabolism by protein acetylation. Trends in biochemical sciences 36: 108-116.
66. Zhao S, Xu W, Jiang W, Yu W, Lin Y, Zhang T, Yao J, Zhou L, Zeng Y, Li H, Li Y, Shi J, An W, Hancock SM, He F, Qin L, Chin J, Yang P, Chen X, Lei Q, Xiong Y, Guan KL (2010) Regulation of cellular metabolism by protein lysine acetylation. Science 327: 1000-1004.

67. Devi MA, Das NP (1993) In vitro effects of natural plant polyphenols on the proliferation of normal and abnormal human lymphocytes and their secretions of interleukin-2. Cancer Lett 69: 191-196.
68. Kobori M, Shinmoto H, Tsushida T, Shinohara K (1997) Phloretin-induced apoptosis in B16 melanoma 4A5 cells by inhibition of glucose transmembrane transport. Cancer Lett 119: 207-212.
69. Porporato PE, Dhup S, Dadhich RK, Copetti T, Sonveaux P (2011) Anticancer targets in the glycolytic metabolism of tumors: a comprehensive review. Front Pharmacol 2: 49.
70. Tennant DA, Duran RV, Gottlieb E (2010) Targeting metabolic transformation for cancer therapy. Nat Rev Cancer 10: 267-277.
71. Ko YH, Verhoeven HA, Lee MJ, Corbin DJ, Vogl TJ, Pedersen PL (2012) A translational study "case report" on the small molecule "energy blocker" 3-bromopyruvate (3BP) as a potent anticancer agent: from bench side to bedside. J Bioenerg Biomembr 44: 163-170.
72. Ko YH, Smith BL, Wang Y, Pomper MG, Rini DA, Torbenson MS, Hullihen J, Pedersen PL (2004) Advanced cancers: eradication in all cases using 3-bromopyruvate therapy to deplete ATP. Biochem Biophys Res Commun 324: 269-275.
73. Biolato M, Marrone G, Racco S, Di Stasi C, Miele L, Gasbarrini G, Landolfi R, Grieco A (2010) Transarterial chemoembolization (TACE) for unresectable HCC: a new life begins? Eur Rev Med Pharmacol Sci 14: 356-362.
74. DeBerardinis RJ, Mancuso A, Daikhin E, Nissim I, Yudkoff M, Wehrli S, Thompson CB (2007) Beyond aerobic glycolysis: transformed cells can engage in glutamine metabolism that exceeds the requirement for protein and nucleotide synthesis. Proc Natl Acad Sci U S A 104: 19345-19350.
75. Hutson SM, Sweatt AJ, Lanoue KF (2005) Branched-chain [corrected] amino acid metabolism: implications for establishing safe intakes. J Nutr 135: 1557S-1564S.
76. Gupta V, Bamezai RN (2010) Human pyruvate kinase M2: a multifunctional protein. Protein Sci 19: 2031-2044.
77. Takenaka M, Noguchi T, Sadahiro S, Hirai H, Yamada K, Matsuda T, Imai E, Tanaka T (1991) Isolation and characterization of the human pyruvate kinase M gene. Eur J Biochem 198: 101-106.
78. Noguchi T, Inoue H, Tanaka T (1986) The M1- and M2-type isozymes of rat pyruvate kinase are produced from the same gene by alternative RNA splicing. J Biol Chem 261: 13807-13812.
79. Munoz ME, Ponce E (2003) Pyruvate kinase: current status of regulatory and functional properties. Comp Biochem Physiol B Biochem Mol Biol 135: 197-218.
80. Wong N, De Melo J, Tang D (2013) PKM2, a Central Point of Regulation in Cancer Metabolism. Int J Cell Biol 2013: 242513.
81. Imamura K, Tanaka T (1972) Multimolecular forms of pyruvate kinase from rat and other mammalian tissues. I. Electrophoretic studies. J Biochem 71: 1043-1051.

82. Mazurek S (2011) Pyruvate kinase type M2: a key regulator of the metabolic budget system in tumor cells. Int J Biochem Cell Biol 43: 969-980.
83. Anastasiou D, Yu Y, Israelsen WJ, Jiang JK, Boxer MB, Hong BS, Tempel W, Dimov S, Shen M, Jha A, Yang H, Mattaini KR, Metallo CM, Fiske BP, Courtney KD, Malstrom S, Khan TM, Kung C, Skoumbourdis AP, Veith H, Southall N, Walsh MJ, Brimacombe KR, Leister W, Lunt SY, Johnson ZR, Yen KE, Kunii K, Davidson SM, Christofk HR, Austin CP, Inglese J, Harris MH, Asara JM, Stephanopoulos G, Salituro FG, Jin S, Dang L, Auld DS, Park HW, Cantley LC, Thomas CJ, Vander Heiden MG (2012) Pyruvate kinase M2 activators promote tetramer formation and suppress tumorigenesis. Nat Chem Biol 8: 839-847.
84. Christofk HR, Vander Heiden MG, Harris MH, Ramanathan A, Gerszten RE, Wei R, Fleming MD, Schreiber SL, Cantley LC (2008) The M2 splice isoform of pyruvate kinase is important for cancer metabolism and tumour growth. Nature 452: 230-233.
85. Lv L, Li D, Zhao D, Lin R, Chu Y, Zhang H, Zha Z, Liu Y, Li Z, Xu Y, Wang G, Huang Y, Xiong Y, Guan KL, Lei QY (2011) Acetylation targets the M2 isoform of pyruvate kinase for degradation through chaperone-mediated autophagy and promotes tumor growth. Mol Cell 42: 719-730.
86. Hitosugi T, Kang S, Vander Heiden MG, Chung TW, Elf S, Lythgoe K, Dong S, Lonial S, Wang X, Chen GZ, Xie J, Gu TL, Polakiewicz RD, Roesel JL, Boggon TJ, Khuri FR, Gilliland DG, Cantley LC, Kaufman J, Chen J (2009) Tyrosine phosphorylation inhibits PKM2 to promote the Warburg effect and tumor growth. Sci Signal 2: ra73.
87. Christofk HR, Vander Heiden MG, Wu N, Asara JM, Cantley LC (2008) Pyruvate kinase M2 is a phosphotyrosine-binding protein. Nature 452: 181-186.
88. Ashizawa K, Willingham MC, Liang CM, Cheng SY (1991) In vivo regulation of monomer-tetramer conversion of pyruvate kinase subtype M2 by glucose is mediated via fructose 1,6-bisphosphate. J Biol Chem 266: 16842-16846.
89. Israelsen WJ, Dayton TL, Davidson SM, Fiske BP, Hosios AM, Bellinger G, Li J, Yu Y, Sasaki M, Horner JW, Burga LN, Xie J, Jurczak MJ, DePinho RA, Clish CB, Jacks T, Kibbey RG, Wulf GM, Di Vizio D, Mills GB, Cantley LC, Vander Heiden MG (2013) PKM2 isoform-specific deletion reveals a differential requirement for pyruvate kinase in tumor cells. Cell 155: 397-409.
90. Walsh MJ, Brimacombe KR, Anastasiou D, Yu Y, Israelsen WJ, Hong BS, Tempel W, Dimov S, Veith H, Yang H, Kung C, Yen KE, Dang L, Salituro F, Auld DS, Park HW, Vander Heiden MG, Thomas CJ, Shen M, Boxer MB (2010) ML265: A potent PKM2 activator induces tetramerization and reduces tumor formation and size in a mouse xenograft modelProbe Reports from the NIH Molecular Libraries Program, Bethesda (MD).
91. Parnell KM, Foulks JM, Nix RN, Clifford A, Bullough J, Luo B, Senina A, Vollmer D, Liu J, McCarthy V, Xu Y, Saunders M, Liu XH, Pearce S, Wright K, O'Reilly M, McCullar MV, Ho KK, Kanner SB (2013) Pharmacologic activation of PKM2 slows lung tumor xenograft growth. Mol Cancer Ther 12: 1453-1460.

92. Michelakis ED, Webster L, Mackey JR (2008) Dichloroacetate (DCA) as a potential metabolic-targeting therapy for cancer. Br J Cancer 99: 989-994.
93. Sutendra G, Michelakis ED (2014) The metabolic basis of pulmonary arterial hypertension. Cell Metab 19: 558-573.
94. Michelakis ED, Sutendra G, Dromparis P, Webster L, Haromy A, Niven E, Maguire C, Gammer TL, Mackey JR, Fulton D, Abdulkarim B, McMurtry MS, Petruk KC (2010) Metabolic modulation of glioblastoma with dichloroacetate. Sci Transl Med 2: 31ra34.
95. Bowker-Kinley MM, Davis WI, Wu P, Harris RA, Popov KM (1998) Evidence for existence of tissue-specific regulation of the mammalian pyruvate dehydrogenase complex. Biochem J 329 (Pt 1): 191-196.
96. Stacpoole PW (1989) The pharmacology of dichloroacetate. Metabolism 38: 1124-1144.
97. Bonnet S, Archer SL, Allalunis-Turner J, Haromy A, Beaulieu C, Thompson R, Lee CT, Lopaschuk GD, Puttagunta L, Harry G, Hashimoto K, Porter CJ, Andrade MA, Thebaud B, Michelakis ED (2007) A mitochondria-K+ channel axis is suppressed in cancer and its normalization promotes apoptosis and inhibits cancer growth. Cancer Cell 11: 37-51.
98. Stacpoole PW, Moore GW, Kornhauser DM (1978) Metabolic effects of dichloroacetate in patients with diabetes mellitus and hyperlipoproteinemia. N Engl J Med 298: 526-530.
99. Stacpoole PW, Wright EC, Baumgartner TG, Bersin RM, Buchalter S, Curry SH, Duncan CA, Harman EM, Henderson GN, Jenkinson S, et al. (1992) A controlled clinical trial of dichloroacetate for treatment of lactic acidosis in adults. The Dichloroacetate-Lactic Acidosis Study Group. N Engl J Med 327: 1564-1569.
100. Stacpoole PW, Kerr DS, Barnes C, Bunch ST, Carney PR, Fennell EM, Felitsyn NM, Gilmore RL, Greer M, Henderson GN, Hutson AD, Neiberger RE, O'Brien RG, Perkins LA, Quisling RG, Shroads AL, Shuster JJ, Silverstein JH, Theriaque DW, Valenstein E (2006) Controlled clinical trial of dichloroacetate for treatment of congenital lactic acidosis in children. Pediatrics 117: 1519-1531.
101. McMurtry MS, Bonnet S, Wu X, Dyck JR, Haromy A, Hashimoto K, Michelakis ED (2004) Dichloroacetate prevents and reverses pulmonary hypertension by inducing pulmonary artery smooth muscle cell apoptosis. Circ Res 95: 830-840.
102. Krishna S, Supanaranond W, Pukrittayakamee S, Kuile FT, Ruprah M, White NJ (1996) The disposition and effects of two doses of dichloroacetate in adults with severe falciparum malaria. Br J Clin Pharmacol 41: 29-34.
103. Bersin RM, Wolfe C, Kwasman M, Lau D, Klinski C, Tanaka K, Khorrami P, Henderson GN, de Marco T, Chatterjee K (1994) Improved hemodynamic function and mechanical efficiency in congestive heart failure with sodium dichloroacetate. J Am Coll Cardiol 23: 1617-1624.
104. Calvert LD, Shelley R, Singh SJ, Greenhaff PL, Bankart J, Morgan MD, Steiner MC (2008) Dichloroacetate enhances performance and reduces blood lactate during maximal cycle exercise in chronic obstructive pulmonary disease. Am J Respir Crit Care Med 177: 1090-1094.

105. Stacpoole PW (1969) Review of the pharmacologic and therapeutic effects of diisopropylammonium dichloroacetate (DIPA). J Clin Pharmacol J New Drugs 9: 282-291.
106. Holloway PA, Knox K, Bajaj N, Chapman D, White NJ, O'Brien R, Stacpoole PW, Krishna S (1995) Plasmodium berghei infection: dichloroacetate improves survival in rats with lactic acidosis. Exp Parasitol 80: 624-632.
107. Cao W, Yacoub S, Shiverick KT, Namiki K, Sakai Y, Porvasnik S, Urbanek C, Rosser CJ (2008) Dichloroacetate (DCA) sensitizes both wild-type and over expressing Bcl-2 prostate cancer cells in vitro to radiation. Prostate 68: 1223-1231.
108. Sanchez-Arago M, Chamorro M, Cuezva JM (2010) Selection of cancer cells with repressed mitochondria triggers colon cancer progression. Carcinogenesis 31: 567-576.
109. Madhok BM, Yeluri S, Perry SL, Hughes TA, Jayne DG (2010) Dichloroacetate induces apoptosis and cell-cycle arrest in colorectal cancer cells. Br J Cancer 102: 1746-1752.
110. Sebastian C, Zwaans BM, Silberman DM, Gymrek M, Goren A, Zhong L, Ram O, Truelove J, Guimaraes AR, Toiber D, Cosentino C, Greenson JK, MacDonald AI, McGlynn L, Maxwell F, Edwards J, Giacosa S, Guccione E, Weissleder R, Bernstein BE, Regev A, Shiels PG, Lombard DB, Mostoslavsky R (2012) The histone deacetylase SIRT6 is a tumor suppressor that controls cancer metabolism. Cell 151: 1185-1199.
111. Xuan Y, Hur H, Ham IH, Yun J, Lee JY, Shim W, Bae Kim Y, Lee G, Han SU, Kwan Cho Y (2013) Dichloroacetate attenuates hypoxia-induced resistance to 5-fluorouracil in gastric cancer through the regulation of glucose metabolism. Exp Cell Res.
112. Wong JY, Huggins GS, Debidda M, Munshi NC, De Vivo I (2008) Dichloroacetate induces apoptosis in endometrial cancer cells. Gynecol Oncol 109: 394-402.
113. Kumar K, Wigfield S, Gee HE, Devlin CM, Singleton D, Li JL, Buffa F, Huffman M, Sinn AL, Silver J, Turley H, Leek R, Harris AL, Ivan M (2013) Dichloroacetate reverses the hypoxic adaptation to bevacizumab and enhances its antitumor effects in mouse xenografts. J Mol Med (Berl) 91: 749-758.
114. Vella S, Conti M, Tasso R, Cancedda R, Pagano A (2012) Dichloroacetate inhibits neuroblastoma growth by specifically acting against malignant undifferentiated cells. Int J Cancer 130: 1484-1493.
115. Kumar A, Kant S, Singh SM (2012) Novel molecular mechanisms of antitumor action of dichloroacetate against T cell lymphoma: Implication of altered glucose metabolism, pH homeostasis and cell survival regulation. Chem Biol Interact 199: 29-37.
116. Flavin DF (2010) Non-Hodgkin's Lymphoma Reversal with Dichloroacetate. J Oncol 2010.
117. Ishiguro T, Ishiguro R, Ishiguro M, Iwai S (2012) Co-treatment of dichloroacetate, omeprazole and tamoxifen exhibited synergistically antiproliferative effect on malignant tumors: in vivo experiments and a case report. Hepatogastroenterology 59: 994-996.

118. Sun RC, Fadia M, Dahlstrom JE, Parish CR, Board PG, Blackburn AC (2010) Reversal of the glycolytic phenotype by dichloroacetate inhibits metastatic breast cancer cell growth in vitro and in vivo. Breast Cancer Res Treat 120: 253-260.
119. Kaluzova M, Kaluz S, Lerman MI, Stanbridge EJ (2004) DNA damage is a prerequisite for p53-mediated proteasomal degradation of HIF-1alpha in hypoxic cells and downregulation of the hypoxia marker carbonic anhydrase IX. Mol Cell Biol 24: 5757-5766.
120. Kaplon J, Zheng L, Meissl K, Chaneton B, Selivanov VA, Mackay G, van der Burg SH, Verdegaal EM, Cascante M, Shlomi T, Gottlieb E, Peeper DS (2013) A key role for mitochondrial gatekeeper pyruvate dehydrogenase in oncogene-induced senescence. Nature 498: 109-112.
121. Dunbar EM, Coats BS, Shroads AL, Langaee T, Lew A, Forder JR, Shuster JJ, Wagner DA, Stacpoole PW (2013) Phase 1 trial of dichloroacetate (DCA) in adults with recurrent malignant brain tumors. Invest New Drugs.
122. Abdelmalak M, Lew A, Ramezani R, Shroads AL, Coats BS, Langaee T, Shankar MN, Neiberger RE, Subramony SH, Stacpoole PW (2013) Long-term safety of dichloroacetate in congenital lactic acidosis. Mol Genet Metab 109: 139-143.
123. Dhar S, Lippard SJ (2009) Mitaplatin, a potent fusion of cisplatin and the orphan drug dichloroacetate. Proc Natl Acad Sci U S A 106: 22199-22204.
124. Morfouace M, Lalier L, Bahut M, Bonnamain V, Naveilhan P, Guette C, Oliver L, Gueguen N, Reynier P, Vallette FM (2012) Comparison of spheroids formed by rat glioma stem cells and neural stem cells reveals differences in glucose metabolism and promising therapeutic applications. J Biol Chem 287: 33664-33674.
125. Markert CL, Shaklee JB, Whitt GS (1975) Evolution of a gene. Multiple genes for LDH isozymes provide a model of the evolution of gene structure, function and regulation. Science 189: 102-114.
126. Koukourakis MI, Giatromanolaki A, Sivridis E, Bougioukas G, Didilis V, Gatter KC, Harris AL (2003) Lactate dehydrogenase-5 (LDH-5) overexpression in non-small-cell lung cancer tissues is linked to tumour hypoxia, angiogenic factor production and poor prognosis. Br J Cancer 89: 877-885.
127. Leiblich A, Cross SS, Catto JW, Phillips JT, Leung HY, Hamdy FC, Rehman I (2006) Lactate dehydrogenase-B is silenced by promoter hypermethylation in human prostate cancer. Oncogene 25: 2953-2960.
128. Koukourakis MI, Giatromanolaki A, Sivridis E, Gatter KC, Trarbach T, Folprecht G, Shi MM, Lebwohl D, Jalava T, Laurent D, Meinhardt G, Harris AL (2011) Prognostic and predictive role of lactate dehydrogenase 5 expression in colorectal cancer patients treated with PTK787/ZK 222584 (vatalanib) antiangiogenic therapy. Clin Cancer Res 17: 4892-4900.
129. Koukourakis MI, Giatromanolaki A, Winter S, Leek R, Sivridis E, Harris AL (2009) Lactate dehydrogenase 5 expression in squamous cell head and neck cancer relates to prognosis following radical or postoperative radiotherapy. Oncology 77: 285-292.

130. Fantin VR, St-Pierre J, Leder P (2006) Attenuation of LDH-A expression uncovers a link between glycolysis, mitochondrial physiology, and tumor maintenance. Cancer Cell 9: 425-434.
131. Le A, Cooper CR, Gouw AM, Dinavahi R, Maitra A, Deck LM, Royer RE, Vander Jagt DL, Semenza GL, Dang CV (2010) Inhibition of lactate dehydrogenase A induces oxidative stress and inhibits tumor progression. Proc Natl Acad Sci U S A 107: 2037-2042.
132. Granchi C, Roy S, Giacomelli C, Macchia M, Tuccinardi T, Martinelli A, Lanza M, Betti L, Giannaccini G, Lucacchini A, Funel N, Leon LG, Giovannetti E, Peters GJ, Palchaudhuri R, Calvaresi EC, Hergenrother PJ, Minutolo F (2011) Discovery of N-hydroxyindole-based inhibitors of human lactate dehydrogenase isoform A (LDH-A) as starvation agents against cancer cells. J Med Chem 54: 1599-1612.
133. Maftouh M, Avan A, Sciarrillo R, Granchi C, Leon LG, Rani R, Funel N, Smid K, Honeywell R, Boggi U, Minutolo F, Peters GJ, Giovannetti E (2014) Synergistic interaction of novel lactate dehydrogenase inhibitors with gemcitabine against pancreatic cancer cells in hypoxia. Br J Cancer.
134. Golman K, Zandt RI, Lerche M, Pehrson R, Ardenkjaer-Larsen JH (2006) Metabolic imaging by hyperpolarized 13C magnetic resonance imaging for in vivo tumor diagnosis. Cancer Res 66: 10855-10860.
135. Dutta P, Le A, Vander Jagt DL, Tsukamoto T, Martinez GV, Dang CV, Gillies RJ (2013) Evaluation of LDH-A and glutaminase inhibition in vivo by hyperpolarized 13C-pyruvate magnetic resonance spectroscopy of tumors. Cancer Res 73: 4190-4195.
136. Hill DK, Orton MR, Mariotti E, Boult JK, Panek R, Jafar M, Parkes HG, Jamin Y, Miniotis MF, Al-Saffar NM, Beloueche-Babari M, Robinson SP, Leach MO, Chung YL, Eykyn TR (2013) Model free approach to kinetic analysis of real-time hyperpolarized 13C magnetic resonance spectroscopy data. PLoS One 8: e71996.
137. Wang F, Travins J, DeLaBarre B, Penard-Lacronique V, Schalm S, Hansen E, Straley K, Kernytsky A, Liu W, Gliser C, Yang H, Gross S, Artin E, Saada V, Mylonas E, Quivoron C, Popovici-Muller J, Saunders JO, Salituro FG, Yan S, Murray S, Wei W, Gao Y, Dang L, Dorsch M, Agresta S, Schenkein DP, Biller SA, Su SM, de Botton S, Yen KE (2013) Targeted inhibition of mutant IDH2 in leukemia cells induces cellular differentiation. Science 340: 622-626.
138. Rohle D, Popovici-Muller J, Palaskas N, Turcan S, Grommes C, Campos C, Tsoi J, Clark O, Oldrini B, Komisopoulou E, Kunii K, Pedraza A, Schalm S, Silverman L, Miller A, Wang F, Yang H, Chen Y, Kernytsky A, Rosenblum MK, Liu W, Biller SA, Su SM, Brennan CW, Chan TA, Graeber TG, Yen KE, Mellinghoff IK (2013) An inhibitor of mutant IDH1 delays growth and promotes differentiation of glioma cells. Science 340: 626-630.
139. Fathi AT, Sadrzadeh H, Borger DR, Ballen KK, Amrein PC, Attar EC, Foster J, Burke M, Lopez HU, Matulis CR, Edmonds KM, Iafrate AJ, Straley KS, Yen KE, Agresta S, Schenkein DP, Hill C, Emadi A, Neuberg DS, Stone RM, Chen YB (2012) Prospective serial evaluation of 2-hydroxyglutarate, during

treatment of newly diagnosed acute myeloid leukemia, to assess disease activity and therapeutic response. Blood 120: 4649-4652.
140. Folmes CD, Nelson TJ, Martinez-Fernandez A, Arrell DK, Lindor JZ, Dzeja PP, Ikeda Y, Perez-Terzic C, Terzic A (2011) Somatic oxidative bioenergetics transitions into pluripotency-dependent glycolysis to facilitate nuclear reprogramming. Cell Metab 14: 264-271.
141. Xu X, Duan S, Yi F, Ocampo A, Liu GH, Izpisua Belmonte JC (2013) Mitochondrial regulation in pluripotent stem cells. Cell Metab 18: 325-332.
142. Varum S, Rodrigues AS, Moura MB, Momcilovic O, Easley CAt, Ramalho-Santos J, Van Houten B, Schatten G (2011) Energy metabolism in human pluripotent stem cells and their differentiated counterparts. PLoS One 6: e20914.
143. Ye XQ, Li Q, Wang GH, Sun FF, Huang GJ, Bian XW, Yu SC, Qian GS (2011) Mitochondrial and energy metabolism-related properties as novel indicators of lung cancer stem cells. Int J Cancer 129: 820-831.
144. Vega-Naredo I, Loureiro R, Mesquita KA, Barbosa IA, Tavares LC, Branco AF, Erickson JR, Holy J, Perkins EL, Carvalho RA, Oliveira PJ (2014) Mitochondrial metabolism directs stemness and differentiation in P19 embryonal carcinoma stem cells. Cell Death Differ 21: 1560-1574.
145. Figueroa ME, Abdel-Wahab O, Lu C, Ward PS, Patel J, Shih A, Li Y, Bhagwat N, Vasanthakumar A, Fernandez HF, Tallman MS, Sun Z, Wolniak K, Peeters JK, Liu W, Choe SE, Fantin VR, Paietta E, Lowenberg B, Licht JD, Godley LA, Delwel R, Valk PJ, Thompson CB, Levine RL, Melnick A (2010) Leukemic IDH1 and IDH2 mutations result in a hypermethylation phenotype, disrupt TET2 function, and impair hematopoietic differentiation. Cancer Cell 18: 553-567.
146. Minucci S, Pelicci PG (2006) Histone deacetylase inhibitors and the promise of epigenetic (and more) treatments for cancer. Nat Rev Cancer 6: 38-51.
147. Lee JV, Carrer A, Shah S, Snyder NW, Wei S, Venneti S, Worth AJ, Yuan ZF, Lim HW, Liu S, Jackson E, Aiello NM, Haas NB, Rebbeck TR, Judkins A, Won KJ, Chodosh LA, Garcia BA, Stanger BZ, Feldman MD, Blair IA, Wellen KE (2014) Akt-Dependent Metabolic Reprogramming Regulates Tumor Cell Histone Acetylation. Cell Metab.
148. Wellen KE, Hatzivassiliou G, Sachdeva UM, Bui TV, Cross JR, Thompson CB (2009) ATP-citrate lyase links cellular metabolism to histone acetylation. Science 324: 1076-1080.
149. Mullen AR, Wheaton WW, Jin ES, Chen PH, Sullivan LB, Cheng T, Yang Y, Linehan WM, Chandel NS, DeBerardinis RJ (2012) Reductive carboxylation supports growth in tumour cells with defective mitochondria. Nature 481: 385-388.
150. Sutendra G, Kinnaird A, Dromparis P, Paulin R, Stenson TH, Haromy A, Hashimoto K, Zhang N, Flaim E, Michelakis ED (2014) A Nuclear Pyruvate Dehydrogenase Complex Is Important for the Generation of Acetyl-CoA and Histone Acetylation. Cell 158: 84-97.
151. Chueh FY, Leong KF, Cronk RJ, Venkitachalam S, Pabich S, Yu CL (2011) Nuclear localization of pyruvate dehydrogenase complex-E2 (PDC-E2), a

mitochondrial enzyme, and its role in signal transducer and activator of transcription 5 (STAT5)-dependent gene transcription. Cellular signalling 23: 1170-1178.

Chapter Two

Metabolic Modulation of Clear Cell Renal Cell Carcinoma with Dichloroacetate, an Inhibitor of Pyruvate Dehydrogenase Kinase

Abstract

Background: Clear cell renal cell carcinoma (ccRCC) exhibits suppressed mitochondrial function and preferential use of glycolysis even in normoxia, promoting proliferation and suppressing apoptosis. ccRCC's resistance to therapy is driven by a constitutive HIF expression (due to a genetic loss of VHL). In addition to promoting angiogenesis, HIF suppresses mitochondrial function by inducing Pyruvate Dehydrogenase Kinase (PDK), a glucose oxidation-gatekeeping mitochondrial enzyme.

Objective: To reverse the mitochondrial suppression of ccRCC using the PDK inhibitor Dichloroacetate (DCA).

Design, setting, and participants: Radical nephrectomy specimens from patients with ccRCC were assessed for PDK expression. The 786-O ccRCC line and two animal models (chicken in ovo and murine xenografts) were used for mechanistic studies.

Outcome measurements and statistical analysis: Mitochondrial function, proliferation, apoptosis, HIF transcriptional activity, angiogenesis and tumor size were measured in vitro and in vivo. Independent samples t-test and ANOVA were used.

Results: PDK was elevated in ccRCC compared to normal kidney tissues from the same patients, as well as in 786-O cells. DCA reactivated mitochondrial function [increased: respiration, Krebs' cycle metabolites like α-ketoglutarate -a cofactor of Factor Inhibiting HIF (FIH)-, mitochondrial reactive oxygen species] increased p53 activity and apoptosis, while decreasing proliferation in 786-O cells. DCA reduced HIF transcriptional activity in a FIH-dependent manner, inhibiting angiogenesis in vitro. In vivo, DCA reduced tumor size and angiogenesis in both animal models.

Conclusions: DCA can reverse the mitochondrial suppression of ccRCC and decrease HIF's

transcriptional activity, “bypassing” its constitutive expression. Its previous clinical use in humans makes it an attractive candidate for translation to ccRCC patients.

Patient Summary: We show that an energy-boosting drug decreases tumor growth and tumor blood vessels in animals carrying human kidney cancer cells. This generic drug has been used in patients for other conditions and thus could be tested in kidney cancer that remains incurable.

Introduction

Renal Cell Carcinoma (RCC) affects more than 270,000 patients annually worldwide but remains deadly and resistant to radiation and chemotherapies (1). Current treatments with vascular endothelial growth factor (VEGF), platelet-derived growth factor (PDGF), and mammalian target of rapamycin (mTOR) antibodies and inhibitors, despite improving progression free survival, rarely provide a durable response (2). The most common subtype of RCC, clear cell (ccRCC), exhibits loss-of-function mutations or gene silencing of the von Hippel-Lindau (VHL) factor in 70-90% of patients, which leads to elevated levels of hypoxia inducible factor (HIF), even in normoxia, due to the inhibition of the prolyl-hydroxylase-dependent proteasome machinery that normally destabilizes HIF (3-5). In addition to directly promoting angiogenesis by the induction of several pro-angiogenic genes, HIF upregulates many enzymes of cytoplasmic glycolysis and a suppression of mitochondrial glucose oxidation, in part by up-regulation of its gate-keeping enzyme Pyruvate Dehydrogenase Kinase (PDK) (6-8). This normoxic suppression of mitochondrial function, known as the Warburg Effect, promotes suppression of mitochondrial-dependent apoptosis, as well as a shift of carbohydrates toward biomass biosynthesis, in part via the pentose phosphate pathway (since they are no longer oxidized in mitochondria) (9-11). In addition, this suppression leads to a decrease in the production of Krebs' cycle metabolites such as α-ketoglutarate (αKG), and mitochondrial reactive oxygen species (mROS) generation from the electron transport chain. Both are diffusible and their decrease can have secondary tumor promoting biologic effects, including the inhibition of the redox-sensitive transcription factor p53, further promoting proliferation and resistance to apoptosis (10, 12).

Thus, in ccRCC the activation of HIF underlies the strong pro-angiogenic and, largely through mitochondrial suppression, the anti-apoptotic and pro-proliferative environment as well. However, the presence of a genetic trigger for the stability of HIF (i.e. VHL loss) limits the pharmacologic therapy options, although there are early efforts for the development of small molecule HIF inhibitors (13, 14). The essentially constitutive activation of HIF in normoxia is a

constant driver of the metabolic downstream effects and the angiogenic products, perhaps explaining the long-term failure of essentially all ccRCC therapies.

While HIF does not get ubiquitinated in the absence of VHL, its transcriptional activity can still be inhibited by other pathways. For example, Factor Inhibiting HIF (FIH) hydroxylates HIF at a site different than the prolyl-hydroxylases (that promote its ubiquitination), preventing its DNA binding onto "hypoxia response elements". FIH is linked to mitochondrial function since it requires αKG as a co-factor. Thus, the decrease in the levels of αKG would inhibit the function of FIH, removing this potential "defense" to the activation of HIF. Another way to inhibit HIF's transcriptional activity may be the activation of p53 (which is inhibited by suppressed mitochondria) (15), since they both compete for p300, a cofactor for the transcriptional machinery of both p53 and HIF (16). A promising ccRCC therapy may be a mitochondrial activator that, in addition to promoting apoptosis and suppressing non-HIF-driven pathways, via an increase in αKG, or activation of p53, may also inhibit HIF function. Such a therapy will be more attractive if it is a small molecule with an acceptable toxicity profile in humans. The objective of this study was to reverse the mitochondrial suppression of ccRCC using Dichloroacetate (DCA), a small molecule that has several of these properties. Our group and others have previously shown that by inhibiting PDK, DCA is a potent mitochondrial activator with anti-tumor activity in several solid tumors (10, 17-20). We report that by inhibiting PDK, DCA activates pyruvate dehydrogenase (PDH) and thus increases the flux of pyruvate into mitochondria in ccRCC. This leads to an increase in the production of Krebs' cycle metabolites such as αKG and mROS, activating p53 and inhibiting tumor growth in vitro and in vivo. We also show that DCA inhibits HIF's transcriptional activity and decreases angiogenesis in ccRCC, and propose an αKG and FIH-dependent mechanism.

Results

2.1 Pyruvate Dehydrogenase Kinase is up-regulated in ccRCC.

We compared PDK levels in ccRCC versus normal kidney cells at the tissue and cellular level. We used radical nephrectomy surgical specimens that were handled in an identical manner for both the tumor (ccRCC) and the non-cancer kidney tissue as part of a prospective tissue registry. This allowed us to directly compare the levels of PDK in the tumor and normal tissue from the same patient, minimizing potentially confounding differential effects on PDK levels. The age, tumor grade and stage of the patients is shown in the inset of Figure 2-1A.We found a significant increase in PDK1 levels in the tumor compared to normal tissues at both the protein level (confocal immunohistochemistry) and the mRNA level (qRT-PCR). While there was not a significant increase in the PDK2 isoform, there was also an increase in the PDK4 isoform (of the four PDK isoforms, PDK3 expression is typically restricted in the testis) (Figures 3-1A and 3-2A). Similarly, the commonly studied human 786-O ccRCC cell line, which lacks functional VHL and shows a sustained expression of HIF (mostly HIF2α), expresses significantly more PDK1 and 4 compared to a human proximal tubule cell line, i.e. the cell type from which ccRCC is derived (Figures 3-1B and 3-2B).

2.2 DCA increases PDH activity and Mitochondrial Function.

We studied the effects of PDK inhibition by DCA in ccRCC cells (Figure 2-3A). DCA decreased the PDK-mediated Serine 293 phosphorylation of PDH (Figure 2-3B), causing an increase in PDH activity, measured by a standard immunocapture dipstick assay (Figure 2-3C). Since activated PDH causes a shift to pyruvate metabolism away from lactate and toward acetyl-CoA, which enters and drives the Krebs' cycle, we found an increase in acetyl-CoA levels in the DCA-treated cells. To ensure that the measured acetyl-CoA is only derived from pyruvate we used mass spectrometry and measured the levels of ^{13}C isotope-labeled acetyl-CoA in cells grown in the presence of ^{13}C isotope-labeled pyruvate (Figure 2-3D). Accordingly, we also found a decrease in both pyruvate and lactate levels in the DCA treated cells (Figure 2-3E). The predicted activation of the Krebs' cycle was confirmed by increased levels of the Krebs' cycle

intermediates oxaloacetate, succinate and fumarate, measured by mass spectroscopy (Figure 2-4A). More importantly, the overall increase in mitochondrial function was shown by an increase in respiration of the DCA-treated cells (Figure 2-3F).

We have previously shown that cancer cells (glioblastoma, lung and breast cancer) have increased mitochondrial membrane potential and decreased production of mROS, i.e superoxide, when compared to normal matching epithelial cells (17). We used the mitochondria-specific membrane potential and ROS-sensitive dyes TMRM and MitoSox and now showed that this is also true in ccRCC cells, which exhibit increased mitochondrial membrane potential and decreased mROS production compared to proximal tubule cells. DCA reversed the mitochondrial suppression of ccRCC cells, decreasing the membrane potential and increasing mROS levels (Figure 2-3G). Since an increase in mitochondrial membrane potential and a decrease in mROS is thought to facilitate a state of resistance to mitochondrial driven apoptosis, these effects of DCA may unlock cancer cells from apoptosis-resistance (11, 12). DCA may restore the mitochondrial activity that is required for apoptosis (an energy-dependent process) and this is in keeping with its lack of effects on normal cells, which already have normal mitochondrial function (perhaps in part because of their much lower expression of PDK). Accordingly, DCA did not alter the mitochondrial membrane potential nor mROS levels in the normal proximal tubule cells, which have a lower mitochondrial potential and higher levels of mROS than the ccRCC cells at baseline (Figure 2-3G).

We then studied 786-O ccRCC cells stably transfected with VHL (+VHL 786-O cells (21)) and found that DCA does not alter mitochondrial function (i.e. respiration) in these cells, which do not express HIF2α in normoxia (Figure 2-4B). The lack of DCA effects suggests that its mitochondrial effects in 786-O cells depend largely on the expression of HIF. Thus, we studied the mechanism by which DCA may modulate HIF function in ccRCC.

2.3 DCA inhibits ccRCC HIF activity and decreases angiogenesis in vitro.

As expected, DCA does not reduce the levels of HIF2α protein expression in ccRCC cells, since the main regulatory mechanism, i.e. ubiquitination and degradation by the

proteasome, requires VHL which is absent in VHL-deficient 786-O ccRCA cells (Figure 2-5A). Despite this, DCA decreased the expression of the HIF responsive genes VEGF and PDGF (Figure 2-5B) (22), suggesting that DCA may inhibit HIF's transcriptional activity. This was confirmed by a direct measurement of HIF's transcriptional activity using a widely used dual reporter luciferase assay (Figure 2-5B). There are two ways that HIF's transcriptional activity can be inhibited even in a state of constitutive HIF protein expression (Figure 2-5C):

a) Activation of p53: as p53 and HIF transcriptional machineries compete for the same cofactor (i.e. p300), loss of p53 promotes HIF activation (16). The inhibition of p53 can actually be caused by a suppression of mitochondria-driven redox signals, like a decrease in mROS followed, in the presence of MnSOD, by a decrease in the more stable and diffusible mROS, H_2O, which is known to activate p53 (10, 15, 23).

b) Inhibition of FIH: this αKG-dependent hydroxylase, hydroxylates HIF and prevents its binding to DNA (24). Thus, a lack of αKG due to the suppressed Krebs' cycle activity may suppress FIH further contributing to the enhanced HIF transcription in cancer, although this has not been studied in ccRCC. Nevertheless, in ccRCC tissues, inhibited FIH is a strong independent predictor of poor survival (25).

DCA increased the overall expression, nuclear localization, and transcriptional activity of p53 in ccRCC cells, measured by immunoblot, confocal microscopy and a dual reporter luciferase assay (Figure 2-6). In keeping with increased p53 activity, p21 (a downstream p53 target) was significantly increased by DCA treatment (Figure 2-6B). Furthermore, DCA increased the co-localization coefficient of p53 with its cofactor p300, while reducing the co-localization coefficient of HIF2α with p300 (Figure 2-7). The pro-carcinogenic effects of p53 inhibition are broad and include inhibition of mitochondrial complexes and activation of glycolysis (23). They also promote a shift toward the pentose phosphate pathway, a metabolic pathway that is critical to biomass biosynthesis, by directly inhibiting its first enzyme, Glucose-6-Phosphate Dehydrogenase (G6PD) (26). Cells treated with DCA had significantly less 6-phosphogluconolactone (the product of G6PD) as well as lower levels of other PPP intermediates

including the nucleotide precursors Ribulose-5-Phosphate, Ribose-5-Phosphate and NADPH, a co-factor used in many anabolic reactions (Figure 2-6C).

We then studied HIF transcriptional activity using a dual reporter luciferase assay in ccRCC cells treated with FIH siRNA, which effectively decreased the expression of FIH mRNA by more than 90% and increased HIF activity by more than 2.5 fold (Figure 2-8A). However in the absence of FIH, DCA failed to inhibit HIF, suggesting a critical role of FIH in this mechanism (Figure 2-8A). We speculate that DCA increased FIH activity by increasing the levels of αKG, which we confirmed by measuring the production of αKG in ccRCC exposed to DCA (Figure 2-8B). This increase in αKG is in keeping with the increase in other Krebs' cycle metabolites caused by DCA (Figure 2-4A). Our hypothesized model (Figure 2-5C) suggested a dual mechanism for HIF inhibition by DCA. However, the complete inhibition of DCA's effects in the absence of FIH suggests that the primary mechanism is the increase in FIH activity, rather than the activation of p53; although both mechanisms may play a role in different conditions. Nevertheless, p53 activation by DCA may contribute to its overall antitumor effects besides HIF, i.e. limiting proliferation and promoting apoptosis.

We then used an *in vitro* matrigel model for angiogenesis, where the supernatant from ccRCC cells pretreated with DCA versus vehicle (water) is applied to microvascular endothelial cells, and showed that DCA reduced paracrine angiogenic signaling as both metrics of angiogenesis in this assay, complete structures and total tubule length, were significantly reduced (Figure 2-8C). We have previously shown that DCA does not have any direct effects on normal microvascular endothelial cells, suggesting that its effects are mediated by the decrease in the production of pro-angiogenic factors in ccRCC due to HIF inhibition (Figure 2-5B) (10).

2.4 HIF is essential for DCA's effects on ccRCC

Our data presented above emphasized the role of HIF on DCA's effects. We then designed a series of experiments to prove the hypothesis that HIF is indeed essential for the effects of DCA that we studied so far. We used two strategies: a) an effective inhibition of HIF2α using siRNA, which we hypothesized would prevent DCA's effects; and b) a physiologic restoration of HIF by

placing stably expressing VHL cells (that do not express much HIF in normoxia) into hypoxia. Here we hypothesized that the restoration of HIF expression will restore the responsiveness to DCA. Using these strategies we measured the effects of DCA on apoptosis, angiogenesis and mitochondrial respiration.

To explore the essential role of HIF on the response of ccRCC to DCA we studied two strategies, using: (1) HIF2α siRNA (vs. Scrambled) treated –VHL 786-O cells (these cells show constitutive HIF activation due to lack of VHL); and (2) 786-O cells stably transfected with functional VHL (+VHL 786-O cells: this is a rescue phenotype) in hypoxia (vs. normoxia). In other words we used a condition where we artificially inhibited HIF2α (to achieve a 'loss of HIF' state, hypothesizing loss of DCA's effect on the cells lacking HIF), vs. a physiologic induction of HIF (hypoxia) on 786-O cells in which we had genetically replenished VHL (to achieve a 'gain of HIF' state); hypothesizing a gain of DCA's effect on these cells, in which we showed lack of significant DCA effects on respiration (Figure 2-4B). Compared to the –VHL 786-O scrambled RNA-treated cells, -VHL 786-O siHIF2α-treated cells express significantly reduced HIF2α levels (both at the mRNA and protein level), as well as reduced GLUT1 and PDK1 (HIF targets) (Figure 2-9A). In contrast, +VHL 786-O cells placed in hypoxia for 48 hours significantly upregulated HIF2α as well as both HIF targets compared to +VHL cells in normoxia. In both of these strategies, the expression of PDK1 varied accordingly to the amount of HIF (the higher the HIF, the higher the PDK expression) and allowed us to study whether the response to DCA varies accordingly.

We next asked whether the effect of DCA on apoptosis (Figure 2-8B) and angiogenesis (Figure 2-9C) depend on the expression of HIF. Following the above 2 strategies we showed that DCA increased apoptosis and decreased angiogenesis in conditions where HIF2α and PDK1 levels are higher (i.e. –VHL scrambled RNA-treated 786-O cells and hypoxic +VHL 786-O cells). In contrast, DCA does not alter apoptosis and angiogenesis in cells where HIF2α and PDK1 levels are low (siHIF2α –VHL 786-O cells and normoxic +VHL 786-O cells). Similarly, DCA increased respiration in +VHL 786-O cells exposed to hypoxia (high HIF state) while it did not alter respirations in their normoxic controls (low HIF state) (Figures 3-4B and 3-9D).

Taken together, these data suggest that the inhibitory effect of DCA on angiogenesis, apoptosis, and mitochondrial respiration in ccRCC cells requires the presence of HIF activity.

2.5 DCA reduces angiogenesis and tumor growth in vivo in ccRCC

In order to test the effect of DCA on tumor angiogenesis and tumor growth in animals, we used two models: the chick chorioallantoic membrane (CAM) in ovo xenograft and a standard nude mouse xenotransplant model. Compared to the effects of oral DCA in mice, the chick onplant model allows the examination of the direct effects of DCA as the drug is directly applied on the tumor (rather than those of DCA metabolites or indirect effects on other tissues, like circulating cells). It also allows a precise and quantitative assessment of angiogenesis as tumor cells grow on gridded plugs that are placed on the CAM, allowing the direct measurement of vessels in a standardized surface area under microscopy.

Using the *in ovo* xenograft model with ccRCC cells, we tested the effects of DCA on tumor development, using prevention (DCA starting at the day of ccRCC injection for 4 days) and reversal protocols (DCA given 4 days after tumor development and for 4 more days) (Figure 2-10A). In the prevention model, 45% of tumors grew when treated with DCA, compared to 75% of tumors treated with vehicle injections (Figure 2-10B). Of the tumors that did grow in the prevention protocol, those treated with DCA were significantly smaller (18.5 vs. 8.3 mg). In the reversal protocol where DCA was given after measurable tumors were established, DCA reduced the tumor weight (73.8 vs. 17.6 mg).

In a variation of the *in ovo* model, grids carrying wild-type 786-0 cells (which lack functional VHL protein) versus 786-0 cells with a stable transfection of a VHL gene (carrying functional VHL protein and lacking HIF; see Figure 2-4B) were attached in the CAM. DCA versus vehicle (water) was applied directly on the grids once a day for two days and the grids were explanted for assessment of angiogenesis on the third day. The wild type 786-0 cells exhibited an angiogenic index of 69% compared to 35% in transgenic 786-O cells constitutively expressing VHL (Figure 2-10C). DCA treatment reduced the angiogenic index of wild-type 786-O cells to 44%.

In the second model, nude mice were injected with 786-0 cells and tumors were allowed to grow to a mean volume of 40mm^3 prior to initiation of oral DCA treatment (in the drinking water). After 4 weeks, mice receiving DCA had significantly smaller volume tumors (387.8 vs. 152.2 mm^3) as well as significantly lower tumor weights (684.3 vs. 279.1 mg) (Figure 2-11A,B). There were no observable side effects in the DCA treated animals (appetite, grooming, mobility) and throughout the entire treatment course there were no differences in overall mouse weight (Figure 2-11B). Excised tumor tissue stained for ki67 demonstrated a 3-fold reduction in the number of proliferating tumor cells in DCA-treated animals as well as an increase in the number of cells staining positive for TUNEL (Figure 2-11C). These effects on proliferation and apoptosis were not due to the inhibition of angiogenesis alone but also due to direct effects of DCA on the cancer cells, as DCA in cultured wild type 786-0 cells also increased apoptosis (% TUNEL positive cells) and decreased proliferation (% ki67 positive cells) (Figure 2-12). In addition, tumors from DCA-treated mouse xenografts stained less for VEGF and had significantly less vascularity as measured by lectin staining (injected to the animals prior to sacrifice, thus staining perfused vessels), using 3D stereotactically reconstructed images following stacked confocal imaging (Figure 2-11C,D).

Discussion

We showed that the small molecule DCA inhibits a gate-keeping enzyme for glucose oxidation (i.e. PDK) and reverses the mitochondrial suppression in ccRCC, resulting in both reduced angiogenesis and tumor growth in vitro and in vivo in two animal models. Our work supports the emerging evidence that mitochondrial suppression contributes to the apoptosis-resistance and proliferation potential of cancer cells. The novel aspect of our work is that the strong metabolic remodeling in ccRCC (one of the most chemotherapy-resistant tumors) is reversible, despite the fact that perhaps the main driver for this mitochondrial suppression is the sustained expression of HIF due to lack of VHL. The fact that the lack of VHL is mostly based on mutations, makes this metabolic remodeling challenging for pharmacological approaches. We report that this sustained protein expression of HIF, can be "bypassed" by attacking its FIH-dependent transcriptional activity instead. This may make DCA more attractive than angiogenesis inhibitors that target products of HIF (like VEGF).

We, and others, have shown that DCA can reverse the mitochondrial suppression in several tumors, unlocking the cancer cells from a state of resistance to mitochondria-dependent apoptosis (17-20). The target of DCA (i.e. PDK) is up-regulated in ccRCC tumors (as well as in a widely used ccRCC cell line, i.e. 786-O) compared to the normal surrounding kidney from the same patient in radical nephrectomy specimens (27), a finding that we confirmed in our cohort of ccRCC patients (Figure 2-1). Despite being a small molecule, DCA's mechanism of action is quite specific. It inhibits PDK by lodging at a specific site on the protein (confirmed by crystallization models of DCA on the PDK protein), changing its configuration and preventing the phosphorylation of PDH (28). DCA completely mimics effective inhibition of PDK by siRNA, and DCA added to PDK siRNA does not have additional effects (10, 17). The DCA-induced reactivation of mitochondria (Krebs' cycle activity and glucose oxidation) leads to mitochondrial depolarization (facilitating the opening of the voltage-dependent mitochondrial transition pore from where pro-apoptotic mediators like cytochrome c or apoptosis inducing factor leak to induce apoptosis) and an increase in mROS that can promote apoptosis as well (Figure 2-3G) (29). Other mechanisms like a redox-dependent activation of p53 are now

confirmed in RCC as well (Figure 2-6D,E), contributing to DCA's pro-apoptotic and anti-proliferative effects (Figures 3-9, 3-11C, and 3-12) (30). Although the precise role of p53 in ccRCC remains controversial (31), there is evidence that in the majority of ccRCC tumors, p53 is reversibly inhibited. While in other cancers p53 can be inhibited by mitochondrial suppression, this has not been studied directly in ccRCC, but the trigger may not be loss of function mutations (as in many tumors) since the majority of ccRCC tumors do not carry p53 mutations (32, 33). Thus our work provides another mechanism that may contribute to this p53 suppression in ccRCC, i.e. mitochondrial suppression. While p53 loss is known to contribute to mitochondrial suppression, the presence of the opposite arm (i.e. mitochondrial suppression inhibiting p53) suggests a potentially powerful feed forward loop that may be blocked by DCA.

Another effect of the DCA-induced activation of the Krebs' cycle is the increase in the production of diffusible metabolites, like αKG with well-described biologic effects (Figures 3-4A and 3-8B). For example, αKG is a critical cofactor for FIH and in its absence FIH is inhibited. Thus the increase in αKG may underlie the activation of FIH and explain the decrease in HIF transcriptional activity despite the fact that the HIF protein levels remain unaltered (Figures 3-5A,B). In summary, our finding that PDK inhibition and mitochondrial reactivation may offer an alternate mechanism for the inhibition of HIF transcriptional activity, in addition to several other pro-apoptotic and anti-proliferative signals, makes DCA a potential candidate for translation in RCC patients (Figure 2-13).

DCA has been used for over 4 decades to treat mostly children with congenital mitochondrial abnormalities (for example PDH deficiencies) (34, 35). Its toxicity profile is good with the only significant toxicity being a non-demyelinating peripheral neuropathy that is dose-dependent and reversible upon discontinuation of the drug (36). A small but mechanistic early-phase trial of oral DCA in patients with glioblastoma showed the operation of the mechanism described in animal models, in actual human tumors (18). In this trial we obtained glioblastoma biopsies before and after treatment with DCA. Activation of PDH, mitochondrial depolarization, increase in mROS, activation of apoptosis and decrease in proliferation were shown in the tumors from DCA-treated patients. Importantly, when compared with non-cancer brain tissue

(taken form epilepsy surgery) PDK expression was shown to be significantly higher in glioblastoma, in a manner similar to our data provided here with ccRCC (Figure 2-1). In another early phase dose-finding trial in patients with advanced and metastatic cancer (lung, breast, colon) that had failed all standard previous therapies, we showed that a dose of 6.25mg/kg po tid is well-tolerated (37). At that dose, the trough serum levels of DCA (despite some variability among patients) reached the levels required for the pharmacologic inhibition of its target enzyme. However, DCA has initially a short half-life (less than one hour) but it inhibits its own metabolism requiring perhaps around 3 months before it reaches a plateau of sustainable trough levels (18, 35, 37). The survival of the patients in this trial was very limited due to the advanced stage of disease at the time of enrollment, not allowing perhaps enough exposure to DCA to show a meaningful clinical response (although waterfall analysis suggested that the longer the exposure to the drug the higher the trough levels, the stronger the clinical response (decrease in tumor size) and the more the predicted decrease in the FDG-PET signal) (37).

DCA is not a cytotoxic drug, but perhaps can be seen as a "facilitator" of apoptosis, making it an attractive component of combination treatments (12). For example, in such a scheme, a cytotoxic drug may limit the tumor burden decreasing disease progression and thus prolonging the exposure to DCA, which can contribute by facilitating the effectiveness of the standard chemotherapy and by prevention of recurrence (38, 39). In the GBM trial, *in vitro* addition of DCA to standard chemotherapy (temozolomide) showed promising pro-apoptotic effects in patient-derived putative GBM cancer stem cells, suggesting more positive long-term effects of the DCA therapy (18).

Such a combination therapy in ccRCC may include DCA plus tyrosine kinase inhibitors (TKI) (22, 40). There is early evidence that this combination with DCA may prove effective in overcoming resistance to TKIs in other tumor types (30). Interestingly, TKIs may also partially inhibit PDK, as well as activate PDH by inhibiting tyrosine phosphorylation of these two proteins (41, 42). It is important to note that the inhibition caused by these tyrosine phosphylated sites is independent from DCA activity (which causes a serine phosphorylation in PDK). This means that there is a possibility for a synergistic combination of TKIs with DCA to more

completely activate PDH (and therefore inhibit HIF activity) while the TKIs themselves directly antagonize downstream HIF targets and other anti-apoptotic signals in ccRCC. A challenge in the translation of DCA to early-phase clinical trials with DCA is the fact that it is a generic drug, with limited options for intellectual property protection. This makes the involvement of industry challenging. However, there do remain options for the conduction of early-phase trials driven by academic institutions or clinical networks supported by the National Cancer Institute in North America or similar organizations.

In summary, our work suggests that, a) it is possible that metabolic modulators like DCA can "bypass" the persisting activity of HIF that is genetically driven (and thus difficult to be reversed pharmacologically) by targeting its transcriptional machinery in a FIH-dependent manner and b) its in vivo beneficial effects along with the recent experience of its use as an oral agent in patients with cancer, establishing a dose-limiting dose and proving that the mechanisms in human tumors in vivo (glioblastoma) are identical to the ones described in preclinical models, make its translation to humans with ccRCC attractive.

Materials and Methods

Patient Samples: We received institutional Health Research Ethics Board approval (Pro00051169) to obtain specimens from patients undergoing radical nephrectomy for RCC. All specimens were formalin fixed, paraffin embedded, pathologist diagnosed ccRCC. In each case, the pathologist microscopically examined and separated normal kidney sections from tumor sections. All tissues were processed identically and sliced into 5μm sections. RNA was isolated using the RNeasy FFPE Kit (Qiagen) or stained for confocal immunofluoresence using a monoclonal PDK1 antibody (Abcam, ab110025).

Cell Culture and Reagents*:* The 786-O human ccRCC line was purchased from ATCC, maintained in RMPI 1640 media (GIBCO, 10% FBS, 1% PSF). –VHL 786-O and +VHL 786-O cell lines (stably infected with an empty vector or functional, Hemagglutinin-tagged VHL, respectively) were a gift from Dr. Kaelin (Harvard Medical School). Human renal proximal tubular cells were purchased from ScienCell and maintained in EpiCM media. DCA powder was purchased from TCI America and diluted in sterile water adjusting the pH of the solution to 7.4.

Confocal imaging: Confocal microscopy was performed using a two-photon Zeiss LSM 510 NLO model (Carl Zeiss). Live cell TMRM (Life Technologies) and Mitosox (Invitrogen) imaging as well as TUNEL Apoptosis Detection Kit (Millipore) were completed as previously described (10). Co-localization coefficients were calculated by the Zen Software (Carl Zeiss) by quantifying the degree of pixel overlap between the FITC and TRITC channels after samples were stained in an identical manner. Antibodies used were: ki67 (Abcam, ab16667), p53 (Cell Signaling, CS9282), VEGF (Abcam, ab46154), p300 (Abcam, ab14984) and HIF2α (Novus Biologicals, NB100-122).

Oxygen Consumption Rate: An XF^e 24 Analyzer (Seahorse Bioscience) was used to determine oxygen consumption rate in 24 well plates. Results were normalized to protein concentration determined by BCA (Thermo Scientific).

PDH Activity Assay and α-Ketoglutarate Assay Kit: PDH activity was determined by an immunocapture assay (MitoSciences) and α-Ketoglutarate levels measured using the BioVision α-Ketoglutarate Assay Kit, as previously described (10).

Nude Mouse Xenografts: 6 week old male nu/nu mice (Charles River) were injected with ~3 million 786-O cells (in 250 µl PBS) in a 1:1 ratio with Matrigel using a previously published protocol (43). Tumors were measured twice per week using electronic calipers and allowed to grow to a volume of $40mm^3$ prior to initiation of DCA treatment. DCA was administered in the drinking water as previously published (10).

Lectin Imaging: Anesthetized mice were injected intraperitoneally with 50µl of Heparin (1000 units/ml; American Pharmaceuticals Partners) followed by intravenous injection of 100µl (0.5µg) FITC-conjugated Ricinus Communis Agglutinin I (Vector Laboratories) through the internal jugular vein. Lectin was perfused for 15 minutes prior to sacrifice. Tumors were immediately frozen in OCT, cut into 50µm sections and imaged in 3-dimensional z-stacks.

Matrigel Assay: Matrigel (BD Biosciences) was prepared as a 1:1: mixture with serum free, supplemented Medium 131 (Cascade Biologics) and plated (300µl per well) on a 24-well dish, as previously described (10). Once the matrigel solidified, human microvascular endothelial cells were plated at 60,000 cells/well. Fully supplemented RMPI media or supernatant from cancer cells (normalized to cell count) was then added to the well. After 5 hours pictures were taken and analyzed for total tubule length and number of complete structures using Image-Pro software (MediaCybernetics).

Mass spectroscopy*:* Cells were washed with ice-cold PBS and metabolites extracted by freeze-thaw in 80% methanol. Samples were flow injected into a 4000 QTRAP mass spectrometer (AB Sciex) measuring either enhanced product ion (EPI; IonSpray voltage of 4,500 V) or enhanced

MS (EMS; IonSpray voltage of 5,500 V). In ^{13}C labeled experiments, cells were exposed to $^{13}C_2$-pyruvate (Cambridge Isotope Laboratories) for 24hr before the experiment was terminated with the addition of ice-cold PBS.

Immunoblotting: Immunoblotting with standard SDS-PAGE was performed as previously described (17). Antibodies used were: PDK1 (Abcam, ab110025), PDK4 (Abcam, ab110336), PDH (Santa Cruz Biotechnology, sc-377092), Phospho-Ser293 PDH (EMD Millipore, AP1062), p21 (Abcam, ab7960), p53 (Cell Signaling, CS9282), HA-tag (Abcam, ab9134), GLUT1 (Abcam, ab115730), Tubulin (Sigma, T6199), HIF2α (Novus Biologicals, NB100-122), VHL (BD Biosciences, BD556347), and Actin (Abcam, ab3280).

siRNA transfection and qRT-PCR: Cells were grown to 60% confluence in 6-well plates and transfected using the RNAiMAX transfection reagent (Invitrogen). Experiments were carried out 72hrs post siRNA transfection. qRT-PCR was performed using gene specific primers from Life Technologies, using an ABI Prism 7900 Sequence Detector (Applied Biosystems), as previously described (10). 18S rRNA and Beta-2 Microglobulin were used as housekeeping genes.

HIF and p53 luciferase assays: HIF and p53 Cignal dual-luciferase reporter kits (SA Biosciences) were used as previously described (10). 48hrs after transfection, activity was assessed using a dual luciferase reporter assay kit (Promega). HIF and p53 activity was normalized to the Renilla luminescence.

Chick chorioallantoic membrane (CAM) angiogenesis assay: The anti-angiogenic activity of DCA was tested using an onplant assay in an *ex ovo* chicken embryo CAM model as previously described (44-46). In brief, fertilized White Leghorn chicken eggs were received from the University of Alberta Poultry research Centre (Edmonton, AB) and incubated in a humidified environmental chamber at 38˚C, with regular rocking. At day 4, egg shells were removed and the embryos cultured under shell-less conditions, in a covered plastic dish at 38˚C, 85% humidity.

Onplants were assembled by overlaying two gridded nylon meshes and embedding them into 28 uL of 1.6 mg/mL collagen I (sc-136157, Santa Cruz Biotechnology). Collagen was then supplemented with 786-O or 786-O+VHL +/- 0.5mM DCA diluted in water. Each onplant contained $0.5x10^6$ cells. Onplants (4 per embryo) were placed on the CAM of day 10 shell less embryos and incubated for an additional 72 hours, with at least 36 embryos used for each experimental compound. Each onplant was covered with 20 uL of DCA or water once every 24hrs for a total of two treatments. At 72hrs, each onplant was imaged using a dissecting microscope, after which groups were randomized and *de novo* angiogenesis was quantified independently by two individuals. The percentage of grids that showed new blood vessels compared to the total number of grids scored was considered the angiogenic index. Lectin was injected intravenously for visualization of representative images.

Chick chorioallantoic membrane (CAM) In Ovo assay: Fertilized White Leghorn chicken eggs were received from the University of Alberta Poultry research Centre (Edmonton, AB) and incubated in a humidified environmental chamber at 38˚C, with regular rocking. At day 10 of development, eggs were prepared for *in ovo* assays as previously described (47-49). Briefly, following identification and marking of the chorioallantoic vein by candling, a small hole is first drilled using a rotating cutting tool (Dremel) fitted with a silicone carbide grinding stone (Dremel part #84922) into the air sac, then a secondary but smaller hole next to the location of the chorioallantoic vein. Using the suction from an automatic pipette, the CAM is gently detached from the eggshell membrane in the area of the second hole next to the chorioallantoic vein. After the CAM is dropped, an opening of ~$1cm^2$ is cut around the second hole used to provide access to the surface of the dropped CAM. The holes located in the square near the chorioallantoic vein and the air sac are sealed with a piece of laboratory tape. Next, using a cotton-tipped applicator the CAM was abraded 3 times. Immediately after damaging the CAM, 25-30µl of a 786-0 cell suspension was placed onto the damaged area. 786-O cells were prepared into a single cell suspension by trypsinization and 4×10^6 786-0 cells were applied to the abraded area of each CAM by pipette. Xenografts were allowed to grow for 7 days (at 38˚C, 85%

humidity). For DCA treated groups, 200 uL of 0.5mM DCA was applied directly each day, with the control receiving a similar volume of PBS. At the end of the treatment period, embryos were killed and tumors excised; excess CAM was removed and tumors then weighed.

Statistics: We used Independent-Samples T test when comparing two groups and one-way ANOVA with Tukey post hoc analysis for comparison among 3 or more groups. To compare categorical data we used Fisher's Exact Test. All statistics were performed using SPSS Version 21 Software. $p<0.05$ was considered significant.

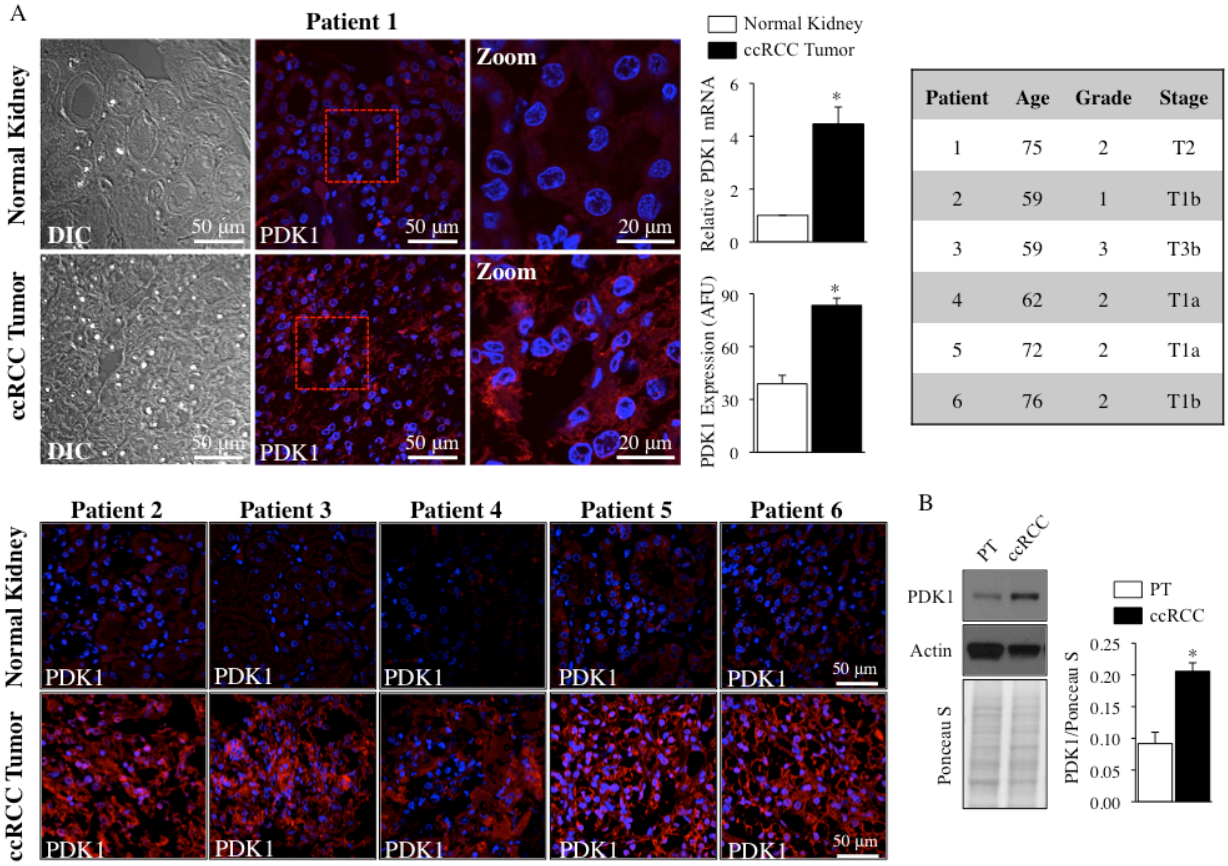

Patient	Age	Grade	Stage
1	75	2	T2
2	59	1	T1b
3	59	3	T3b
4	62	2	T1a
5	72	2	T1a
6	76	2	T1b

Figure 2-1: PDK1 is upregulated in ccRCC cells and tumors from patients compared to healthy kidney tissues removed from the same patient.

(A) qRT-PCR and confocal immunofluorescence imaging show that PDK1 is upregulated in ccRCC tumor samples compared to normal kidney tissue removed from the same patient during radical nephrectomy (PDK1: red, Nuclear stain DAPI: blue; n=6 patients per group; *p<0.01 vs. normal kidney). Patient information is shown in the inset. **(B)** The human ccRCC cell line 786-O, expresses significantly more PDK1 compared to healthy proximal tubules - the cell type from which ccRCC is derived (n=3 per group; *p<0.01 vs. proximal tubules).

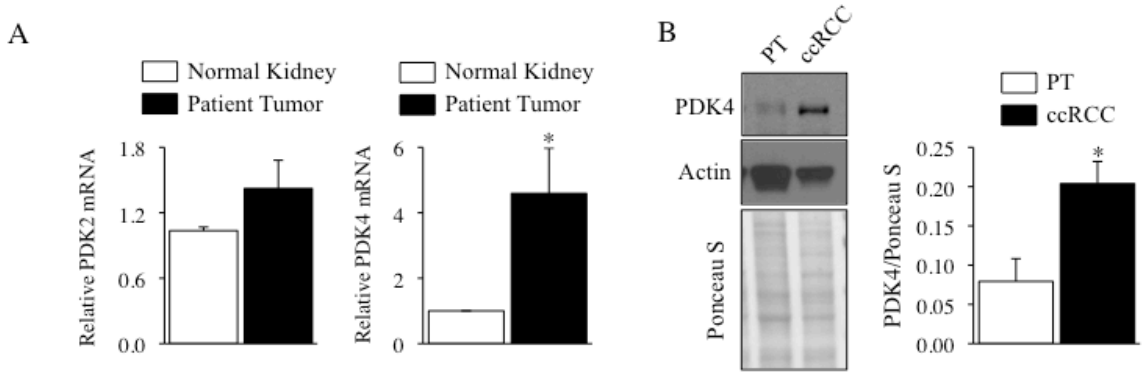

Figure 2-2: Specific PDK isoforms are upregulated in ccRCC

(A) qRT-PCR shows that PDK4 but not PDK2 is upregulated in ccRCC tumor samples compared to normal kidney tissue from the same patient (n=6 patients per group; *p<0.05 vs. normal kidney). **(B)** The ccRCC cell line, 786-O, expresses significantly more PDK4 compared to healthy proximal tubules, the cell type from which ccRCC is derived (n=4 per group; *p<0.05).

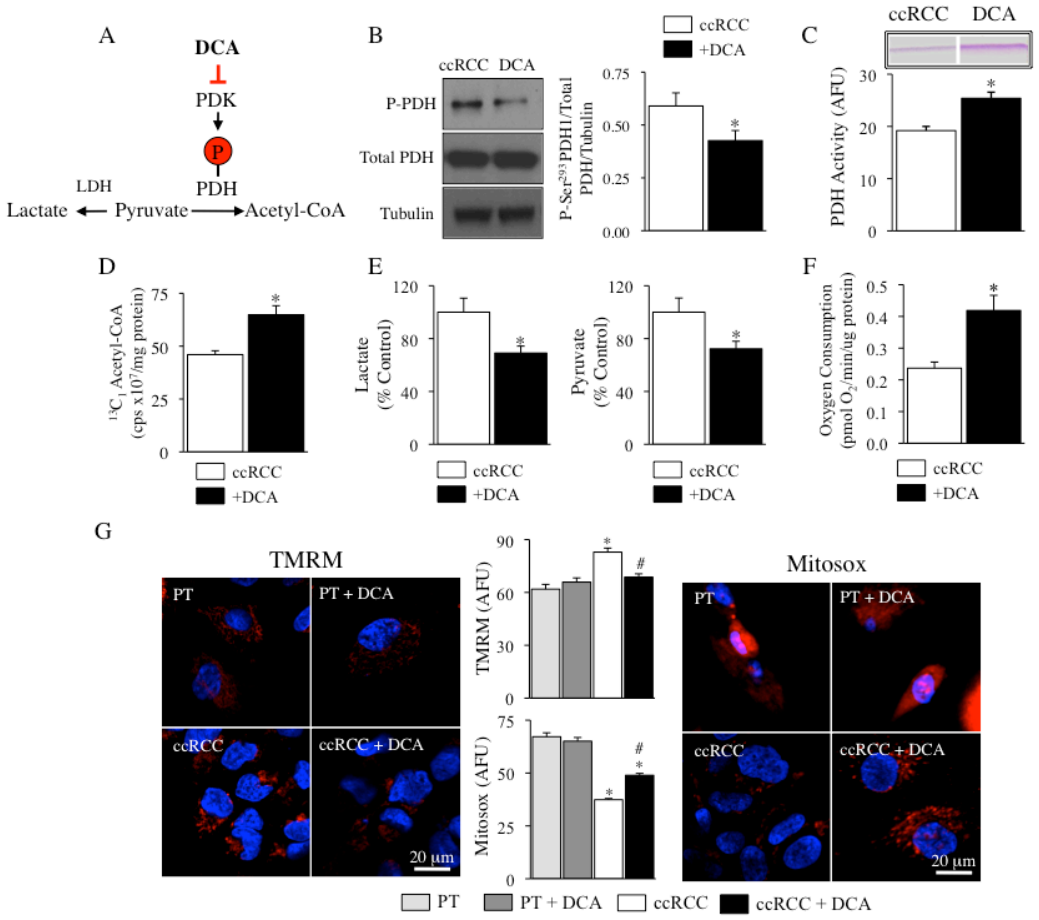

Figure 2-3: DCA increases PDH activity and reactivates mitochondrial function in ccRCC cells.

(A) Schematic showing the mechanism of action for DCA**. (B)** DCA reduces PDK-dependent phosphorylation of serine 293 on PDH (n=4 per group; *p<0.05 vs. ccRCC). **(C)** DCA increases PDH activity measured by a dipstick immunocapture assay (n=3 per group; *p<0.05 vs. ccRCC). **(D)** DCA increases the production of ^{13}C labeled acetyl-CoA when media is supplemented with ^{13}C labeled pyruvate (n=4 per group; *p<0.01 vs. ccRCC). **(E)** DCA reduces both lactate and pyruvate levels measured by mass spectroscopy (n=5 per group; *p<0.05 vs. ccRCC). **(F)** ccRCC cells consume more oxygen after treatment with DCA (n=4 per group; p<0.05 vs. ccRCC). **(G)** ccRCC cells have more hyperpolarized mitochondrial membrane potential (left;

TMRM: red, nuclear stain Hoechst: blue) and a reduced production of mitochondrial reactive oxygen species (mROS) (right; Mitosox: red, nuclear stain Hoechst: blue) compared to normal proximal tubule cells at baseline. DCA treatment repolarizes the mitochondrial membrane potential and increases mROS in ccRCC but not normal proximal tubule cells (PT) (n=100 cells per group; *$p<0.01$ vs. PT, $^{\#}p<0.01$ vs. ccRCC).

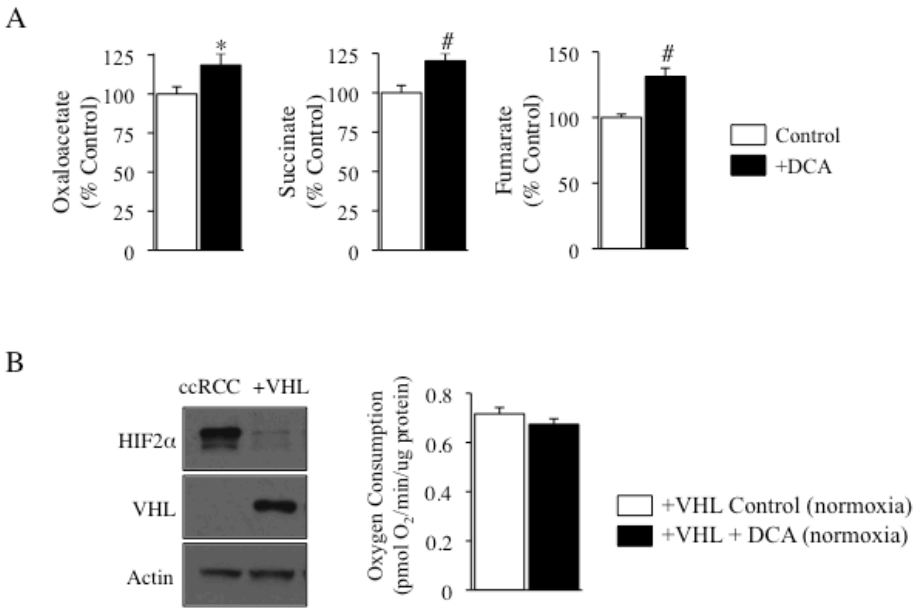

Figure 2-4: DCA increases the production of Krebs' cycle metabolites in VHL-deficient ccRCC cells

(A) DCA treatment increases the production of multiple Krebs' cycle metabolites (n=3 per group; *p=0.052, $^{\#}$p<0.01). **(B)** 786-O cells stably transfected with functional VHL eliminates HIF2α (the main HIF isoform in this cell line) in normoxia and do not increase their respiration after treatment with DCA (n=3 per group).

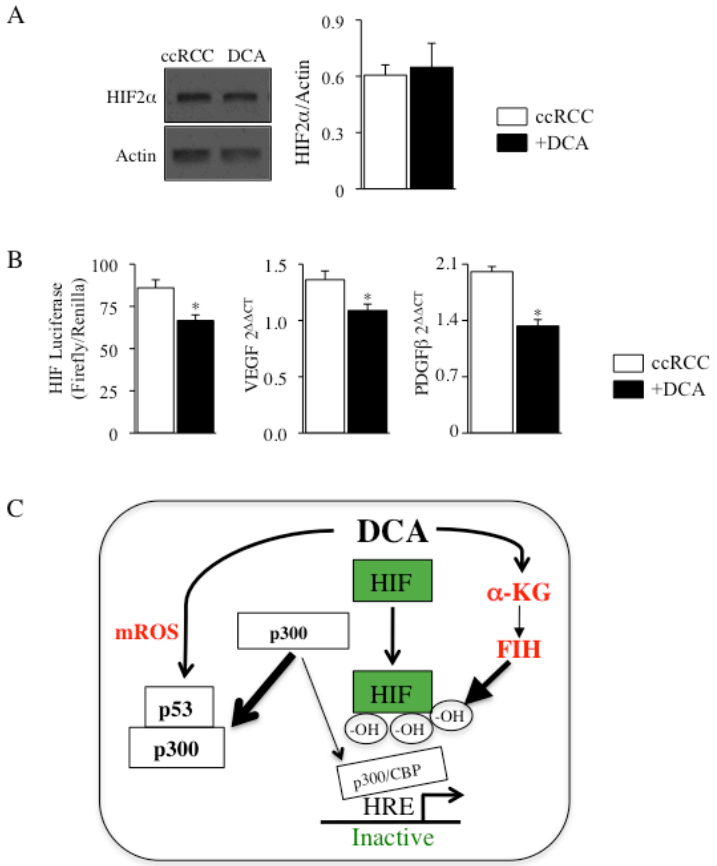

Figure 2-5: DCA inhibits HIF transcriptional activity and increases p53 activity in ccRCC. **(A)** DCA does not alter HIF2α protein level measured by immunoblot (n=4 per group). **(B)** DCA reduces HIF activity measured by a dual reporter HIF luciferase assay (n=3 per group; *p<0.01 vs. ccRCC) and decreases expression of HIF target genes VEGF and PDGFβ (n=4 per group; *p<0.05 vs. ccRCC). **(C)** Schematic showing our hypothesis model of two mechanisms of inhibiting HIF activity without altering protein levels: (1) DCA increases p53 activation via mROS therefore reducing the availability of p300 to bind to HIF and (2) DCA increases the αKG-dependent asparagine hydroxalase Factor Inhibiting HIF (FIH), which directly inhibits HIF activity.

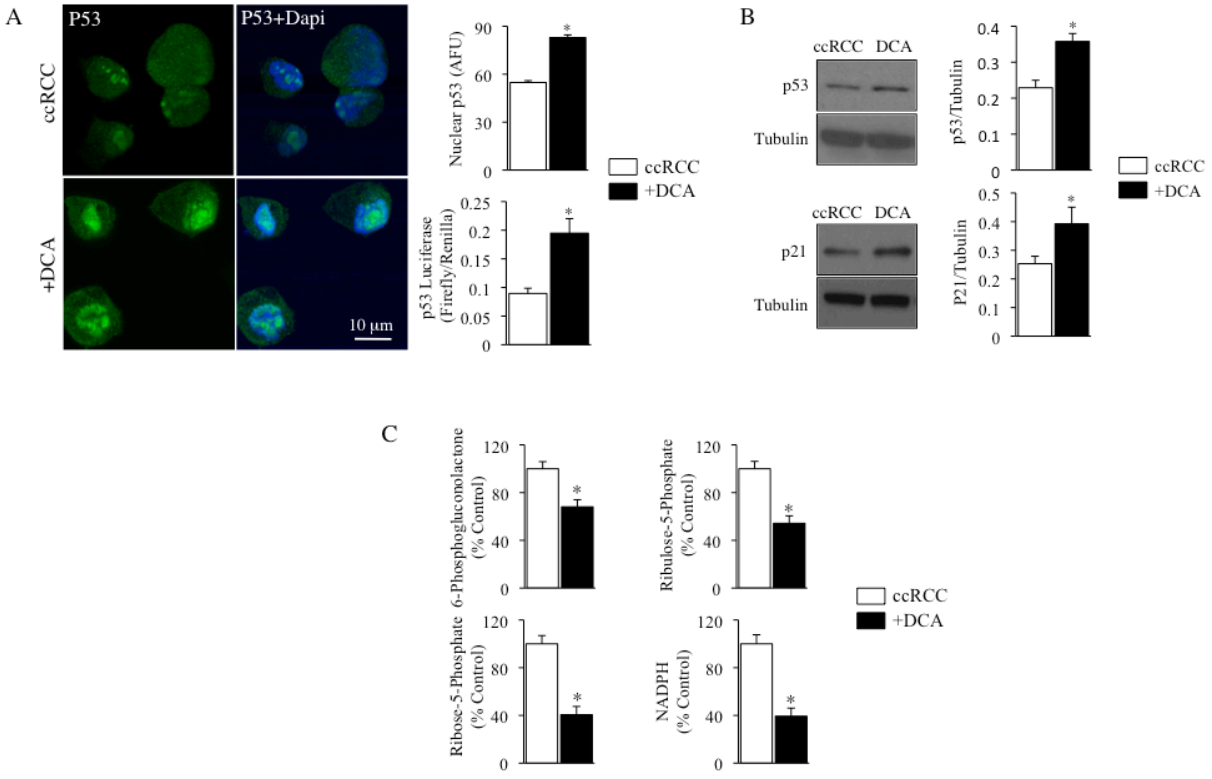

Figure 2-6: DCA increases p53 activity in ccRCC.

(A) DCA increases nuclear localization of p53 (p53: green, nuclear stain DAPI: blue; n=150 cells per group; *p<0.01 vs. ccRCC) and increases p53 activity measured by a dual-reporter p53 luciferase assay (n=4 per group; *p<0.01 vs. ccRCC). **(B)** DCA treatment increases the overall protein level of p53 as well as the expression of the p53 target gene, p21 (n=3 per group; *p<0.05 vs. ccRCC). **(C)** Mass spectroscopy shows that DCA treatment reduces multiple intermediary metabolites in the pentose phosphate pathway (n=6 per group; *p<0.01 vs. ccRCC).

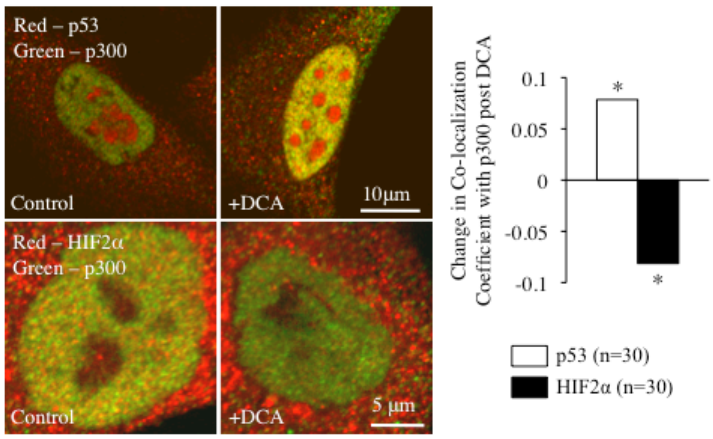

Figure 2-7: DCA treatment promotes association of p300 with p53

DCA treatment increases the co-localization coefficient of p53 with p300 and reduces the co-localization coefficient of HIF2α with p300 (n=30 cells per group; *p<0.05 vs. control). Note that the yellow color that shows co-localization is higher in the right upper quadrant (p53 co-localizes with p300 after DCA) compared to the left upper quadrant (no DCA). In contrast, the amount of yellow is lower in the right lower quadrant (less HIF2a co-localization with p300 after DCA) compared to the left lower quadrant (no DCA).

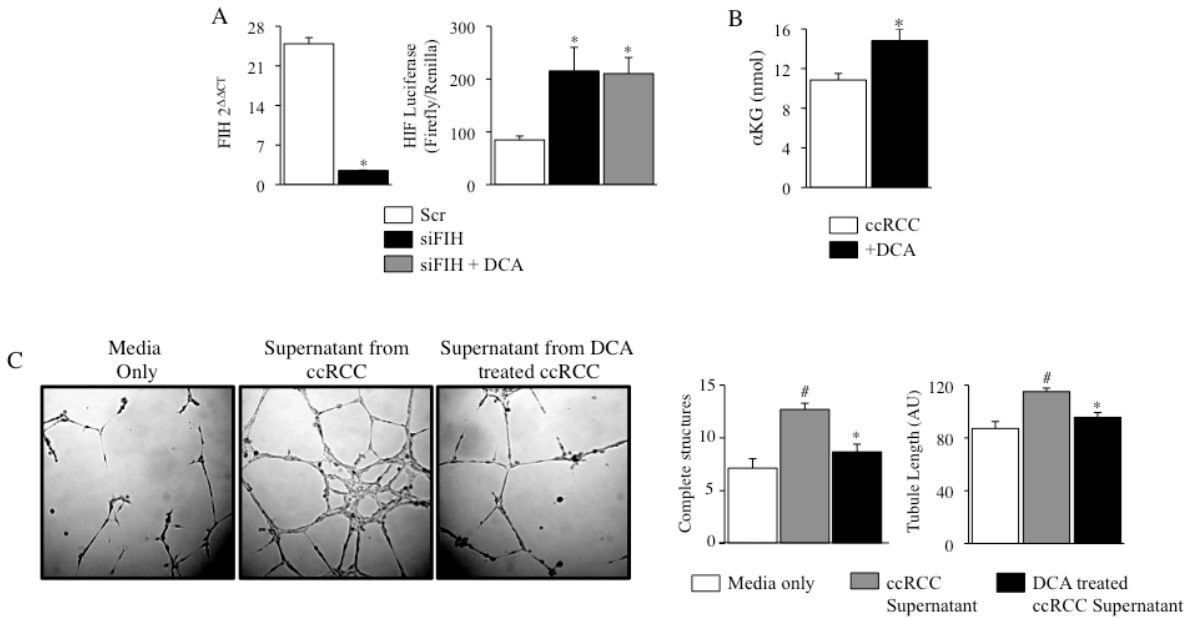

Figure 2-8: DCA inhibits HIF in a FIH-dependent manner and reduces angiogenic signaling in vitro.

(A) siRNA treatment reduces FIH mRNA by >90% (n=3 per group; *p<0.01 vs. Scr). Knockdown of FIH increases HIF activity by >2.5 fold but DCA treatment no longer reduces HIF activity (n=4 per group; *p<0.01 vs. Scr). **(B)** DCA treatment increases intracellular αKG levels (n=6; *p<0.05). **(C)** Matrigel assay shows that supernatant from ccRCC induces microvasculature endothelial cell tubule formation and increases the number of complete structures, while supernatant from DCA-treated ccRCC cells does not (n=3; #p<0.01 vs. media only, *p<0.01 vs. ccRCC supernatant).

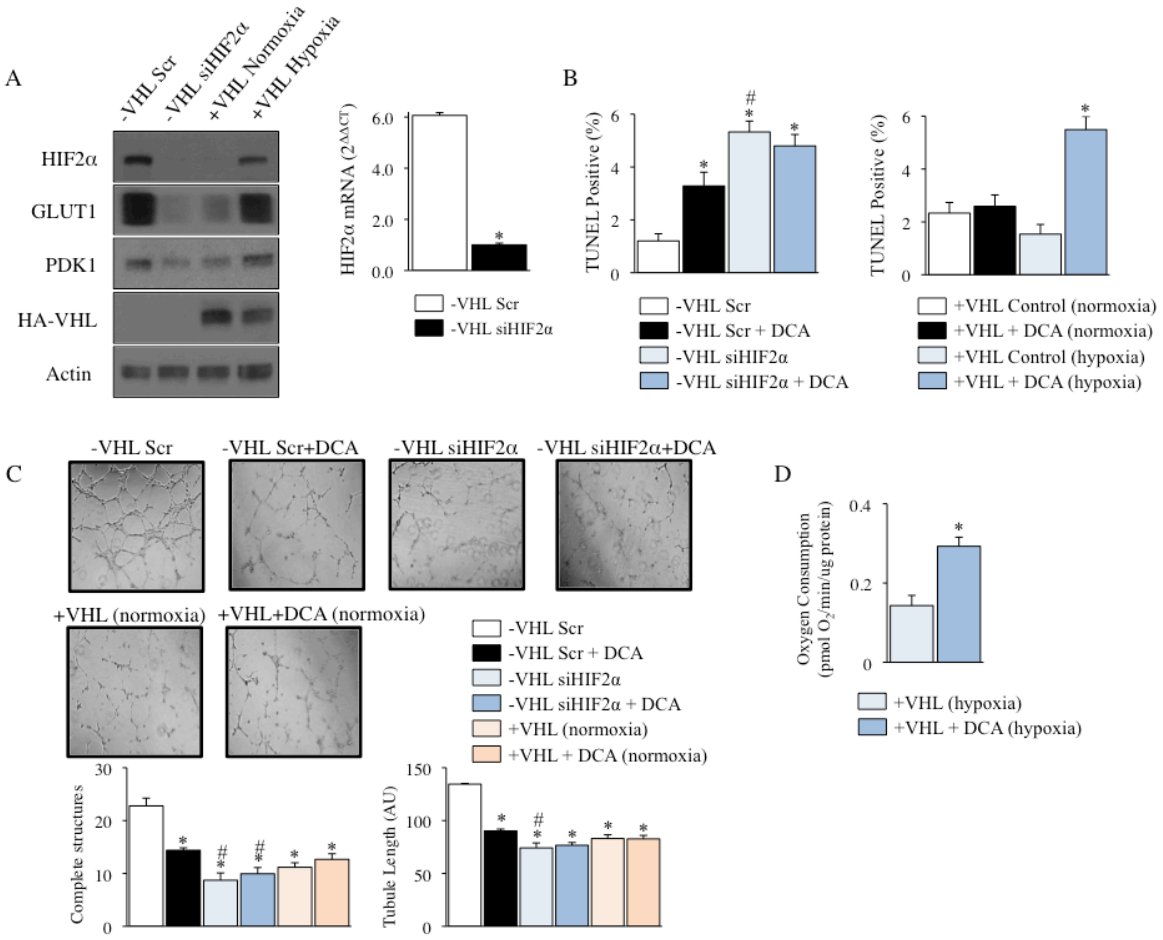

Figure 2-9: HIF is essential for DCA's effects of ccRCC

(A) HIF2α siRNA significantly reduces HIF2α mRNA and protein level as well as reduces the expression of downstream HIF targets, GLUT1 and PDK1, in -VHL 786-O cells (n=3 / group; *p<0.01 vs. Scr). In contrast, +VHL 786-O cells, which lack HIF2α expression in normoxia, regain HIF2α protein expression (and GLUT1, PDK1) when placed in 1% hypoxia for 48hrs. VHL is tagged by hemaglutinin (HA). **(B)** Both DCA and siHIF2α treatments significantly increased the amount of TUNEL staining in –VHL 786-O cells individually, however their combination did not further increase the rate of apoptosis over siHIF2α alone (n=3 per group; *p<0.05 vs. –VHL 786-O Scr, $^{\#}$p<0.05 vs. –VHL 786-O Scr + DCA). DCA treatment increases

TUNEL staining when +VHL 786-O cells are in hypoxia, but not normoxia (n=3 per group; *p<0.05 vs. +VHL 786-O Control). **(C)** DCA treatment, HIF2α siRNA and +VHL 786-O cells in normoxia reduce the number of complete structures and total tubule length compared to –VHL 786-O Scr (n=6 wells per group; *p<0.01 vs. –VHL 786-O Scr, $^{\#}$p<0.05 vs. –VHL 786-O Scr + DCA). The addition of DCA to –VHL 786-O siHIF2α or normoxic +VHL 786-O cells does not further reduce these angiogenesis indices. **(D)** DCA treatment increases respiration in hypoxic +VHL 786-O cells (n=5 per group; *p<0.01 vs. +VHL 786-O (hypoxia)).

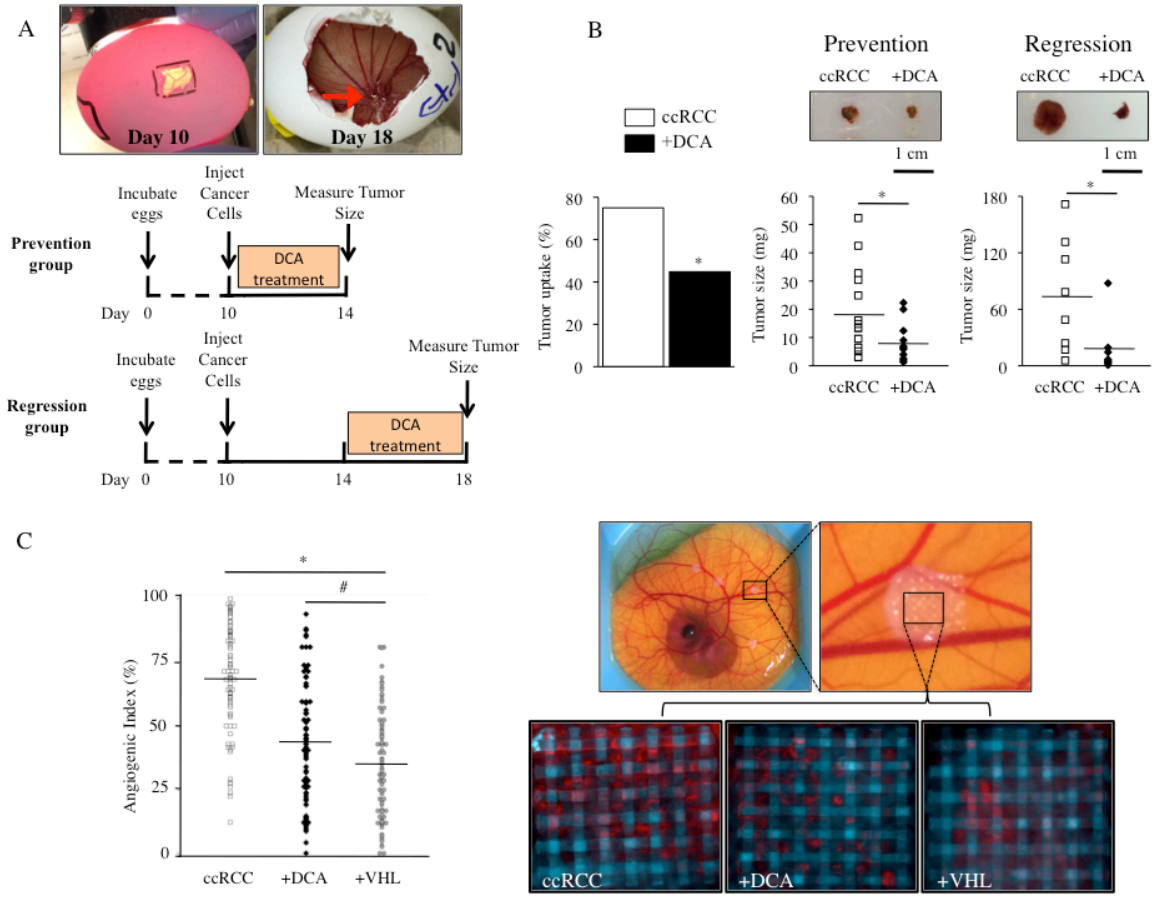

Figure 2-10: DCA reduces tumor formation, size and angiogenesis in vivo in fertilized egg "*in ovo*" xenograft models.

(A) Schematic shows in ovo xenograft prevention and regression protocols (red arrow points to developed Day 18 tumor with multiple blood vessels perfusing the tumor. **(B)** DCA reduces tumor uptake (left) as well as size of tumor in both prevention (middle) and regression (right) protocols (n≥8 eggs per group; *p<0.05 vs. ccRCC). **(C)** Ex ovo onplant angiogenesis assay shows that both DCA treatment and reintroduction of functional VHL in ccRCC cells (via stable transfection) reduce angiogenic index (n>75 onplants per group; *p<0.01 vs. ccRCC, $^{\#}$p<0.05 vs. DCA). The microphotographs show the grid with the ccRCC cells in situ (top) and after removal under the microscope.

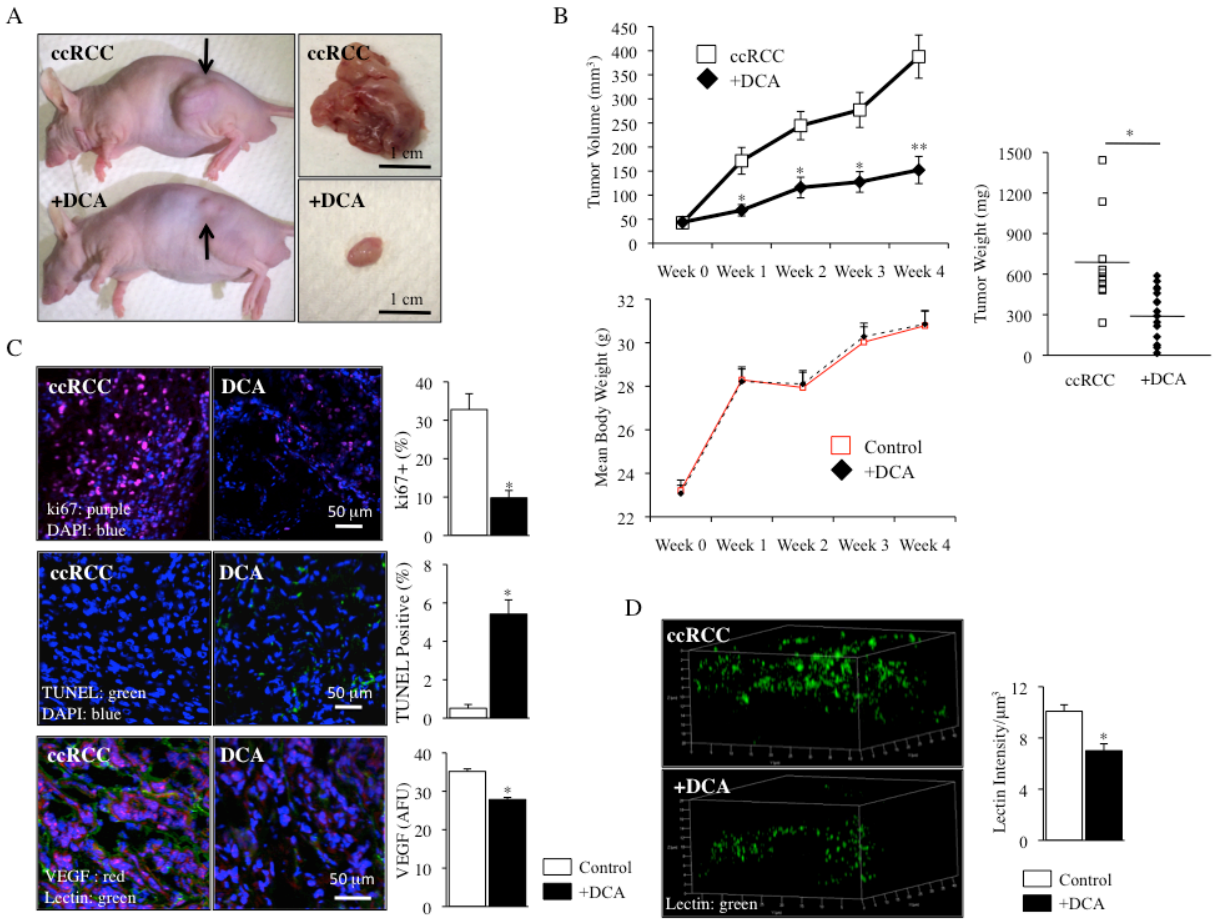

Figure 2-11: DCA reduces tumor size, proliferation and angiogenesis in a nude mouse xenograft model.

(A) Representative photographs of flank xenograft tumors. DCA reduces tumor volume **(B)** (n≥10 mice per group; *p<0.01 vs. ccRCC, **p<0.001 vs. ccRCC) and weight after one month of DCA treatment in the drinking water (n≥10 mice per group; *p<0.001 vs. ccRCC), but does not alter mean mouse body weight for up to one month compared to untreated animals (n≥10 mice per group). **(C)** Immunofluorescent staining shows a reduction in the proliferative marker ki67 in tumors from DCA-treated animals (n=4 mice per group; *p<0.01 vs. ccRCC), an increase in the amount of apoptosis (TUNEL) in tumors from DCA-treated animals (n=3 mice per group; *p<0.01 vs. ccRCC), as well as a reduction in the amount of VEGF in tumors from DCA treated

animals (n=3 mice per group; *p<0.01 vs. ccRCC). **(D)** 3D stereotactic analysis of stacked confocal imaging of lectin injected tumors shows reduced vascular density in tumors from DCA-treated animals (n=3 mice per group; *p<0.01 vs. ccRCC).

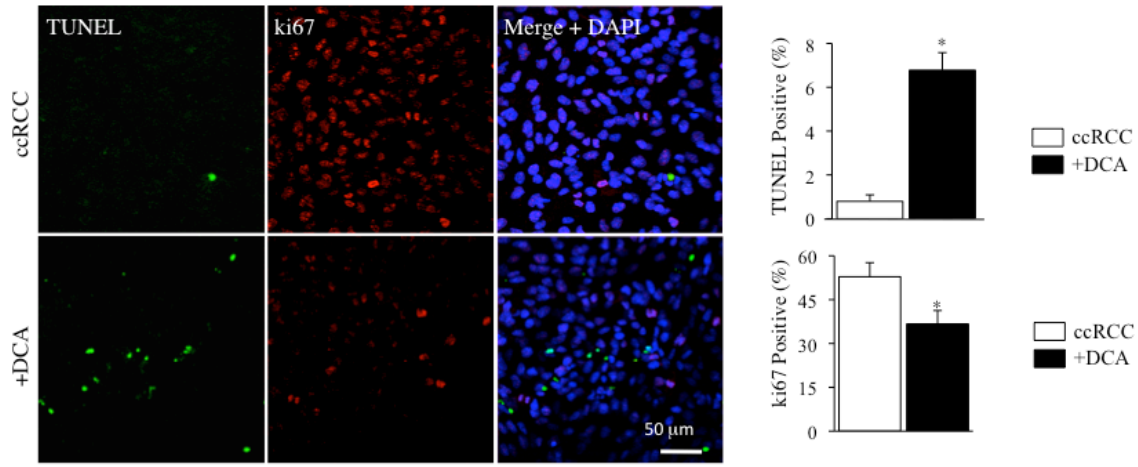

Figure 2-12: DCA treatment increases apoptosis and reduces proliferation

DCA treatment increases the apoptotic marker TUNEL (green) and reduces the proliferation marker ki67 (red) staining in 786-O cells (nuclear marker DAPI: blue; n=3 per group; *p<0.05 vs. ccRCC).

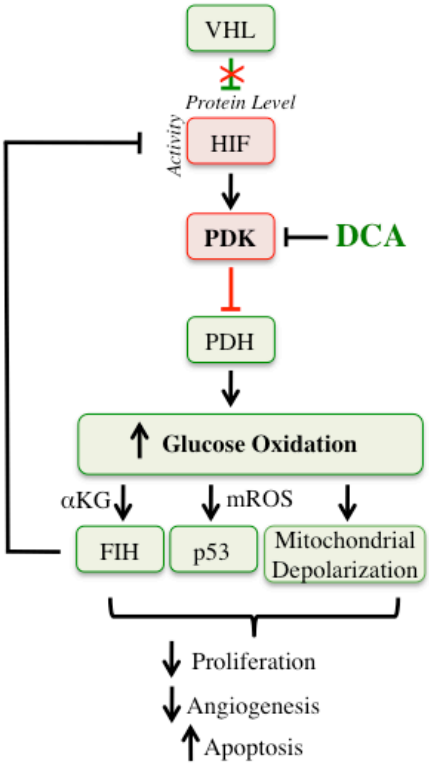

Figure 2-13: Proposed mechanism for the effect of DCA in ccRCC (see discussion).

References

1. Srinivasan R, Ricketts CJ, Sourbier C, Linehan WM. New strategies in renal cell carcinoma: targeting the genetic and metabolic basis of disease. Clinical cancer research : an official journal of the American Association for Cancer Research. 2015;21(1):10-7.
2. Coppin C, Kollmannsberger C, Le L, Porzsolt F, Wilt TJ. Targeted therapy for advanced renal cell cancer (RCC): a Cochrane systematic review of published randomised trials. BJU international. 2011;108(10):1556-63.
3. Kim WY, Kaelin WG. Role of VHL gene mutation in human cancer. Journal of clinical oncology : official journal of the American Society of Clinical Oncology. 2004;22(24):4991-5004.
4. Moore LE, Nickerson ML, Brennan P, Toro JR, Jaeger E, Rinsky J, et al. Von Hippel-Lindau (VHL) inactivation in sporadic clear cell renal cancer: associations with germline VHL polymorphisms and etiologic risk factors. PLoS genetics. 2011;7(10):e1002312.
5. Krieg M, Haas R, Brauch H, Acker T, Flamme I, Plate KH. Up-regulation of hypoxia-inducible factors HIF-1alpha and HIF-2alpha under normoxic conditions in renal carcinoma cells by von Hippel-Lindau tumor suppressor gene loss of function. Oncogene. 2000;19(48):5435-43.
6. Kim JW, Tchernyshyov I, Semenza GL, Dang CV. HIF-1-mediated expression of pyruvate dehydrogenase kinase: a metabolic switch required for cellular adaptation to hypoxia. Cell metabolism. 2006;3(3):177-85.
7. Papandreou I, Cairns RA, Fontana L, Lim AL, Denko NC. HIF-1 mediates adaptation to hypoxia by actively downregulating mitochondrial oxygen consumption. Cell metabolism. 2006;3(3):187-97.
8. Sudarshan S, Karam JA, Brugarolas J, Thompson RH, Uzzo R, Rini B, et al. Metabolism of kidney cancer: from the lab to clinical practice. European urology. 2013;63(2):244-51.
9. Vander Heiden MG, Cantley LC, Thompson CB. Understanding the Warburg effect: the metabolic requirements of cell proliferation. Science. 2009;324(5930):1029-33.
10. Sutendra G, Dromparis P, Kinnaird A, Stenson TH, Haromy A, Parker JM, et al. Mitochondrial activation by inhibition of PDKII suppresses HIF1a signaling and angiogenesis in cancer. Oncogene. 2013;32(13):1638-50.
11. Sutendra G, Michelakis ED. Pyruvate dehydrogenase kinase as a novel therapeutic target in oncology. Frontiers in oncology. 2013;3:38.
12. Kinnaird A, Michelakis ED. Metabolic modulation of cancer: a new frontier with great translational potential. J Mol Med (Berl). 2015;93(2):127-42.
13. Scheuermann TH, Li Q, Ma HW, Key J, Zhang L, Chen R, et al. Allosteric inhibition of hypoxia inducible factor-2 with small molecules. Nat Chem Biol. 2013;9(4):271-6.
14. Zimmer M, Ebert BL, Neil C, Brenner K, Papaioannou I, Melas A, et al. Small-molecule inhibitors of HIF-2a translation link its 5'UTR iron-responsive element to oxygen sensing. Mol Cell. 2008;32(6):838-48.

15. Compton S, Kim C, Griner NB, Potluri P, Scheffler IE, Sen S, et al. Mitochondrial dysfunction impairs tumor suppressor p53 expression/function. J Biol Chem. 2011;286(23):20297-312.
16. Schmid T, Zhou J, Kohl R, Brune B. p300 relieves p53-evoked transcriptional repression of hypoxia-inducible factor-1 (HIF-1). Biochem J. 2004;380(Pt 1):289-95.
17. Bonnet S, Archer SL, Allalunis-Turner J, Haromy A, Beaulieu C, Thompson R, et al. A mitochondria-K+ channel axis is suppressed in cancer and its normalization promotes apoptosis and inhibits cancer growth. Cancer cell. 2007;11(1):37-51.
18. Michelakis ED, Sutendra G, Dromparis P, Webster L, Haromy A, Niven E, et al. Metabolic modulation of glioblastoma with dichloroacetate. Science translational medicine. 2010;2(31):31ra4.
19. Cao W, Yacoub S, Shiverick KT, Namiki K, Sakai Y, Porvasnik S, et al. Dichloroacetate (DCA) sensitizes both wild-type and over expressing Bcl-2 prostate cancer cells in vitro to radiation. The Prostate. 2008;68(11):1223-31.
20. Sun RC, Fadia M, Dahlstrom JE, Parish CR, Board PG, Blackburn AC. Reversal of the glycolytic phenotype by dichloroacetate inhibits metastatic breast cancer cell growth in vitro and in vivo. Breast cancer research and treatment. 2010;120(1):253-60.
21. Li L, Zhang L, Zhang X, Yan Q, Minamishima YA, Olumi AF, et al. Hypoxia-inducible factor linked to differential kidney cancer risk seen with type 2A and type 2B VHL mutations. Mol Cell Biol. 2007;27(15):5381-92.
22. Rini BI, Atkins MB. Resistance to targeted therapy in renal-cell carcinoma. The lancet oncology. 2009;10(10):992-1000.
23. Vousden KH, Ryan KM. p53 and metabolism. Nature reviews Cancer. 2009;9(10):691-700.
24. Keith B, Johnson RS, Simon MC. HIF1alpha and HIF2alpha: sibling rivalry in hypoxic tumour growth and progression. Nature reviews Cancer. 2012;12(1):9-22.
25. Kroeze SG, Vermaat JS, van Brussel A, van Melick HH, Voest EE, Jonges TG, et al. Expression of nuclear FIH independently predicts overall survival of clear cell renal cell carcinoma patients. Eur J Cancer. 2010;46(18):3375-82.
26. Jiang P, Du W, Wang X, Mancuso A, Gao X, Wu M, et al. p53 regulates biosynthesis through direct inactivation of glucose-6-phosphate dehydrogenase. Nature cell biology. 2011;13(3):310-6.
27. Lim HY, Yip YM, Chiong E, Tiong HY, Halliwell B, Esuvaranathan K, et al. Metabolic signatures of renal cell carcinoma. Biochem Biophys Res Commun. 2015;460(4):938-43.
28. Kato M, Li J, Chuang JL, Chuang DT. Distinct structural mechanisms for inhibition of pyruvate dehydrogenase kinase isoforms by AZD7545, dichloroacetate, and radicicol. Structure. 2007;15(8):992-1004.
29. Kaplon J, Zheng L, Meissl K, Chaneton B, Selivanov VA, Mackay G, et al. A key role for mitochondrial gatekeeper pyruvate dehydrogenase in oncogene-induced senescence. Nature. 2013;498(7452):109-12.

30. Shen YC, Ou DL, Hsu C, Lin KL, Chang CY, Lin CY, et al. Activating oxidative phosphorylation by a pyruvate dehydrogenase kinase inhibitor overcomes sorafenib resistance of hepatocellular carcinoma. Br J Cancer. 2013;108(1):72-81.
31. Warburton HE, Brady M, Vlatkovic N, Linehan WM, Parsons K, Boyd MT. p53 regulation and function in renal cell carcinoma. Cancer research. 2005;65(15):6498-503.
32. Gurova KV, Hill JE, Razorenova OV, Chumakov PM, Gudkov AV. p53 pathway in renal cell carcinoma is repressed by a dominant mechanism. Cancer research. 2004;64(6):1951-8.
33. Roberts AM, Watson IR, Evans AJ, Foster DA, Irwin MS, Ohh M. Suppression of hypoxia-inducible factor 2alpha restores p53 activity via Hdm2 and reverses chemoresistance of renal carcinoma cells. Cancer research. 2009;69(23):9056-64.
34. Stacpoole PW, Kerr DS, Barnes C, Bunch ST, Carney PR, Fennell EM, et al. Controlled clinical trial of dichloroacetate for treatment of congenital lactic acidosis in children. Pediatrics. 2006;117(5):1519-31.
35. Stacpoole PW. The pharmacology of dichloroacetate. Metabolism. 1989;38(11):1124-44.
36. Abdelmalak M, Lew A, Ramezani R, Shroads AL, Coats BS, Langaee T, et al. Long-term safety of dichloroacetate in congenital lactic acidosis. Mol Genet Metab. 2013;109(2):139-43.
37. Chu QS, Sangha R, Spratlin J, L JV, Mackey JR, McEwan AJ, et al. A phase I open-labeled, single-arm, dose-escalation, study of dichloroacetate (DCA) in patients with advanced solid tumors. Invest New Drugs. 2015;33(3):603-10.
38. Dhar S, Lippard SJ. Mitaplatin, a potent fusion of cisplatin and the orphan drug dichloroacetate. Proc Natl Acad Sci U S A. 2009;106(52):22199-204.
39. Kumar K, Wigfield S, Gee HE, Devlin CM, Singleton D, Li JL, et al. Dichloroacetate reverses the hypoxic adaptation to bevacizumab and enhances its antitumor effects in mouse xenografts. J Mol Med (Berl). 2013;91(6):749-58.
40. Buczek M, Escudier B, Bartnik E, Szczylik C, Czarnecka A. Resistance to tyrosine kinase inhibitors in clear cell renal cell carcinoma: from the patient's bed to molecular mechanisms. Biochimica et biophysica acta. 2014;1845(1):31-41.
41. Hitosugi T, Fan J, Chung TW, Lythgoe K, Wang X, Xie J, et al. Tyrosine phosphorylation of mitochondrial pyruvate dehydrogenase kinase 1 is important for cancer metabolism. Mol Cell. 2011;44(6):864-77.
42. Fan J, Kang HB, Shan C, Elf S, Lin R, Xie J, et al. Tyr-301 phosphorylation inhibits pyruvate dehydrogenase by blocking substrate binding and promotes the Warburg effect. J Biol Chem. 2014;289(38):26533-41.
43. Mullen P. The use of Matrigel to facilitate the establishment of human cancer cell lines as xenografts. Methods in molecular medicine. 2004;88:287-92.
44. Quail DF, Walsh LA, Zhang G, Findlay SD, Moreno J, Fung L, et al. Embryonic protein nodal promotes breast cancer vascularization. Cancer research. 2012;72(15):3851-63.

45. Pink DB, Schulte W, Parseghian MH, Zijlstra A, Lewis JD. Real-time visualization and quantitation of vascular permeability in vivo: implications for drug delivery. PLoS One. 2012;7(3):e33760.
46. Leong HS, Steinmetz NF, Ablack A, Destito G, Zijlstra A, Stuhlmann H, et al. Intravital imaging of embryonic and tumor neovasculature using viral nanoparticles. Nat Protoc. 2010;5(8):1406-17.
47. Kain KH, Miller JW, Jones-Paris CR, Thomason RT, Lewis JD, Bader DM, et al. The chick embryo as an expanding experimental model for cancer and cardiovascular research. Dev Dyn. 2014;243(2):216-28.
48. Goulet B, Kennette W, Ablack A, Postenka CO, Hague MN, Mymryk JS, et al. Nuclear localization of maspin is essential for its inhibition of tumor growth and metastasis. Lab Invest. 2011;91(8):1181-7.
49. Palmer TD, Lewis J, Zijlstra A. Quantitative analysis of cancer metastasis using an avian embryo model. J Vis Exp. 2011(51).

Chapter Three

A Nuclear Pyruvate Dehydrogenase Complex is Important for the Generation of Acetyl-CoA and Histone Acetylation

Abstract

DNA transcription, replication and repair are regulated by histone acetylation, a process that requires the generation of acetyl-CoA. Here we show that all the subunits of the mitochondrial pyruvate dehydrogenase complex (PDC) are also present and functional in the nucleus of mammalian cells. We found that knockdown of nuclear PDC in isolated functional nuclei decreased the de-novo synthesis of acetyl-CoA and acetylation of core histones. Nuclear PDC levels increased in a cell-cycle dependent manner and in response to serum, epidermal growth factor or mitochondrial stress; this was accompanied by a corresponding decrease in mitochondrial PDC levels, suggesting a translocation from the mitochondria to the nucleus. Inhibition of nuclear PDC decreased acetylation of specific lysine residues on histones important for G1-S-phase progression and expression of S phase markers. Dynamic translocation of mitochondrial PDC to the nucleus provides a novel pathway for nuclear acetyl-CoA synthesis required for histone acetylation and epigenetic regulation.

Introduction

Epigenetic regulation of gene expression is essential for embryonic development and differentiation, protection against viruses and progression of cancer (Jaenisch and Bird, 2003). It includes modifications of core histones by either methylation or acetylation. By neutralizing the positive charges of lysine residues in histones, acetylation promotes the relaxation of DNA, necessary for replication and transcription (Vogelauer et al., 2002). A recent high-resolution mass spectrometry analysis identified a large number of nuclear proteins with multiple acetylation sites, suggesting that the role of acetylation extends beyond histones (Choudhary et al., 2009). In Eukaryotes, the biosynthesis of acetyl-CoA is thought to occur in the sub-cellular compartment in which it is required, because it is membrane impermeable and very unstable, due to the high-energy thioester bond that joins the acetyl- and -CoA groups. Our understanding of how the nucleus generates acetyl-CoA in metazoan cells is incomplete. Acetyl-CoA synthetase (AceCS1) and ATP-citrate lyase (ACL) are both present in the nucleus (Wellen et al., 2009). ACL is be the predominant pathway for nuclear acetyl-CoA generation in mammalian cells since it utilizes glucose oxidation-derived mitochondrial citrate as its substrate, as opposed to AceCS1 which uses acetate, a fuel that is not an important energy source for mammalian cells (Wellen et al., 2009). However, in cells with decreased citrate levels due to mitochondrial suppression by Bcl-xL over-expression, levels of acetyl-CoA and N-α acetylated proteins decreased in the cytoplasm with no apparent decrease in histone acetylation (Yi et al., 2011). This suggested the presence of a yet unidentified mitochondria-independent mechanism for histone acetylation in the nucleus.

Primitive protozoan cells that lack mitochondria, like *Entamoeba histolytica*, utilize pyruvate:ferrodoxin oxidoreductase (PFO) to generate acetyl-CoA (Rodriguez et al., 1998). Mammalian cells do not express PFO, but generate acetyl-CoA in mitochondria with a similar complex of nucleus-encoded proteins known as pyruvate dehydrogenase complex (PDC) (Horner et al., 1999). The generation of acetyl-CoA from both PFO and PDC is dependent on the glycolysis-

derived product pyruvate. The nuclear presence of several metabolic enzymes has been observed as early as the 1960s, with many shown to interact with nuclear proteins and DNA and "moonlight" to the nucleus in conditions of cellular stress (Kim and Dang, 2005; Siebert and Humphrey, 1965; Yang et al., 2012; Yogev et al., 2010). For example, the M2 isoform of the glycolytic enzyme pyruvate kinase (PKM2) translocates to the nucleus and functions as a protein kinase, phosphorylating nuclear proteins, like threonine-11 of histone 3 (H3) and enhancing the acetylation of lysine 9 on H3 (H3K9) (Yang et al., 2012). The protein kinase function of PKM2 utilizes the glycolytic intermediate phosphoenolpyruvate (PEP) and not ATP as its phosphate donor (Vander Heiden et al., 2010), resulting in the subsequent generation of pyruvate (Gao et al., 2012; Yang et al., 2012). However, the fate of pyruvate in the nucleus and whether this is related to the acetyl-CoA used in the H3K9 acetylation remain unknown.

Intact and functional PDC can translocate across mitochondrial membranes from the matrix to the outer mitochondrial membrane (Hitosugi et al., 2011). Thus it would be possible for a chaperone protein to bind PDC from the outer mitochondrial membrane and bring it to the nucleus under conditions that stimulate S-phase entry and cell cycle progression, where histone acetylation is critical.

We provide evidence that supports the hypothesis that functional PDC can translocate from the mitochondria to the nucleus during cell cycle progression, generating a nuclear pool of acetyl-CoA from pyruvate, and increasing the acetylation of core histones important for S-phase entry. The mitochondrial pyruvate dehydrogenase kinase (PDK), which phosphorylates and inhibits mitochondrial PDC was not detectable in the nucleus, suggesting that nuclear PDC may be constitutively active and regulated differently than mitochondrial PDC. The nuclear translocation of PDC was triggered by growth signals like serum and epidermal growth factor, or mitochondrial inhibitors, like rotenone. Nuclear PDC provides a novel means for the nucleus to generate acetyl-CoA in an autonomous fashion. The implications of this work extend to many conditions

where nuclear acetylation is altered, like development, cancer, neurodegeneration or cardiovascular disease.

Results

3.1 All Components of PDC are Present in the Nucleus

PDC is comprised of subunits from three catalytic enzymes: pyruvate dehydrogenase (E1), dihydrolipoamide transacetylase (E2) and dihydrolipoamide dehydrogenase (E3) as well as the tethering protein, E3 binding protein (E3BP) (Behal et al., 1993). We first identified the nuclear presence of PDC-E1 (α subunit) in human spermatozoa, which compartmentalize the nucleus (in the head) away from mitochondria (in the mid-section), allowing for more clear visualization of nuclear versus mitochondrial PDC (Figure 3-2A). To confirm the nuclear presence of PDC-E1 in a terminally differentiated primary cell line, we isolated primary fibroblasts from human lungs and detected its nuclear presence (Figure 3-1A). We then performed a more detailed assessment for the presence of nuclear PDC using microscopy in two commercially available cell lines, normal small airway epithelial cells (SAEC) and A549 cells (non-small cell lung cancer cells). In intact SAEC and A549 cells co-stained with an antibody against PDC-E1 and the mitochondrial marker MitoTracker Red, co-localization of the two signals was evident in the cytoplasm as expected, but PDC-E1 was also evident within the nucleus (marked by DAPI) without any mitochondrial signal (Figures 3-1B and 3-1C). For our imaging we generated 25 separate images in each intact cell, systematically scanning in the z-axis at 0.2μm in depth for each image. We used these stacked images to generate 3D videos that show the presence of PDC-E1 throughout the nucleus (Supplementary Video 1 and 2). We selected specific planes that "cut through the nucleus" from the z-stacked images, as shown in the top image of Figure 3-1D. Then, in the XY axis, we quantified the nuclear PDC-E1 and MitoTracker Red signals by measuring the fluorescence intensity. As we move from left to right in the image plane, an area of mitochondria is followed by an area where only the nucleus is present. PDC-E1 is highly detected in the mitochondria and co-localizes with the MitoTracker Red signal. However, while the MitoTracker Red signal intensity is absent in the nucleus, the PDC-E1 signal

is present, though with lesser intensity than the mitochondrial PDC-E1 signal (Figure 3-1D). Furthermore, nuclear PDC-E1 followed a similar signal pattern to the nuclear protein histone 3, confirming the specificity of the nuclear PDC-E1 signal (Figure 3-2B). In addition, a clear nuclear signal of PDC-E1 was also detected in the nucleus using electron microscopy (Figure 3-2C). These data show that the nuclear PDC-E1 signal is not a "contamination" from overlapping mitochondria.

To address the possibility that our PDC-E1 antibody non-specifically binds to other nuclear proteins, we transfected A549 and SAEC with a plasmid encoding for cloned human E1α subunit of PDC in frame with enhanced green fluorescent protein (EGFP). Based on EGFP fluorescence we detected the presence of the fused EGFP-E1 protein in mitochondria as well as the nucleus of both cell types (Figure 3-1E and Figure 3-2D). We then identified the nuclear presence for other subunits of the PDC complex, including PDC-E2, PDC-E3 and the ancillary subunit PDC-E3BP in intact cells using immunofluorescence (Figure 3-1F-H). For all confocal and electron microscopy experiments a "secondary antibody-only" control staining was performed, which in all experiments showed no signal (Figure 3-2E).

3.2 Nuclear PDC is Functional and Can Generate Acetyl-CoA from Pyruvate

To assess if nuclear PDC is functional, we isolated nuclei using a nuclei-specific high sucrose gradient centrifugation protocol. As even a small amount of mitochondrial membranes could be a confounding factor, we took several steps to ensure that our nuclei were not contaminated with any mitochondria. We showed that nuclear membranes were intact by the lamin staining pattern and that our nuclear preparations were free of mitochondrial membranes, as assessed by nonyl-acridine orange (NAO) and MitoTracker Red imaging (Figures 3-3A and 3-3B), as well as free of cytoplasmic, mitochondrial matrix and membrane proteins, as assessed by immunoblots with antibodies against α-tubulin, citrate synthase (CS), isocitrate dehydrogenase 2 (IDH2), succinyl-CoA synthetase (SCS) and succinate dehydrogenase (SDH) (Figure 3-3C). These vigorous purity indices

were used in all of our experiments with isolated nuclear preparations throughout this work. In these pure nuclei preparations, we confirmed the presence of PDC-E1 in nuclei from the EGFP-transfected cells, as well as from intact nuclei from A549 and SAEC cells, using immunofluorescence; with absence of any detectable signal in secondary-only antibody straining (Figure 3-4A, upper panels). In addition to the α subunit of the PDC-E1, all the subunits of the PDC complex were present in isolated nuclei (Figure 3-4A, bottom panels). We then used immunoblots and showed the nuclear presence of all PDC subunits in isolated nuclei from A549 cells (Figure 3-3D) as well as a separate cancer cell line, 786-0 renal cell carcinoma cells, in the absence of cytoplasmic or mitochondrial contamination (Figure 3-3E). As NAD(H) is abundant in the nucleus, our finding that PDC-E2 appears to be lipoylated (implying the nuclear presence of lipoic acid, not present in our media), suggests that nuclear PDC has all the necessary co-factors to be functional (Figure 3-4B).

To study the function of nuclear PDC without interference from mitochondrial PDC, we performed our initial experiments on isolated nuclei. We detected many glycolytic intermediates including PEP, pyruvate and acetyl-CoA using collision-induced dissociation mass spectrometry (Figure 3-3F). We then designed an experiment to study whether nuclear PDC is functional in terms of the *de-novo* biosynthesis of acetyl-CoA.

We first isolated intact and pure nuclei from either A549 or 786-0 cells previously treated with scrambled vs. PDC-E1 siRNA. We obtained an efficient knockdown of PDC-E1 resulting in no detectable immunoblot signal (Figure 3-3G; top). This was in keeping with the absence of any PDC activity in nuclei lacking PDC, measured by a standard dipstick assay that measures the NADH produced by the immunocaptured enzyme (Figure 3-3G; bottom).

We then treated these nuclei with an isotope-labeled form of pyruvate ($^{13}C_2$-pyruvate) for 8hrs and measured the production of labeled acetyl-CoA ($^{13}C_1$-acetyl-CoA; Figure 3-3H). Since the only way to synthesize acetyl-CoA from pyruvate is by PDC, the detection of labeled acetyl-CoA in our nuclear preparations reflects the activity of nuclear PDC. We detected a significant

decrease in the levels of $^{13}C_1$-labeled acetyl-CoA in nuclei from PDC-E1 siRNA-treated cells compared to those from scrambled siRNA, using two separate mass spectrometry acquisition modes in A549 and 786-0 nuclei (Figure 3-3I and 3-4C). We also detected increasing levels of labeled acetyl-CoA in response to increasing levels of labeled pyruvate, suggesting the presence of non-limiting amounts of functional PDC in the isolated nuclei (Figure 3-3I and 3-4C).

3.3 Nuclear PDC is Important for Histone Acetylation

We then assessed whether the acetyl-CoA generated from nuclear PDC is important for histone acetylation. Since histone acetylation depends on glucose and not free-fatty acid metabolism (Wellen et al., 2009), we first deprived the A549 cells of glucose for 24 hours in order to synchronize acetylation, in the presence of scrambled or PDC-E1 siRNA. Next, we isolated functional nuclei from scrambled and PDC-E1 siRNA-treated cells and exposed them to pyruvate (10mM) for 8hrs and measured histone acetylation (Figure 3-5A). Prior to the addition of pyruvate to our isolated nuclei (time=0), no significant differences were apparent in acetylated lysine levels at the molecular weight of histones between scrambled and PDC-E1 siRNA groups (Figure 3-5B), confirming the synchronization of acetylation. After exposure to pyruvate, nuclei from PDC-E1 siRNA-treated cells had decreased levels of all three acetylated (Ac) core histones H2B, H3 and H4, compared to nuclei from scrambled siRNA-treated cells (Figure 3-5C).

On the other hand, inhibition of nuclear PDC did not appear to change the acetylation of p53 and FOXO1 in these cancer cells, suggesting that the acetylation of targets in the nucleus is regulated, perhaps by the availability or proximity of acetyl-transferases or de-acetylases with acetyl-CoA generating enzymes, like PDC (Figure 3-6). Alternatively, a rapid turnover of acetyl-groups in histones, compared to those of other proteins, may also explain why the inhibition of nuclear PDC preferentially showed a decrease in histone acetylation.

Since the role of ACL on nuclear acetylation has not been studied in A549 cells, we used ACL or PDC-E1 siRNA in order to study the relative importance of

these two enzymes in nuclear acetylation. Extracted histones from either PDC-E1 or ACL siRNA-treated cells had decreased histone acetylation compared to scrambled siRNA-treated cells (Figure 3-5D). Nevertheless, in these cells the impact of PDC-E1 silencing on histone acetylation appears to be larger than that of ACL-silencing. This may be explained by the fact that PDC is also involved in the ACL-mediated production of nuclear acetyl-CoA, as mitochondrial PDC is also an important regulator of citrate production (i.e. ACL's substrate) via the Krebs' cycle. The effects of ACL and PDC-E1 silencing were not the same on the acetylation of specific histones, suggesting that the source of acetyl-CoA may play a role on which target is acetylated.

3.4 Pyruvate Dehydrogenase Kinase is Not Present in the Nucleus

Mitochondrial PDC-E1 is tonically inhibited by PDC kinases (PDKs) and activated by PDC phosphatases (PDPs). PDKs phosphorylate serine-293 of the α subunit of PDC-E1, resulting in its inactivation (Behal et al., 1993). While PDK I and II are ubiquitously expressed, PDK III and IV are only expressed in the testis and under starvation conditions in muscle, respectively (Bowker-Kinley et al., 1998). Hypoxia-inducible factor 1α (HIF1α) is activated in many cancers and can suppress mitochondrial PDC by inducing PDK expression (Kim et al., 2006). We detected PDKI and II in mitochondria, but not in isolated nuclei of A549 (which express both isoforms) and 786-O cancer cells, (which only express PDKI) (Figure 3-7A and 3-7B). On the other hand, we detected the presence of PDPI (but not PDPII) in nuclei of A549 and 786-O cells (Figure 3-7A and 3-7B). We found higher levels of PDC-E1 serine-293 phosphorylation in A549 mitochondria compared to normal cells (Figure 3-7C), in keeping with the finding that cancer cells have higher levels of PDK (Michelakis et al., 2010). Furthermore, PDC-E1 phosphorylated serine-293 was present in mitochondria but not in nuclei (Figure 3-7A), in keeping with the absence of PDK. This suggested that in certain conditions (like in cancer or hypoxia, where HIF1α is activated) while mitochondrial PDC can be relatively inactive, nuclear PDC could remain constitutively active.

We then treated isolated nuclei from A549 and 786-O cancer cells with the small molecule PDK inhibitor Dichloroacetate (DCA), which primarily inhibits PDK I and II (Bonnet et al., 2007; Michelakis et al., 2010) and showed no differences in Ac-H3 levels (Figure 3-7D). However, DCA treatment of whole A549 cells resulted in both increased Ac-H3 (nuclear acetylation) and Ac-tubulin (cytoplasmic acetylation) (Figure 3-7E, 3-8A and 3-8B). The increase in acetylation by DCA in whole cells may be due to acetyl-CoA biosynthesis by cytoplasmic and nuclear ACL, which produces acetyl-CoA using citrate as substrate (Figure 3-7F). We confirmed the expected DCA-induced increase in citrate, along with another Krebs' cycle intermediate (succinate) and the expected decrease in lactate (Figure 3-8C). Thus the differential effects of DCA [which has known anti-cancer properties (Bonnet et al., 2007; Dhar and Lippard, 2009; Michelakis et al., 2010)] between mitochondrial and nuclear PDC, reflect the differential expression of PDK in the two cellular compartments and suggests that factors that can increase or decrease PDK function (like HIF1α and DCA, respectively) can be used to exploit the functional significance of nuclear PDC, an idea that we explored later on.

3.5 PDC Translocates from the Mitochondria to the Nucleus During S-phase

To study whether histone acetylation occurs prior to DNA replication during S-phase in our cells, we first synchronized cells to the G1 phase by serum starvation for 24 hrs. We then introduced serum and serially measured Ac-H3 and cyclin A. Ac-H3 levels increased first, followed by cyclin A (Figure 3-9A). By isolating pure nuclei from these cells we also showed that nuclear PDC-E1 levels followed a similar increase pattern to Ac-H3 and then began to decrease towards baseline, but only after Ac-H3 levels peaked (Figure 3-10A). Furthermore, using microscopy, we showed that both PDC-E1 and Ac-H3 were higher during late S-phase compared to baseline in isolated nuclei (Figure 3-10B).

We then measured both nuclear and mitochondrial PDC-E1 levels upon serum stimulation after cell-cycle synchronization, at the same time points. We found that the increase in nuclear PDC-E1 levels during cell cycle progression

was associated with a parallel decrease in mitochondrial PDC-E1 levels, before both PDC fractions returned toward their baseline levels (Figure 3-9B). The decrease in mitochondrial PDC was not due to enhanced degradation since PDC levels remained unaltered in whole cells in response to increasing concentrations of serum (Figure 3-10C), suggesting the decrease in mitochondrial PDC was due to its translocation to the nucleus.

To measure the relative distribution of PDC in the mitochondria and nucleus, we loaded on the same gel the same amount of protein from isolated nuclei and mitochondria at baseline and 3hrs post-serum stimulation. Although PDC-E1 levels were clearly higher in mitochondria than the nuclei, the percent ratio of nuclear to mitochondrial PDC-E1 increased from 17% to 30% after 3 hours of serum stimulation (Figure 3-10D). A similar increase in the percent ratio of nuclear to mitochondrial PDC in response to serum stimulation was also observed with the E2 component using immunofluorescence, where we were able to measure mitochondrial PDC (overlap with MitoRed) and nuclear PDC (overlap with DAPI) within the same cell (Figure 3-9C).

We then performed a series of experiments to further support the fact that nuclear PDC translocates from the mitochondria. To exclude the possibility that the increase in nuclear PDC in response to serum stimulation is a newly translated product from the endoplasmic reticulum (ER), we inhibited ribosomal translation with cycloheximide (CHX) and measured nuclear PDC levels (see Figure 3-9D). Serum stimulation increased nuclear PDC (E1 and E2) and this was not altered by CHX, although the translation of c-myc [a protein with a short half-life, previously shown to be decreased within 2 hrs of CHX treatment (Alarcon-Vargas et al., 2002)] was decreased during this timeframe (Figure 3-9E).

Newly synthesized mitochondrial proteins from the ER contain an N-terminus mitochondrial localization sequence (MLS) and upon entry into the matrix, the MLS is cleaved by the mitochondrial processing peptidase (MPP; see Figure 3-9D). The cleavage of these (otherwise destabilizing) sequences (~15-50 amino acids) of mitochondrial proteins is required to prevent degradation and facilitate subsequent assembly of subunits (Chacinska et al., 2009). Only mature

(cleaved MLS) PDC proteins are able to re-fold and form complexes in the mitochondria. Therefore, we hypothesized that if nuclear PDC is directly translocated to the nucleus after its translation in ribosomes, we should be able to detect the precursor form in the nucleus. Using two separate siRNA transfection approaches for the β-catalytic subunit of mitochondrial processing peptidase (MPP), we were able to inhibit the mRNA levels by 65% and 90% respectively, resulting in the accumulation of increasing levels of the precursor form of PDC-E1 (Figure 3-9F, see arrowhead) along with the mature form. We then used MPP siRNA-treated whole cells and probed for PDC-E1 on the same membrane with isolated nuclei and mitochondrial protein from untreated cells. While the precursor form was clearly seen in the MPP-silenced whole cells in the same gel, only the mature form of PDC was detected in isolated nuclei and mitochondria (Figure 3-9G; top). We also isolated nuclei from both scrambled and MPP siRNA-treated cells and could not detect the presence of the precursor; only mature PDC was present in the nucleus (Figure 3-9G; bottom). As MPP is a mitochondria-specific protease, our data suggest that nuclear PDC is processed in the mitochondria prior to translocation to the nucleus.

All of the subunits of PDC are translated in the ER and are transported separately to the mitochondria, where they are processed prior to complex formation. We hypothesized that if we inhibit only one of the subunits and thus disturb the stoichiometry balance of the subunits within the complex, we may affect the nuclear levels of the other subunits. Indeed, knockdown of only PDC-E1 by siRNA resulted in decreased levels of all catalytic components of PDC in the nucleus, without changing their overall protein expression in whole cell preparations (Figure 3-10E). This suggests that PDC is translocated from the mitochondria to the nucleus as a functional complex.

3.6 Signals Increasing Nuclear PDC Levels

We then studied signals that may trigger the nuclear translocation of PDC. Epidermal growth factor (EGF) signaling is important for S-phase entry and cell cycle progression (Kato et al., 1998) and has been shown to increase the nuclear

translocation of PKM2 in cancer (Yang et al., 2012). We found that recombinant human EGF (rhEGF) increased the nuclear levels of PDC components, along with PKM2, in A549 cells (Figure 3-11A and 3-12A). The increase in nuclear levels was through translocation since rhEGF did not change the total cellular expression of PDC subunits, while it predictably increased tyrosine-204 phosphorylation of MAPK (Figure 3-11B). Similarly, gefitinib, an EGF receptor inhibitor, decreased nuclear (Figure 3-11C), but not whole-cell PDC levels (Figure 3-11D). We then used confocal imaging and studied the relative distribution of PDC subunits within the same cell, in 786-0 cells. Similar to A549 cells, rhEGF increased the relative distribution of PDC-E1 and PDC-E2 from the mitochondria to the nucleus (Figure 3-11E).

We speculated that a mitochondrial stressor might trigger translocation of PDC from the mitochondria to the nucleus. We studied the electron transport chain (ETC) complex I inhibitor rotenone, since inhibition of ETC complexes is a well-known cause of mitochondrial stress (Durieux et al., 2011). We found that rotenone caused a significant translocation of PDC into the nucleus over and above serum and rhEGF (Figure 3-11E and 3-12B). Mitochondria adapt to stress by initiating the mitochondria unfolded protein response (mtUPR), which results in increased expression of mitochondrial import proteins, folding chaperones and heat shock proteins, amplifying the communication with the nucleus (Zhao et al., 2002). We speculated that a heat shock chaperone may be involved in the nuclear translocation of PDC.

We studied heat shock protein 70 (Hsp70) based on evidence that: (**1**) induction of Hsp70 is cell-cycle dependent, with its highest expression and nuclear localization observed during S-phase (Milarski and Morimoto, 1986), (**2**) Hsp70 is involved in the nuclear translocation of several proteins (Shi and Thomas, 1992) and (**3**) Hsp70 binds to and activates mitochondrial PDC (Kiang et al., 2006). We confirmed that nuclear levels of Hsp70 increase in a cell-cycle dependent manner, similarly to the increase in nuclear PDC-E1 following serum stimulation (Figure 3-12C). We performed immunoprecipitation studies on A549 cells and MRC-9 cells (fibroblasts) with Hsp70 and detected the presence of

PDC-E1 and PDC-E2 (Figure 3-11F and 3-12D), suggesting that Hsp70 may bind to these components of the complex. Sequence and structural analysis of potential binding motifs for Hsp70 within the PDC complex showed a putative Hsp70 binding motif (i.e. hydrophobic peptide regions) (Mayer and Bukau, 2005) within the PDK binding site on PDC (Figure 3-12E). PDK did not co-immunoprecipitate with Hsp70 (Figure 3-11F and 3-12D), suggesting that Hsp70 and PDK may compete for similar binding domains within PDC.

We pre-treated serum-starved A549 and 786-0 cells with either vehicle (DMSO) or KNK437, an inhibitor of heat shock factor 1 (HSF1), which results in decreased expression of inducible Hsp70 (Koishi et al., 2001), prior to serum stimulation for 4hrs. KNK437 decreased mRNA expression (Figure 3-12F) and nuclear levels of both Hsp70 and PDC-E1, compared to vehicle (Figure 3-11G and S6G). Nuclear Hsp70 levels correlated positively with nuclear PDC-E1 levels in both vehicle and KNK437-treated A549 cells (Figure 3-11H and 3-12H). Similar to KNK437, a specific siRNA against Hsp70 also decreased nuclear levels of both Hsp70 and PDC-E1 in response to serum stimulation (Figure 3-11I).

3.7 Nuclear PDC is Important for S-phase Entry and Cell Cycle Progression

Our data on the dynamic translocation of PDC from the mitochondria to the nucleus suggest that it is the same enzymatic complex that is present in both compartments, rather than perhaps a different variant. This makes the study of the relative biological role of PDC on histone acetylation and cell cycle progression in the two cellular compartments challenging, particularly in the intact cell setting. We took advantage of PDK's localization in mitochondria, but not the nucleus, and designed experiments in an intact cell setting, in which by subtracting the effects of selective mitochondrial PDC inhibition (by the induction of PDK) from the effects of total cellular PDC inhibition (by PDC-E1 siRNA), we could expose the role of nuclear PDC.

While PDK is already induced in cancer cells, we aimed to maximally inhibit mitochondrial PDC by two methods: first, inducing endogenous PDK by activation of HIF1α and second, increasing exogenous PDKI via transfection with

a PDKI plasmid (see Figure 3-13A). With either method, mitochondrial PDC should be maximally inhibited (condition 1). Then by inhibiting total cellular PDC by siRNA gene silencing (condition 2), we could expose the effects of nuclear PDC on histone acetylation and cell cycle progression by subtracting condition 1 from condition 2 (Figure 3-13A).

For the first experiment, we infected A549 cells with an adenovirus encoding for CA5 (AdCA5), a constitutively active mutant form of HIF1α (mHIF1α) (Manalo et al., 2005), avoiding the confounding effects of hypoxia. Compared to an adenovirus encoding for LacZ (AdLacZ), increased expression of mHIF1α by AdCA5 (Figure 3-14A and 3-14B) resulted in a significant increase in the expression of PDKI (Figure 3-13B) and phosphorylation of serine-293 on mitochondrial, but not nuclear PDC-E1 (Figure 3-13C). Mutant HIF1α increased mitochondrial membrane potential (Figure 3-14C), further supporting the mitochondrial PDC suppression and its impact on mitochondrial function in our model, as we have previously described (Bonnet et al., 2007). We then treated AdCA5-infected cells with scrambled (condition 1) versus PDC-E1 siRNA (condition 2). We also gave scrambled siRNA to AdLacZ-infected cells (control). We synchronized all the groups to the G1 phase by serum starvation for 24hrs, followed by re-introduction of serum, and 24 hours later we measured S-phase markers and specific histone-3 acetylation sites that are involved in cell cycle progression. AdCA5-infected cells treated with scrambled siRNA had increased acetylation of H3K9 and H3K18, both important for S-phase progression (Cai et al., 2011), increased G1-S-phase progression shown by increased levels of phosphorylated retinoblastoma (P-Rb), as well as elongation-2-factor (E2F), cyclin A and cyclin-dependent kinase 2 (Cdk2), markers for S-phase entry, compared to AdLacZ-infected cells treated with scrambled siRNA (Figure 3-13D). These effects (condition 1) are in agreement with the described effects of HIF1α on proliferation (Semenza, 2010) and the recruitment of histone acetyl-transferases (HATs) (Luo et al., 2011). In contrast, AdCA5-infected cells treated with PDC-E1 siRNA (condition 2) had significantly decreased acetylation of H3K9 and H3K18 and decreased levels of P-Rb, E2F, cyclin A and Cdk2,

compared to AdCA5-infected cells treated with scrambled siRNA (condition 1) (Figure 3-13D). Since both conditions had activated HIF1α and inhibited mitochondrial PDC, subtraction of condition 2 (grey bars) from condition 1 (black bars) in Figure 3-13D shows that nuclear PDC inhibition decreases Ac-H3K9 and Ac-H3K18 (while total H3 levels remain relatively stable) as well as P-Rb and S-phase regulators (E2F, cyclin A, Cdk2).

For the second experiment, transfection with a PDKI plasmid increased the expression of PDKI (Figure 3-14D) and phosphorylation of PDC-E1 serine-293 (Figure 3-13E), compared to the empty vector control. PDKI over-expression did not change histone acetylation or cell cycle progression (Figure 3-13E, compare white bars [control] to black bars [condition 1]), compatible with the fact that mitochondrial PDC is significantly inhibited in these cancer cells at baseline and further inhibition may not elicit any measurable effects. However, similar to the first experiment, PDC siRNA (condition 2), decreased H3K9 and H3K18 acetylation and decreased P-Rb, E2F, cyclin A and Cdk2, compared to scrambled siRNA controls (condition 1; Figure 3-13E). Thus, two different approaches of inhibiting nuclear PDC support its role in S-phase progression.

Discussion

Here we show for the first time that PDC is present and functional in the nucleus. Nuclear PDC can generate acetyl-CoA utilized for histone acetylation and S-phase entry, providing a novel link between metabolism and epigenetic or cell cycle regulation. This newly discovered source of nuclear acetyl-CoA may also be important in conditions where the availability of cytoplasmic citrate (which can cross the nuclear membrane and produce acetyl-CoA through ACL) is decreased due to suppressed production or shift toward lipid synthesis. Our work suggests that nuclear PDC has a mitochondrial origin since it lacks the MLS (which can only be cleaved in the mitochondria) and its nuclear increase in response to serum is not affected by inhibition of ribosomal translation. In addition to serum, nuclear PDC translocation increases under growth factors (EGF) or mitochondrial inhibitors (rotenone), suggesting a potential role in disease states with proliferative signals or mitochondrial dysfunction, like cancer.

It is intriguing that our data suggest translocation of PDC in the nucleus, given the large size of this enzymatic complex. High-resolution electron microscopy and structural analysis have recorded its size and diameter within the range of 8-10MDa and 25-45nm, respectively (Sumegi et al., 1987; Zhou et al., 2001b). However, there is evidence for size and conformational variability of PDC with identification of complexes as small as 1MDa (Sumegi et al., 1987; Zhou et al., 2001a). Although the stoichiometry of the individual components in the complex (i.e. the relative amount of E1, E2, E3 subunits) varies, in keeping with the reported variability in its size among tissues, only the interplay of all subunits within a functional complex can produce acetyl-CoA. The fact that we find *de-novo* production of acetyl-CoA in isolated nuclei in response to pyruvate, suggests that a functional complex is present. The fact that we can decrease the nuclear levels of all subunits by only silencing the gene for one subunit, suggests that the complex travels as a whole from the mitochondria into the nucleus. PDC was recently identified as an intact functional complex on the outer mitochondrial membrane (Hitosugi et al., 2011), suggesting that it can translocate across mitochondrial membranes, a more complex process than translocation across the

nuclear membrane. Since the nuclear pore complex can accommodate the entry of large complexes of similar diameter to PDC, like ribonucleoprotein complexes (Lodish et al., 2000) or intact nucleocapsids of viruses (Pante and Kann, 2002), it is possible that an intact PDC complex could translocate to the nucleus.

We provide evidence that Hsp70 may promote the nuclear translocation of a constitutively active form of PDC. By competing with PDK for binding to PDC, Hsp70 may allow PDC to remain active when translocated to the nucleus (Figure 3-13F). Kiang *et al* (Kiang et al., 2006) showed that Hsp70 binds to and activates mitochondrial PDC, but did not show the mechanism of this activation. It may be that by competing with PDK, Hsp70 removes this inhibitory kinase and thus activates PDC. It is possible that EGF can promote nuclear acetylation by a coordinated translocation of PKM2 and PDC, potentially by increasing Hsp70 levels (Milarski and Morimoto, 1986) (Figure 3-13F). This model may contribute to the recently described effects of nuclear PKM2 on tumor growth via histone acetylation, offering a source and mechanism for the nuclear acetyl-CoA generation used for the acetylation of H3K9 (Yang et al., 2012). It is appealing to consider that there is a mechanism by which several factors required for the nuclear response to proliferative stimuli (for example PKM2 and PDC) can be transferred simultaneously, increasing efficiency. Although our collective data support the existence of the translocation model shown in Figure 3-13F, we cannot rule out the possibility that individual subunits may be transported independently in the nucleus, where they could potentially be assembled in an intact complex with the help of a chaperone like Hsp70.

Tyrosine phosphorylation by growth factor signaling, including EGFR, activates PDKI providing a mechanism for suppression of mitochondrial PDC in cancer (Hitosugi et al., 2011), in addition to the induction of PDK expression by HIF1α (Kim et al., 2006). Therefore, in a "double hit" manner, EGF stimulation can activate PDK, suppressing mitochondrial PDC [which has been shown to inhibit mitochondria-dependent apoptosis in cancer (Bonnet et al., 2007)] in tandem with Hsp70-mediated nuclear translocation of PDC, promoting histone acetylation and cell cycle progression (Figure 3-13F). The inhibition of PDK by

siRNA, DCA or hybrid drugs [like mitoplatin, a drug that structurally combines cisplatin with DCA molecules (Dhar and Lippard, 2009)] decreases cancer growth in animal models (Bonnet et al., 2007) and a small human trial (Michelakis et al., 2010), by activating glucose oxidation, reversing the Warburg effect and the resistance to apoptosis in cancer cells. Our work now suggests that the nuclear pool of PDC is "immune" to this strategy. It raises the possibility that in response to these interventions cancer cells may "escape" by promoting a transfer of PDC in the nucleus, where PDC may promote proliferation. It also suggests that anti-cancer strategies, in which PDK inhibition is used, may perhaps be strengthened by simultaneous inhibition of EGFR signaling or Hsp70 function. As PDC plays a prominent role in many metabolic disorders, it will be important for scientists to be aware that their efforts to target PDC may have direct and previously unrecognized effects on nuclear biology.

Our work suggests an alternative pathway to ACL for the nucleus to generate acetyl-CoA for histone acetylation. It is possible that in specific tissues or disease states, the relative importance of ACL or nuclear PDC may be different. ACL has been shown to be important for histone acetylation during differentiation (Wellen et al., 2009), while our work suggests that histone acetylation by nuclear PDC may be important for cell cycle progression. ACL and PDC should be studied together when assessing histone acetylation and epigenetic regulation in conditions that both differentiation and proliferation are taking place, including development, cancer and other proliferative conditions or stem cell biology.

Materials and Methods

Cell culture

Human A549 non-small cell lung cancer cells, 786-O renal cell carcinoma and MRC-9 fibroblasts were purchased from ATCC (Manassas, VA). A549 cells were maintained on F12K medium, while 786-O cells in RPMI-1640 media and MRC-9 cells in EMEN. Primary human fibroblasts were isolated from the lung of a transplant patient in accordance with the Human Ethics Committee at the University of Alberta and maintained in DMEN. Primary human fibroblasts were isolated from the lung using an enzymatic cocktail containing papin (1mg/ml), dithiothreitol (0.5mg/ml), collagenase (0.6mg/ml) and bovine serum albumin (0.6mg/ml) (Sigma-Aldrich) as previously described (Sutendra et al., 2011). Human small airway epithelial cells (SAECs) were purchased from ScienCell (Carisbad, CA). SAECs were maintained in SAEpiCM, which was provided by the company. Media for all cell lines were supplemented with 10% FBS (unless stated otherwise) and 5% antibiotic and antimycotic (Invitrogen-Gibco Canada, Burlington, Canada).

Confocal Microscopy

Confocal microscopy imaging was performed using a Zeiss LSM 510 NLO confocal microscope with two-photon capability (Carl Zeiss Microscopy, Jena, Germany). PDC-E1α, E2, PDKI, PDKII and Hsp70 antibodies were purchased from Santa Cruz Biotechnology (Santa Cruz, CA) and used at a 1:50 dilution. PDC-E1β, E3, E1BP, lamin and PKM2 antibodies were purchased from Abcam (Cambridge, MA) and used at a dilution of 1:100. Ac-H3 antibody (against all N-terminal acetyl-lysine residues) was purchased from Cell Signaling Technology and used at a dilution of 1:100. MitoTracker Red (250nM; Invitrogen-Gibco) and Nonyl acridine orange (100nM; Invitrogen-Molecular Probes, Burlington, Canada) were used as mitochondrial membrane markers. Quantification of both the mitochondria and nuclear PDC signal was assessed using the Zeiss physiology option software, which can quantify fluorescence units along the plane (line) of a specified region, using the Profile setting. As depicted in Figure 3-1D, a plane that

crosses through the mitochondria and nucleus was selected to directly compare the intensity of signal between the two organelles and to also show the purity of the nuclear signal for PDC as the signal for the mitochondrial marker Mitotracker Red was not detected in the portion of the plane that crosses the nucleus. Image J 64 software was used to measure the nuclear (signal present within the DAPI region of the cell) and mitochondrial (signal present within MitoRed region of the same cell) PDC signal (using the integrated density parameters) in response to serum stimulation, rhEGF or rotenone treatment. All images were scanned in mid-plane of the cell in the z-axis as shown in Figure 3-1D, using a 100X NA 1.3 oil objective lens at 2X zoom, allowing for an pixel size of 0.04μm x 0.04μm x 0.2μm. This allows for the clear visualization of PDC in the mid-plane of the nucleus. Fluorophore conjugated secondary antibodies (DAKO, Carpinteria, CA and Invitrogen, Molecular Probes, Eugene OR) and the nuclear stain DAPI (Molecular Probes) were used for immunofluorescence imaging with specific excitations of 488 nm (Fitc), 543 (Tritc), 633 (Far Red) and 750 nm two photon (DAPI) and the corresponding emissions were detected with the following filter sets. Fitc: BP 505-615, Tritc: BP 565-615, Far red: LP 650 and DAPI: BP 390-465. Overlap was eliminated between the emissions of any secondary antibodies, mitochondrial-specific dyes, EGFP and nuclear stains by imaging each channel independently and sequentially with only one excitation wavelength active during each scan.

Reconstructed Video: Twenty-five stacked images consisting of 0.2μm sections in depth were acquired using confocal microscopy. The frame size was 2048x2048 pixels. These stacked images covering an area of 46.1μm (length) x 46.1μm (width) x 5μm (depth) generated the constructed video using the Zeiss 3D for LSM software. All experiments included negative control secondary antibody-only staining (Figure 3-2E, 3-4A and 3-12A), which in all presented experiments showed no signal, supporting the specificity of the antibodies used.

EGFP-PDC-E1 plasmid

EGFP-PDC-E1 plasmid was generated by OriGene Technologies (Rockville, MD). Briefly, cDNA ORF clone of *homo sapiens* pyruvate dehydrogenase alpha 1 (PDHA1) (OriGene Technologies; Rockville, MD) was cloned into pEGFP-N1 vector (Clontech, Mountain View, CA) and transfected into A549 and SAECs using Xfect transfection agent (Clontech).

Spermatozoa isolation

Human spermatozoa were isolated from semen by centrifugation for 10 minutes at 700 x g. Spermatozoa were then plated on slides coated with cell-tak (BD Biosciences, Mississauga, Canada) before immunofluorescence staining and confocal microscopy.

Immunogold electron microscopy

A549 cells were grown on coverslips, fixed in 3% freshly prepared paraformaldehyde plus 0.05% glutaraldehyde and permeabilized with 0.05% saponin. Following blocking, cells were incubated with a mouse monoclonal antibody against PDC-E1α (Santa Cruz Biotechnlology) for one hour and then with fluro-nanogold anti mouse Fab Alexa Fluor 488 (Nanoprobes, Yaphank, NY) secondary antibody over night at 4°C. Cells were further fixed in 2.5% glutaraldehyde in PBS plus 2% sucrose, and nanogold particles were gold-enhanced (Gold Enhance, Nanoprobes). Cells were then dehydrated and embedded in EMbed-812. Seventy-millimeter thin sections were prepared and observed using a Philips 410 electron microscope (Philips Research, Briarcliff Manor, NY). A Hitachi H-7000 (Hitachi High Technologies America, Schaumburg, IL) Transmission Electron Microscopy (TEM) was used at 15,000x magnification and 80kV, in order to image isolated nuclei and confirm their purity.

Functional nuclear isolation

Isolation of nuclei was performed using the commercially available nuclei isolation kit: nuclei PURE prep from Sigma Aldrich. Briefly, adherent cells were washed with PBS and scraped from the plate in the presence of lysis buffer. Cells (in lysis media) were carefully placed on top of a 1.8M sucrose gradient and the resulting suspension was centrifuged at 30,000 x g for 45 minutes in a pre-cooled swinging bucket ultracentrifuge. Nuclei were collected as a white pellet at the bottom of the centrifuge and washed with nuclei storage buffer (provided with the kit). Purity of nuclei was assessed by immunocytochemistry and immunoblot. For functional experiments, isolated nuclei were used immediately.

PDC Activity Assay

PDC activity was measured using the MitoProfile Dipstick Assay Kit (MitoSciences, Eugene, OR). Protein (50μL of 1μg/μL) was collected from isolated nuclei and placed in a 96-well dish and incubated with the dipstick containing the PDC antibody. The enzyme complex is immunocaptured in its native form and activity is visualized by coupling PDC-dependent production of NADH to the reduction of NBT in the presence of excess diaphorase, forming an insoluble intensely colored precipitate at the capture line. PDC activity was measured by the intensity of band using a flat top scanner.

siRNA treatment

PDC-E1, ACL, Hsp70 and scrambled-siRNA (Ambion, Austin, TX) were transfected at a final concentration of 20nM with $CaCl_2$. MPPβ was transfected at a final concentration of 200nM with $CaCl_2$. After 18 hrs, media was changed and experiments were performed 48 hrs later.

Isolated nuclei experimental protocol for acetyl-CoA measurement and histone acetylation

A549 or 786-0 cells transfected with scrambled or PDC-E1 siRNA were maintained in glucose free media 24 hours prior to nuclear isolation. Immediately

following nuclear isolation, isolated nuclei were incubated with 10mM pyruvate in nuclear storage buffer (Sigma Aldrich) for 8 hrs at 37°C. The experiments were terminated by the addition of ice-cold nuclear storage buffer and the nuclei were centrifuged at 500 x g before they were washed with ice-cold storage buffer to remove any excess pyruvate. Nuclei were then prepared for either metabolite extraction and acetyl-CoA measurements by mass spectrometry or protein extraction and histone acetylation by immunoblots.

Metabolite extraction: Nuclei and cells were re-suspended in 800µL of ice-cold 80% methanol and 20% ddH_2O. Samples were vigorously vortexed and placed in liquid N_2 for 10 minutes to freeze. Samples were then thawed on ice for 10 minutes, before freeze-thaw cycle was repeated. Samples were centrifuged at 13,000 x g to pellet cell debris, lipids and proteins. Supernatant was evaporated and resulting metabolites were re-suspended in HPLC-grade H_2O. Metabolites were normalized to protein concentration.

Mass spectrometry for $^{13}C_1$-acetyl-CoA: Isolated nuclei from scrambled and PDC-E1 siRNA-treated cells were exposed to $^{13}C_2$-pyruvate (Cambridge Isotope Laboratories, Andover, MA) for 8 hrs, before the experiment was terminated with the addition of ice-cold storage buffer. Metabolites were extracted and 30µL of samples was diluted to 120µL with methanol and flow injected to the MS using 4000 QTRAP mass spectrometer (AB Sciex, Concord, Canada) with either enhanced product ion (EPI; IonSpray voltage of -4500V) or enhanced MS (EMS; IonSpray voltage of 5500V).

Mass spectrometry for glycolytic intermediates

Seven microliters of sample was injected using a 4000 QTRAP mass spectrometer (AB Sciex) equipped with a UHPLC 1290 system (Agilent Technologies, Mississauga, Canada) via SRM for all 9 glycolytic intermediates and acetyl-CoA. Samples were delivered to the MS with mobile phases A (20mM NH_4OH, 20mM NH_4Ac in 95%/5% H_2O/CH_3CN) and B (98% CH_3CN, 2% H_2O) via a 2.0mm i.d. x 10cm HILIC Luna NH_2 column (Phenomenex, Torrance, CA) at 250µl/min using negative ion LC/MS/MS analytical run. The dwell time was 5ms per SRM

transition, and collision energy was optimized for each SRM transition. Total cycle time was 2.09s.

Histone extraction

Histone extraction was performed using the commercially available EpiQuik Global Histone Acetylation Assay kit (Epigentek, Brooklyn, NY). Briefly isolated nuclei and whole cells were lysed and proteins were precipitated with 25% trichloracetic acid. Extracted histone pellets were dissolved in HPLC-grade distilled water.

^{1}H-Nuclear Magnetic Resonance (^{1}H-NMR)

^{1}H-NMR spectra was acquired on an 800-MHz Inova spectrometer (Agilent formerly Varian Inc, Palo Alto, CA) equipped with a HCN Z-axis gradient cold-probe. ^{1}H-NMR spectra were acquired at 25°C using the first increment of a 2D-^{1}H-^{1}H-NOESY probe sequence, commonly referred to as the metnosey (ie. 1D-^{1}H-NOESY). Spectra were collected with 128 transients and 8 steady state scans using a 4 second acquisition time and a 990 millisecond presaturation, with saturation during the 100 millisecond-mixing period.

Cycloheximide Experiments

786-0 cells were serum starved and pre-treated with either vehicle (DMSO) or 100μg/ml cycloheximide (Cell Signaling) for 24hrs prior to serum stimulation for 4 hrs in the presence of either vehicle or cycloheximide. After nuclear isolation, protein was extracted and immunoblots were performed.

Adenoviral Infection

A549 cells were infected with AdCA5 or AdLacZ at a multiplicity of infection of 500 for 48 hrs allowing an infection rate of ~100% (Figure 3-14A) as previously described (Manalo et al., 2005; Sutendra et al., 2013). After 48hrs cells were than transfected with scrambled vs. PDC-E1 siRNA.

Pyruvate dehydrogenase kinase I (PDKI) Transfection

PDKI plasmid was generated by OriGene Technologies (Rockville, MD) and 40μg of plasmid was transfected into A549 cells using Xfect transfection agent (Clontech). After 48hrs cells were transfected with either scrambled or PDC-E1 siRNA.

Epidermal Growth Factor (EGF) Experiments

A549 cells were treated with vehicle (PBS) or 500ng/mL rhEGF (Sigma Aldrich) or 10μM Gefitinib (Cayman Chemicals) for 24 hrs prior to nuclear isolation. After nuclear isolation, nuclei were prepared for either immunocytochemistry or immunoblots. 786-0 cells were treated with either vehicle (DMSO) or 5μM rotenone (Sigma Aldrich) in the presence of rhEGF for 24hrs prior to fixation in paraformaldehyde (4%), immunofluorescence staining and confocal imaging.

KNK437 Experiments

A549 or 786-0 cells were serum starved and pre-treated with either vehicle (DMSO) or 100μM KNK437 (Santa Cruz Biotechnology) for 24hrs prior to serum stimulation for 4 hrs in the presence of either vehicle or KNK437. After nuclear isolation, protein was extracted and immunoblots were performed.

Immunoprecipitation

The Dynabeads co-immunoprecipitation kit (Invitrogen Canada) was used as per manufacturer's instructions. Immunoprecipitation was performed on conjugated beads with Hsp70 (mouse host; Santa Cruz Biotechnology). Immunoblots were then performed using a rabbit host to Hsp70 (abcam), PDC-E1 (abcam) and PDC-E2 (abcam) and a goat host to PDK I (Santa Cruz Biotechnology).

Immunoblotting

Standard SDS-PAGE and immunoblotting was performed as previously described (Bonnet et al., 2007) and with antibody dilutions as recommended by the manufacturer. Where required, SDS-PAGE of purified histones as well as nuclear,

mitochondrial and cellular protein was performed on 16.5% Tricine gels (Bio-Rad, Montreal, Quebec) followed by immunoblotting to low-pore size (0.2 μm) nitrocellulose (Bio-Rad). Primary antibodies were the same as in confocal microscopy plus antibodies against: actin, Ac-H3K9, Ac-H3K18, ATP-citrate lyase, citrate synthase, ^{Ser293}P-E1α, isocitrate dehydrogenase 2, lamin, lipoic acid, succinyl-CoA dehydrogenase, succinyl-CoA synthethase purchased from Abcam; HIF1α purchased from BD Biosciences; MAPK, ^{Tyr204}P-MAPK, Ac-lysine (against all acetyl-lysine residues) and acetyl-p53 (against acetyl-lysine residue 382) were purchased from Cell Signaling Technology; Ac-H2B (against acetyl-lysine residues 5, 12, 15 and 20), Ac-H4 (against acetyl-lysine residues 5, 8, 12 and 16), Cdk2, cyclin A and E2F purchased from Millipore; PDPI & PDPII and α-tubulin & Ac-tubulin purchased from Sigma Aldrich; E3BP was purchased from GeneTex; Ac-Foxo1 (against acetyl-lysine residues 259, 262 and 271) was purchased from Santa Cruz Biotechnology. Data on PDC immunoblots were also confirmed with additional antibodies to PDC E1 (and its competing peptide) from Abgent. For all PDC antibodies (E1, E2 and E3), there was only one clear band at the correct molecular weight and the competing peptide to PDC-E1 eliminated the band of interest, confirming the specificity of the antibodies used.

Statistical analyses

Unpaired Student's *t*-test was used for statistical calculations when comparing the effects of treatment between two sample groups. Error bars indicate standard error of the mean. For correlation studies, a Pearson Product-Moment Correlation Coefficient Test was used (Figure 3-11H).

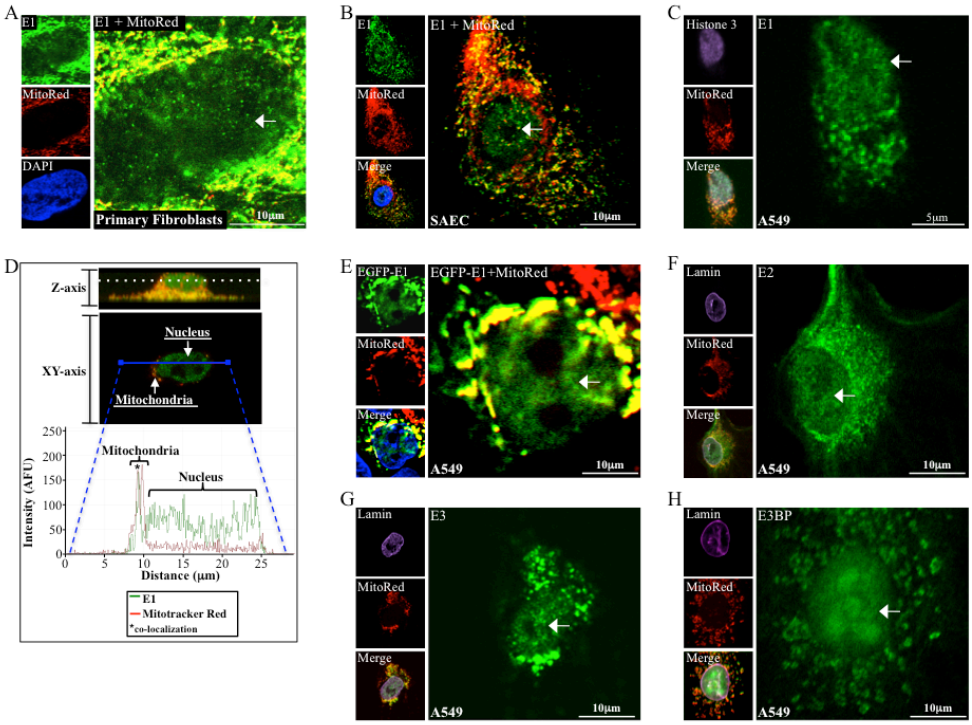

Figure 3-1. PDC is present in the nucleus of human cells.

(A-C) Primary fibroblasts **(A)**, small airway epithelial cells (SAECs) **(B)** and A549 cells **(C)** were co-stained with an antibody to the α subunit of PDC-E1 (green), the mitochondrial marker MitoTracker Red (red) and either the nuclear marker DAPI (blue for **(A-B)**) or histone 3 (purple for **(C)**). The arrow shows PDC-E1 localized in the nucleus in the absence of a mitochondrial signal. **(D)** An A549 cell was co-stained with PDC-E1 (green) and MitoTracker Red (red) and scanned at 2μm increments along the z-axis using confocal microscopy (top image). The fluorescence intensities mid-lane in the cell in the XY axis are shown (top and middle images). **(E)** A549 cells were transfected with a plasmid encoding for EGFP-PDC-E1 and co-stained with MitoTracker Red and DAPI. EGFP-PDC-E1 is clearly seen in the nucleus (white arrow). **(F-H)** A549 cells were co-stained with PDC-E2 **(F)**, PDC-E3 **(G)** and PDC-E3BP **(H)** (all in green), MitoTracker Red and lamin (purple). The images were taken at the mid-plane of the cell, and clearly show the nuclear presence of PDC (white arrow).

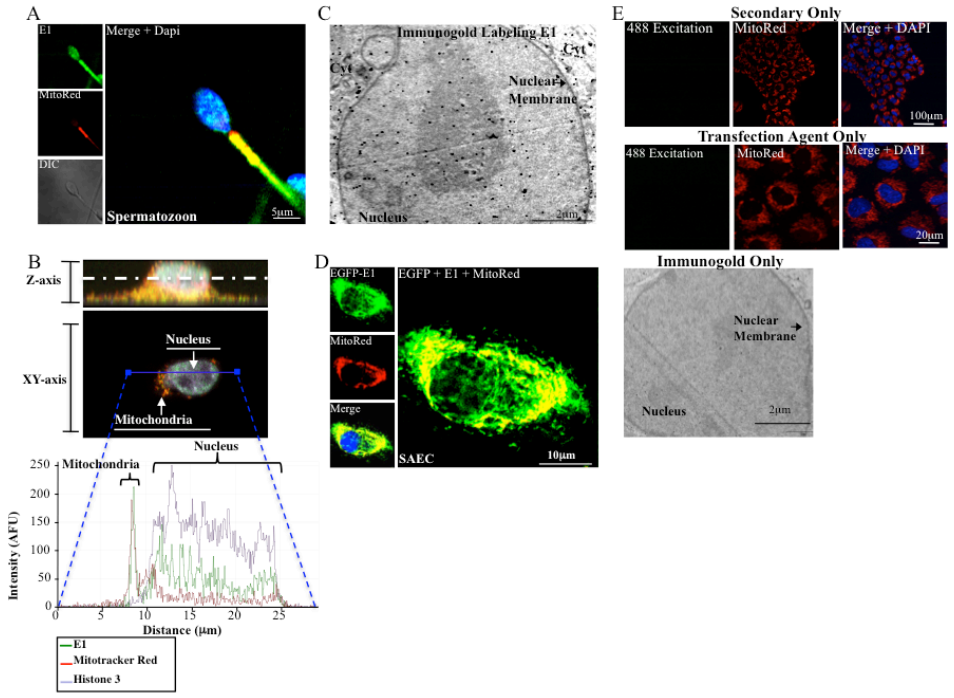

Figure 3-2. PDC-E1 is localized in the mitochondria and nucleus (related to Figure 3-1).

(A) Spermatozoa were co-stained with an antibody to the α subunit of PDC-E1 (green), the mitochondrial marker MitoTracker Red (red) and the nuclear stain DAPI (blue) and imaged using confocal microscopy. PDC-E1 co-localizes with the mitochondria (yellow), shown in the merged panel, but also localizes in the nucleus, which lacks mitochondria. DIC shows morphology of a spermatozoon.

(B) An intact A549 cell co-stained with PDC-E1 (green), MitoTracker Red (red) and the nuclear marker histone 3 (purple) was systematically scanned at 2μm increments along the z-axis using confocal microscopy (top image). Zeiss physiology option software was used to analyze the fluorescence intensity mid-plane in the cell at the XY axis. PDC-E1 and histone 3 have a similar signal pattern in the nucleus. The histone 3 fluorescence signal was not detected in the mitochondria, while the MitoTracker signal was not detected in the nucleus.

(C) A549 cells were labeled using immunogold staining with an antibody against the α subunit of PDC-E1 (black dots) and imaged using transmission electron microscopy. PDC-E1 was highly expressed in the nucleus within the nuclear membrane (Cyt=cytosol). PDC-E1 presence in the cytoplasm and the nuclear membrane is also compatible with the trafficking of PDC-E1 from the mitochondria to the nucleus as discussed in the text. The negative control (immunogold only) labeling is presented in Figure 3-2E.

(D) SAECs were transfected with a plasmid encoding for enhanced green fluorescent protein in-frame with the α subunit of PDC-E1 (EGFP-PDC; green) and co-stained with MitoTracker Red (red) and the nuclear stain DAPI (blue). EGFP-PDC-E1 co-localization with the mitochondria (yellow) is shown in the merged panel (left). EGFP-PDC-E1 is also localized in the nucleus as shown by the EGFP signal, obtained at a mid-plane level cutting through the nucleus.

(E) Secondary-only antibody to Fitc did not provide a fluorescence signal, validating the specificity of the antibody used. MitoTracker Red (red) and the nuclear stain DAPI (blue) are also shown (top). The EGFP signal detected was not due to our transfection agent, as there was no detectable fluorescence signal with our transfection agent-only control sample. MitoTracker (red) and the nuclear stain DAPI (blue) are also shown (middle). Immunogold-only staining and electron microscopy shows the specificity of our immunogold labeling.

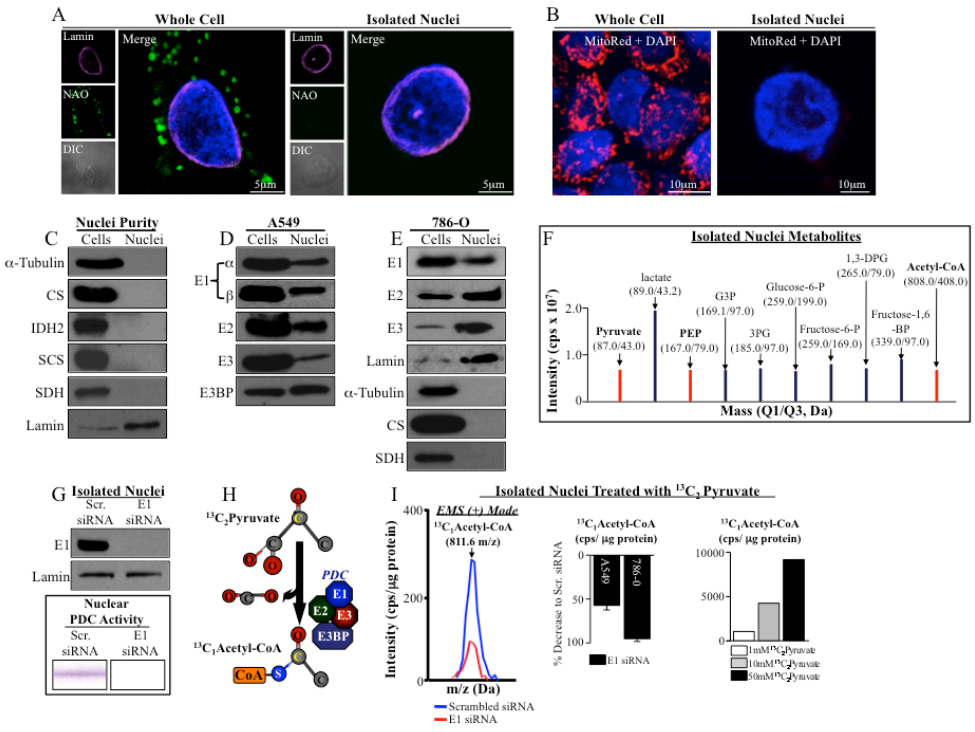

Figure 3-3. Nuclear PDC is functional and can synthesize acetyl-CoA.

(A-B) The mitochondrial membrane markers nonyl-acridine orange [NAO (green; **(A)**)] and MitoTracker Red **(B)** stained whole cells, but signal was not detectable in isolated nuclei preparations. Nuclei were stained with lamin (purple) or DAPI (blue). **(C)** Our isolated nuclear preparations had no detectable levels of the cytoplasmic marker α-tubulin and mitochondrial markers citrate synthase (CS), isocitrate dehydrogenase 2 (IDH2), succinyl-CoA synthetase (SCS) and succinate dehydrogenase (SDH); (an example from A549 cells is shown). **(D-E)** Immunoblots showing that all subunits of PDC were present in isolated pure nuclei of A549 and 786-O cells. **(F)** Many glycolytic intermediates including phosphoenolopyruvate (PEP), pyruvate, and acetyl-CoA (red) were detected in isolated nuclei from A549 cells, using collision-induced mass spectrometry. **(G)** There was no detectable PDC-E1 protein (immunoblot, top) or enzymatic activity measured by a dipstick assay from nuclei isolated from PDC-E1 siRNA-treated cells. **(H)** Mechanism for the $^{13}C_2$-pyruvate experiments. **(I)** Isolated nuclei from

A549 or 786-0 cells previously treated with either PDC-E1 or scrambled siRNA were incubated with $^{13}C_2$-pyruvate for 8 hrs. The nuclei lacking PDC-E1 had decreased levels of $^{13}C_1$-acetyl-CoA compared to scrambled siRNA controls, measured by mass spectrometry and normalized to protein concentration. Increasing doses of labeled pyruvate showed a dose-dependent increase in labeled acetyl-CoA.

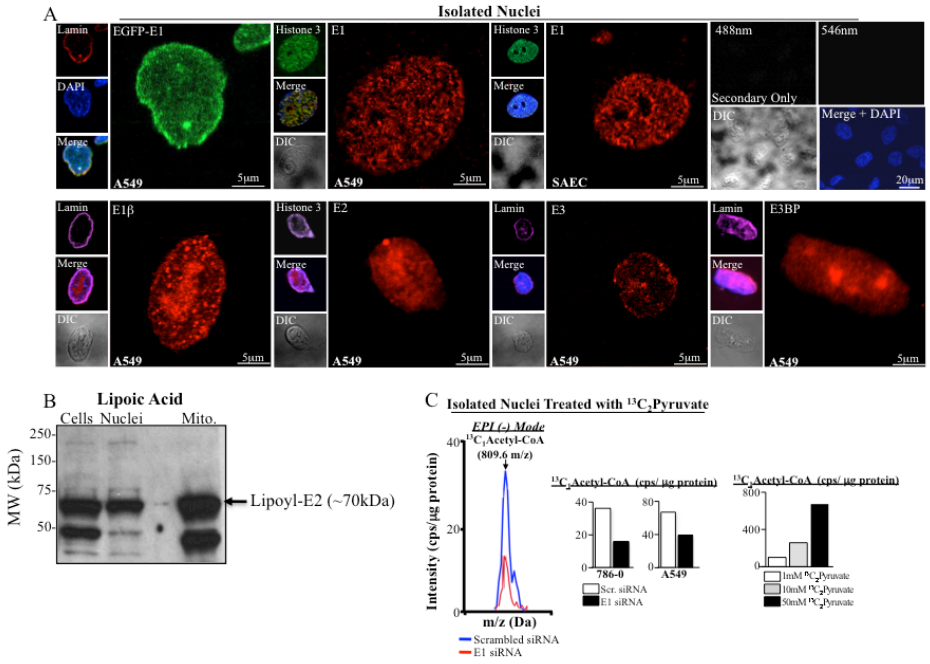

Figure 3-4. PDC is present in isolated highly pure intact nuclei free of mitochondrial membranes from A549 and SAEC cells and is important for nuclear generation of acetyl-CoA (related to Figure 3-3).

(A) Isolated nuclei from A549 cells transfected with EGFP-PDC-E1 plasmid (green) were intact as assessed by the nuclear membrane marker lamin (red). EGFP-PDC-E1 localization within the nuclei (stained blue with DAPI) is shown in the merged panel (upper left). Isolated nuclei from A549 and SAECs (upper middle) were co-stained with antibodies to the α subunit of PDC-E1 (red) and histone 3 (green) and the nuclear stain DAPI (blue). Both PDC-E1 and histone 3 were detected in isolated nuclei, using confocal microscopy. DIC shows morphology of isolated nuclei. Secondary only antibodies did not provide a fluorescence signal, validating the specificity of the antibodies used. The nuclear stain DAPI is in blue and DIC shows the morphology of our isolated nuclei (upper right). All four components of PDC (E1, E2, E3 and E3BP) are localized in isolated nuclei from A549 cells (red). In addition our nuclei had intact membranes

as assessed by lamin (purple) and expressed histones (purple) in indicated panels (bottom).

(B) Isolated nuclei contain a lipoylated protein at the molecular weight of E2 (~ 70kDa) as assessed by an antibody to lipoic acid and immunoblots. The same lipoylated protein is also highly detected in isolated mitochondria. The purity of the nuclear samples are shown in Figure 3-3C.

(C) Nuclei from PDC-E1 siRNA-treated A549 and 786-0 cells had decreased levels of $^{13}C_1$-acetyl-CoA compared to scrambled siRNA controls, measured by mass spectrometry (EPI mode) and normalized to protein concentration. Furthermore, isolated nuclei had a dose-dependent increase of labeled acetyl-CoA from labeled pyruvate using EPI mode mass spectrometry.

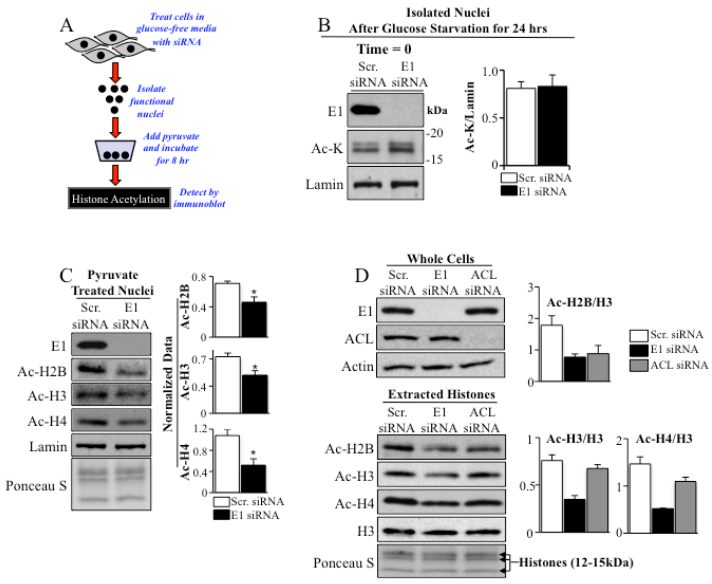

Figure 3-5. PDC is important for histone acetylation.

(A) Experimental design for acetylation experiments in isolated nuclei. **(B)** In the absence of pyruvate at time = 0, there were no differences in acetyl-lysine of proteins within the molecular weight of acetylated histones (n=3 experiments) between nuclei isolated from PDC-E1 siRNA or scramble-treated cells. **(C)** Nuclei lacking PDC-E1 exposed to 10mM pyruvate for 8hrs, had decreased levels of acetylated H2B, H3 and H4, compared to control. Lamin and Ponceau S were loading controls. Representative immunoblots are shown to the left and quantified mean data normalized to lamin are shown to the right (n=3 experiments, *$p<0.05$). **(D)** PDC-E1 and ACL siRNA-treated A549 cells had almost complete knockdown of PDC-E1 and ACL respectively, compared to scrambled siRNA-treated cells (top). Extracted histones from PDC-E1 and ACL siRNA-treated A549 cells exposed to 10mM glucose had decreased levels of acetylated H2B, H3 and H4 compared to scrambled siRNA control (bottom). Quantified mean data (to total H3) are shown on the right (n=3 experiments).

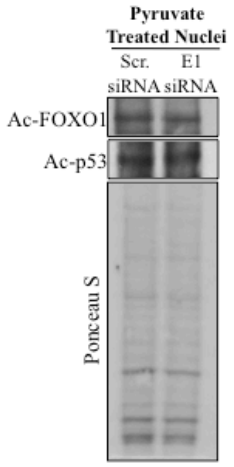

Figure 3-6. Acetyl-CoA generated from nuclear PDC is not required for acetylation of the tumor suppressor proteins p53 and FOXO1 in A549 cells (related to Figure 3-5).

Isolated nuclei from PDC-E1 siRNA-treated cells exposed to 10mM pyruvate for 8hrs showed no differences in acetylated p53 and acetylated FOXO1, compared to nuclei from scrambled siRNA-treated cells. Total protein levels as measured by Ponceau S were unchanged between isolated nuclei from scrambled versus PDC-E1 siRNA-treated cells. Representative gels are shown.

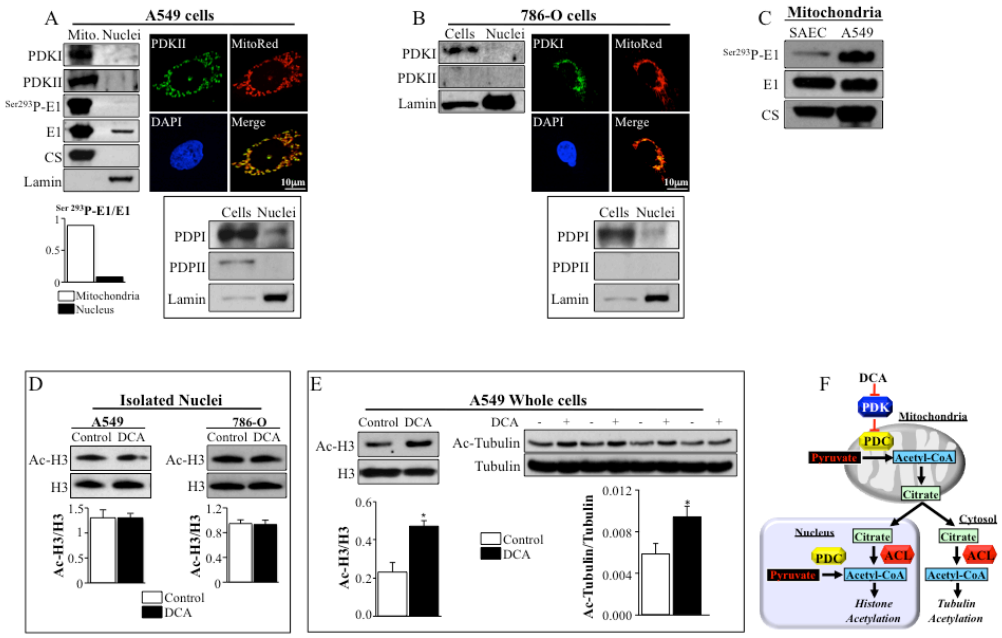

Figure 3-7. Nuclear PDC is regulated differently than mitochondrial PDC.

(A) A549 cells have high levels of PDKI and PDKII in isolated mitochondria, but no detectable levels in isolated nuclei. Phosphorylated PDC-E1 serine-293 was present in isolated mitochondria (where PDK is present) but not in isolated nuclei (where PDK is absent) and the ratio of P-E1/E1 is shown below. Confocal microscopy shows the presence of PDKII (green) in the mitochondria as assessed by co-localization (yellow) with MitoTracker Red in the merge panel, but not in the nucleus, stained with DAPI (blue) (upper right). Immunoblot showing that PDPI, but not PDPII, is present in isolated nuclei from A549 cells (bottom right). **(B)** In 786-O cells PDKI (but not PDKII) is present in whole-cell preparations, but not in isolated nuclei (left). The absence of PDK in the nucleus is confirmed by confocal microscopy (top right). PDPI, but not PDPII is present in isolated nuclei from 786-O cells (bottom right). **(C)** A549 cells had higher levels phosphorylated serine-293 on PDC-E1 compared to isolated mitochondria from normal SAECs (CS=citrate synthase). **(D)** Extracted histones from isolated A549 (left) and 786-O (right) nuclei exposed to DCA (5mM) had similar levels of

acetylated H3 compared to vehicle-treated control cells. **(E)** In contrast, DCA increased the acetylation of H3 (left) and tubulin (right) in whole A549 cells, reflecting the activation of mitochondrial PDC. Representative immunoblots (top) and quantified mean data normalized to total H3 (left) or tubulin (right) are shown (n=4 experiments, *$p<0.05$). **(F)** Mechanism for DCA-mediated increase in acetylation (see results section for discussion).

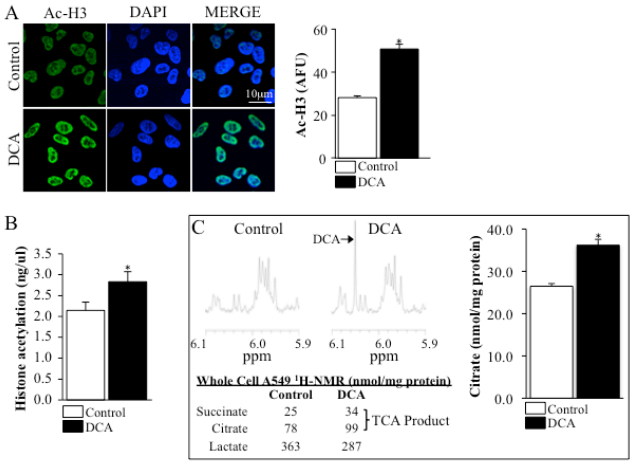

Figure 3-8. The PDK inhibitor Dichloroacetate (DCA) increases acetyl-H3 and acetyl-tubulin in whole cell preparations (related to Figure 3-7).

(A) A549 cells treated with DCA had increased levels of acetylated-H3 (green) compared to vehicle-treated controls, using immunofluorescence and confocal microscopy. Acetylated-H3 co-localized with the nuclear stain DAPI (blue). Representative images (left) and quantified mean data (right) are shown (n=4 experiments, *$p<0.05$).

(B) A549 cells treated with DCA had increased levels of acetylated-H3, using a commercially available H3 Elisa assay (n=3 experiments, *$p<0.05$).

(C) A549 cells treated with DCA had increased levels of succinate and citrate, and had decreased levels of lactate, using proton-nuclear magnetic resonance (^{1}H-NMR; left). Representative image showing the peak for DCA (top) and levels of metabolites (below) are shown. A549 cells treated with DCA had increased levels of citrate, using a commercially available citrate assay kit (right; n=3 experiments, *$p<0.05$).

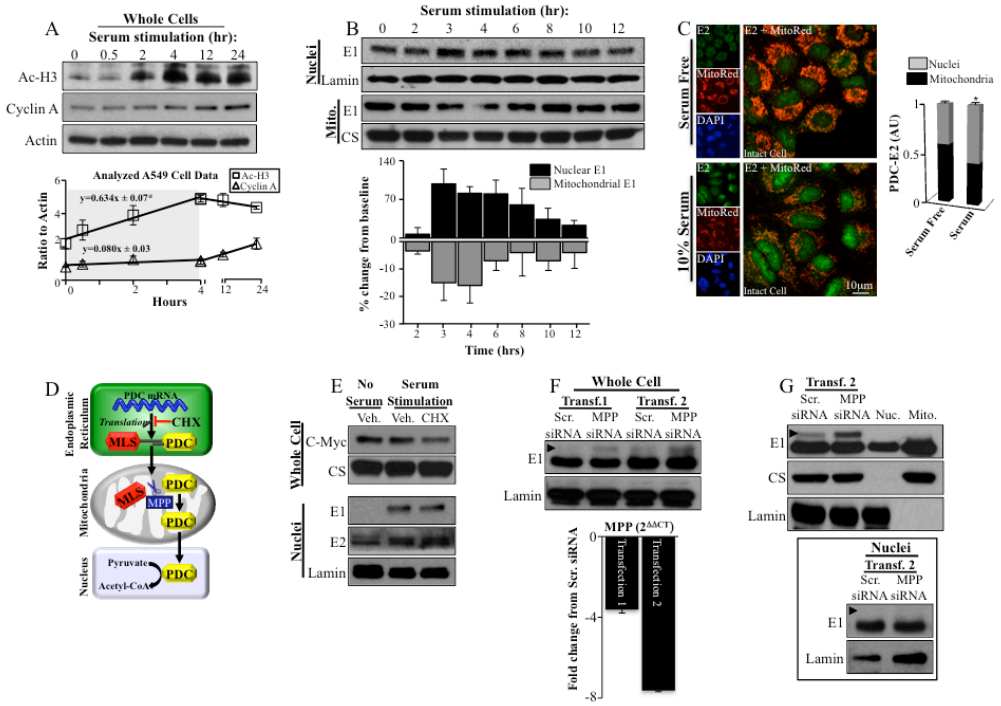

Figure 3-9. PDC is translocated from the mitochondria to the nucleus.

(A) Serum stimulation time course after cell cycle synchronization in G1phase showed an early increase in acetylation of H3, followed by an increase in the S-phase marker cyclin A. Representative immunoblots are shown above. The rate of acetylation of H3 is faster than cyclin A expression within the first 4 hrs after introduction of serum. Note the brake in the time scale showing a later relative plateau in H3 acetylation, while cyclin A levels continue to increase (n=3 experiments, *p<0.001 for Ac-H3 of compared to cyclin A slopes). **(B)** Serum stimulation time course shows an increase in nuclear levels of PDC-E1 peaking at 3-4hrs, associated with a parallel decrease in mitochondrial PDC-E1. This was followed by a return toward baseline levels of both the mitochondrial and nuclear PDC levels. Representative immunoblots are shown above and quantified data normalized to either lamin (nuclei) or citrate synthase (CS) (mitochondria) are shown below (n=4 experiments). **(C)** A549 cells were co-stained with PDC-E2 (green), MitoTracker Red (red) and DAPI (blue). The mitochondrial E2 signal was quantified by signal overlap with MitoTracker Red, while nuclear signal was

quantified by signal overlap with DAPI in the same cell, and the ratio of the two for each cell was calculated. Serum stimulation increased the nuclear to mitochondrial ratio suggesting nuclear translocation from mitochondria (n=25 cells, *$p<0.05$). **(D)** Experimental design for the study of nuclear PDC translocation using Cycloheximide (CHX) and gene silencing of MPP. **(E)** In response to serum stimulation (4hrs) nuclear PDC-E1 and PDC-E2 increased and this was not altered by CHX, which decreased the levels of c-myc. **(F)** Using two siRNA transfection approaches to silence MPP we found a clear signal of the unprocessed (precursor) form of PDC-E1 (arrowhead). Lamin was used as a loading control. qRT-PCR shows the relative fold change for both MPP siRNA transfection approaches. Note that more effective silencing (transfection 2) resulted in higher levels of the PDC-E1 precursor. **(G)** The PDC-E1 precursor was not detected in protein from isolated nuclei or mitochondria loaded in the same gel with whole-cell protein from MPP siRNA-treated cells, which clearly showed the presence of the precursor (top; arrowhead shows precursor form). The precursor PDC-E1 was not detectable in nuclei isolated from the MPP siRNA-treated cells (arrowhead represents where the precursor band would have been detected).

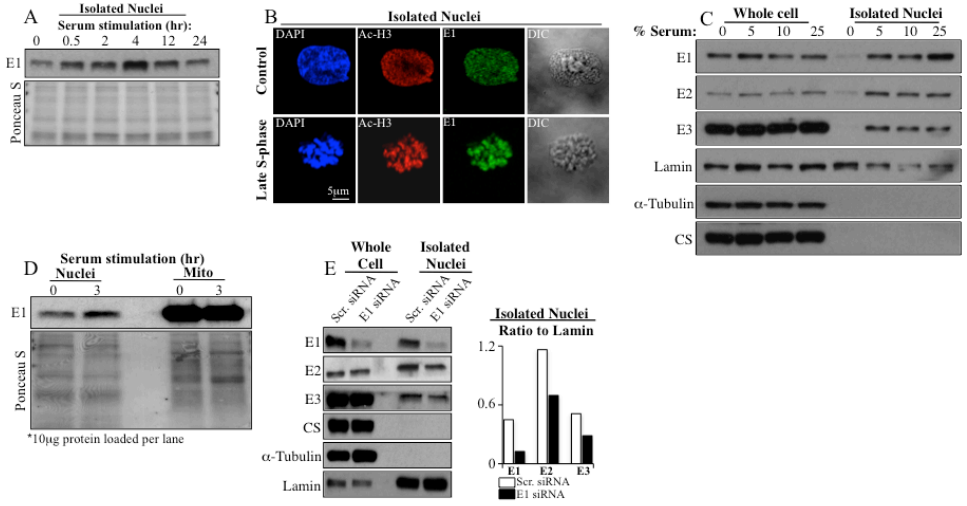

Figure 3-10. Nuclear/mito PDC-E1 ratio increases during serum stimulation and PDC translocates to the nucleus as an intact unit (related to Figure 3-9).

(A) Nuclear PDC-E1 shows a similar increase to acetyl-H3 peaking (shown in Figure 3-9A) at 4hrs post serum stimulation. Total protein levels as measured by Ponceau S remained similar between all timepoints.

(B) Isolated nuclei from A549 cells were co-stained with antibodies to Ac-H3 (red), the α subunit of PDC-E1 (green) and the nuclear stain DAPI (blue). Both PDC-E1 and Ac-H3 were increased in isolated nuclei during late S-phase. DIC shows morphology of isolated nuclei.

(C) Serum stimulation as low as 5% increases nuclear levels of all catalytic components of PDC, while serum stimulation, even as high as 25%, does not decrease overall PDC levels in whole cells. This suggests that the associated decrease in mitochondrial PDC components that we show earlier is not due to protein degradation, but it represents translocation to the nucleus.

(D) The same amount of protein (10μg) from isolated nuclei and mitochondria preparations at baseline and 3hrs post-serum stimulation (as shown in Figure 3-

9B) was loaded on the same immunoblot. Total protein levels were similar between the 0 and 3 hours groups, although there are apparent differences in the bands between the nuclear and mitochondria on Ponceau S, reflecting the different proteome in the two organelles.

(E) PDC translocates to the nucleus as an intact unit as knockdown of one specific component of PDC (i.e. gene silencing of the E1 gene by siRNA) results in decreased nuclear levels of other PDC components (E2 and E3), but does not alter overall levels of these components in whole cells. Nuclear purity was shown by absence of citrate synthase (CS) and tubulin in the nucleus. The ratios of PDC components to lamin are shown on the right.

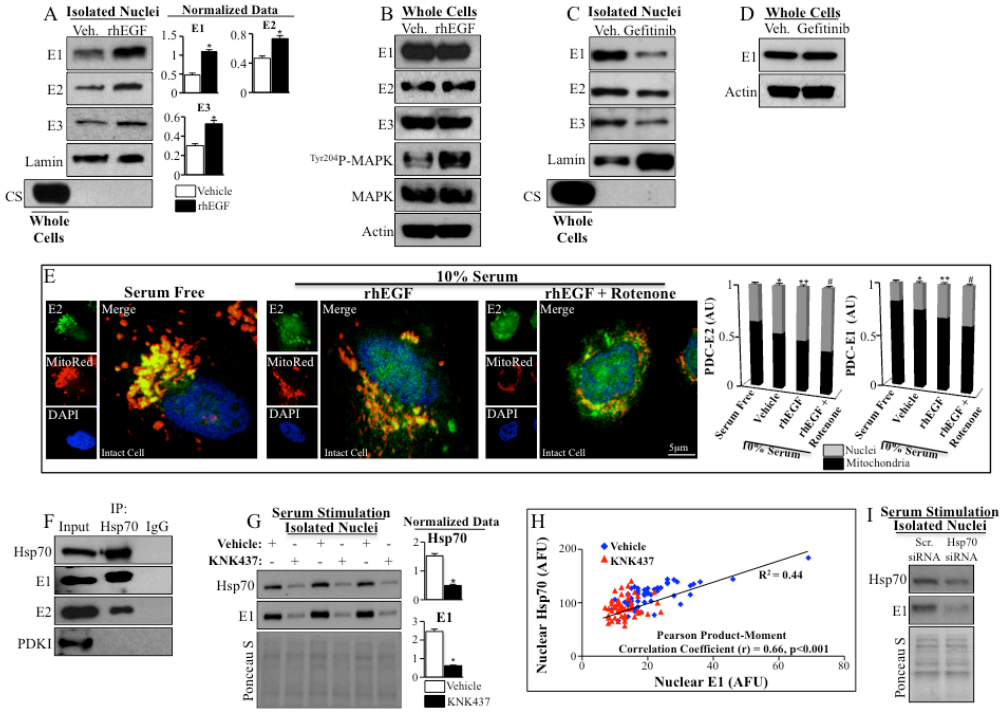

Figure 3-11. Signals increasing the nuclear translocation of PDC.

(A-B) Isolated nuclei from rhEGF-treated A549 cells have increased levels of PDC-E1, E2 and E3 compared to the vehicle-treated cells (n=3 experiments, *p<0.05) **(A)**, without changing total cellular levels, while rhEGF treatment increased tyrosine-204 phosphorylation of MAPK **(B)**. Lamin and actin were used as loading controls. **(C-D)** Gefitinib (Gef) decreased nuclear levels of all three PDC subunits, as shown by immunoblots, without changing the total cellular expression. **(E)** 786-0 cells were co-stained with PDC-E2 (green), MitoTracker Red (red) and DAPI (blue). Serum stimulation increased the nuclear to mitochondrial ratio, compared to serum-free treated cells; this was enhanced by rhEGF and further enhanced by the addition of rotenone (5μM) (n=25 cells, *p<0.05 compared to serum free, **p<0.05 compared to vehicle, #p<0.05 compared to rhEGF). A similar pattern was seen in PDC-E1translocation (representative images shown in Figure 3-12B). **(F)** Hsp70 co-immunoprecipitates with PDC-E1 and PDC-E2, but not with PDKI in A549 cells. Input represents 2.5μg of whole cell lysate. **(G)** Serum-stimulated (4hrs) A549 cells pre-treated

with KNK437 (100μM) show decreased nuclear levels of both Hsp70 and PDC-E1 compared to vehicle (DMSO)-treated cells. Mean data are normalized to Ponceau S (n=3 experiments, *p>0.05). **(H)** The same cells as in **(G)** were co-stained with Hsp70 and PDC-E1, imaged with confocal microscopy and the nuclear fluorescence intensity was measured. A Pearson product-moment correlation plot showed that nuclear levels of Hsp70 and PDC-E1 correlate positively ($r=0.66$; $p<0.001$; n=50 cells/group). Representative images are shown in Figure 3-12H. **(I)** Serum stimulated (4hrs) A549 cells transfected with Hsp70 siRNA show decreased nuclear levels of both Hsp70 and PDC-E1, compared to scrambled-transfected cells.

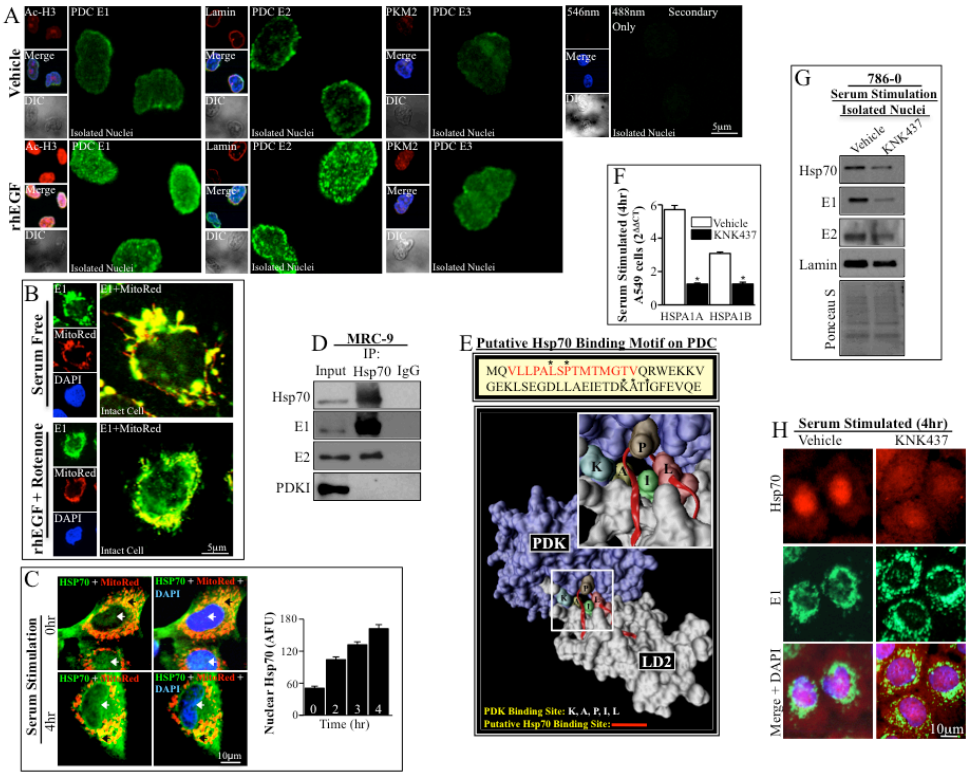

Figure 3-12. rhEGF, rotenone and Hsp70 can increase nuclear localization of PDC (related to Figure 3-11).

(A) Isolated nuclei from recombinant human EGF (rhEGF)-treated A549 cells have increased nuclear levels of PDC (E1, E2 and E3), using immunofluorescence and confocal microscopy. rhEGF treatment increased nuclear localization of PDC-E1 (green; top panel) and Ac-H3 (red; top panel), PDC-E2 (green; middle panel), PDC-E3 (green; bottom panel) and PKM2 (red; bottom panel). All images included the nuclear stain DAPI (blue). The nuclei had intact membranes as indicated by lamin staining (red; middle panel). DIC shows the morphology and structural integrity of the isolated nuclei. Secondary only antibodies did not provide a fluorescence signal, validating the specificity of the antibodies used.

(B) 786-0 cells were co-stained with PDC-E1 (green), the mitochondrial marker MitoTracker Red (red) and the nuclear stain DAPI (blue) and imaged using confocal microscopy. Mitochondrial E1 signal was quantified by signal overlap with MitoTracker Red, while nuclear signal was quantified by signal overlap with

DAPI, using the Image J 64 processing software. These are representative images of the mean data shown in Figure 3-11E.

(C) Serum stimulation of A549 cells for 4hrs shows progressively increasing nuclear Hsp70 levels compared to baseline control cells. Hsp70 is shown in green, the mitochondrial marker MitoTracker Red is shown in red and the nuclear stain DAPI is shown in blue. Black arrows show Hsp70 co-localization with MitoTracker Red (yellow) and white arrows show nuclear Hsp70. Representative images are shown on the left and quantified mean data for nuclear Hsp70 are shown on the right (n=50 cells per group).

(D) Hsp70 co-immunoprecipitates with PDC-E1 and PDC-E2, but not with PDKI in MRC-9 cells as shown by immunoblots. Input represents 2.5μg of whole cell lysate.

(E) Sequence of residues 133-182 of PDC-E2 encoding for part of the lipoyl-domain 2 (LD2), reveals putative Hsp70 binding motifs (red) and known PDK interacting residues (highlighted by *). These include Leu 140 (L), Pro 142 (P), Lys 173 (K), Ala 174 (A) and Ile 176 (I) of LD2 (Kato et al., 2005; Roche et al., 2003) (top). Ribbon representation of putative Hsp70 binding motifs (red), shows a potential binding region within the PDK binding site for LD2. PDK is shown in purple and LD2 is shown in grey surface representation. Inset shows higher magnification of putative Hsp70 and PDK binding sites on LD2 of PDC-E2. PDB code 1Y8O (Kato et al., 2005) and the visual molecular dynamics program was used to generate structural images.

(F) Serum stimulated (4hrs) A549 cells, previously serum starved and pre-treated with 100μM of KNK437, show decreased mRNA levels of HSPA1A and HSPA1B, the two genes responsible for inducible Hsp70, compared to vehicle (DMSO)-treated cells (n=3 experiments, *$p<0.05$).

(G) Serum stimulated (4hrs) 786-0 cells previously serum starved and pre-treated with 100μM of KNK437 (which inhibits induced Hsp70) show decreased nuclear levels of Hsp70, PDC-E1 and PDC-E2 compared to vehicle (DMSO)-treated cells, as shown by immunoblots. Lamin and Ponceau S show similar protein loading between vehicle and KNK437 treated cells.

(H) Serum stimulated (4hrs) A549 cells, previously serum starved and pre-treated with 100μM of KNK437 show decreased nuclear levels of Hsp70 (red) and PDC-E1 (green) compared to vehicle (DMSO)-treated cells as shown by immunofluorescence and confocal microscopy. These are representative images of the mean data shown in Figure 3-11H for a Pearson product-moment correlation plot between nuclear Hsp70 and nuclear PDC-E1.

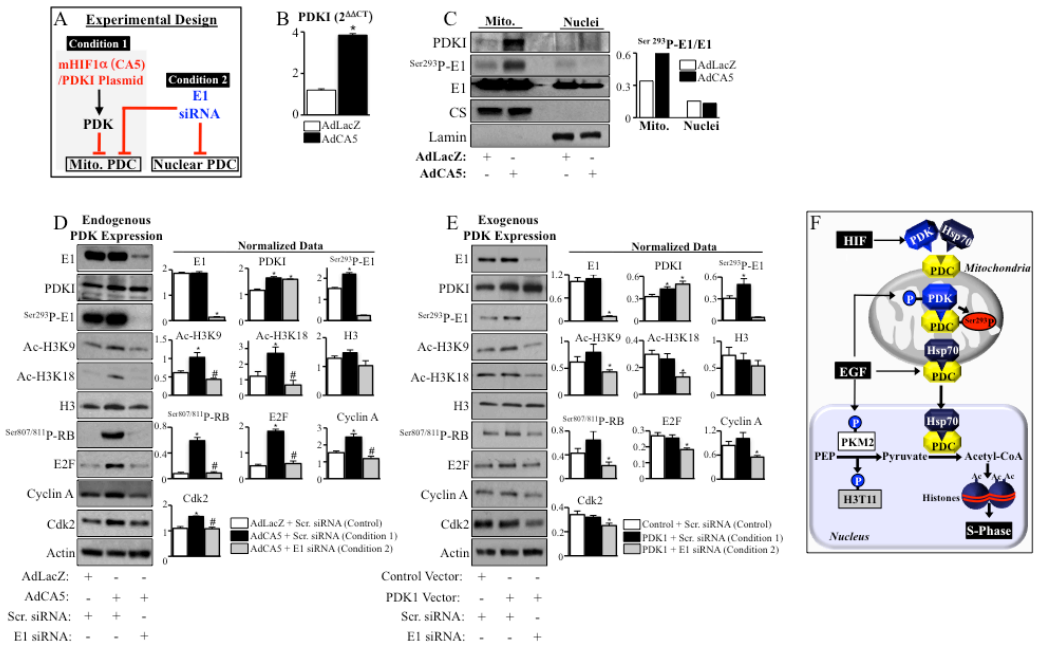

Figure 3-13. Nuclear PDC is important for S-phase entry.

(A) Experimental design for the study of nuclear PDC on S-phase entry in whole cells (see results section). **(B-C)** AdCA5-treated cells had higher PDKI mRNA levels (n=3 experiments, *p<0.01); and higher PDKI protein levels and phosphorylated PDC-E1 serine-293, compared to AdLacZ-treated cells in isolated mitochondria, but no detectable levels of PDKI were seen in isolated nuclei from both groups compared to AdLacZ-treated cells (quantification of the immunoblots is shown to the right). **(D)** A549 cells treated with AdCA5 (condition 1) followed by scrambled siRNA had increased levels of PDKI, phosphorylated PDC-E1, Ac-H3K9, Ac-H3K18, the G1-S-phase progression marker P-Rb, and the S-phase markers elongation-2-factor (E2F), cyclin A and cyclin-dependent kinase 2 (Cdk2), compared to AdLacZ-treated scrambled siRNA cells. In contrast, A549 cells treated with AdCA5 followed by PDC-E1 siRNA (condition 2) had decreased levels of both PDC-E1 and phosphorylated PDC-E1, similar levels of PDK and decreased levels of Ac-H3K9, Ac-H3K18, P-Rb, E2F, cyclin A and Cdk2 compared to AdCA5-treated scrambled siRNA cells (n=3 experiments,

*p<0.05 vs AdLacZ scr. siRNA, #p<0.05 vs AdCA5 scr. siRNA). **(E)** Transfection with PDKI plasmid followed by PDC-E1 siRNA (condition 2) decreased the levels of PDC-E1, phosphorylated PDC-E1, Ac-H3K9, Ac-H3K18, P-Rb, E2F, cyclin A and Cdk2, compared to transfection with PDKI plasmid but treated with scrambled siRNA (condition 1) (n=3 experiments, *p<0.05 vs scr. siRNA). **(F)** Proposed model for the translocation of PDC from mitochondria to the nucleus and its functional role (see discussion).

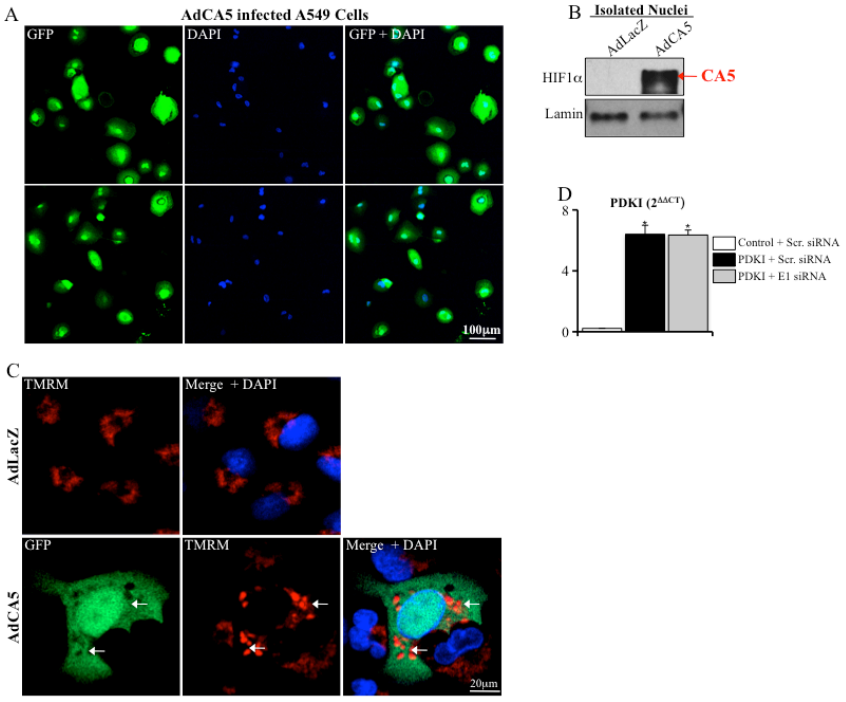

Figure 3-14. AdCA5 infection increases mitochondrial membrane potential and PDKI plasmid increases PDKI expression (related to Figure 3-13).

(A) Infection of A549 cells with AdCA5, which co-expresses green fluorescent protein (GFP) at a multiplicity of infection (MOI) of 500 results in almost 100% infection of cells as indicated by GFP (green). The nuclear stain DAPI is shown in blue. Two different images of the infected A549 cells are shown in the two rows.

(B) Isolated nuclei from AdLacZ and AdCA5-treated A549 cells shows that the CA5 mutant form of HIF1α, which has deletion of amino acids 392-520 and is present at a lower molecular weight than endogenous HIF1α (Manalo et al., 2005), (thus allowing its clear separation from endogenous HIF1α, is only present in the AdCA5-treated cells.

(C) Infection of A549 cells with AdCA5 (GFP; green) results in increased mitochondrial membrane potential (measured the mitochondria specific voltage-sensitive dye TMRM in red; i.e. the more the red the higher the membrane potential) compared to non-infected cells in the same image and AdLacZ infected A549 cells. The nuclei stain Hoechst is shown in blue. This shows that the

mutant, constitutively active HIF1α has the expected effects on mitochondria, as we have previously published (see text).

(D) A549 cells transfected with a PDKI plasmid had higher PDKI mRNA levels compared to empty vector transfected cells, measured by qRT-PCR. Treatment with PDC-E1 siRNA of A549 cells transfected with the PDKI plasmid did not alter PDKI mRNA levels compared to scrambled siRNA-treated cells (n=3 experiments, *$p<0.01$ compared to empty control vector and scrambled siRNA).

Supplementary Video 1 and 2. PDC E1 is present throughout the nucleus of an intact cell (related to Figure 3-1).

Stacked images using confocal microscopy as represented in this video clearly shows the presence of PDC-E1 (green) throughout the nucleus in two separate cell lines (see text). PDC E1 is also localized in the mitochondria as assessed by the yellow co-localization with the mitochondrial stain MitoTracker Red (red). Videos are available on the CellPress website: www.cell.com

References

Alarcon-Vargas, D., Tansey, W.P., and Ronai, Z. (2002). Regulation of c-myc stability by selective stress conditions and by MEKK1 requires aa 127-189 of c-myc. Oncogene *21*, 4384-4391.

Behal, R.H., Buxton, D.B., Robertson, J.G., and Olson, M.S. (1993). Regulation of the pyruvate dehydrogenase multienzyme complex. Annu Rev Nutr *13*, 497-520.

Bonnet, S., Archer, S.L., Allalunis-Turner, J., Haromy, A., Beaulieu, C., Thompson, R., Lee, C.T., Lopaschuk, G.D., Puttagunta, L., Harry, G.*, et al.* (2007). A mitochondria-K+ channel axis is suppressed in cancer and its normalization promotes apoptosis and inhibits cancer growth. Cancer Cell *11*, 37-51.

Bowker-Kinley, M.M., Davis, W.I., Wu, P., Harris, R.A., and Popov, K.M. (1998). Evidence for existence of tissue-specific regulation of the mammalian pyruvate dehydrogenase complex. Biochem J *329 (Pt 1)*, 191-196.

Cai, L., Sutter, B.M., Li, B., and Tu, B.P. (2011). Acetyl-CoA induces cell growth and proliferation by promoting the acetylation of histones at growth genes. Mol Cell *42*, 426-437.

Chacinska, A., Koehler, C.M., Milenkovic, D., Lithgow, T., and Pfanner, N. (2009). Importing mitochondrial proteins: machineries and mechanisms. Cell *138*, 628-644.

Choudhary, C., Kumar, C., Gnad, F., Nielsen, M.L., Rehman, M., Walther, T.C., Olsen, J.V., and Mann, M. (2009). Lysine acetylation targets protein complexes and co-regulates major cellular functions. Science *325*, 834-840.

Dhar, S., and Lippard, S.J. (2009). Mitaplatin, a potent fusion of cisplatin and the orphan drug dichloroacetate. Proc Natl Acad Sci U S A *106*, 22199-22204.

Durieux, J., Wolff, S., and Dillin, A. (2011). The cell-non-autonomous nature of electron transport chain-mediated longevity. Cell *144*, 79-91.

Gao, X., Wang, H., Yang, J.J., Liu, X., and Liu, Z.R. (2012). Pyruvate kinase M2 regulates gene transcription by acting as a protein kinase. Mol Cell *45*, 598-609.

Hitosugi, T., Fan, J., Chung, T.W., Lythgoe, K., Wang, X., Xie, J., Ge, Q., Gu, T.L., Polakiewicz, R.D., Roesel, J.L.*, et al.* (2011). Tyrosine phosphorylation of mitochondrial pyruvate dehydrogenase kinase 1 is important for cancer metabolism. Mol Cell *44*, 864-877.

Horner, D.S., Hirt, R.P., and Embley, T.M. (1999). A single eubacterial origin of eukaryotic pyruvate: ferredoxin oxidoreductase genes: implications for the evolution of anaerobic eukaryotes. Mol Biol Evol *16*, 1280-1291.

Jaenisch, R., and Bird, A. (2003). Epigenetic regulation of gene expression: how the genome integrates intrinsic and environmental signals. Nat Genet *33 Suppl*, 245-254.

Kato, M., Chuang, J.L., Tso, S.C., Wynn, R.M., and Chuang, D.T. (2005). Crystal structure of pyruvate dehydrogenase kinase 3 bound to lipoyl domain 2 of human pyruvate dehydrogenase complex. EMBO J *24*, 1763-1774.

Kato, Y., Tapping, R.I., Huang, S., Watson, M.H., Ulevitch, R.J., and Lee, J.D. (1998). Bmk1/Erk5 is required for cell proliferation induced by epidermal growth factor. Nature *395*, 713-716.
Kiang, J.G., Bowman, P.D., Lu, X., Li, Y., Ding, X.Z., Zhao, B., Juang, Y.T., Atkins, J.L., and Tsokos, G.C. (2006). Geldanamycin prevents hemorrhage-induced ATP loss by overexpressing inducible HSP70 and activating pyruvate dehydrogenase. Am J Physiol Gastrointest Liver Physiol *291*, G117-127.
Kim, J.W., and Dang, C.V. (2005). Multifaceted roles of glycolytic enzymes. Trends Biochem Sci *30*, 142-150.
Kim, J.W., Tchernyshyov, I., Semenza, G.L., and Dang, C.V. (2006). HIF-1-mediated expression of pyruvate dehydrogenase kinase: a metabolic switch required for cellular adaptation to hypoxia. Cell Metab *3*, 177-185.
Koishi, M., Yokota, S., Mae, T., Nishimura, Y., Kanamori, S., Horii, N., Shibuya, K., Sasai, K., and Hiraoka, M. (2001). The effects of KNK437, a novel inhibitor of heat shock protein synthesis, on the acquisition of thermotolerance in a murine transplantable tumor in vivo. Clin Cancer Res *7*, 215-219.
Lodish, H., Berk, A., Zipursky, S.L., Matsudaira, P., Baltimore, D., and Darnell, J. (2000). Section 11.4, Signal-Mediated Transport through Nuclear Pore Complexes. In Molecular Cell Biology, 4th Edition, W.H. Freeman, ed. (New York: W.H. Freemand and Company).
Luo, W., Hu, H., Chang, R., Zhong, J., Knabel, M., O'Meally, R., Cole, R.N., Pandey, A., and Semenza, G.L. (2011). Pyruvate kinase M2 is a PHD3-stimulated coactivator for hypoxia-inducible factor 1. Cell *145*, 732-744.
Manalo, D.J., Rowan, A., Lavoie, T., Natarajan, L., Kelly, B.D., Ye, S.Q., Garcia, J.G., and Semenza, G.L. (2005). Transcriptional regulation of vascular endothelial cell responses to hypoxia by HIF-1. Blood *105*, 659-669.
Mayer, M.P., and Bukau, B. (2005). Hsp70 chaperones: cellular functions and molecular mechanism. Cell Mol Life Sci *62*, 670-684.
Michelakis, E.D., Sutendra, G., Dromparis, P., Webster, L., Haromy, A., Niven, E., Maguire, C., Gammer, T.L., Mackey, J.R., Fulton, D.*, et al.* (2010). Metabolic modulation of glioblastoma with dichloroacetate. Sci Transl Med *2*, 31ra34.
Milarski, K.L., and Morimoto, R.I. (1986). Expression of human HSP70 during the synthetic phase of the cell cycle. Proc Natl Acad Sci U S A *83*, 9517-9521.
Pante, N., and Kann, M. (2002). Nuclear pore complex is able to transport macromolecules with diameters of about 39 nm. Mol Biol Cell *13*, 425-434.
Roche, T.E., Hiromasa, Y., Turkan, A., Gong, X., Peng, T., Yan, X., Kasten, S.A., Bao, H., and Dong, J. (2003). Essential roles of lipoyl domains in the activated function and control of pyruvate dehydrogenase kinases and phosphatase isoform 1. Eur J Biochem *270*, 1050-1056.
Rodriguez, M.A., Garcia-Perez, R.M., Mendoza, L., Sanchez, T., Guillen, N., and Orozco, E. (1998). The pyruvate:ferredoxin oxidoreductase enzyme is located in the plasma membrane and in a cytoplasmic structure in Entamoeba. Microb Pathog *25*, 1-10.
Semenza, G.L. (2010). Defining the role of hypoxia-inducible factor 1 in cancer biology and therapeutics. Oncogene *29*, 625-634.

Shi, Y., and Thomas, J.O. (1992). The transport of proteins into the nucleus requires the 70-kilodalton heat shock protein or its cytosolic cognate. Mol Cell Biol *12*, 2186-2192.
Siebert, G., and Humphrey, G.B. (1965). Enzymology of the nucleus. Adv Enzymol Relat Areas Mol Biol *27*, 239-288.
Sumegi, B., Liposits, Z., Inman, L., Paull, W.K., and Srere, P.A. (1987). Electron microscopic study on the size of pyruvate dehydrogenase complex in situ. Eur J Biochem *169*, 223-230.
Sutendra, G., Dromparis, P., Kinnaird, A., Stenson, T.H., Haromy, A., Parker, J.M., McMurtry, M.S., and Michelakis, E.D. (2013). Mitochondrial activation by inhibition of PDKII suppresses HIF1a signaling and angiogenesis in cancer. Oncogene *32*, 1638-1650.
Sutendra, G., Dromparis, P., Wright, P., Bonnet, S., Haromy, A., Hao, Z., McMurtry, M.S., Michalak, M., Vance, J.E., Sessa, W.C.*, et al.* (2011). The role of Nogo and the mitochondria-endoplasmic reticulum unit in pulmonary hypertension. Sci Transl Med *3*, 88ra55.
Vander Heiden, M.G., Locasale, J.W., Swanson, K.D., Sharfi, H., Heffron, G.J., Amador-Noguez, D., Christofk, H.R., Wagner, G., Rabinowitz, J.D., Asara, J.M.*, et al.* (2010). Evidence for an alternative glycolytic pathway in rapidly proliferating cells. Science *329*, 1492-1499.
Vogelauer, M., Rubbi, L., Lucas, I., Brewer, B.J., and Grunstein, M. (2002). Histone acetylation regulates the time of replication origin firing. Mol Cell *10*, 1223-1233.
Wellen, K.E., Hatzivassiliou, G., Sachdeva, U.M., Bui, T.V., Cross, J.R., and Thompson, C.B. (2009). ATP-citrate lyase links cellular metabolism to histone acetylation. Science *324*, 1076-1080.
Yang, W., Xia, Y., Hawke, D., Li, X., Liang, J., Xing, D., Aldape, K., Hunter, T., Alfred Yung, W.K., and Lu, Z. (2012). PKM2 phosphorylates histone H3 and promotes gene transcription and tumorigenesis. Cell *150*, 685-696.
Yi, C.H., Pan, H., Seebacher, J., Jang, I.H., Hyberts, S.G., Heffron, G.J., Vander Heiden, M.G., Yang, R., Li, F., Locasale, J.W.*, et al.* (2011). Metabolic regulation of protein N-alpha-acetylation by Bcl-xL promotes cell survival. Cell *146*, 607-620.
Yogev, O., Singer, E., Shaulian, E., Goldberg, M., Fox, T.D., and Pines, O. (2010). Fumarase: a mitochondrial metabolic enzyme and a cytosolic/nuclear component of the DNA damage response. PLoS biology *8*, e1000328.
Zhao, Q., Wang, J., Levichkin, I.V., Stasinopoulos, S., Ryan, M.T., and Hoogenraad, N.J. (2002). A mitochondrial specific stress response in mammalian cells. EMBO J *21*, 4411-4419.
Zhou, Z.H., Liao, W., Cheng, R.H., Lawson, J.E., McCarthy, D.B., Reed, L.J., and Stoops, J.K. (2001a). Direct evidence for the size and conformational variability of the pyruvate dehydrogenase complex revealed by three-dimensional electron microscopy. The "breathing" core and its functional relationship to protein dynamics. J Biol Chem *276*, 21704-21713.
Zhou, Z.H., McCarthy, D.B., O'Connor, C.M., Reed, L.J., and Stoops, J.K. (2001b). The remarkable structural and functional organization of the eukaryotic

pyruvate dehydrogenase complexes. Proc Natl Acad Sci U S A *98*, 14802-14807.

Chapter Four

VHL attenuates p53-dependent gene regulation

Abstract

The von Hippel Lindau (VHL) tumour suppressor is known to bind and degrade hypoxia inducible factors (HIF). Furthermore, it has been shown to physically interact with approximately 60 different proteins, and loss of VHL paradoxically results in increased cell proliferation and apoptosis-resistance. Hre, we report that VHL directly interacts with p53, preventing its tetramerization, promoter binding and expression of its target genes, p21 and PUMA, in response to p53-inducing stimuli. This process is independent of prolyl-hydroxylation, HIF activity and VHL mediated HIF degradation. Finally, we show that VHL-deficiency results in an attenuation of p53-inducing therapies in multiple tumor types, *in vivo*. In conclusion, this study suggests that VHL is a multifaceted protein, balancing anti-tumor HIF degradation with pro-tumor p53 inhibition.

Introduction

VHL is described as a tumor suppressor due to its ability to bind hydroxylated hypoxia inducible factors (HIF) and target them for proteasomal degradation (Gossage et al., 2015). Loss of VHL function through either mutation, loss of heterozygosity or epigenetic silencing by promoter methylation is an important event in renal cancer initiation, found in up to ~90% of clear cell renal cell carcinomas (ccRCC) (Moore et al., 2011). However, while VHL-deficiency is strongly associated with ccRCC and HIF activation, it has not been correlated with tumor stage, grade or proliferative index (ki-67 staining) (Gimenez-Bachs et al., 2006; Kondo et al., 2002; Schraml et al., 2002). Furthermore, the impact on overall and cancer-specific survival is not definitive, with some studies suggesting improved survival (Patard et al., 2008; Yao et al., 2002) and others suggesting impaired survival (Kim et al., 2005). This is discrepant from a systematic review which identified high nuclear levels of HIF1α (i.e. VHL's 'target') to be associated with a poor overall survival (Fan et al., 2015).

A possible explanation for these discrepancies is that VHL has functions that are independent of HIF. VHL has been shown to interact with several proteins such as tubulin (Hergovich et al., 2003), RNA Polymerase II (Kuznetsova et al., 2003), transcription factor Sp1 (Cohen et al., 1999; Mukhopadhyay et al., 1997), and the tumor suppressor p53 (Lai et al., 2011). However, these HIF-independent effects of VHL on tumor growth remain unclear.

Recently, several studies have shown that VHL may in fact paradoxically potentiate tumor growth. In order to determine the HIF-independent effects of VHL on ccRCC growth, Yi et al. (2010) created VHL-deficient (-VHL) and wild-type (+VHL) ccRCC lines that expressed similar levels of HIF; by genetically silencing PHD2, which is the critical hydroxylase responsible for marking HIF for recognition by VHL, HIF is no longer ubiquitinated and degraded by the proteasome in +VHL cells (Berra et al., 2003). Surprisingly, when HIF is present in both –VHL and +VHL cells, +VHL cells proliferate faster and grow larger

tumors in xenograft models (Yi et al., 2010). Similarly, using the well-studied RENCA renal cancer model, VHL-deficient RENCA cells (created using CRISPR) have more HIF activation but paradoxically have an unexplained reduction in cell proliferation compared to wild-type VHL RENCA cells (Schokrpur et al., 2016). Finally, when VHL expression is inhibited, by microRNA-101, the low VHL state induces cell cycle arrest and apoptosis (Liu et al., 2016).

Therefore, as p53 is a critical regulator of proliferation and apoptosis and a known VHL interaction partner, we hypothesized that VHL may be negatively regulating p53-dependent gene expression (like p21 and the p53 up-regulated modulator of apoptosis (PUMA)) and that conditions that induce p53, like chemotherapy would have an attenuated effect in VHL-expressing cells.

Results

4.1 VHL inhibits p53 binding to the promoters and expression of its target genes, p21 and PUMA, in response to a p53 inducing stimulus

We confirm that VHL co-immunoprecipitates with p53 (Figure 4-1A), as has been previously shown (Lai et al., 2011; Roe et al., 2006). However, in order to understand the significance of this interaction we analyzed the effect of VHL on p53 target genes, p21 and PUMA, using VHL-expressing (+VHL) and VHL-deficient (-VHL) 786-O cells. Furthermore, we used doxorubicin, a clinically utilized DNA damaging anthracycline chemotherapy, which induces p53 in order to stop the cell cycle to repair or induce apoptosis, as a model to explore VHL-dependent regulation of p53 stimulation. We show that VHL blunts the induction of p53 target genes, p21 and PUMA, in response to doxorubicin treatment (Figure 4-1B). As DNA damage may have off target effects, we verified these results using a second model of p53 induction, nutlin, which causes accumulation of p53 by inhibiting MDM2-dependent proteasomal degradation rather than DNA damage (Figure 4-2A). Furthermore, using chromatin immunoprecipitation, we show that VHL reduces p53 binding to the promoters of its target genes, p21 and PUMA, in response to p53 stimulation (Figure 4-1C). p53 binds its targets' promoters with varying affinity based on quaternary protein structure, with the formation of p53 tetramers facilitating binding (Chene, 2001). Using disuccinimidyl suberate to irreversibly crosslink intracellular proteins, we show that VHL reduces the formation of p53 tetramers in response to p53 stimulation (Figure 4-1D).

When we exclude p53 from the regulation of p21, by overexpressing an exogenous FLAG-p21 protein driven from a CMV promoter (i.e. p53-independent promoter) in +VHL cells, we find that p21 mRNA is restored to levels seen in –VHL cells (Figure 4-2B). Critically, only endogenous (p53-dependent) p21 protein is reduced in +VHL cells, while exogenous FLAG-p21 (p53-independent) protein is expressed at levels that are similar to p21 in –VHL cells (Figure 4-1E). This suggests that VHL inhibits p53-dependent p21 mRNA transcription and does not affect p21 at the protein level. Furthermore, we show that VHL does not co-

immunoprecipitate with p21 protein, even when p21 levels are artificially elevated in the cell by preventing its degradation using the proteasome inhibitor, MG-132 (Figure 4-2C).

These results suggest that VHL inhibits p53-dependent mRNA transcription by preventing the formation of p53 quaternary structures that have higher binding affinity for target promoters.

4.2 VHL inhibits p53-dependent target gene p21 expression, promoting cell proliferation

VHL-expressing 786-O cells (+VHL) express significantly less p21 than VHL-deficient 786-O cells (-VHL) (Figure 4-3A and B). These findings are replicated in a second model of VHL-deficiency with stable re-expression, in RCC4 cells (Figure 4-3C) as well as in a loss-of-function model using CRISPR to deplete VHL in A549 cells, which express wild-type VHL at baseline (Figure 4-3D and Figure 4-4A and B). Furthermore, acute adenoviral reintroduction of full length, wild-type VHL (AdVHL30) but not a mutated VHL (AdVHLΔ114-154), which lacks Exon 2 (a region critical for binding other proteins), reduces p21 levels to those seen in stably VHL-expressing 786-O cells (Figure 4-3E). Taken together, these four models suggest that VHL inhibits p21 expression, possibly through interaction with another protein (i.e. p53).

As p21 is well-known to be regulated by p53, we sought to determine whether this inhibition by VHL is specific to p53. To do this we knocked down p53 using siRNA in -VHL and +VHL cells to show: 1. +VHL alone mimics p21 levels observed with p53 knockdown in –VHL and 2. p53 knockdown does not further decrease p21 expression in the presence of VHL (Figure 4-3F). These results suggest that VHL is inhibiting p53-dependent p21 expression.

Importantly, VHL did not reduce the expression or nuclear localization of p53, suggesting its effect is not via p53 degradation or nuclear export (Figure 4-4C). Furthermore, to ensure that this effect is relatively specific to a VHL-p53 axis, we performed a similar experiment, knocking down Sp1, which like p53 is a transcription factor that can regulate p21 and that has been shown to interact with

VHL (Abbas and Dutta, 2009; Cohen et al., 1999; Mukhopadhyay et al., 1997). Unlike the changes observed with p53 knockdown, we show that loss of Sp1 does not reduce p21 expression regardless of VHL status (Figure 4-4D).

Functionally, p21 is an important cell cycle inhibitor. Therefore, we measured cell proliferation using two metrics, ki67 staining and cell number, and show that +VHL cells, which express less p21, are more proliferative than –VHL cells (Figure 4-3G and H).

4.3 VHL inhibits p21 independent of HIF and does not require prolyl hydroxylation

As the canonical effect of VHL is HIF degradation, we sought to determine if the inhibition of p21 expression by VHL is secondary to VHL-mediated HIF degradation. In order to examine this possible relationship, we performed a series of experiments that alter HIF expression or activity, independent of VHL status, such as: HIF siRNA, hypoxia, pharmacological inhibition of HIF degradation, knockdown of prolyl hydroxylases (that mark HIF for degradation), and overexpression of a HIF isoform that cannot be recognized by VHL.

We took advantage of 786-O cells, which are known to express only HIF2α (and not HIF1α) protein in order to create HIF-deficient, –VHL and +VHL cells using HIF2α siRNA (Figure 4-5A and B; note that VHL degrades HIF2α protein and therefore while HIF2α mRNA is present, HIF2α protein is not)(Hu et al., 2003). We show that although expression of the HIF target gene, GLUT1, is reduced to similar levels in +VHL and –VHL cells treated with siHIF2α, p21 mRNA is only reduced when VHL is present and not in HIF-deficient cells lacking VHL (Figure 4-5A and B). Importantly, we show that neither HIF2α knockdown nor VHL, reduced p53 expression in these cells (Figure 4-6A).

Classically, VHL recognizes and binds hydroxylated proteins, like HIF. Hydroxylation is an oxygen and α-ketoglutarate dependent enzymatic reaction performed by prolyl hydroxylases (PHD), with PHD2 identified as the major

regulator of HIF hydroxylation(Berra et al., 2003). We show that, neither hypoxia, which induces HIF2α, nor infection with AdCA5 (an adenovirus encoding a HIF1α mutant that cannot be hydroxylated) in +VHL cells restores p21 expression to levels measured in –VHL cells (Figure 4-5B). Similarly, treatment with DMOG (a competitive inhibitor of αKG for PHD), restores HIF-driven GLUT1 expression but not p21 expression in +VHL cells (Figure 4-5C). Furthermore, siRNA knockdown of specific PHD isoforms (1, 2, and 3) shows that while knockdown of PHD2 induces GLUT1 expression in +VHL cells, no PHD knockdown restores p21 to levels seen in –VHL cells (Figure 4-5D and Figure 4-6B). These data suggest that VHL-mediated inhibition of p21 expression is independent of both the VHL-HIF interaction, HIF activity, and prolyl hydroxylation.

4.4 VHL inhibits induction of p53-dependent apoptosis and attenuates the response to anthracycline chemotherapy *in vivo*

The growth of tumors cells *in vitro* is a balance of proliferation and apoptosis. While we have shown that VHL increases proliferation (Figure 4-3G and H), we next sought to examine if VHL inhibits p53-dependent apoptosis. In keeping with our results that demonstrate VHL-dependent inhibition of p53 activity, we show that while p53 protein is induced equally, regardless of VHL status, in response to doxorubicin or nutlin treatment, expression of p53-dependent target genes, p21 and PUMA, are not significantly increased in VHL-expressing cells (Figure 4-7A and Figure 4-8A). Functionally, we show that VHL dramatically reduces apoptosis in response to a p53-inducing stimulus, measured using two markers of apoptosis (cleaved PARP and cleaved Caspase 3, Figure 4-7A).

In vivo, tumor growth is dependent on proliferation and apoptosis as well as other factors such as angiogenesis, which is largely regulated by HIF-driven factors such as VEGF and PDGF; any perturbation of VHL will have significant impact on tumor growth *in vivo* secondary to direct effects on HIF. In fact, it has been previously shown that VHL-expressing renal tumor xenografts develop less

frequently and grow more slowly than VHL-deficient renal tumor xenografts(Iliopoulos et al., 1995). Therefore, we used an optimized xenograft protocol, co-injecting matrigel to improve tumor establishment and yield (Mullen, 2004). We used two models of VHL-deficiency: 1. VHL rescue (786-O cells vs. 786-O cells stably expressing VHL) and 2. VHL depletion (A549 cells vs. A549 CRISPR VHL), injecting VHL-deficient tumors on the left flank of the animal and VHL-expressing tumors on the right. We permitted these tumors to grow for 4 weeks and then initiated doxorubicin treatment for another 4 weeks (Figure 4-8B). As hypothesized, we show that VHL-deficient tumors initially grow to be larger than VHL-expressing tumors (Figure 4-7B), likely secondary to the effect of VHL on HIF. However, after p53 induction using doxorubicin, we find that VHL-deficient tumors are much more sensitive to treatment than VHL-expressing tumors, measured by the ratio of the final tumor volume (i.e. after treatment) to the pre-treatment tumor volume (Figure 4-7C). These results suggest that VHL is attenuating the effect of anthracycline treatment on tumors *in vivo*.

Discussion

In this paper, we show that VHL reduces binding of p53 at the promoters of its target genes, p21 and PUMA, thereby attenuating production of these in response to a p53 inducing stimulus (Figure 4-9). This results in increased proliferation and reduced apoptosis in VHL-expressing cancer cells as well as a relative insensitivity to treatment with p53-targeted therapy *in vivo*.

These findings suggest VHL straddles a delicate balance between anti-tumor HIF degradation and pro-tumor p53 inhibition. This is critical for understanding renal tumorigenesis as there is now mounting evidence that VHL-deficiency alone is insufficient for renal cancer initiation (Albers et al., 2013). In fact, several papers have found that normal kidney cells spontaneously form tumors only when both sides of this axis, VHL and p53, have been knocked out, but not with VHL knockout alone (Albers et al., 2013; Harlander et al., 2017). Moreover, in another tissue type, VHL knockout mouse embryonic fibroblasts (MEFs) and fibrosarcomas express more HIF targets and are more vascular, yet proliferate more slowly and express more p21 than wild-type VHL MEFs and fibrosarcomas (Mack et al., 2005). In keeping with this balancing act, Albers et al. 2013 found that VHL knockout lead to proliferation arrest that was abrogated if simultaneous knockout of p53 was performed (Albers et al., 2013).

It must be noted, that while there is accumulating evidence, as discussed above (Albers et al., 2013; Liu et al., 2016; Mack et al., 2005; Schokrpur et al., 2016; Yi et al., 2010), which demonstrate an inhibitory effect of VHL on p53 and proliferation, there is a publication that suggests VHL activates p53 through a direct protein interaction (Roe et al., 2006). In this paper, different cell and tissue types were used compared with our studies. Therefore, it is possible, as VHL has been described as an adapter protein (Frew and Krek, 2008), which physically interacts with at least 60 different proteins (Lai et al., 2011), that the inhibitory interaction between VHL and p53 identified in our work requires binding of an unidentified protein to the VHL-p53 complex and that this factor is not expressed at a significant level in the cell types used by that study. Logically, it would make sense that a process as critical as regulation of p53 would have several layers of

regulation that may be cell type or tissue specific and may explain the differences between the studies.

Importantly, this newly identified duality of VHL may potentially be exploited clinically in a number of ways. For example, VHL-deficient tumors such as ccRCC and pheochromocytomas may be sensitive to treatment with p53 inducers like doxorubicin or nutlin. Similarly, malignancies that have VHL may be sensitized to p53 inducers by combining recently developed cell permeable small molecules that inhibit VHL interaction with other proteins with specific HIF inhibitors already in early phase clinical trial, in order to inhibit VHL-p53 interaction while mitigating undesirable induction of HIF (Chen et al., 2016; Frost et al., 2016; Soares et al., 2017). Conversely, VHL may be induced in normal tissues in order to prevent side effects of p53 inducing chemotherapies. For example, a strategy to induce VHL in cardiac tissues (potentially using targeted antagomirs to MiR-101), may prevent chemotherapy induced cardiomyopathy, which is secondary to induction of p53 in the hearts of patients treated with doxorubicin (Chatterjee et al., 2010).

We believe that this elucidation of a fundamental intracellular process, between two critical proteins, may lead to novel therapies in cancer and vascular diseases.

Materials and Methods

All animal studies were approved and performed under the University of Alberta Animal Care and Use Committee (ACUC).

Cell Culture: 786-O -/+VHL cells (generous gift from Dr. Kaelin, Harvard) (Li et al., 2007), RCC4 -/+VHL cells (ATCC) and A549 cells (ATCC) were cultured in RMPI-1640 (Gibco) or F12 media (Gibco) with 10% FBS, 1% PSF at 5% CO_2.

Reagents: Doxorubicin (5μM, Cell Signaling), Nutlin (20μM, Cell Signaling), DMOG (1mM, Sigma-Aldrich), and MG-132 (10μM, Sigma-Aldrich) were used for *in vitro* experiments.

siRNA: RNAiMax (Invitrogen) was used to deliver gene specific siRNAs for p53, Sp1, HIF2α, PHD1, PHD2, and PHD3 (Ambion) as previously described(Kinnaird et al., 2016).

Plasmid Transfections: Cells were plated at 70% confluency 24hrs prior to transfection in antibiotic-free media. Lipofectamine 2000 (Thermofisher) was used to transfect 10μg of DNA per T25 flask. Cells were washed 6 hours later and transfection was assayed 48 hours later. Human Flag-p21 plasmid was purchased from Addgene (Plasmid 16240)

Adenoviral infection: AdLacZ and AdCA5 (generous gifts from Dr. Semenza, Johns Hopkins) or AdGFP, AdVHL30, and AdVHLΔ114-154 (Vector Biolabs) were infected into cells in serum-free media. Complete media was added after 6 hours and experiments performed 72 hours after infection.

CRISPR/Cas9 Genome Editing: Plasmids were made by Origene (KN208875) with a guide plasmid against VHL along with Cas9 and a donor plasmid that had turbo GFP (under endogenous promoter control) and puromycin resistance gene under PGK promoter. Cells were transfected with plasmids and single cell sorted into 96 well plates using flow cytometry to select the top 1% of tGFP-positive cells. tGFP-positive cells were then grown in 1μg/ml Puromycin for 10 days. Single cell clones were expanded and tested for genomic integration of the plasmid by PCR as well as VHL expression via immunoblotting and qRT-PCR.

Confocal imaging/Immunofluorescence: Imaging was done using Zeiss LSM 710 confocal microscope. Cells on glass coverslips were fixed with 2% PFA at

37˚C for 15 min, permeabilized with Triton X (0.5%) for 10-15 min, followed by PBS washes and blocking in Image-iT FX Signal Enhancer (Thermofisher I36933) for 30 min at room temperature. Primary antibodies were then added in primary diluent (Dako) overnight at 4˚C. Alexa Fluor secondary antibodies (Molecular Probes) were then added in secondary antibody diluent (Dako) at 1:1000 at 37˚C for 1hr in the dark. Slides were then washed in PBS for 20 min and DAPI was added at room temperature for 10 min, prior to fixation in ProLong Gold (Thermofisher) for 24hrs at room temperature.

Immunoblots: Cells were lysed in NP-40 (Santa Cruz) supplemented with protease inhibitor cocktail, and PMSF for 30 min on ice with frequent vortexing. Lysates were spun down at 10,000 RPM at 4˚C. Pierce BCA protein Assay (Thermofisher) was used to measure concentrations and samples were prepared in 2x Laemmli's (Sigma) and boiled for 7 min at 100˚C. Proteins were separated on SDS-PAGE and transferred onto nitrocellulose membranes, blocked at room temperature for 1h in 5% non-fat dry milk or 5% BSA in TBST (0.1% Tween-20) and incubated with primary antibodies (Cell Signaling and Santa Cruz) overnight at 4˚C. Membranes were then washed for 30' in TBST and incubated with horseradish-peroxidase-coupled secondary antibodies (Santa Cruz) at room temperature for 1 hr and visualized with enhanced chemiluminescence (Pierce, ThermoFisher).

RNA isolation and qRT PCR: RNA was isolated using Qiagen RNeasy Kit. Taqman RNA-to-CT 1 step (Applied Biosystems 4392938) was used as recommended for quantitative RT PCR. Primers were purchased from Ambion.

Co-immunoprecipitation: Co-Immunoprecipitations were done using Dynabeads Co-IP kit (Thermofisher 14321D). Briefly, beads were conjugated with glycerol-free antibody for 24hrs before protein extraction. Cells were rinsed with ice cold PBS and trypsinized at room temperature followed by lysis with IP buffer. 50mg equivalent of cell pellet volume were added to 1µg of antibody conjugated to beads and incubated at 4˚C overnight. Beads were then washed, eluted and boiled with 4x Laemmli's buffer (BioRad).

Disuccinimidyl Suberate (DSS) Cross-Linking: Cells were pelleted and washed twice in cold PBS and re-suspended in 1ml of cold PBS. 100mM stock of DSS was made fresh in DMSO and 25µL were added to 1ml of cell-PBS suspension and mixed by pipetting immediately after addition and incubated at room temperature for 45 min with mixing every 10 min. The reaction was then stopped with 20µL of 1M Tris-HCl (20mM final concentration) and incubated for another 15 min at room temperature.

Cell counting: 40,000 cells were plated per well in 24-well dish and allowed to grow for 24, 48 or 72 hours. At each time point cells were trypsinized and resuspended in 1mL of PBS. 10µL of trypan blue was combined with of 10µL of cell suspension then measured in duplicate in a Countess automated cell counter (ThermoFisher).

Chromatin immunoprecipitation: SimpleChIP (Cell Signaling), a magnetic-bead based chromatin immunoprecipitation kit was used as per manufacturer's specifications. Quantitative PCR (SYBR green, ThermoFisher) with primers to the promoters of p21 (Cell Signaling) and PUMA(Gomes and Espinosa, 2010) were used. Results are expressed as the amount of qPCR amplification in the immunoprecipitated samples normalized to the amplification of the input samples.

Bilateral tumor xenograft model: Male nu/nu mice (6 wk old; Charles River, Wilmington, MA, USA) mice were subcutaneously injected in the left flank with VHL-deficient (786-O or A549) cells and in the right flank with VHL-expressing (786-O or A549) cells. 786-O cells were resuspended with PBS and matrigel (Corning) in a 1:1 ratio. After four weeks of tumor growth, animals were treated with 2mg/kg Doxorubicin (Teva Standard) given as an intraperitoneal injection weekly for four weeks.

Statistics: Values are expressed as mean ± SEM. Independent-samples T-test or ANOVA were used for most experiments. The non-parametric Mann-Whitney *U* test was used for the VHL-rescue group in Figure 4-7C. Significance was considered at $p < 0.05$.

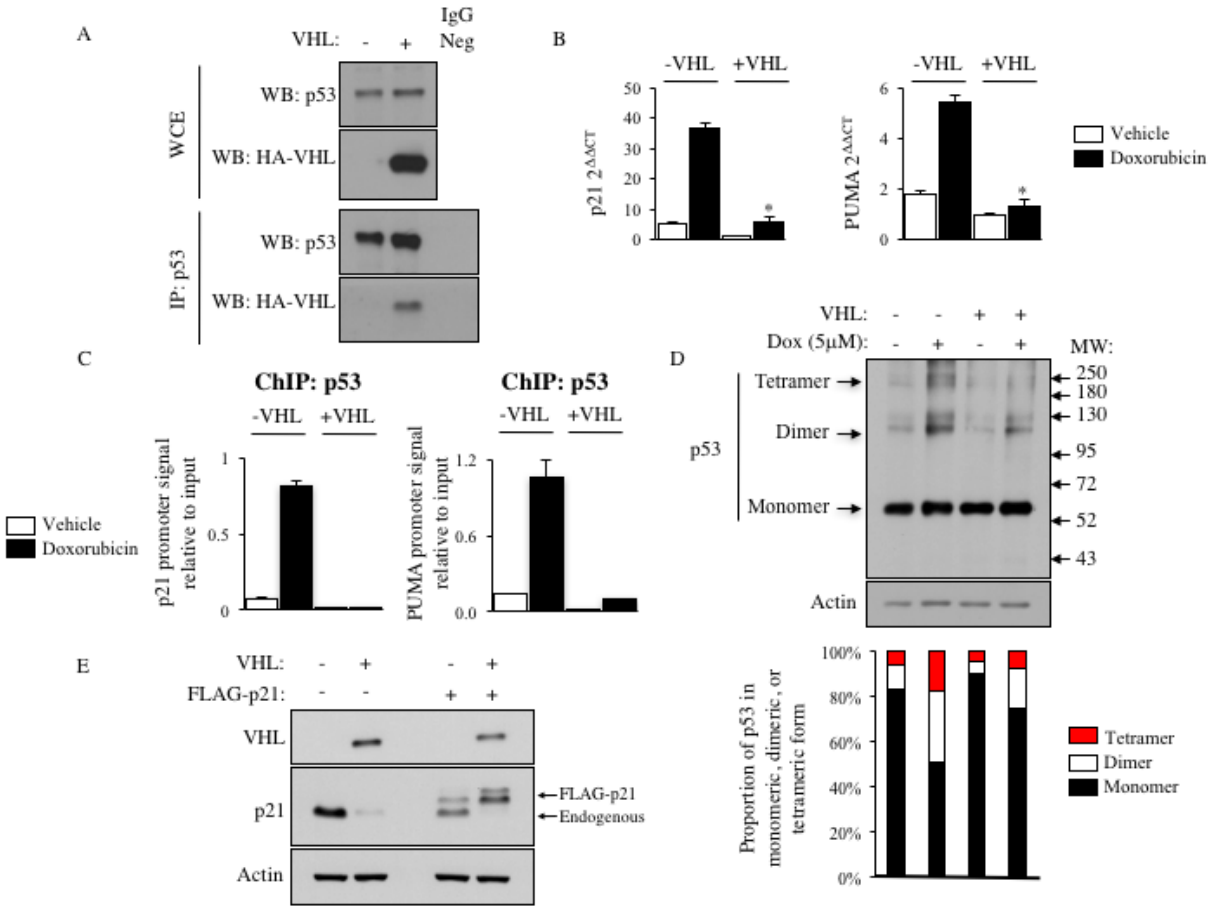

Figure 4-1: VHL inhibits p53 tetramerization, binding the promoters and expression of its target genes

(A) VHL co-immunoprecipitates with p53. (B) qRT-PCR shows that VHL inhibits expression of p53 target genes, p21 and PUMA, in response to a p53 stimulus with doxorubicin (n=3; $p<0.01$ vs. –VHL Doxorubicin) (C) Chromatin immunoprecipitation shows that VHL reduces p53 binding at the promoters of its target genes, p21 and PUMA, in response to a p53 stimulus (doxorubicin). (D) Irreversible protein crosslinking with disuccinimidyl suberate shows that VHL reduces the formation of p53 tetramers in response to a p53 stimulus (doxorubicin). (E) VHL inhibits expression of endogenous p21 (p53 promoter controlled), but not exogenous (CMV promoter controlled plasmid) FLAG-p21 protein.

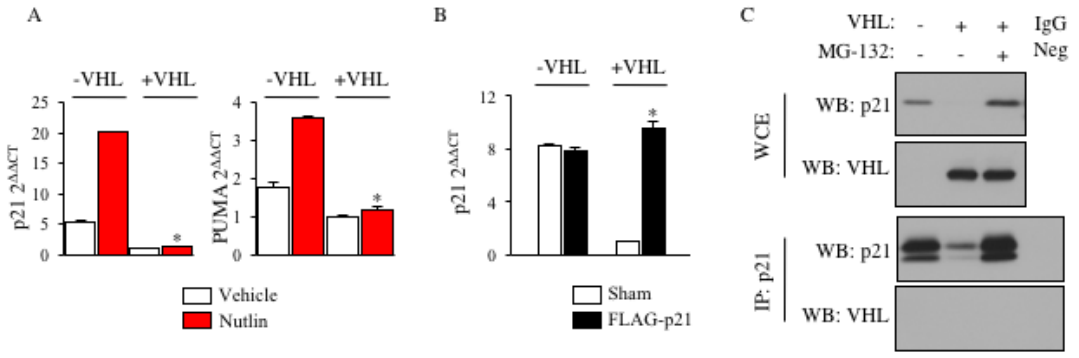

Figure 4-2: VHL does not interact with p21 protein, but inhibits induction of p21 mRNA in response to p53 stimulation with nutlin

(A) qRT-PCR shows that VHL inhibits expression of p53 target genes, p21 and PUMA, in response to a p53 stimulus with nutlin (n=3; $p<0.01$ vs. –VHL Doxorubicin). (B) Exogenous (CMV promoter controlled) FLAG-p21 restores p21 mRNA levels in +VHL cells to at least those measured in –VHL cells (n=3; $p<0.001$ vs. +VHL Sham). (C) VHL does not co-immunoprecipitate with p21.

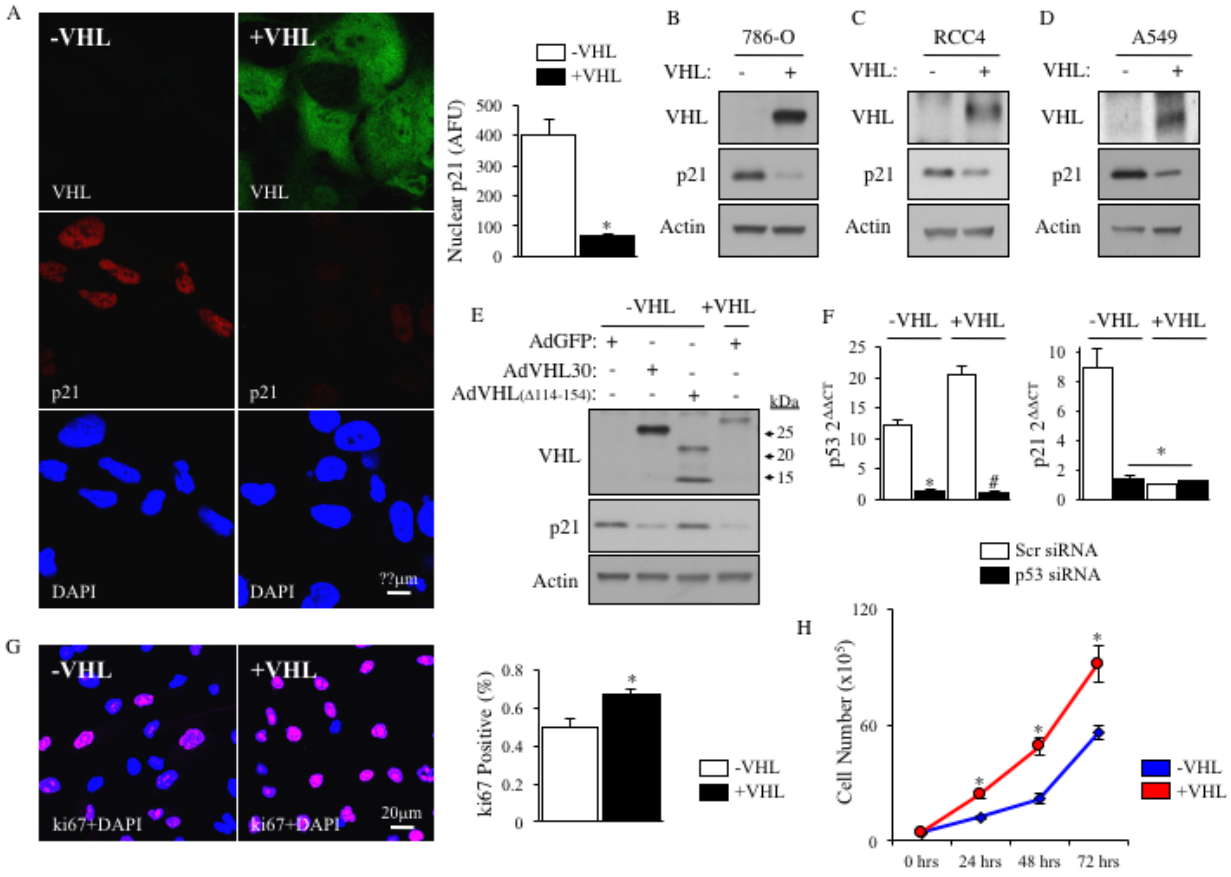

Figure 4-3: VHL inhibits p53-dependent target gene p21 expression, promoting cell proliferation

(A) Confocal imaging shows +VHL cells express less p21 than –VHL cells (VHL: green, p21: red, DAPI: blue, n=15 fields of view; *p<0.01 vs. –VHL). (B) VHL reduces p21 protein expression in 786-O, (C) RCC4, and (D) A549 cancer cells. (E) Adenoviral expression of wild-type, but not mutant VHL reduces p21 expression. (F) p53 knockdown mimics VHL expression's reduction in p21 (n=3; *p<0.01 vs. –VHL Scr, #p<0.01 vs. +VHL Scr). (G) More +VHL than -VHL cells stain positive for ki67 (n=3; *p<0.05). (H) More +VHL than –VHL cells are counted at 24, 48 and 72 hours after plating equal numbers of cells at time 0 hours (n=4; *p<0.01 vs. -VHL).

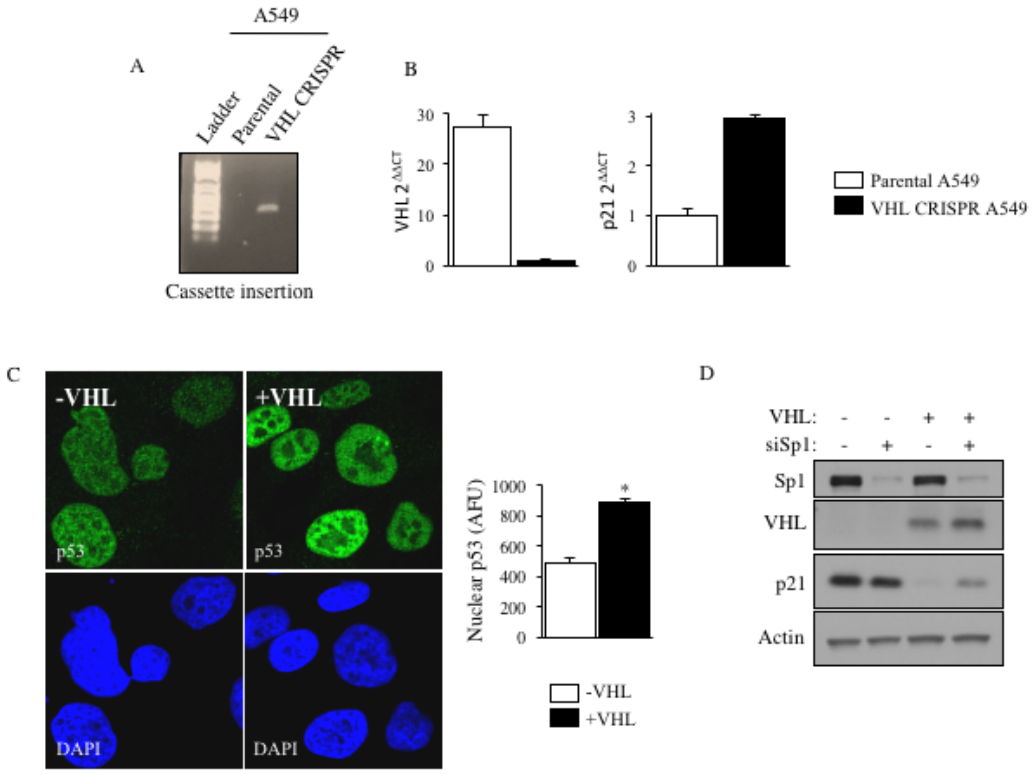

Figure 4-4: Validation of VHL expression in several models
(A) Confirmation of CRISPR plasmid insertion into genomic DNA from A549 cells (left). VHL mRNA is depleted in VHL CRISPR A549 cells compared to parental A549 cells (middle). p21 mRNA is increased in VHL CRISPR A549 cells compared to parental A549 cells (right). Confocal microscopy shows that p53 has similar nuclear localization and increased expression in +VHL cells (n= n=15 fields of view; *p<0.01 vs. -VHL). (C) Sp1 knockdown does not reduce p21 expression.

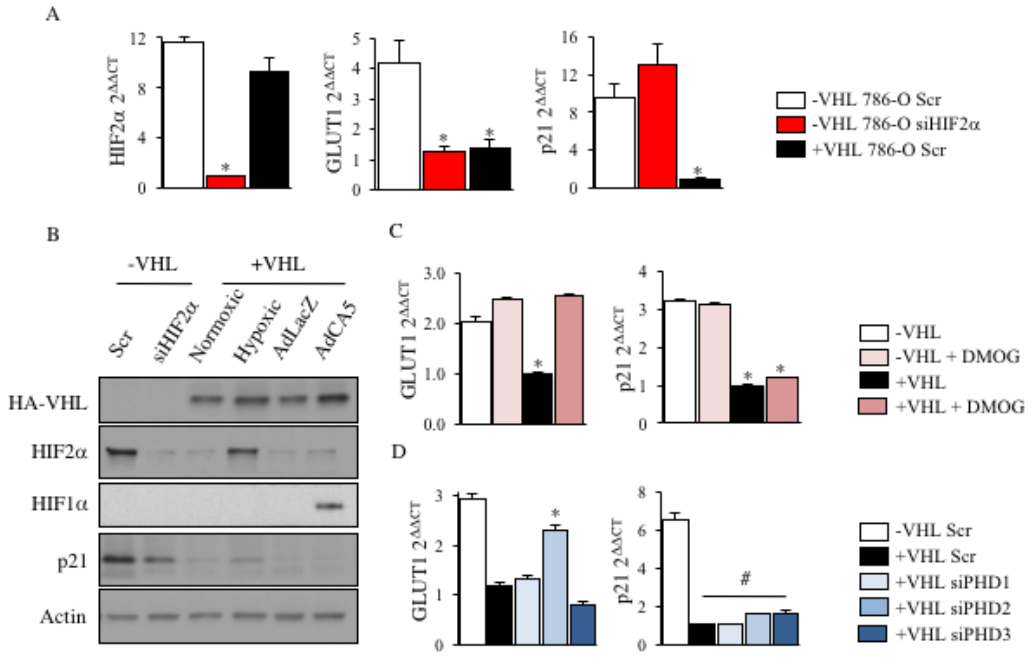

Figure 4-5: VHL inhibits p53 target gene, p21, independent of HIF and prolyl-hydroxylation

(A) VHL expression inhibits both GLUT1 and p21, but HIF2α knockdown only inhibits GLUT1 (n=3; *p<0.01 vs. –VHL Scr). (B) VHL, but not HIF2α knockdown, inhibits p21 expression regardless of hypoxia or expression of a non-degradable HIF1α isoform (AdCA5). (C) DMOG restores GLUT1 but not p21 expression (n=3; *p<0.01 vs. -VHL). (D) Only PHD2 knockdown increases GLUT1, but no PHD knockdown increases p21 expression (n=3; *p<0.01 vs. +VHL Scr, #p<0.01 vs. –VHL Scr).

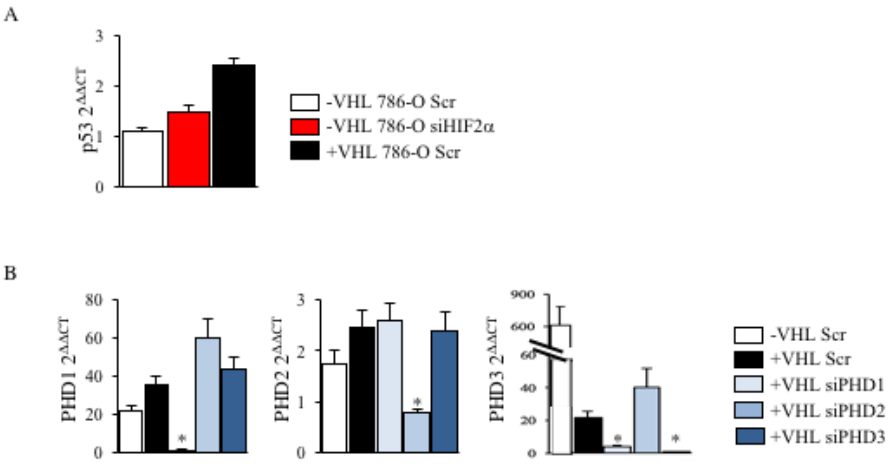

Figure 4-6: HIF knockdown does not reduce p53 expression and verification of PHD knockdown

(A) Neither HIF2α knockdown nor VHL reduce p53 mRNA expression. (B) qRT-PCR showing knockdown of PHD1, PHD2, and PHD3 mRNA (n=3; *p<0.01 vs. +VHL Scr).

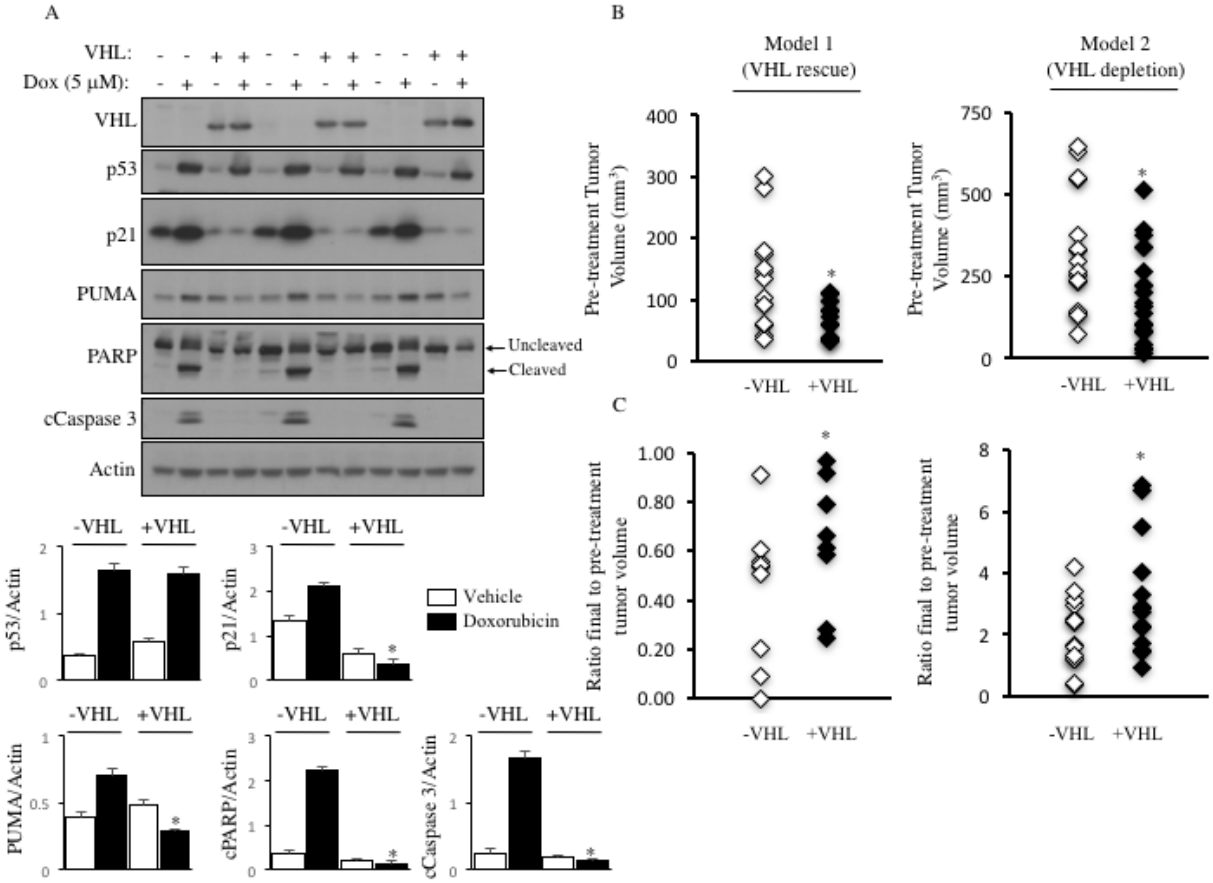

Figure 4-7: VHL attenuates p53-mediated apoptosis-induction and response to treatment in vivo with p53 stimulation with doxorubicin

(A) Immunoblot shows that VHL inhibits expression of p53 target genes, p21 and PUMA, but not induction of p53 protein, in response to a p53 stimulus with doxorubicin. VHL also reduces two markers of apoptosis, cleaved PARP and cleaved Caspase 3, after treatment with doxorubicin (n=3, *p<0.05 vs. –VHL Doxorubicin). (B) –VHL tumor xenografts volume is larger than +VHL tumor xenografts after 4 weeks (n=9 VHL rescue model, n=14 VHL depletion model; *p<0.05 vs. –VHL). (C) +VHL tumor xenografts have a higher ratio of post-treatment to pre-treatment tumor volume, showing the effect of doxorubicin treatment on tumor growth is attenuated in +VHL cells compared to –VHL cells (n=9 VHL rescue model, n=14 VHL depletion model; *p<0.05 vs. –VHL, note: Mann-Whitney-U test for VHL rescue model).

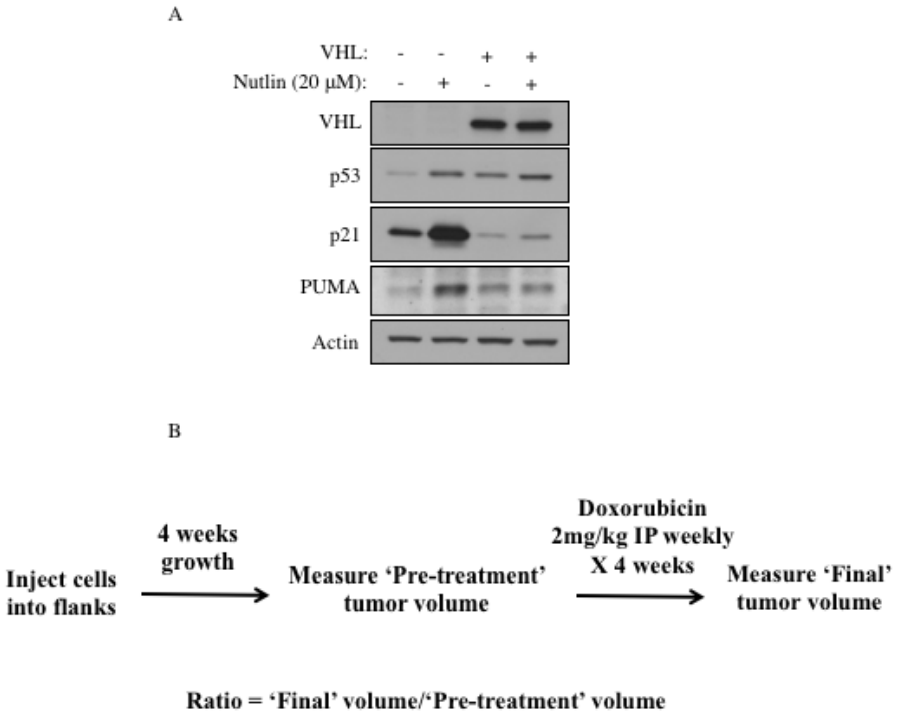

Figure 4-8: VHL attenuates p53-mediated gene induction in response to p53 stimulation with nutlin

(A) Immunoblot shows that VHL inhibits expression of p53 target genes, p21 and PUMA, but not induction of p53 protein, in response to a p53 stimulus with nutlin. (B) Schematic of in vivo tumor xenograft experiments with –VHL and +VHL cells.

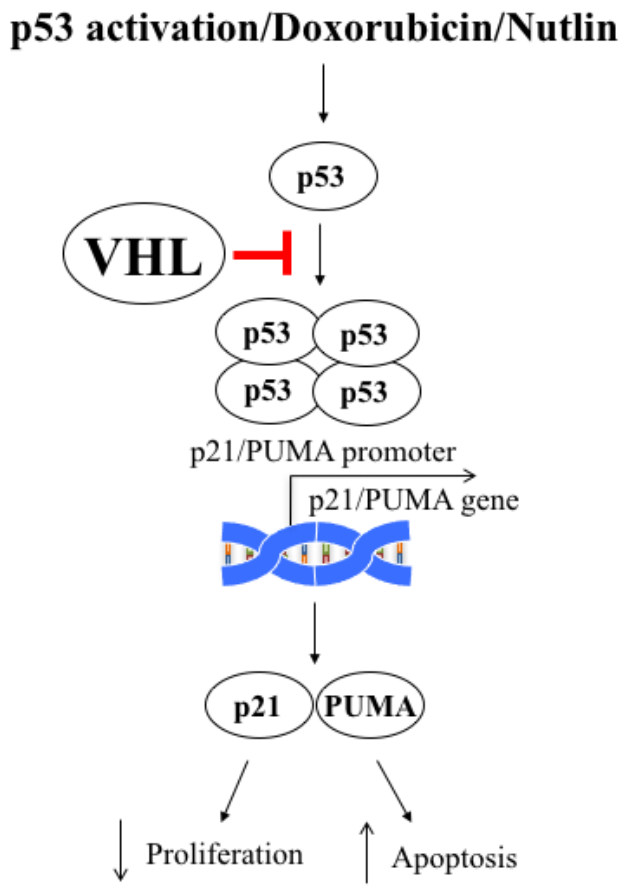

Figure 4-9: Schematic mechanism of VHL-mediated inhibition of p53 (see Discussion).

References

Abbas, T., and Dutta, A. (2009). p21 in cancer: intricate networks and multiple activities. Nat Rev Cancer *9*, 400-414.

Albers, J., Rajski, M., Schonenberger, D., Harlander, S., Schraml, P., von Teichman, A., Georgiev, S., Wild, P. J., Moch, H., Krek, W., and Frew, I. J. (2013). Combined mutation of Vhl and Trp53 causes renal cysts and tumours in mice. EMBO Mol Med *5*, 949-964.

Berra, E., Benizri, E., Ginouves, A., Volmat, V., Roux, D., and Pouyssegur, J. (2003). HIF prolyl-hydroxylase 2 is the key oxygen sensor setting low steady-state levels of HIF-1alpha in normoxia. EMBO J *22*, 4082-4090.

Chatterjee, K., Zhang, J., Honbo, N., and Karliner, J. S. (2010). Doxorubicin cardiomyopathy. Cardiology *115*, 155-162.

Chen, W., Hill, H., Christie, A., Kim, M. S., Holloman, E., Pavia-Jimenez, A., Homayoun, F., Ma, Y., Patel, N., Yell, P.*, et al.* (2016). Targeting renal cell carcinoma with a HIF-2 antagonist. Nature *539*, 112-117.

Chene, P. (2001). The role of tetramerization in p53 function. Oncogene *20*, 2611-2617.

Cohen, H. T., Zhou, M., Welsh, A. M., Zarghamee, S., Scholz, H., Mukhopadhyay, D., Kishida, T., Zbar, B., Knebelmann, B., and Sukhatme, V. P. (1999). An important von Hippel-Lindau tumor suppressor domain mediates Sp1-binding and self-association. Biochem Biophys Res Commun *266*, 43-50.

Fan, Y., Li, H., Ma, X., Gao, Y., Chen, L., Li, X., Bao, X., Du, Q., Zhang, Y., and Zhang, X. (2015). Prognostic Significance of Hypoxia-Inducible Factor Expression in Renal Cell Carcinoma: A PRISMA-compliant Systematic Review and Meta-Analysis. Medicine (Baltimore) *94*, e1646.

Frew, I. J., and Krek, W. (2008). pVHL: a multipurpose adaptor protein. Sci Signal *1*, pe30.

Frost, J., Galdeano, C., Soares, P., Gadd, M. S., Grzes, K. M., Ellis, L., Epemolu, O., Shimamura, S., Bantscheff, M., Grandi, P.*, et al.* (2016). Potent and selective chemical probe of hypoxic signalling downstream of HIF-alpha hydroxylation via VHL inhibition. Nat Commun *7*, 13312.

Gimenez-Bachs, J. M., Salinas-Sanchez, A. S., Sanchez-Sanchez, F., Lorenzo-Romero, J. G., Donate-Moreno, M. J., Pastor-Navarro, H., Garcia-Olmo, D. C., Escribano-Martinez, J., and Virseda-Rodriguez, J. A. (2006). Determination of vhl gene mutations in sporadic renal cell carcinoma. Eur Urol *49*, 1051-1057.

Gomes, N. P., and Espinosa, J. M. (2010). Gene-specific repression of the p53 target gene PUMA via intragenic CTCF-Cohesin binding. Genes Dev *24*, 1022-1034.

Gossage, L., Eisen, T., and Maher, E. R. (2015). VHL, the story of a tumour suppressor gene. Nat Rev Cancer *15*, 55-64.

Harlander, S., Schonenberger, D., Toussaint, N. C., Prummer, M., Catalano, A., Brandt, L., Moch, H., Wild, P. J., and Frew, I. J. (2017). Combined mutation in Vhl, Trp53 and Rb1 causes clear cell renal cell carcinoma in mice. Nat Med *23*, 869-877.

Hergovich, A., Lisztwan, J., Barry, R., Ballschmieter, P., and Krek, W. (2003). Regulation of microtubule stability by the von Hippel-Lindau tumour suppressor protein pVHL. Nat Cell Biol *5*, 64-70.
Hu, C. J., Wang, L. Y., Chodosh, L. A., Keith, B., and Simon, M. C. (2003). Differential roles of hypoxia-inducible factor 1alpha (HIF-1alpha) and HIF-2alpha in hypoxic gene regulation. Mol Cell Biol *23*, 9361-9374.
Iliopoulos, O., Kibel, A., Gray, S., and Kaelin, W. G., Jr. (1995). Tumour suppression by the human von Hippel-Lindau gene product. Nat Med *1*, 822-826.
Kim, J. H., Jung, C. W., Cho, Y. H., Lee, J., Lee, S. H., Kim, H. Y., Park, J., Park, J. O., Kim, K., Kim, W. S.*, et al.* (2005). Somatic VHL alteration and its impact on prognosis in patients with clear cell renal cell carcinoma. Oncol Rep *13*, 859-864.
Kinnaird, A., Dromparis, P., Saleme, B., Gurtu, V., Watson, K., Paulin, R., Zervopoulos, S., Stenson, T., Sutendra, G., Pink, D. B.*, et al.* (2016). Metabolic Modulation of Clear-cell Renal Cell Carcinoma with Dichloroacetate, an Inhibitor of Pyruvate Dehydrogenase Kinase. Eur Urol *69*, 734-744.
Kondo, K., Yao, M., Yoshida, M., Kishida, T., Shuin, T., Miura, T., Moriyama, M., Kobayashi, K., Sakai, N., Kaneko, S.*, et al.* (2002). Comprehensive mutational analysis of the VHL gene in sporadic renal cell carcinoma: relationship to clinicopathological parameters. Genes Chromosomes Cancer *34*, 58-68.
Kuznetsova, A. V., Meller, J., Schnell, P. O., Nash, J. A., Ignacak, M. L., Sanchez, Y., Conaway, J. W., Conaway, R. C., and Czyzyk-Krzeska, M. F. (2003). von Hippel-Lindau protein binds hyperphosphorylated large subunit of RNA polymerase II through a proline hydroxylation motif and targets it for ubiquitination. Proc Natl Acad Sci U S A *100*, 2706-2711.
Lai, Y., Song, M., Hakala, K., Weintraub, S. T., and Shiio, Y. (2011). Proteomic dissection of the von Hippel-Lindau (VHL) interactome. J Proteome Res *10*, 5175-5182.
Li, L., Zhang, L., Zhang, X., Yan, Q., Minamishima, Y. A., Olumi, A. F., Mao, M., Bartz, S., and Kaelin, W. G., Jr. (2007). Hypoxia-inducible factor linked to differential kidney cancer risk seen with type 2A and type 2B VHL mutations. Mol Cell Biol *27*, 5381-5392.
Liu, N., Xia, W. Y., Liu, S. S., Chen, H. Y., Sun, L., Liu, M. Y., Li, L. F., Lu, H. M., Fu, Y. J., Wang, P.*, et al.* (2016). MicroRNA-101 targets von Hippel-Lindau tumor suppressor (VHL) to induce HIF1alpha mediated apoptosis and cell cycle arrest in normoxia condition. Sci Rep *6*, 20489.
Mack, F. A., Patel, J. H., Biju, M. P., Haase, V. H., and Simon, M. C. (2005). Decreased growth of Vhl-/- fibrosarcomas is associated with elevated levels of cyclin kinase inhibitors p21 and p27. Mol Cell Biol *25*, 4565-4578.
Moore, L. E., Nickerson, M. L., Brennan, P., Toro, J. R., Jaeger, E., Rinsky, J., Han, S. S., Zaridze, D., Matveev, V., Janout, V.*, et al.* (2011). Von Hippel-Lindau (VHL) inactivation in sporadic clear cell renal cancer: associations with germline VHL polymorphisms and etiologic risk factors. PLoS Genet *7*, e1002312.

Mukhopadhyay, D., Knebelmann, B., Cohen, H. T., Ananth, S., and Sukhatme, V. P. (1997). The von Hippel-Lindau tumor suppressor gene product interacts with Sp1 to repress vascular endothelial growth factor promoter activity. Mol Cell Biol *17*, 5629-5639.
Mullen, P. (2004). The use of Matrigel to facilitate the establishment of human cancer cell lines as xenografts. Methods Mol Med *88*, 287-292.
Patard, J. J., Fergelot, P., Karakiewicz, P. I., Klatte, T., Trinh, Q. D., Rioux-Leclercq, N., Said, J. W., Belldegrun, A. S., and Pantuck, A. J. (2008). Low CAIX expression and absence of VHL gene mutation are associated with tumor aggressiveness and poor survival of clear cell renal cell carcinoma. Int J Cancer *123*, 395-400.
Roe, J. S., Kim, H., Lee, S. M., Kim, S. T., Cho, E. J., and Youn, H. D. (2006). p53 stabilization and transactivation by a von Hippel-Lindau protein. Mol Cell *22*, 395-405.
Schokrpur, S., Hu, J., Moughon, D. L., Liu, P., Lin, L. C., Hermann, K., Mangul, S., Guan, W., Pellegrini, M., Xu, H., and Wu, L. (2016). CRISPR-Mediated VHL Knockout Generates an Improved Model for Metastatic Renal Cell Carcinoma. Sci Rep *6*, 29032.
Schraml, P., Struckmann, K., Hatz, F., Sonnet, S., Kully, C., Gasser, T., Sauter, G., Mihatsch, M. J., and Moch, H. (2002). VHL mutations and their correlation with tumour cell proliferation, microvessel density, and patient prognosis in clear cell renal cell carcinoma. J Pathol *196*, 186-193.
Soares, P., Gadd, M. S., Frost, J., Galdeano, C., Ellis, L., Epemolu, O., Rocha, S., Read, K. D., and Ciulli, A. (2017). Group-Based Optimization of Potent and Cell-Active Inhibitors of the von Hippel-Lindau (VHL) E3 Ubiquitin Ligase: Structure-Activity Relationships Leading to the Chemical Probe (2S,4R)-1-((S)-2-(1-Cyanocyclopropanecarboxamido)-3,3-dimethylbutanoyl)-4-hydroxy -N-(4-(4-methylthiazol-5-yl)benzyl)pyrrolidine-2-carboxamide (VH298). J Med Chem.
Yao, M., Yoshida, M., Kishida, T., Nakaigawa, N., Baba, M., Kobayashi, K., Miura, T., Moriyama, M., Nagashima, Y., Nakatani, Y.*, et al.* (2002). VHL tumor suppressor gene alterations associated with good prognosis in sporadic clear-cell renal carcinoma. J Natl Cancer Inst *94*, 1569-1575.
Yi, Y., Mikhaylova, O., Mamedova, A., Bastola, P., Biesiada, J., Alshaikh, E., Levin, L., Sheridan, R. M., Meller, J., and Czyzyk-Krzeska, M. F. (2010). von Hippel-Lindau-dependent patterns of RNA polymerase II hydroxylation in human renal clear cell carcinomas. Clin Cancer Res *16*, 5142-5152.

Chapter Five

Myocyte Enhancer Factor 2A is up-regulated, increases CCL20 expression and promotes tumor growth in clear cell renal cell carcinoma

Abstract

Background: Advanced clear cell renal cell carcinoma (ccRCC) remains a deadly disease driven by metabolic derangement, immune evasion and propensity for invasion and metastasis. Myocyte Enhancer Factor 2A (Mef2A) is a growth factor driven transcription factor involved in cell growth, metabolism, invasion, immunomodulation and apoptosis-resistance.

Objective: We hypothesized that Mef2A is up-regulated in ccRCC, promoting tumor growth.

Design, Setting, and Participants: Fifty-two pathologist reviewed ccRCC tumors and surrounding normal kidney tissues (from the same patients) were stained for Mef2A using immunofluorescent confocal microscopy. ccRCC and proximal tubule cells lines as well as nude mouse xenografts were used for in-vitro and in-vivo experiments, respectively.

Interventions: Mef2A was inhibited using RNA interference.

Outcomes: Unbiased GeneChip screening (confirmed by qRT-PCR) identified Mef2A target genes. Proliferation (ki67, BrdU and phosphorylated retinoblastoma), apoptosis (TUNEL), migration (scratch assay), invasion (basement membrane extract) and xenograft tumor growth were measured using standard techniques.

Results: Mef2A expression is higher in ccRCC tumors compared to the surrounding normal kidney. Mef2A transcriptional activity is higher in ccRCC cells vs. proximal tubule cells and in VHL-deficient (high growth factor) vs. VHL-expressing (low growth factor) 786-O cells. The pro-tumorigenic, secretable molecule Chemokine Ligand 20 (CCL20) is the most reduced target in Mef2A knockdown. Mef2A knockdown reduces cell proliferation, migration, invasion, and increases apoptosis in-vitro, as well as reducing tumor growth in a nude mouse model. Mef2A levels correlate with tumor size in large tumors.

Conclusions: Mef2A is up-regulated in ccRCC, drives expression of the pro-tumorigenic chemokine CCL20 and is important for tumor growth.

Patient Summary: In this report we identify the protein Mef2A to be important for kidney cancer growth and find that it correlates with tumor size in large kidney cancers. Mef2A may be involved in tumor cell growth and death as well as local regulation of the immune system. Inhibition of Mef2A reduces tumor growth in the dish as well as in an animal model.

Introduction

More than 330,000 patients are diagnosed with renal cell carcinoma (RCC) annually, with approximately 30% presenting with metastases at the time of diagnosis(1, 2). Current first-line agents for advanced clear cell RCC (ccRCC), such as tyrosine kinase inhibitors like sunitinib, only increase progression free survival by 11 months(3). Therefore, we must link together several fundamental mechanisms contributing to the pathogenesis of ccRCC, such as the recent identification of local immune suppression and advancement of immune checkpoint inhibitors, to find novel therapeutic targets to treat this deadly cancer(4).

Deregulated cellular energetics, apoptosis-resistance, evading the immune system and activating invasion and metastasis are critical hallmarks of cancer(5). Identifying a mechanism that controls multiple hallmarks of cancer is a desirable therapeutic target.

Myocyte enhancer factor 2A (Mef2A) is a master transcription factor involved in cell survival, metabolism, apoptosis-resistance, immunomodulation, and invasion(6-10), Mef2A has recently been identified in several solid organ tumors (breast, liver, and lung), however its role in ccRCC has not yet been described(6). Mef2A is activated by growth factor dependent phosphorylation through the epidermal growth factor receptor (EGFR) signaling pathway(6, 11). This signaling cascade is highly active in ccRCC due to loss of the von Hippel Lindau (VHL) tumor suppressor, leading to accumulation of hypoxia inducible factor (HIF) and overexpression of HIF target genes such as transforming growth factor alpha (TGFα) (12-14). TGFα has been shown to be a potent ligand for EGFR, strongly activating the EGFR signaling pathway in ccRCC and potentially activating Mef2A(15).

Chemokine Ligand 20 (CCL20) is a pro-proliferation(16-18), pro-migration(17-19) and pro-invasion(16, 19, 20) molecule that has been shown to be secreted by several solid tumors including renal cell carcinoma(20-25). CCL20 exerts its physiological effect by binding to a highly specific G-coupled protein receptor, CCR6(26).

In this manuscript, we show that Mef2A is up-regulated and transcriptionally activated in ccRCC. Furthermore, we use unbiased screening to identify that Mef2A promotes the expression of the pro-proliferative and invasive chemokine CCL20, as well as increases cell proliferation, apoptosis-resistance and tumor growth.

Results

5.1 Mef2A expression is up-regulated in renal tumor tissue

In order to determine the relative expression of Mef2A in ccRCC compared to the normal kidney parenchyma in our patients, we obtained 52 ccRCC tumors and compared the amount of Mef2A expression in the tumors to normal kidney tissues removed from the same patients at the time of their radical nephrectomy. Nuclear Mef2A protein and mRNA expression were significantly elevated in tumors compared to the normal kidney samples (Figure 5-1A-C). The patient and tumor characteristics are outlined in Figure 5-2A.

Mef2A protein is expressed in ccRCC but not proximal tubule cells, which are the healthy tissue type from which ccRCC is derived (Figure 5-1D). This increase in Mef2A expression in cancer cells compared to the normal cell type from which the cancer initiates was also found in several other cancer/normal tissues pairings (non-small cell lung cancer vs. small airway epithelial cells and melanoma vs. melanocytes; Figure 5-2B). Similarly, the transcriptional activity of Mef2 is increased in ccRCC compared to proximal tubule cells as measured using a promoter firefly luciferase assay (Figure 5-1E).

5.2 Mef2A regulates expression of CCL20 in kidney tumor cells

In order to determine the effect of Mef2A in ccRCC we performed a GeneChip screening assay on a loss-of-function model using siRNA knockdown. We achieved an ~90% knockdown of Mef2A at both the mRNA and protein levels (Figure 5-3A). GeneChip screening demonstrated that Mef2A knockdown resulted in a >6-fold reduction of CCL20 mRNA (Figure 5-3B; see Table 5-1 for complete list of all genes with ≥1.5 fold change). Decreased CCL20 expression was confirmed by primer specific qRT-PCR (Figure 5-3C). Similarly, we found an increased expression of CCL20 mRNA in patient tumors (high Mef2A) compared to normal kidney (low Mef2A) tissues (Figure 5-3D). As CCL20 is a secretable chemokine, we measured CCL20 levels in the supernatant after Mef2A knockdown. We found the concentration of CCL20 to be reduced in the supernatant of ccRCC cells that had decreased Mef2A expression (Figure 5-3E).

CCL20 is known to exert its pro-proliferative and pro-invasive effects by binding to a specific G-coupled protein receptor, called CCR6, on several tissues such as breast and immune cells. CCR6 has previously been identified in both ccRCC tumor and infiltrating T regulatory cells within the tumors of patients with ccRCC(24). We confirm that the CCR6 receptor is expressed in ccRCC cells and at a high level compared to benign proximal tubule cells (Figure 5-3F).

5.3 Loss of Mef2A inhibits proliferation, migration and invasion and promotes mitochondrial activity and apoptosis of ccRCC cells

We used three metrics to determine the effect of Mef2A on proliferation: ki67, BrdU incorporation and phosphorylated retinoblastoma (p-Rb) protein levels. Mef2A knockdown reduced ki67 staining (Figure 5-4A), BrdU incorporation (Figure 5-4B) and p-Rb (Figure 5-4C) suggesting loss of Mef2A inhibits proliferation. Mef2A knockdown increased mitochondrial activity measured by a depolarized mitochondrial membrane potential as well as increased mitochondrial reactive oxygen species (Figure 5-4D). This may be due to up-regulation of a known Mef2 regulated gene, PGC1α and its downstream target, the major mitochondrial deacetylase and activator Sirtuin 3 (Figure 5-4E) (27-29). Mef2A knockdown increased staining of the apoptotic marker TUNEL in ccRCC in keeping with its anti-apoptotic role previously described and the increase in mitochondrial activity (Figure 5-4F)(10). Mef2A knockdown reduced tumor cell migration as assessed using a standard scratch assay (Figure 5-4G). Similarly, knockdown of Mef2A reduced the invasiveness of ccRCC cells measured using a commercially available in-vitro invasion assay (Figure 5-4H).

5.4 VHL-deficiency increases Mef2A transcriptional activity

VHL-deficient 786-O ccRCC cells overexpress HIF2a in normoxia (Figure 5-5A). This leads to an increased expression of the HIF2a target gene, Transforming growth factor alpha (TGFα) (Figure 5-5B), and activation of the EGFR phosphorylation pathway for which it has previously been shown to be a potent ligand (Figure 5-5C)(15). Mef2A is significantly more phosphorylated at

Threonine 312, which is a stimulatory phosphorylation that can be triggered by EGFR signaling, in VHL-deficient compared to VHL-expressing ccRCC cells (Figure 5-5D). Moreover, the transcriptional activity of Mef2 is significantly higher in the VHL-deficient, hyperphosphorylated T312 Mef2A, ccRCC cells (Figure 5-5E). The model of VHL deficiency leading to increased Mef2A activity is outlined in Figure 5-5F.

5.5 Mef2A knockdown reduces tumor growth in-vivo

We developed a stable knockdown model of Mef2A using expression of a short-hairpin RNA Mef2A plasmid (shMef2A) in order to assess the effect of Mef2A inhibition on tumor growth *in vivo* (Figure 5-6A). Tumors initiated in 7/9 (78%) of animals injected with shScr and in 12/13 (92%) of animals injected with shMef2A tumors suggesting that Mef2A is not critical for tumor establishment. However, after 10 days, tumors with Mef2A knockdown failed to significantly enlarge, while shScr control tumors continued to grow (Figure 5-6B). After 30 days, excised shMef2A tumors were significantly smaller in volume and weight than shScr control tumors (Figure 5-6B and C). Stratification of human tumor samples by size as either pT1 (early tumors, <7cm) or pT2 (established tumors, >7cm) suggests that nuclear Mef2A expression is correlated with tumor size in established (pT2) tumors (R=0.829; p=0.042; Figure 5-6D) but not in early (pT1) tumors (Spearman correlation R=0.192; p=0.242; Figure 5-7). Inclusion of pT3 tumors that are >7cm, (i.e. pT2 by size) into the pT2 data also suggests a trend in larger tumor size and nuclear Mef2A levels (R=0.506; p=0.078; Figure 5-6D).

Discussion

We show that the expression and activity of Mef2A is increased in ccRCC compared to normal kidney tissues. This leads to increased transcription and secretion of the pro-proliferative chemokine CCL20. Inhibition of Mef2A reduces CCL20 production and decreases cancer cell proliferation and tumor growth.

The molecular phenotype of ccRCC predisposes this malignancy to Mef2A activation. VHL-deficiency leads to increased HIF activation, which drives TGFα expression. TGFα activates the EGF receptor and downstream cascade of protein kinases, which phosphorylate Mef2A threonine 312, increasing transcriptional activity and subsequent activation of downstream targets like CCL20 (Figure 5-6E). This is important because VHL is the most commonly altered gene in ccRCC, being mutated or having its promoter hypermethylated in up to 90% of all ccRCC tumors. Therefore, Mef2A may not only be up-regulated in our patients, as we show, but potently activated in these tumors as well. These findings are in keeping with results from The Cancer Genome Atlas and the Human Protein Atlas (www.proteinatlas.org), which identify RCC as having the highest median expression of Mef2A RNA across the 17 malignancies studied(30).

We identified CCL20 as an important target gene of Mef2A using an unbiased GeneChip screening assay and confirmed its reduction in Mef2A knockdown cells at both the mRNA and secreted protein levels. CCL20 is a chemokine secreted by both immune and tumor cells and exerts its effects by binding in an autocrine and paracrine manner to the CCR6 G-coupled protein receptor. There is evidence that CCL20/CCR6 promote tumorigenesis in two manners: First by promoting proliferation, migration and invasion of the tumor cells themselves as has been identified in several other tumor types such as breast, lung, thyroid, colon and pancreatic cancers(17-20, 25). Secondly, CCL20/CCR6 mediates effector T-cell suppression by recruiting inhibitory T-regulatory cells to the tumour microenvironment, thus locally suppressing the immune system(24, 31). Therefore, the overall effect of CCL20 is tumor tropism and immune tolerance. This means that while we observe a significant reduction in tumour cell

growth in the Mef2A knockdown ccRCC cells, we may not be capturing the complete effect of Mef2A/CCL20 inhibition as we are missing the effects on immune suppression. Indeed, the anti-tumor effects we observed in-vivo (in mice lacking cell-mediated immunity) for Mef2A knockdown cells are likely limited to the anti-proliferative effects, and may actually be more accentuated tumor inhibition in our patients where immune suppression would also be targeted.

Furthermore, ccRCC has been identified as a cancer that hijacks the immune system to increase its growth, and immune checkpoint inhibitors are quickly becoming the new cornerstone of advanced ccRCC management(4). Interestingly, we show that two other cancer types for which immune checkpoint inhibitors have been approved, NSCLC and melanoma both have increased expression of Mef2A compared to their normal tissues from which they develop. Mef2A may be playing an important role in immune evasion as ~25% of the top 25 targets identified on GeneChip screening were immune activators such as CCL20, tumor necrosis factor, and interleukin 8, which were all up-regulated in Mef2A expressing compared to Mef2A inhibited ccRCC cells (Table 5-1).

Our work suggests that Mef2A functions as an important node in ccRCC growth and that Mef2A/CCL20/CCR6 inhibition may represent a new therapeutic target. While there are no specific Mef2A inhibitors available, the underlying driving force of Mef2A activation in ccRCC (EGFR activation by TGFα) can be pharmacologically targeted as an adjuvant to current therapies(32). Early attempts at targeting CCL20 have been attempted both specifically with monoclonal antibodies(33) and non-specifically using commonly prescribed agents such as statins(34). Similarly, specific microRNAs that inhibit CCR6 have been identified, which have been shown to inhibit tumor invasion and metastasis(35). While we have identified a new pro-tumor pathway, further work will need to be performed to inhibit the Mef2A/CCL20/CCR6 axis in ccRCC.

Materials and Methods

Patient Samples: We received institutional Health Research Ethics Board approval to obtain specimens from patients undergoing radical nephrectomy for RCC. All specimens (tumor and surrounding normal tissue from each patient) were formalin fixed, paraffin embedded and diagnosed by a pathologist as ccRCC versus normal kidney tissue. All tissue was processed for mRNA isolation and staining as previously described(36).

Cell Culture and Reagents: The 786-O human ccRCC line was purchased from ATCC, maintained in RMPI 1640 media (GIBCO, 10% FBS, 1% PSF). –VHL 786-O and +VHL 786-O cell lines (stably infected with an empty vector or functional, Hemagglutinin-tagged VHL, respectively) were a gift from Dr. Kaelin (Harvard Medical School)(37). Human renal proximal tubular cells were purchased from ScienCell and maintained in EpiCM media.

siRNA knockdown and qRT-PCR: Mef2A specific or scrambled siRNAs were transfected using Lipofectamine RNAiMax reagent as previously described(36). After 72 hours, RNA was isolated (Qiagen) and qRT-PCR using gene specific primers and TaqMan reagents (ThermoFisher) were used in a QuantStudio 7 Flex Real-time PCR system (ThermoFisher).

shRNA knockdown: 786-O cells were transfected with plasmid using the xfect transfection reagent (Clontech). Stable integration of the plasmid was selected for using puromycin (1ug/mL).

***Luciferase*:** Cignal dual-luciferase (Mef2/Renilla) reporter kits (SA Biosciences) were used as previously described(38). 48hrs after transfection, activity was assessed using a dual luciferase reporter assay kit (Promega). Mef2 activity was normalized to the Renilla luminescence.

Genechip: 200ng of total RNA was labeled using the Affymetrix GeneChip 3' IVT PLUS Reagent kit. Poly-A controls were added to each sample at the beginning of the labeling. 10ug of fragmented, biotin-modified aRNA was hybridized to the Affymetrix PrimeView Human microarray in the Affymetrix GeneChip Hybridization Oven 645 set at 45°C with 60rpm for 16 hours. Hybridization controls were added to each sample before the arrays were

hybridized. The arrays were washed and stained with Affymetrix GeneChip Wash and Stain Kit on the Affymetrix GeneChip Fluidics Station 450. Arrays were scanned on the Affymetrix GeneChip Scanner 3000 7G to generate the raw data files.

Nude Mouse Xenografts: 6 week old male nu/nu mice (Charles River) were injected with ~3 million cells (in 250μl PBS) in a 1:1 ratio with Matrigel and after institutional animal ethics committee approval as previously described(36).

CCL20 ELISA: Supernatant was collected, centrifuged at 1500rpm for 5 minutes to remove any remaining cellular debris and the CCL20 ELISA performed as per the manufacturer's specifications (Abcam). Concentrations were normalized to milligrams of cell protein from the wells.

BrdU assay: Colorimetric BrdU ELISA assay was used as per the manufacturer's specifications (Roche). In summary cells were incubated with 20 μM of BrdU solution for 2 hours and then fixed for 30 minutes. Cells were then incubated with an anti-BrdU-POD solution for 90 minutes and were subsequently washed and incubated with a substrate solution for 5 minutes before measuring the absorbance at 370 nm and 492 nm.

Confocal microscopy was used for immunofluorescence and live cell (TMRM, Mitosox) imaging as previously described(36).

Immunoblotting: Immunoblotting with standard SDS-PAGE was performed as previously described(39).

Statistics: We used Paired and Independent-Samples T tests to compare two samples when appropriate and Spearman's correlation coefficient to determine association between two variables. $p<0.05$ was considered significant.

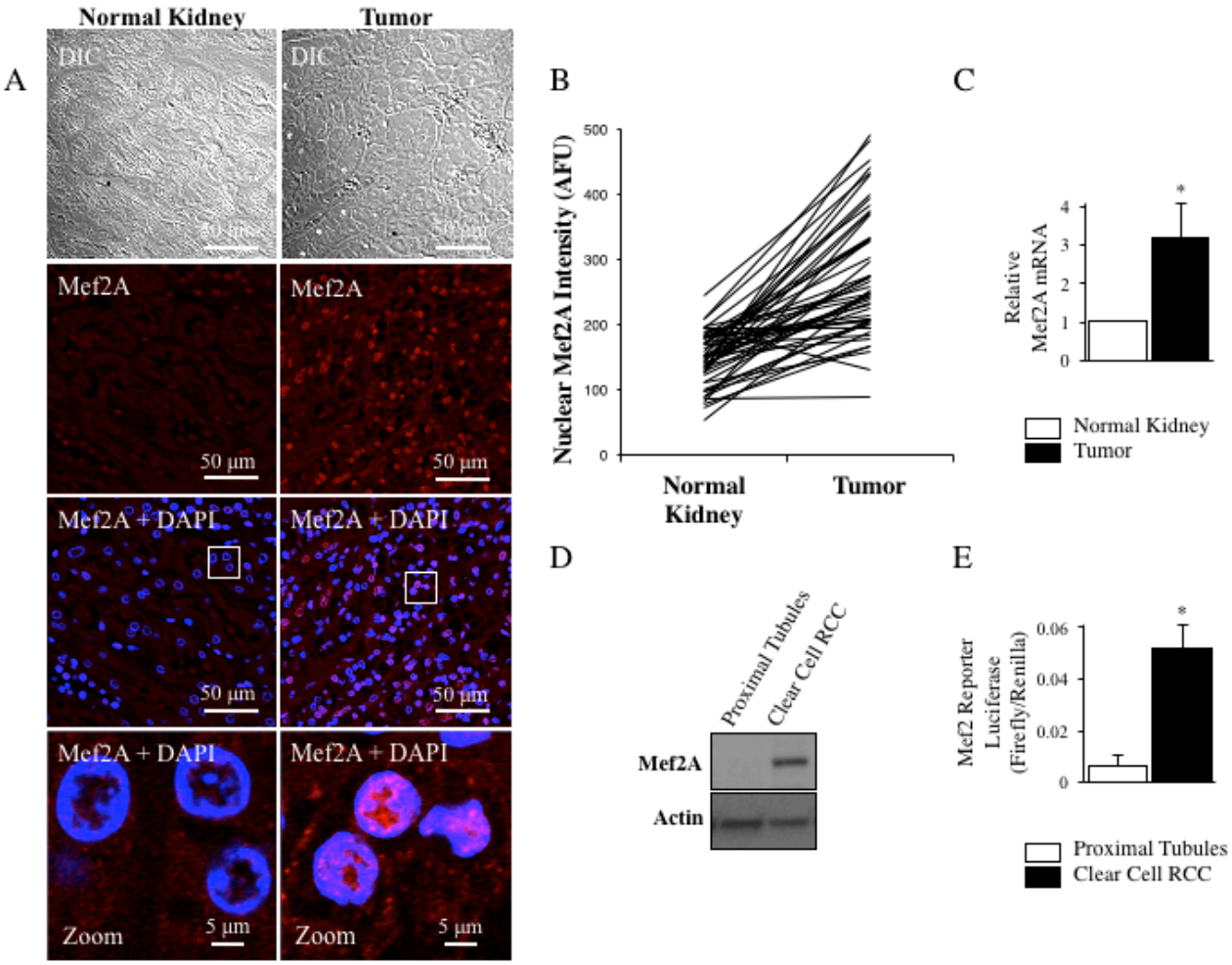

Figure 5-1: Mef2A is upregulated in ccRCC cells and tumors from patients compared to healthy kidney tissues removed from the same patient.

(A) Representative confocal immunofluorescence imaging shows that Mef2A is upregulated in the nuclei of ccRCC tumor samples compared to normal kidney tissues removed from the same patient during radical nephrectomy (Mef2A: red, Nuclear stain DAPI: blue; bottom image is a zoom of the region of interest outlined by a white box). (B) Nuclear Mef2A intensity plotted for normal and tumor tissues from each patient (n=52 patients per group; *p<0.01 vs. normal kidney). (C) Mef2A mRNA levels in tumor and normal kidney tissues (n=5 patients per group; *p<0.05 vs. normal kidney). (D) Protein expression levels of Mef2A in human ccRCC and proximal tubule cells. (E) ccRCC cells have significantly more Mef2 transcriptional activity then proximal tubule cells (n=3 per group; *p<0.01 vs. proximal tubules).

A

Patient/Tumor Characteristics		n=52
Median Age (Range)		62 (36-84)
Female (%)		21 (40.4%)
Stage	T1	33 (63.5%)
	T2	6 (11.5%)
	T3	13 (25%)
	T4	0 (0%)
Grade	1	13 (25%)
	2	25 (48.1%)
	3	13 (25%)
	4	1 (1.9%)

B

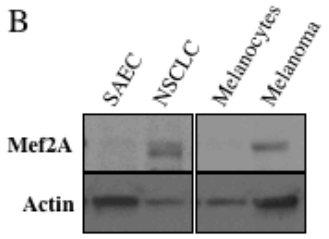

Figure 5-2: Patient and tumor characteristics

(A) Patient and tumor characteristics from the 52 patients studied. (B) Mef2A protein levels are higher in non-small cell lung cancer and melanoma compared to the normal cell type from which they derive, small airway epithelial cells and melanocytes, respectively.

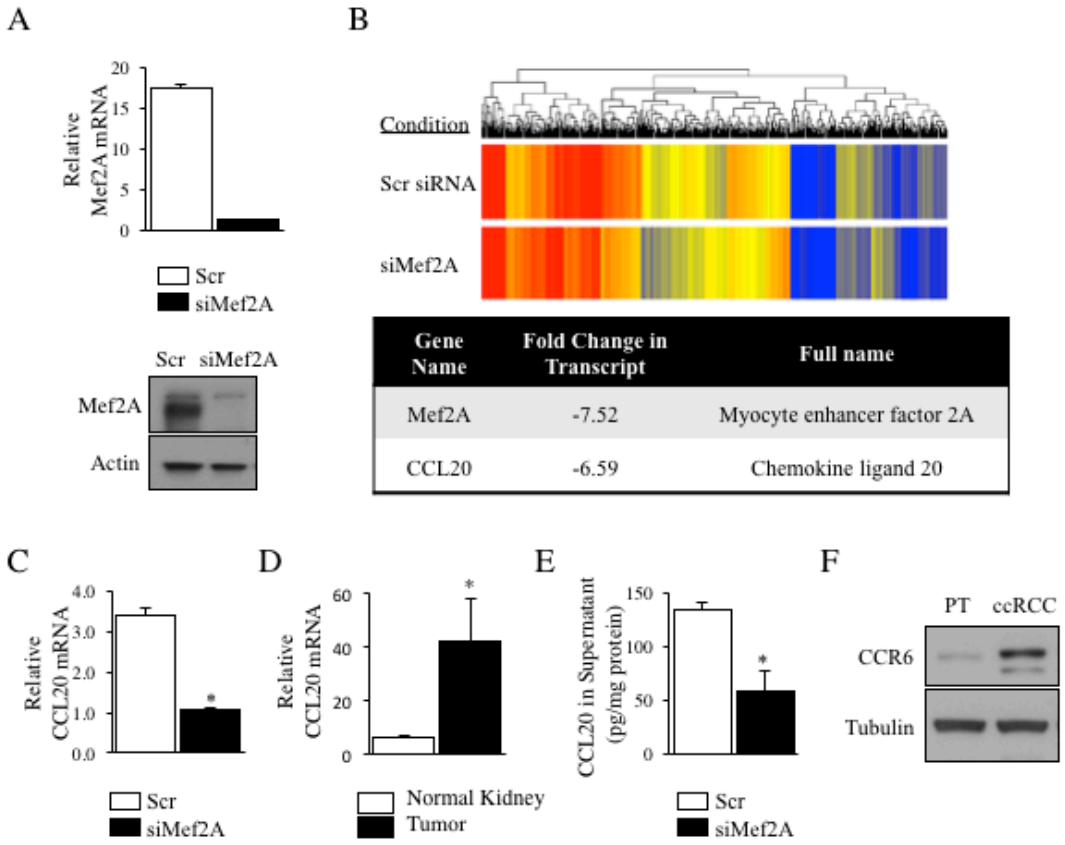

Gene Name	Fold Change in Transcript	Full name
Mef2A	-7.52	Myocyte enhancer factor 2A
CCL20	-6.59	Chemokine ligand 20

Figure 5-3: Mef2A regulates expression of CCL20 in kidney tumor cells

(A) siRNA knocks down Mef2A mRNA and protein in ccRCC cells used for GeneChip analysis shown in B. (B) CCL20 mRNA is the most altered target (reduced by ~6.6 fold) in a GeneChip assay comparing siMef2A against Scr siRNA treated ccRCC cells. (C) Mef2A knockdown significantly reduces CCL20 expression in ccRCC cells by primer specific qRT-PCR (n=3; *p<0.01 vs. Scr). (D) CCL20 mRNA levels in tumor and normal kidney tissues (n=6 patients per group; *p<0.05 vs. normal kidney). (E) Less CCL20 is measured in the supernatant of Mef2A knockdown compared to Scr siRNA treated ccRCC cells (n=3; *p<0.05 vs. Scr). (F) The CCL20 receptor, CCR6 is present and highly expressed on ccRCC cells compared to proximal tubule cells.

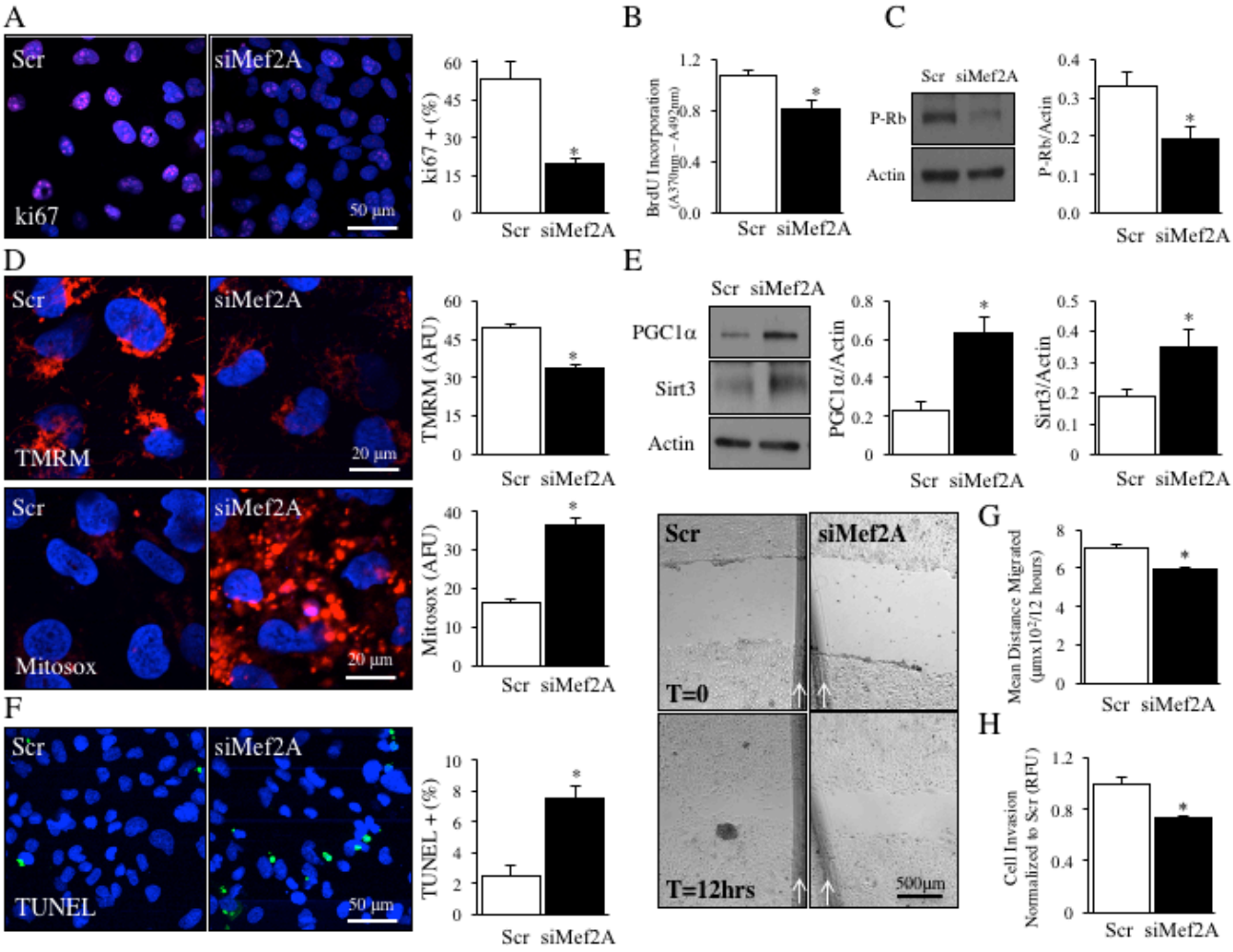

Figure 5-4: Mef2A inhibition reduces proliferation, migration and invasion and promotes apoptosis in ccRCC cells

(A) Mef2A knockdown reduces the cell proliferative markers: ki67 (n=15 fields from 3 different experiments, *p<0.05 vs. Scr), (B) Brdu incorporation (n=9, *p<0.05 vs. Scr) and (C) phosphorylated retinoblastoma protein (n=3, *p<0.05 vs. Scr) in ccRCC cells. (D) Mef2A knockdown depolarizes mitochondrial membrane potential (TMRM) and increases mitochondrial reactive oxygen species detection (Mitosox; n=100 cells/group, *p<0.01 compared to Scr). (E) Mef2A knockdown increases PGC1α and Sirt3 protein levels (n=3, *p<0.05 vs. Scr). (F) Mef2A knockdown increases apoptosis in ccRCC cells, measured by TUNEL staining (n=3, *p<0.05 compared to Scr). (G) Mef2A knockdown decreases mean distance migrated after 12 hours in a standard scratch assay (n=18, *p<0.05 vs. Scr), and (H) cell invasion measured in an in-vitro invasion assay (n=12, *p<0.05 vs. Scr).

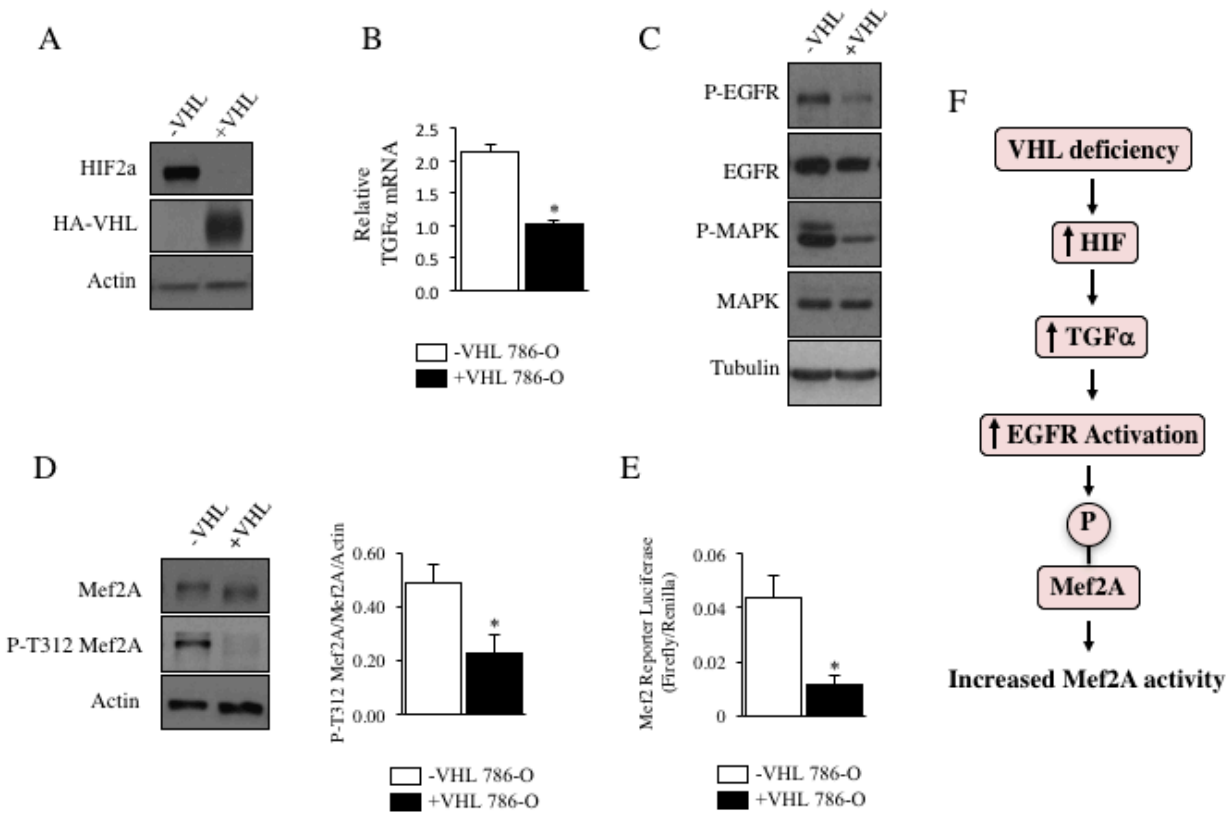

Figure 5-5: VHL deficiency activates Mef2A in ccRCC

(A) VHL-deficient (-VHL) 786-O ccRCC cells express significantly more HIF2a than VHL-expressing (+VHL) 786-O ccRCC cells. (B) TGFα mRNA is expressed at a higher level in -VHL ccRCC cells (n=3; *p<0.05 vs. -VHL). (C) The EGFR receptor and downstream MAP kinase are hyperphosphorylated in -VHL ccRCC cells. (D) Mef2A is significantly more phosphorylated at threonine 312 in -VHL ccRCC cells (n=3; *p<0.05 vs. +VHL ccRCC cells). (E) Mef2 transcriptional activity is higher in -VHL ccRCC cells (n=9; *p<0.01 vs. +VHL ccRCC cells). (F) Schematic of Mef2A activation in VHL-deficient ccRCC cells.

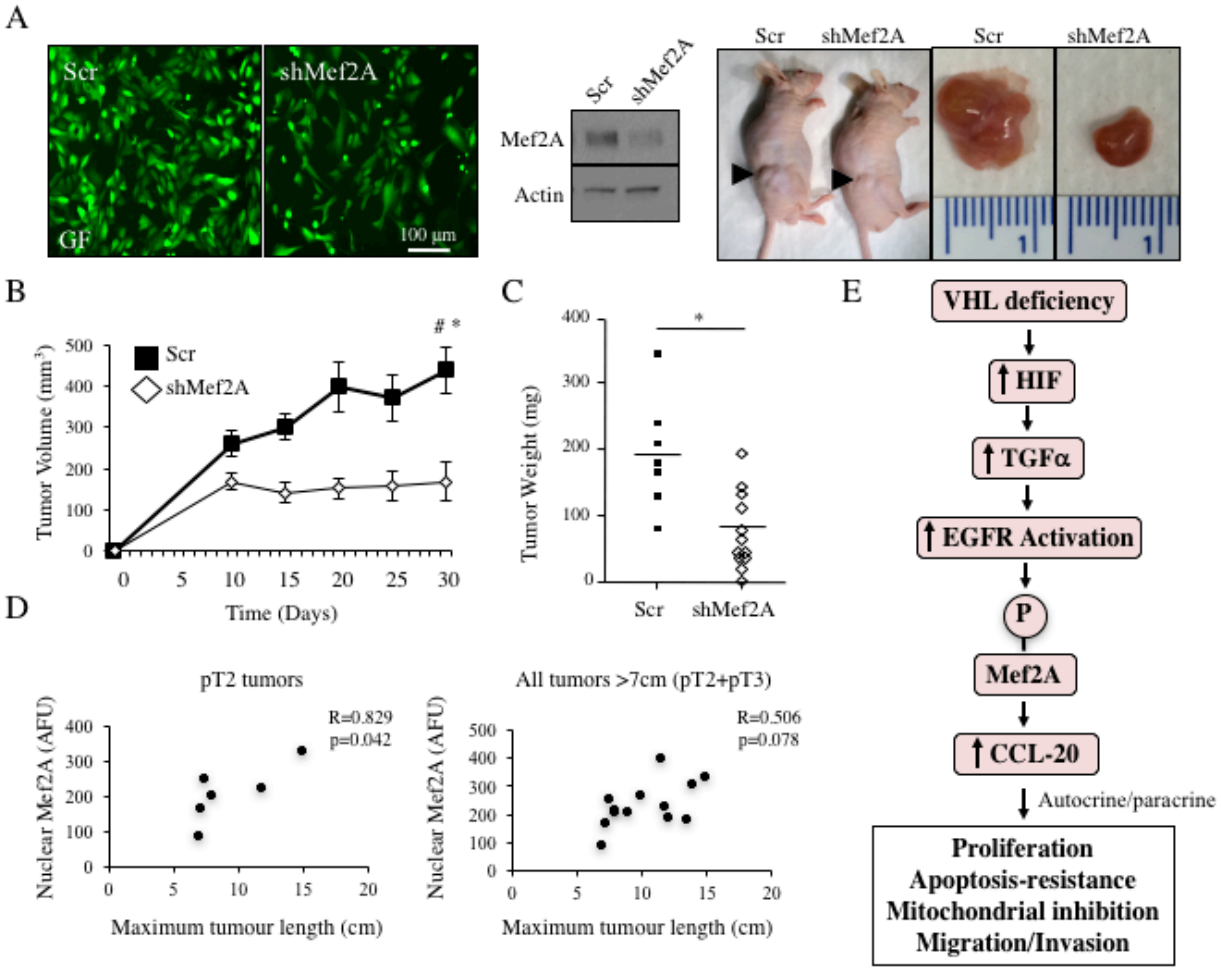

Figure 5-6: Mef2A knockdown reduces tumor growth in a nude mouse flank xenograft model

(A) Stable knockdown of Mef2A using a Mef2A short-hairpin RNA plasmid, which co-expresses GFP and representative flank tumor xenografts formed by Scr (left) and shMef2A (right) ccRCC cells. (B) Mef2A knockdown ccRCC cells grow tumors that are smaller volume and (C) weight after 30 days (n=7 (Scr) and 12 (shMef2A); *p<0.01 vs. Scr, #p<0.01 vs. shMef2A at 11 days). (D) Positive correlation between nuclear Mef2A levels and maximal tumor length from patient samples, stratified by pT2 (left; R=0.829, p<0.05) and all tumours >7cm (right; R=0.506, p=0.078). (E) Mechanism of Mef2A activation leading to proliferation, apoptosis-resistance, mitochondrial inhibition, migration and invasion in ccRCC (see Discussion).

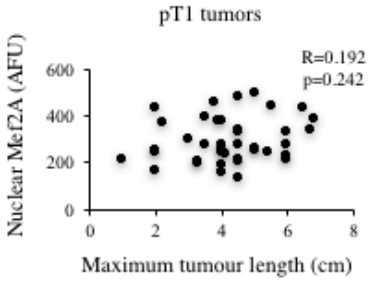

Figure 5-7: Correlation between Mef2A and maximal tumor length in pT1 tumors

No correlation between nuclear Mef2A levels and maximal tumor length from pT1 patient samples (R=0.192, p=0.242).

Table 5-1 (available upon request):

All mRNA targets with >1.5-fold change in expression after Mef2A knockdown, measured by GeneChip assay.

References

1. Ferlay J, Soerjomataram I, Dikshit R, Eser S, Mathers C, Rebelo M, et al. Cancer incidence and mortality worldwide: sources, methods and major patterns in GLOBOCAN 2012. Int J Cancer. 2015;136(5):E359-86.
2. Fisher R, Gore M, Larkin J. Current and future systemic treatments for renal cell carcinoma. Semin Cancer Biol. 2013;23(1):38-45.
3. Motzer RJ, Hutson TE, Tomczak P, Michaelson MD, Bukowski RM, Rixe O, et al. Sunitinib versus interferon alfa in metastatic renal-cell carcinoma. N Engl J Med. 2007;356(2):115-24.
4. Motzer RJ, Escudier B, McDermott DF, George S, Hammers HJ, Srinivas S, et al. Nivolumab versus Everolimus in Advanced Renal-Cell Carcinoma. N Engl J Med. 2015;373(19):1803-13.
5. Hanahan D, Weinberg RA. Hallmarks of cancer: the next generation. Cell. 2011;144(5):646-74.
6. Pon JR, Marra MA. MEF2 transcription factors: developmental regulators and emerging cancer genes. Oncotarget. 2016;7(3):2297-312.
7. Yu W, Huang C, Wang Q, Huang T, Ding Y, Ma C, et al. MEF2 transcription factors promotes EMT and invasiveness of hepatocellular carcinoma through TGF-beta1 autoregulation circuitry. Tumour Biol. 2014;35(11):10943-51.
8. Clark RI, Tan SW, Pean CB, Roostalu U, Vivancos V, Bronda K, et al. MEF2 is an in vivo immune-metabolic switch. Cell. 2013;155(2):435-47.
9. Naya FJ, Black BL, Wu H, Bassel-Duby R, Richardson JA, Hill JA, et al. Mitochondrial deficiency and cardiac sudden death in mice lacking the MEF2A transcription factor. Nat Med. 2002;8(11):1303-9.
10. Hashemi S, Salma J, Wales S, McDermott JC. Pro-survival function of MEF2 in cardiomyocytes is enhanced by beta-blockers. Cell Death Discov. 2015;1:15019.
11. Kato Y, Zhao M, Morikawa A, Sugiyama T, Chakravortty D, Koide N, et al. Big mitogen-activated kinase regulates multiple members of the MEF2 protein family. J Biol Chem. 2000;275(24):18534-40.
12. Chen W, Hill H, Christie A, Kim MS, Holloman E, Pavia-Jimenez A, et al. Targeting renal cell carcinoma with a HIF-2 antagonist. Nature. 2016;539(7627):112-7.
13. Gossage L, Eisen T, Maher ER. VHL, the story of a tumour suppressor gene. Nat Rev Cancer. 2015;15(1):55-64.
14. Keith B, Johnson RS, Simon MC. HIF1alpha and HIF2alpha: sibling rivalry in hypoxic tumour growth and progression. Nat Rev Cancer. 2011;12(1):9-22.
15. Gunaratnam L, Morley M, Franovic A, de Paulsen N, Mekhail K, Parolin DA, et al. Hypoxia inducible factor activates the transforming growth factor-alpha/epidermal growth factor receptor growth stimulatory pathway in VHL(-/-) renal cell carcinoma cells. J Biol Chem. 2003;278(45):44966-74.

16. Beider K, Abraham M, Begin M, Wald H, Weiss ID, Wald O, et al. Interaction between CXCR4 and CCL20 pathways regulates tumor growth. PLoS One. 2009;4(4):e5125.
17. Marsigliante S, Vetrugno C, Muscella A. CCL20 induces migration and proliferation on breast epithelial cells. J Cell Physiol. 2013;228(9):1873-83.
18. Ghadjar P, Rubie C, Aebersold DM, Keilholz U. The chemokine CCL20 and its receptor CCR6 in human malignancy with focus on colorectal cancer. Int J Cancer. 2009;125(4):741-5.
19. Zeng W, Chang H, Ma M, Li Y. CCL20/CCR6 promotes the invasion and migration of thyroid cancer cells via NF-kappa B signaling-induced MMP-3 production. Exp Mol Pathol. 2014;97(1):184-90.
20. Kimsey TF, Campbell AS, Albo D, Wilson M, Wang TN. Co-localization of macrophage inflammatory protein-3alpha (Mip-3alpha) and its receptor, CCR6, promotes pancreatic cancer cell invasion. Cancer J. 2004;10(6):374-80.
21. Middel P, Brauneck S, Meyer W, Radzun HJ. Chemokine-mediated distribution of dendritic cell subsets in renal cell carcinoma. BMC Cancer. 2010;10:578.
22. Rubie C, Frick VO, Ghadjar P, Wagner M, Grimm H, Vicinus B, et al. CCL20/CCR6 expression profile in pancreatic cancer. J Transl Med. 2010;8:45.
23. Nandi B, Pai C, Huang Q, Prabhala RH, Munshi NC, Gold JS. CCR6, the sole receptor for the chemokine CCL20, promotes spontaneous intestinal tumorigenesis. PLoS One. 2014;9(5):e97566.
24. Oldham KA, Parsonage G, Bhatt RI, Wallace DM, Deshmukh N, Chaudhri S, et al. T lymphocyte recruitment into renal cell carcinoma tissue: a role for chemokine receptors CXCR3, CXCR6, CCR5, and CCR6. Eur Urol. 2012;61(2):385-94.
25. Wang B, Shi L, Sun X, Wang L, Wang X, Chen C. Production of CCL20 from lung cancer cells induces the cell migration and proliferation through PI3K pathway. J Cell Mol Med. 2016;20(5):920-9.
26. Schutyser E, Struyf S, Van Damme J. The CC chemokine CCL20 and its receptor CCR6. Cytokine Growth Factor Rev. 2003;14(5):409-26.
27. Paulin R, Dromparis P, Sutendra G, Gurtu V, Zervopoulos S, Bowers L, et al. Sirtuin 3 deficiency is associated with inhibited mitochondrial function and pulmonary arterial hypertension in rodents and humans. Cell Metab. 2014;20(5):827-39.
28. Kong X, Wang R, Xue Y, Liu X, Zhang H, Chen Y, et al. Sirtuin 3, a new target of PGC-1alpha, plays an important role in the suppression of ROS and mitochondrial biogenesis. PLoS One. 2010;5(7):e11707.
29. Czubryt MP, McAnally J, Fishman GI, Olson EN. Regulation of peroxisome proliferator-activated receptor gamma coactivator 1 alpha (PGC-1 alpha) and mitochondrial function by MEF2 and HDAC5. Proc Natl Acad Sci U S A. 2003;100(4):1711-6.
30. Uhlen M, Zhang C, Lee S, Sjostedt E, Fagerberg L, Bidkhori G, et al. A pathology atlas of the human cancer transcriptome. Science. 2017;357(6352).

31. Xu L, Xu W, Qiu S, Xiong S. Enrichment of CCR6+Foxp3+ regulatory T cells in the tumor mass correlates with impaired CD8+ T cell function and poor prognosis of breast cancer. Clin Immunol. 2010;135(3):466-75.
32. Bukowski RM, Kabbinavar FF, Figlin RA, Flaherty K, Srinivas S, Vaishampayan U, et al. Randomized phase II study of erlotinib combined with bevacizumab compared with bevacizumab alone in metastatic renal cell cancer. J Clin Oncol. 2007;25(29):4536-41.
33. Kitagawa Y, Kikuchi S, Arita Y, Nishimura M, Mizuno K, Ogasawara H, et al. Inhibition of CCL20 increases mortality in models of mouse sepsis with intestinal apoptosis. Surgery. 2013;154(1):78-88.
34. Kim TG, Byamba D, Wu WH, Lee MG. Statins inhibit chemotactic interaction between CCL20 and CCR6 in vitro: possible relevance to psoriasis treatment. Exp Dermatol. 2011;20(10):855-7.
35. Ito M, Teshima K, Ikeda S, Kitadate A, Watanabe A, Nara M, et al. MicroRNA-150 inhibits tumor invasion and metastasis by targeting the chemokine receptor CCR6, in advanced cutaneous T-cell lymphoma. Blood. 2014;123(10):1499-511.
36. Kinnaird A, Dromparis P, Saleme B, Gurtu V, Watson K, Paulin R, et al. Metabolic Modulation of Clear-cell Renal Cell Carcinoma with Dichloroacetate, an Inhibitor of Pyruvate Dehydrogenase Kinase. Eur Urol. 2016;69(4):734-44.
37. Li L, Zhang L, Zhang X, Yan Q, Minamishima YA, Olumi AF, et al. Hypoxia-inducible factor linked to differential kidney cancer risk seen with type 2A and type 2B VHL mutations. Mol Cell Biol. 2007;27(15):5381-92.
38. Sutendra G, Dromparis P, Kinnaird A, Stenson TH, Haromy A, Parker JM, et al. Mitochondrial activation by inhibition of PDKII suppresses HIF1a signaling and angiogenesis in cancer. Oncogene. 2013;32(13):1638-50.
39. Sutendra G, Kinnaird A, Dromparis P, Paulin R, Stenson TH, Haromy A, et al. A nuclear pyruvate dehydrogenase complex is important for the generation of acetyl-CoA and histone acetylation. Cell. 2014;158(1):84-97.

Chapter Six

Overall Conclusions and Future Directions

6.1 Discussion and Conclusions

Metabolic oncology is an exciting new field in cancer research, offering a new window to cancer's molecular plasticity and promise for the development of effective, cancer-selective therapies and novel biomarkers.

In Chapter One of this thesis, I synthesize the metabolic basis of malignancy. It is based on the realization that cancer's unique metabolism (known since Warburg's report in 1923) with suppression of mitochondrial glucose oxidation and up-regulation of cytoplasmic glycolysis is not a secondary but a primary event, offering many growth advantages to cancer cells. Several mechanisms are discussed, including growth factor signaling, oncogenes, and mutations, all contributing to a suppression of mitochondria, similar to what takes place in hypoxia. This suppression leads to inhibition of mitochondria-driven apoptosis, promotes proliferation, and enhances angiogenesis and metastatic potential. Furthermore, most chromatin-modifying enzymes require substrates or cofactors that are intermediates of cell metabolism. Such metabolites, and often the enzymes that produce them, can transfer into the nucleus, directly linking metabolism to nuclear transcription in cancer.

In Chapter Two of this dissertation, I explored the therapeutic effect of reversing the suppression of mitochondrial glucose oxidation (GO) in clear cell renal cell carcinoma (ccRCC) – a malignancy driven by metabolic derangement due to constitutive HIF up-regulation secondary to von Hippel Lindau (VHL) deficiency. Inhibition of Pyruvate dehydrogenase kinase (PDK) with dichloroacetate (DCA) resulted in **(1)** increased production of mitochondrial acetyl-CoA by PDK's target, the Pyruvate dehydrogenase complex (PDC) **(2)** depolarized mitochondrial membrane potential **(3)** increased production of mitochondria-derived reactive oxygen species **(4)** increased production of Krebs' cycle intermediates, including α-ketoglutarate and **(5)** increased mitochondrial respiration. This activation of mitochondrial GO leads to an inhibition of HIF activity (and production of angiogenic signaling molecules), via the α-ketoglutarate–dependent enzyme Factor Inhibiting HIF, without altering HIF protein levels (as ccRCC cells are VHL-deficient). Furthermore, depolarized

mitochondrial membrane potential lead to an induction of mitochondrial-driven apoptosis while increased production of mitochondrial reactive oxygen species increased the nuclear localization and activity of the redox sensitive tumor suppressor, p53, to reduce cell proliferation. In vivo analysis using both ex ovo chicken, and nude mouse flank, xenografts demonstrate DCA inhibits angiogenesis and reduces tumor growth in animal models. This work supports the concept of mitochondrial GO activation as a therapeutic strategy in ccRCC. Furthermore, it identifies a method to suppress HIF activity in a malignancy that has lost the ability to efficiently regulate its expression.

In Chapter Three of this thesis, we identify a novel link between cellular metabolism and epigenetic regulation. We show that mitochondrial PDC **(1)** dynamically translocates to the nucleus in response to growth stimuli **(2)** generates acetyl-CoA from pyruvate locally, within the nucleus, and **(3)** this acetyl-CoA is used to acetylate core histones involved in S-phase progression and cell proliferation. This work provides key insights into the recent identification of localized production of metabolites within the nuclear domain in which they are used for epigenetic modification. The Histone Code has been discussed for nearly two decades, with histone acetyltransferases, which add acetyl- groups representing 'writers' and histone deacetylases, which remove the acetyl- groups known as the 'erasers'. However, it has not been until recently that the 'ink' for these writers has been established. This paper identifies PDC as one of the three major producers of this nuclear acetyl-CoA 'ink', along with ATP-Citrate Lyase (producing acetyl-CoA from citrate) and Acetyl-CoA Synthetase 2 (producing acetyl-CoA from acetate). Furthermore, this paper establishes a new link between carbohydrate metabolism and cell proliferation and offers early mechanistic insight into mitochondrial-nuclear communication with the transfer of a large enzymatic complex between the two organelles.

In Chapter Four of this thesis, we identify a new function of VHL in cancer. We show that VHL **(1)** physically interacts with p53 **(2)** prevents p53 binding to the promoters and expression of its target genes, p21 and PUMA, in response to p53-inducing stimuli **(3)** inhibits p53 independent of its effects on HIF and **(4)**

attenuates p53-inducing therapies on tumor growth in animals. These results are paradoxical as VHL is classically described as a tumor suppressor and VHL loss has been suggested as a key event in ccRCC initiation. In fact, this work suggests VHL to possess a Janus effect; eliciting anti-tumor HIF degradation, while promoting pro-tumor p53 inhibition. This is in keeping with recent publications that suggest VHL-deficiency alone is insufficient for tumorigenesis, however when p53-deficiency is combined with VHL-deficiency, tumors initiate. Furthermore, the identification of this balance provides a new treatment rationale that may be exploited clinically, as discussed below, in 6.2.

In Chapter Five of this dissertation, explore the role of Myocyte Enhancer Factor 2A (Mef2A) in ccRCC. Mef2A is a transcription factor that controls mitochondrial metabolism, immune response and tumor invasion. We show that Mef2A **(1)** expression and activity is up-regulated in ccRCC tumors and VHL-deficient cells compared to normal kidney tissues **(2)** increases expression of several immune factors including the pro-tumor chemokine CCL-20 **(3)** knockdown reduces cell proliferation, migration and invasion as well as increases mitochondrial activity and apoptosis, and reduces tumor growth in an animal model and **(4)** nuclear levels correlate positively with larger tumor size in patients. This work suggests that Mef2A is an important transcription factor for ccRCC growth. In keeping with this, the Cancer Genome Atlas identifies RCC to express the highest level of Mef2A amongst the 17 malignancies studied. While the effect of Mef2A on cell metabolism, proliferation and apoptosis is important, a key finding is the regulation of immune factors. Mef2A induces CCL-20, which has been shown to recruit inhibitory T-regulatory cells in order to locally suppress immune response in the tumor microenvironment. Therefore, Mef2A inhibition may represent a new target in the setting of a tumor that has been recently described and therapeutically targeted for its immune evasion using immune checkpoint inhibitors.

6.2 Future Directions

This work has multiple new and exciting implications for future basic science, translational, and clinical research:

- Activation of mitochondrial glucose oxidation using dichloroacetate has now successfully been shown in early phase clinical trials in Glioblastoma Multiforme and Pulmonary Arterial Hypertension. Our results may allow for rapid translation to phase 2 and phase 3 randomized controlled clinical trials of dichloroacetate in combination with tyrosine kinase inhibitors for patients with advanced ccRCC. This combination will not only inhibit tumor cell growth but also angiogenesis, thereby depleting the developing tumors of nutrients and limiting metastatic potential. Based on this rationale and the early success of dichloroacetate, companies are currently developing more potent PDK inhibitors.
- This work uncovers early insight into dynamic translocation of large, mitochondrial protein complexes into the nucleus with the assistance of a chaperone. This will be an important process to further explore as there is accumulating evidence that at least 20 cytoplasmic or mitochondrial metabolic enzymes, such as hexokinase, fumarase, isocitrate dehydrogenase and carnitine acetyltransferase, 'moonlight' in the nucleus, either providing local production of metabolites or performing newly discovered functions. Alternative mechanisms for transfer of large mitochondrial proteins into the nucleus that require further research include mitochondria-derived vesicles and direct mitochondrial-nuclear contact points.
- Our identification of VHL-mediated p53 inhibition opens the door to accurately identifying susceptible tumors as well as new strategies to sensitize or desensitize tissues to p53 inducing therapies. For example, a personalized medicine approach for treatment with anthracyclines may be taken based on the abundance of VHL expression in a tumor biopsy. Alternatively, tumor biopsies from patients may be implanted into animal models and sensitives to anthracyclines tested to determine efficacy for each patient's specific tumor prior to administering systemic therapy to the

patient. Furthermore, malignancies that have high levels of VHL may be sensitized to p53 inducers by combining recently developed cell permeable small molecules that inhibit VHL interaction with other proteins. Conversely, strategies to increase VHL expression may prevent side effects of p53 inducing chemotherapies, like anthracycline induced cardiotoxicity.

- This works suggests that Mef2A or CCL20 inhibition may represent new therapeutic targets in ccRCC. Development of small molecule inhibitors of these proteins or the CCL20 receptor, CCR6, may advance treatment of this deadly cancer. Furthermore, as ccRCC known to evade the immune system and immune checkpoint inhibitors are quickly becoming the new cornerstone of advanced ccRCC management, it will be critical to further explore the role of local CCL20 production on immune tolerance in the tumor microenvironment.

Bibliography

Abbas, T., and A. Dutta. "P21 in Cancer: Intricate Networks and Multiple Activities." *Nat Rev Cancer* 9, no. 6 (Jun 2009): 400-14.

Abdelmalak, M., A. Lew, R. Ramezani, A. L. Shroads, B. S. Coats, T. Langaee, M. N. Shankar*, et al.* "Long-Term Safety of Dichloroacetate in Congenital Lactic Acidosis." *Mol Genet Metab* 109, no. 2 (Jun 2013): 139-43.

Ahn, B. H., H. S. Kim, S. Song, I. H. Lee, J. Liu, A. Vassilopoulos, C. X. Deng, and T. Finkel. "A Role for the Mitochondrial Deacetylase Sirt3 in Regulating Energy Homeostasis." *Proc Natl Acad Sci U S A* 105, no. 38 (Sep 23 2008): 14447-52.

Alarcon-Vargas, D., W. P. Tansey, and Z. Ronai. "Regulation of C-Myc Stability by Selective Stress Conditions and by Mekk1 Requires Aa 127-189 of C-Myc." [In eng]. *Oncogene* 21, no. 28 (Jun 27 2002): 4384-91.

Albaugh, B. N., K. M. Arnold, and J. M. Denu. "Kat(Ching) Metabolism by the Tail: Insight into the Links between Lysine Acetyltransferases and Metabolism." *Chembiochem* 12, no. 2 (Jan 24 2011): 290-8.

Albers, J., M. Rajski, D. Schonenberger, S. Harlander, P. Schraml, A. von Teichman, S. Georgiev*, et al.* "Combined Mutation of Vhl and Trp53 Causes Renal Cysts and Tumours in Mice." *EMBO Mol Med* 5, no. 6 (Jun 2013): 949-64.

Albert, M., and K. Helin. "Histone Methyltransferases in Cancer." *Semin Cell Dev Biol* 21, no. 2 (Apr 2010): 209-20.

Bachman, K. E., B. H. Park, I. Rhee, H. Rajagopalan, J. G. Herman, S. B. Baylin, K. W. Kinzler, and B. Vogelstein. "Histone Modifications and Silencing Prior to DNA Methylation of a Tumor Suppressor Gene." *Cancer Cell* 3, no. 1 (Jan 2003): 89-95.

Ballantyne, C. M., M. H. Davidson, D. E. Macdougall, H. E. Bays, L. A. Dicarlo, N. L. Rosenberg, J. Margulies, and R. S. Newton. "Efficacy and Safety of a Novel Dual Modulator of Adenosine Triphosphate-Citrate Lyase and Adenosine Monophosphate-Activated Protein Kinase in Patients with Hypercholesterolemia: Results of a Multicenter, Randomized, Double-Blind, Placebo-Controlled, Parallel-Group Trial." *J Am Coll Cardiol* 62, no. 13 (Sep 24 2013): 1154-62.

Bantscheff, M., C. Hopf, M. M. Savitski, A. Dittmann, P. Grandi, A. M. Michon, J. Schlegl*, et al.* "Chemoproteomics Profiling of Hdac Inhibitors Reveals Selective Targeting of Hdac Complexes." *Nat Biotechnol* 29, no. 3 (Mar 2011): 255-65.

Behal, R. H., D. B. Buxton, J. G. Robertson, and M. S. Olson. "Regulation of the Pyruvate Dehydrogenase Multienzyme Complex." [In eng]. *Annu Rev Nutr* 13 (1993): 497-520.

Beider, K., M. Abraham, M. Begin, H. Wald, I. D. Weiss, O. Wald, E. Pikarsky*, et al.* "Interaction between Cxcr4 and Ccl20 Pathways Regulates Tumor Growth." *PLoS One* 4, no. 4 (2009): e5125.

Berra, E., E. Benizri, A. Ginouves, V. Volmat, D. Roux, and J. Pouyssegur. "Hif Prolyl-Hydroxylase 2 Is the Key Oxygen Sensor Setting Low Steady-State Levels of Hif-1alpha in Normoxia." *EMBO J* 22, no. 16 (Aug 15 2003): 4082-90.

Berwick, D. C., I. Hers, K. J. Heesom, S. K. Moule, and J. M. Tavare. "The Identification of Atp-Citrate Lyase as a Protein Kinase B (Akt) Substrate in Primary Adipocytes." *J Biol Chem* 277, no. 37 (Sep 13 2002): 33895-900.

Bharathi, S. S., Y. Zhang, A. W. Mohsen, R. Uppala, M. Balasubramani, E. Schreiber, G. Uechi*, et al.* "Sirtuin 3 (Sirt3) Protein Regulates Long-Chain Acyl-Coa Dehydrogenase by

Deacetylating Conserved Lysines near the Active Site." *J Biol Chem* 288, no. 47 (Nov 22 2013): 33837-47.
Bonnet, S., S. L. Archer, J. Allalunis-Turner, A. Haromy, C. Beaulieu, R. Thompson, C. T. Lee*, et al.* "A Mitochondria-K+ Channel Axis Is Suppressed in Cancer and Its Normalization Promotes Apoptosis and Inhibits Cancer Growth." *Cancer Cell* 11, no. 1 (Jan 2007): 37-51.
Borodovsky, A., V. Salmasi, S. Turcan, A. W. Fabius, G. S. Baia, C. G. Eberhart, J. D. Weingart*, et al.* "5-Azacytidine Reduces Methylation, Promotes Differentiation and Induces Tumor Regression in a Patient-Derived Idh1 Mutant Glioma Xenograft." *Oncotarget* 4, no. 10 (Oct 2013): 1737-47.
Bowker-Kinley, M. M., W. I. Davis, P. Wu, R. A. Harris, and K. M. Popov. "Evidence for Existence of Tissue-Specific Regulation of the Mammalian Pyruvate Dehydrogenase Complex." [In eng]. *Biochem J* 329 (Pt 1) (Jan 1 1998): 191-6.
Buczek, M., B. Escudier, E. Bartnik, C. Szczylik, and A. Czarnecka. "Resistance to Tyrosine Kinase Inhibitors in Clear Cell Renal Cell Carcinoma: From the Patient's Bed to Molecular Mechanisms." *Biochim Biophys Acta* 1845, no. 1 (Jan 2014): 31-41.
Bukowski, R. M., F. F. Kabbinavar, R. A. Figlin, K. Flaherty, S. Srinivas, U. Vaishampayan, H. A. Drabkin*, et al.* "Randomized Phase Ii Study of Erlotinib Combined with Bevacizumab Compared with Bevacizumab Alone in Metastatic Renal Cell Cancer." *J Clin Oncol* 25, no. 29 (Oct 10 2007): 4536-41.
Bungard, D., B. J. Fuerth, P. Y. Zeng, B. Faubert, N. L. Maas, B. Viollet, D. Carling*, et al.* "Signaling Kinase Ampk Activates Stress-Promoted Transcription Via Histone H2b Phosphorylation." *Science* 329, no. 5996 (Sep 3 2010): 1201-5.
Cahill, G. F., Jr. "Fuel Metabolism in Starvation." *Annu Rev Nutr* 26 (2006): 1-22.
Cai, L., B. M. Sutter, B. Li, and B. P. Tu. "Acetyl-Coa Induces Cell Growth and Proliferation by Promoting the Acetylation of Histones at Growth Genes." *Mol Cell* 42, no. 4 (May 20 2011): 426-37.
Cairns, R. A., and T. W. Mak. "Oncogenic Isocitrate Dehydrogenase Mutations: Mechanisms, Models, and Clinical Opportunities." *Cancer Discov* 3, no. 7 (Jul 2013): 730-41.
Cao, W., S. Yacoub, K. T. Shiverick, K. Namiki, Y. Sakai, S. Porvasnik, C. Urbanek, and C. J. Rosser. "Dichloroacetate (Dca) Sensitizes Both Wild-Type and over Expressing Bcl-2 Prostate Cancer Cells in Vitro to Radiation." *Prostate* 68, no. 11 (Aug 1 2008): 1223-31.
Carey, B. W., L. W. Finley, J. R. Cross, C. D. Allis, and C. B. Thompson. "Intracellular Alpha-Ketoglutarate Maintains the Pluripotency of Embryonic Stem Cells." *Nature* 518, no. 7539 (Feb 19 2015): 413-6.
Cederbaum, A. I. "Alcohol Metabolism." *Clin Liver Dis* 16, no. 4 (Nov 2012): 667-85.
Chacinska, A., C. M. Koehler, D. Milenkovic, T. Lithgow, and N. Pfanner. "Importing Mitochondrial Proteins: Machineries and Mechanisms." [In eng]. *Cell* 138, no. 4 (Aug 21 2009): 628-44.
Chatterjee, K., J. Zhang, N. Honbo, and J. S. Karliner. "Doxorubicin Cardiomyopathy." *Cardiology* 115, no. 2 (2010): 155-62.
Chen, L. B. "Mitochondrial Membrane Potential in Living Cells." *Annu Rev Cell Biol* 4 (1988): 155-81.
Chen, R., M. Xu, J. S. Nagati, R. T. Hogg, A. Das, R. D. Gerard, and J. A. Garcia. "The Acetate/Acss2 Switch Regulates Hif-2 Stress Signaling in the Tumor Cell Microenvironment." *PLoS One* 10, no. 2 (2015): e0116515.

Chen, W., H. Hill, A. Christie, M. S. Kim, E. Holloman, A. Pavia-Jimenez, F. Homayoun, *et al.* "Targeting Renal Cell Carcinoma with a Hif-2 Antagonist." *Nature* 539, no. 7627 (Nov 03 2016): 112-17.

Chen, Y., W. Zhao, J. S. Yang, Z. Cheng, H. Luo, Z. Lu, M. Tan, W. Gu, and Y. Zhao. "Quantitative Acetylome Analysis Reveals the Roles of Sirt1 in Regulating Diverse Substrates and Cellular Pathways." *Mol Cell Proteomics* 11, no. 10 (Oct 2012): 1048-62.

Chene, P. "The Role of Tetramerization in P53 Function." *Oncogene* 20, no. 21 (May 10 2001): 2611-7.

Choudhary, C., C. Kumar, F. Gnad, M. L. Nielsen, M. Rehman, T. C. Walther, J. V. Olsen, and M. Mann. "Lysine Acetylation Targets Protein Complexes and Co-Regulates Major Cellular Functions." *Science* 325, no. 5942 (Aug 14 2009): 834-40.

Choudhary, C., B. T. Weinert, Y. Nishida, E. Verdin, and M. Mann. "The Growing Landscape of Lysine Acetylation Links Metabolism and Cell Signalling." *Nat Rev Mol Cell Biol* 15, no. 8 (Aug 2014): 536-50.

Chow, J. D., R. T. Lawrence, M. E. Healy, J. E. Dominy, J. A. Liao, D. S. Breen, F. L. Byrne, *et al.* "Genetic Inhibition of Hepatic Acetyl-Coa Carboxylase Activity Increases Liver Fat and Alters Global Protein Acetylation." *Mol Metab* 3, no. 4 (Jul 2014): 419-31.

Chu, Q. S., R. Sangha, J. Spratlin, J. Vos L, J. R. Mackey, A. J. McEwan, P. Venner, and E. D. Michelakis. "A Phase I Open-Labeled, Single-Arm, Dose-Escalation, Study of Dichloroacetate (Dca) in Patients with Advanced Solid Tumors." *Invest New Drugs* 33, no. 3 (Jun 2015): 603-10.

Cimen, H., M. J. Han, Y. Yang, Q. Tong, H. Koc, and E. C. Koc. "Regulation of Succinate Dehydrogenase Activity by Sirt3 in Mammalian Mitochondria." *Biochemistry* 49, no. 2 (Jan 19 2010): 304-11.

Clark, R. I., S. W. Tan, C. B. Pean, U. Roostalu, V. Vivancos, K. Bronda, M. Pilatova, *et al.* "Mef2 Is an in Vivo Immune-Metabolic Switch." *Cell* 155, no. 2 (Oct 10 2013): 435-47.

Cluntun, A. A., H. Huang, L. Dai, X. Liu, Y. Zhao, and J. W. Locasale. "The Rate of Glycolysis Quantitatively Mediates Specific Histone Acetylation Sites." *Cancer Metab* 3 (2015): 10.

Cohen, H. T., M. Zhou, A. M. Welsh, S. Zarghamee, H. Scholz, D. Mukhopadhyay, T. Kishida, *et al.* "An Important Von Hippel-Lindau Tumor Suppressor Domain Mediates Sp1-Binding and Self-Association." *Biochem Biophys Res Commun* 266, no. 1 (Dec 09 1999): 43-50.

Comerford, S. A., Z. Huang, X. Du, Y. Wang, L. Cai, A. K. Witkiewicz, H. Walters, *et al.* "Acetate Dependence of Tumors." *Cell* 159, no. 7 (Dec 18 2014): 1591-602.

Compton, S., C. Kim, N. B. Griner, P. Potluri, I. E. Scheffler, S. Sen, D. J. Jerry, S. Schneider, and N. Yadava. "Mitochondrial Dysfunction Impairs Tumor Suppressor P53 Expression/Function." *J Biol Chem* 286, no. 23 (Jun 10 2011): 20297-312.

Coppin, C., C. Kollmannsberger, L. Le, F. Porzsolt, and T. J. Wilt. "Targeted Therapy for Advanced Renal Cell Cancer (Rcc): A Cochrane Systematic Review of Published Randomised Trials." *BJU Int* 108, no. 10 (Nov 2011): 1556-63.

Cravo, M. L., A. G. Pinto, P. Chaves, J. A. Cruz, P. Lage, C. Nobre Leitao, and F. Costa Mira. "Effect of Folate Supplementation on DNA Methylation of Rectal Mucosa in Patients with Colonic Adenomas: Correlation with Nutrient Intake." *Clin Nutr* 17, no. 2 (Apr 1998): 45-9.

Czubryt, M. P., J. McAnally, G. I. Fishman, and E. N. Olson. "Regulation of Peroxisome Proliferator-Activated Receptor Gamma Coactivator 1 Alpha (Pgc-1 Alpha) and

Mitochondrial Function by Mef2 and Hdac5." *Proc Natl Acad Sci U S A* 100, no. 4 (Feb 18 2003): 1711-6.
Dang, C. V. "C-Myc Target Genes Involved in Cell Growth, Apoptosis, and Metabolism." *Mol Cell Biol* 19, no. 1 (Jan 1999): 1-11.
———. "Myc, Metabolism, Cell Growth, and Tumorigenesis." *Cold Spring Harb Perspect Med* 3, no. 8 (Aug 2013).
Dang, L., D. W. White, S. Gross, B. D. Bennett, M. A. Bittinger, E. M. Driggers, V. R. Fantin*, et al.* "Cancer-Associated Idh1 Mutations Produce 2-Hydroxyglutarate." *Nature* 462, no. 7274 (Dec 10 2009): 739-44.
Denisov, I. G., and S. G. Sligar. "A Novel Type of Allosteric Regulation: Functional Cooperativity in Monomeric Proteins." *Arch Biochem Biophys* 519, no. 2 (Mar 15 2012): 91-102.
Dhalluin, C., J. E. Carlson, L. Zeng, C. He, A. K. Aggarwal, and M. M. Zhou. "Structure and Ligand of a Histone Acetyltransferase Bromodomain." *Nature* 399, no. 6735 (Jun 3 1999): 491-6.
Dhar, S., and S. J. Lippard. "Mitaplatin, a Potent Fusion of Cisplatin and the Orphan Drug Dichloroacetate." *Proc Natl Acad Sci U S A* 106, no. 52 (Dec 29 2009): 22199-204.
Donohoe, D. R., L. B. Collins, A. Wali, R. Bigler, W. Sun, and S. J. Bultman. "The Warburg Effect Dictates the Mechanism of Butyrate-Mediated Histone Acetylation and Cell Proliferation." *Mol Cell* 48, no. 4 (Nov 30 2012): 612-26.
Dromparis, P., and E. D. Michelakis. "Mitochondria in Vascular Health and Disease." *Annu Rev Physiol* 75 (2013): 95-126.
Dunbar, E. M., B. S. Coats, A. L. Shroads, T. Langaee, A. Lew, J. R. Forder, J. J. Shuster, D. A. Wagner, and P. W. Stacpoole. "Phase 1 Trial of Dichloroacetate (Dca) in Adults with Recurrent Malignant Brain Tumors." *Invest New Drugs* 32, no. 3 (Jun 2014): 452-64.
Durieux, J., S. Wolff, and A. Dillin. "The Cell-Non-Autonomous Nature of Electron Transport Chain-Mediated Longevity." [In eng]. *Cell* 144, no. 1 (Jan 7 2011): 79-91.
Eckel-Mahan, K., and P. Sassone-Corsi. "Metabolism and the Circadian Clock Converge." *Physiol Rev* 93, no. 1 (Jan 2013): 107-35.
Edmunds, L. R., L. Sharma, A. Kang, J. Lu, J. Vockley, S. Basu, R. Uppala*, et al.* "C-Myc Programs Fatty Acid Metabolism and Dictates Acetyl-Coa Abundance and Fate." *J Biol Chem* 289, no. 36 (Sep 5 2014): 25382-92.
Eisenberg, T., S. Schroeder, A. Andryushkova, T. Pendl, V. Kuttner, A. Bhukel, G. Marino*, et al.* "Nucleocytosolic Depletion of the Energy Metabolite Acetyl-Coenzyme a Stimulates Autophagy and Prolongs Lifespan." *Cell Metab* 19, no. 3 (Mar 4 2014): 431-44.
Elsheikh, S. E., A. R. Green, E. A. Rakha, D. G. Powe, R. A. Ahmed, H. M. Collins, D. Soria*, et al.* "Global Histone Modifications in Breast Cancer Correlate with Tumor Phenotypes, Prognostic Factors, and Patient Outcome." *Cancer Res* 69, no. 9 (May 1 2009): 3802-9.
Esteller, M. "Epigenetics in Cancer." *N Engl J Med* 358, no. 11 (Mar 13 2008): 1148-59.
Esteller, M., J. M. Silva, G. Dominguez, F. Bonilla, X. Matias-Guiu, E. Lerma, E. Bussaglia*, et al.* "Promoter Hypermethylation and Brca1 Inactivation in Sporadic Breast and Ovarian Tumors." *J Natl Cancer Inst* 92, no. 7 (Apr 5 2000): 564-9.
Faiola, F., X. Liu, S. Lo, S. Pan, K. Zhang, E. Lymar, A. Farina, and E. Martinez. "Dual Regulation of C-Myc by P300 Via Acetylation-Dependent Control of Myc Protein Turnover and Coactivation of Myc-Induced Transcription." *Mol Cell Biol* 25, no. 23 (Dec 2005): 10220-34.

Falkenberg, K. J., and R. W. Johnstone. "Histone Deacetylases and Their Inhibitors in Cancer, Neurological Diseases and Immune Disorders." *Nat Rev Drug Discov* 13, no. 9 (Sep 2014): 673-91.

Fan, J., H. B. Kang, C. Shan, S. Elf, R. Lin, J. Xie, T. L. Gu*, et al.* "Tyr-301 Phosphorylation Inhibits Pyruvate Dehydrogenase by Blocking Substrate Binding and Promotes the Warburg Effect." *J Biol Chem* 289, no. 38 (Sep 19 2014): 26533-41.

Fan, J., C. Shan, H. B. Kang, S. Elf, J. Xie, M. Tucker, T. L. Gu*, et al.* "Tyr Phosphorylation of Pdp1 Toggles Recruitment between Acat1 and Sirt3 to Regulate the Pyruvate Dehydrogenase Complex." *Mol Cell* 53, no. 4 (Feb 20 2014): 534-48.

Fan, Y., H. Li, X. Ma, Y. Gao, L. Chen, X. Li, X. Bao*, et al.* "Prognostic Significance of Hypoxia-Inducible Factor Expression in Renal Cell Carcinoma: A Prisma-Compliant Systematic Review and Meta-Analysis." *Medicine (Baltimore)* 94, no. 38 (Sep 2015): e1646.

Feinberg, A. P., and B. Vogelstein. "Hypomethylation Distinguishes Genes of Some Human Cancers from Their Normal Counterparts." *Nature* 301, no. 5895 (Jan 6 1983): 89-92.

Ferlay, J., I. Soerjomataram, R. Dikshit, S. Eser, C. Mathers, M. Rebelo, D. M. Parkin, D. Forman, and F. Bray. "Cancer Incidence and Mortality Worldwide: Sources, Methods and Major Patterns in Globocan 2012." *Int J Cancer* 136, no. 5 (Mar 1 2015): E359-86.

Figueroa, M. E., O. Abdel-Wahab, C. Lu, P. S. Ward, J. Patel, A. Shih, Y. Li*, et al.* "Leukemic Idh1 and Idh2 Mutations Result in a Hypermethylation Phenotype, Disrupt Tet2 Function, and Impair Hematopoietic Differentiation." *Cancer Cell* 18, no. 6 (Dec 14 2010): 553-67.

Filippov, S., S. L. Pinkosky, and R. S. Newton. "Ldl-Cholesterol Reduction in Patients with Hypercholesterolemia by Modulation of Adenosine Triphosphate-Citrate Lyase and Adenosine Monophosphate-Activated Protein Kinase." *Curr Opin Lipidol* 25, no. 4 (Aug 2014): 309-15.

Finley, L. W., A. Carracedo, J. Lee, A. Souza, A. Egia, J. Zhang, J. Teruya-Feldstein*, et al.* "Sirt3 Opposes Reprogramming of Cancer Cell Metabolism through Hif1alpha Destabilization." *Cancer Cell* 19, no. 3 (Mar 8 2011): 416-28.

Finley, L. W., W. Haas, V. Desquiret-Dumas, D. C. Wallace, V. Procaccio, S. P. Gygi, and M. C. Haigis. "Succinate Dehydrogenase Is a Direct Target of Sirtuin 3 Deacetylase Activity." *PLoS One* 6, no. 8 (2011): e23295.

Fisher, R., M. Gore, and J. Larkin. "Current and Future Systemic Treatments for Renal Cell Carcinoma." *Semin Cancer Biol* 23, no. 1 (Feb 2013): 38-45.

Flavahan, W. A., Y. Drier, B. B. Liau, S. M. Gillespie, A. S. Venteicher, A. O. Stemmer-Rachamimov, M. L. Suva, and B. E. Bernstein. "Insulator Dysfunction and Oncogene Activation in Idh Mutant Gliomas." *Nature* 529, no. 7584 (Jan 7 2016): 110-4.

Frew, I. J., and W. Krek. "Pvhl: A Multipurpose Adaptor Protein." *Sci Signal* 1, no. 24 (Jun 17 2008): pe30.

Frost, J., C. Galdeano, P. Soares, M. S. Gadd, K. M. Grzes, L. Ellis, O. Epemolu*, et al.* "Potent and Selective Chemical Probe of Hypoxic Signalling Downstream of Hif-Alpha Hydroxylation Via Vhl Inhibition." *Nat Commun* 7 (Nov 04 2016): 13312.

Gao, L., W. Chiou, H. Tang, X. Cheng, H. S. Camp, and D. J. Burns. "Simultaneous Quantification of Malonyl-Coa and Several Other Short-Chain Acyl-Coas in Animal Tissues by Ion-Pairing Reversed-Phase Hplc/Ms." *J Chromatogr B Analyt Technol Biomed Life Sci* 853, no. 1-2 (Jun 15 2007): 303-13.

Gao, X., H. Wang, J. J. Yang, X. Liu, and Z. R. Liu. "Pyruvate Kinase M2 Regulates Gene Transcription by Acting as a Protein Kinase." [In eng]. *Mol Cell* 45, no. 5 (Mar 9 2012): 598-609.

Ghadjar, P., C. Rubie, D. M. Aebersold, and U. Keilholz. "The Chemokine Ccl20 and Its Receptor Ccr6 in Human Malignancy with Focus on Colorectal Cancer." *Int J Cancer* 125, no. 4 (Aug 15 2009): 741-5.

Gimenez-Bachs, J. M., A. S. Salinas-Sanchez, F. Sanchez-Sanchez, J. G. Lorenzo-Romero, M. J. Donate-Moreno, H. Pastor-Navarro, D. C. Garcia-Olmo, J. Escribano-Martinez, and J. A. Virseda-Rodriguez. "Determination of Vhl Gene Mutations in Sporadic Renal Cell Carcinoma." *Eur Urol* 49, no. 6 (Jun 2006): 1051-7.

Gomes, N. P., and J. M. Espinosa. "Gene-Specific Repression of the P53 Target Gene Puma Via Intragenic Ctcf-Cohesin Binding." *Genes Dev* 24, no. 10 (May 15 2010): 1022-34.

Gossage, L., T. Eisen, and E. R. Maher. "Vhl, the Story of a Tumour Suppressor Gene." *Nat Rev Cancer* 15, no. 1 (Jan 2015): 55-64.

Goulet, B., W. Kennette, A. Ablack, C. O. Postenka, M. N. Hague, J. S. Mymryk, A. B. Tuck*, et al.* "Nuclear Localization of Maspin Is Essential for Its Inhibition of Tumor Growth and Metastasis." *Lab Invest* 91, no. 8 (Aug 2011): 1181-7.

Greger, V., E. Passarge, W. Hopping, E. Messmer, and B. Horsthemke. "Epigenetic Changes May Contribute to the Formation and Spontaneous Regression of Retinoblastoma." *Hum Genet* 83, no. 2 (Sep 1989): 155-8.

Gunaratnam, L., M. Morley, A. Franovic, N. de Paulsen, K. Mekhail, D. A. Parolin, E. Nakamura, I. A. Lorimer, and S. Lee. "Hypoxia Inducible Factor Activates the Transforming Growth Factor-Alpha/Epidermal Growth Factor Receptor Growth Stimulatory Pathway in Vhl(-/-) Renal Cell Carcinoma Cells." *J Biol Chem* 278, no. 45 (Nov 07 2003): 44966-74.

Gurova, K. V., J. E. Hill, O. V. Razorenova, P. M. Chumakov, and A. V. Gudkov. "P53 Pathway in Renal Cell Carcinoma Is Repressed by a Dominant Mechanism." *Cancer Res* 64, no. 6 (Mar 15 2004): 1951-8.

Gutierrez, M. J., N. L. Rosenberg, D. E. Macdougall, J. C. Hanselman, J. R. Margulies, P. Strange, M. A. Milad, S. J. McBride, and R. S. Newton. "Efficacy and Safety of Etc-1002, a Novel Investigational Low-Density Lipoprotein-Cholesterol-Lowering Therapy for the Treatment of Patients with Hypercholesterolemia and Type 2 Diabetes Mellitus." *Arterioscler Thromb Vasc Biol* 34, no. 3 (Mar 2014): 676-83.

Hallows, W. C., S. Lee, and J. M. Denu. "Sirtuins Deacetylate and Activate Mammalian Acetyl-Coa Synthetases." *Proc Natl Acad Sci U S A* 103, no. 27 (Jul 5 2006): 10230-5.

Hanahan, D., and R. A. Weinberg. "Hallmarks of Cancer: The Next Generation." *Cell* 144, no. 5 (Mar 4 2011): 646-74.

Hardie, D. G., F. A. Ross, and S. A. Hawley. "Ampk: A Nutrient and Energy Sensor That Maintains Energy Homeostasis." *Nat Rev Mol Cell Biol* 13, no. 4 (Apr 2012): 251-62.

Harlander, S., D. Schonenberger, N. C. Toussaint, M. Prummer, A. Catalano, L. Brandt, H. Moch, P. J. Wild, and I. J. Frew. "Combined Mutation in Vhl, Trp53 and Rb1 Causes Clear Cell Renal Cell Carcinoma in Mice." *Nat Med* 23, no. 7 (Jul 2017): 869-77.

Hashemi, S., J. Salma, S. Wales, and J. C. McDermott. "Pro-Survival Function of Mef2 in Cardiomyocytes Is Enhanced by Beta-Blockers." *Cell Death Discov* 1 (2015): 15019.

Hatzivassiliou, G., F. Zhao, D. E. Bauer, C. Andreadis, A. N. Shaw, D. Dhanak, S. R. Hingorani, D. A. Tuveson, and C. B. Thompson. "Atp Citrate Lyase Inhibition Can Suppress Tumor Cell Growth." *Cancer Cell* 8, no. 4 (Oct 2005): 311-21.

Henry, R. A., Y. M. Kuo, V. Bhattacharjee, T. J. Yen, and A. J. Andrews. "Changing the Selectivity of P300 by Acetyl-Coa Modulation of Histone Acetylation." *ACS Chem Biol* 10, no. 1 (Jan 16 2015): 146-56.

Hergovich, A., J. Lisztwan, R. Barry, P. Ballschmieter, and W. Krek. "Regulation of Microtubule Stability by the Von Hippel-Lindau Tumour Suppressor Protein Pvhl." *Nat Cell Biol* 5, no. 1 (Jan 2003): 64-70.

Herman, J. G., F. Latif, Y. Weng, M. I. Lerman, B. Zbar, S. Liu, D. Samid*, et al.* "Silencing of the Vhl Tumor-Suppressor Gene by DNA Methylation in Renal Carcinoma." *Proc Natl Acad Sci U S A* 91, no. 21 (Oct 11 1994): 9700-4.

Hirschey, M. D., T. Shimazu, E. Goetzman, E. Jing, B. Schwer, D. B. Lombard, C. A. Grueter*, et al.* "Sirt3 Regulates Mitochondrial Fatty-Acid Oxidation by Reversible Enzyme Deacetylation." *Nature* 464, no. 7285 (Mar 4 2010): 121-5.

Hitosugi, T., J. Fan, T. W. Chung, K. Lythgoe, X. Wang, J. Xie, Q. Ge*, et al.* "Tyrosine Phosphorylation of Mitochondrial Pyruvate Dehydrogenase Kinase 1 Is Important for Cancer Metabolism." *Mol Cell* 44, no. 6 (Dec 23 2011): 864-77.

Hnisz, D., A. S. Weintraub, D. S. Day, A. L. Valton, R. O. Bak, C. H. Li, J. Goldmann*, et al.* "Activation of Proto-Oncogenes by Disruption of Chromosome Neighborhoods." *Science* 351, no. 6280 (Mar 25 2016): 1454-8.

Hollebeke, J., P. Van Damme, and K. Gevaert. "N-Terminal Acetylation and Other Functions of Nalpha-Acetyltransferases." *Biol Chem* 393, no. 4 (Apr 2012): 291-8.

Horner, D. S., R. P. Hirt, and T. M. Embley. "A Single Eubacterial Origin of Eukaryotic Pyruvate: Ferredoxin Oxidoreductase Genes: Implications for the Evolution of Anaerobic Eukaryotes." [In eng]. *Mol Biol Evol* 16, no. 9 (Sep 1999): 1280-91.

Houtkooper, R. H., E. Pirinen, and J. Auwerx. "Sirtuins as Regulators of Metabolism and Healthspan." *Nat Rev Mol Cell Biol* 13, no. 4 (Apr 2012): 225-38.

Hu, C. J., L. Y. Wang, L. A. Chodosh, B. Keith, and M. C. Simon. "Differential Roles of Hypoxia-Inducible Factor 1alpha (Hif-1alpha) and Hif-2alpha in Hypoxic Gene Regulation." *Mol Cell Biol* 23, no. 24 (Dec 2003): 9361-74.

Huang, H., S. Lin, B. A. Garcia, and Y. Zhao. "Quantitative Proteomic Analysis of Histone Modifications." *Chem Rev* 115, no. 6 (Mar 25 2015): 2376-418.

Huang, H., B. R. Sabari, B. A. Garcia, C. D. Allis, and Y. Zhao. "Snapshot: Histone Modifications." *Cell* 159, no. 2 (Oct 9 2014): 458-58 e1.

I, H., E. Ko, Y. Kim, E. Y. Cho, J. Han, J. Park, K. Kim, D. H. Kim, and Y. M. Shim. "Association of Global Levels of Histone Modifications with Recurrence-Free Survival in Stage Iib and Iii Esophageal Squamous Cell Carcinomas." *Cancer Epidemiol Biomarkers Prev* 19, no. 2 (Feb 2010): 566-73.

Iliopoulos, O., A. Kibel, S. Gray, and W. G. Kaelin, Jr. "Tumour Suppression by the Human Von Hippel-Lindau Gene Product." *Nat Med* 1, no. 8 (Aug 1995): 822-6.

Intlekofer, A. M., R. G. Dematteo, S. Venneti, L. W. Finley, C. Lu, A. R. Judkins, A. S. Rustenburg*, et al.* "Hypoxia Induces Production of L-2-Hydroxyglutarate." *Cell Metab* 22, no. 2 (Aug 4 2015): 304-11.

Ito, M., K. Teshima, S. Ikeda, A. Kitadate, A. Watanabe, M. Nara, J. Yamashita*, et al.* "Microrna-150 Inhibits Tumor Invasion and Metastasis by Targeting the Chemokine

Receptor Ccr6, in Advanced Cutaneous T-Cell Lymphoma." *Blood* 123, no. 10 (Mar 06 2014): 1499-511.
Izumi, H., R. Ohta, G. Nagatani, T. Ise, Y. Nakayama, M. Nomoto, and K. Kohno. "P300/Cbp-Associated Factor (P/Caf) Interacts with Nuclear Respiratory Factor-1 to Regulate the Udp-N-Acetyl-Alpha-D-Galactosamine: Polypeptide N-Acetylgalactosaminyltransferase-3 Gene." *Biochem J* 373, no. Pt 3 (Aug 1 2003): 713-22.
Jaenisch, R., and A. Bird. "Epigenetic Regulation of Gene Expression: How the Genome Integrates Intrinsic and Environmental Signals." [In eng]. *Nat Genet* 33 Suppl (Mar 2003): 245-54.
Jencks, W.P. *Handbook of Biochemistry and Molecular Biology.* 3rd Edition: Physical and Chemical Data ed. Vol. 1, Boca Raton, FL: CRC Press, 1976.
Jeong, S. M., C. Xiao, L. W. Finley, T. Lahusen, A. L. Souza, K. Pierce, Y. H. Li*, et al.* "Sirt4 Has Tumor-Suppressive Activity and Regulates the Cellular Metabolic Response to DNA Damage by Inhibiting Mitochondrial Glutamine Metabolism." *Cancer Cell* 23, no. 4 (Apr 15 2013): 450-63.
Ji, X., D. B. Dadon, B. E. Powell, Z. P. Fan, D. Borges-Rivera, S. Shachar, A. S. Weintraub*, et al.* "3d Chromosome Regulatory Landscape of Human Pluripotent Cells." *Cell Stem Cell* 18, no. 2 (Feb 4 2016): 262-75.
Jiang, P., W. Du, X. Wang, A. Mancuso, X. Gao, M. Wu, and X. Yang. "P53 Regulates Biosynthesis through Direct Inactivation of Glucose-6-Phosphate Dehydrogenase." *Nat Cell Biol* 13, no. 3 (Mar 2011): 310-6.
Jiang, Y., X. Qian, J. Shen, Y. Wang, X. Li, R. Liu, Y. Xia*, et al.* "Local Generation of Fumarate Promotes DNA Repair through Inhibition of Histone H3 Demethylation." *Nat Cell Biol* 17, no. 9 (Sep 2015): 1158-68.
Kadaveru, K., P. Protiva, E. J. Greenspan, Y. I. Kim, and D. W. Rosenberg. "Dietary Methyl Donor Depletion Protects against Intestinal Tumorigenesis in Apc(Min/+) Mice." *Cancer Prev Res (Phila)* 5, no. 7 (Jul 2012): 911-20.
Kain, K. H., J. W. Miller, C. R. Jones-Paris, R. T. Thomason, J. D. Lewis, D. M. Bader, J. V. Barnett, and A. Zijlstra. "The Chick Embryo as an Expanding Experimental Model for Cancer and Cardiovascular Research." *Dev Dyn* 243, no. 2 (Feb 2014): 216-28.
Kamphorst, J. J., M. K. Chung, J. Fan, and J. D. Rabinowitz. "Quantitative Analysis of Acetyl-Coa Production in Hypoxic Cancer Cells Reveals Substantial Contribution from Acetate." *Cancer Metab* 2 (2014): 23.
Kaplon, J., L. Zheng, K. Meissl, B. Chaneton, V. A. Selivanov, G. Mackay, S. H. van der Burg*, et al.* "A Key Role for Mitochondrial Gatekeeper Pyruvate Dehydrogenase in Oncogene-Induced Senescence." *Nature* 498, no. 7452 (Jun 6 2013): 109-12.
Katainen, R., K. Dave, E. Pitkanen, K. Palin, T. Kivioja, N. Valimaki, A. E. Gylfe*, et al.* "Ctcf/Cohesin-Binding Sites Are Frequently Mutated in Cancer." *Nat Genet* 47, no. 7 (Jul 2015): 818-21.
Kato, M., J. L. Chuang, S. C. Tso, R. M. Wynn, and D. T. Chuang. "Crystal Structure of Pyruvate Dehydrogenase Kinase 3 Bound to Lipoyl Domain 2 of Human Pyruvate Dehydrogenase Complex." [In eng]. *EMBO J* 24, no. 10 (May 18 2005): 1763-74.
Kato, M., J. Li, J. L. Chuang, and D. T. Chuang. "Distinct Structural Mechanisms for Inhibition of Pyruvate Dehydrogenase Kinase Isoforms by Azd7545, Dichloroacetate, and Radicicol." *Structure* 15, no. 8 (Aug 2007): 992-1004.

Kato, Y., R. I. Tapping, S. Huang, M. H. Watson, R. J. Ulevitch, and J. D. Lee. "Bmk1/Erk5 Is Required for Cell Proliferation Induced by Epidermal Growth Factor." [In eng]. *Nature* 395, no. 6703 (Oct 15 1998): 713-6.

Kato, Y., M. Zhao, A. Morikawa, T. Sugiyama, D. Chakravortty, N. Koide, T. Yoshida*, et al.* "Big Mitogen-Activated Kinase Regulates Multiple Members of the Mef2 Protein Family." *J Biol Chem* 275, no. 24 (Jun 16 2000): 18534-40.

Katoh, Y., T. Ikura, Y. Hoshikawa, S. Tashiro, T. Ito, M. Ohta, Y. Kera, T. Noda, and K. Igarashi. "Methionine Adenosyltransferase Ii Serves as a Transcriptional Corepressor of Maf Oncoprotein." *Mol Cell* 41, no. 5 (Mar 4 2011): 554-66.

Keith, B., R. S. Johnson, and M. C. Simon. "Hif1alpha and Hif2alpha: Sibling Rivalry in Hypoxic Tumour Growth and Progression." *Nat Rev Cancer* 12, no. 1 (Jan 2012): 9-22.

Kera, Y., Y. Katoh, M. Ohta, M. Matsumoto, T. Takano-Yamamoto, and K. Igarashi. "Methionine Adenosyltransferase Ii-Dependent Histone H3k9 Methylation at the Cox-2 Gene Locus." *J Biol Chem* 288, no. 19 (May 10 2013): 13592-601.

Kiang, J. G., P. D. Bowman, X. Lu, Y. Li, X. Z. Ding, B. Zhao, Y. T. Juang, J. L. Atkins, and G. C. Tsokos. "Geldanamycin Prevents Hemorrhage-Induced Atp Loss by Overexpressing Inducible Hsp70 and Activating Pyruvate Dehydrogenase." [In eng]. *Am J Physiol Gastrointest Liver Physiol* 291, no. 1 (Jul 2006): G117-27.

Killian, J. K., S. Y. Kim, M. Miettinen, C. Smith, M. Merino, M. Tsokos, M. Quezado*, et al.* "Succinate Dehydrogenase Mutation Underlies Global Epigenomic Divergence in Gastrointestinal Stromal Tumor." *Cancer Discov* 3, no. 6 (Jun 2013): 648-57.

Kim, H. S., K. Patel, K. Muldoon-Jacobs, K. S. Bisht, N. Aykin-Burns, J. D. Pennington, R. van der Meer*, et al.* "Sirt3 Is a Mitochondria-Localized Tumor Suppressor Required for Maintenance of Mitochondrial Integrity and Metabolism During Stress." *Cancer Cell* 17, no. 1 (Jan 19 2010): 41-52.

Kim, J. H., C. W. Jung, Y. H. Cho, J. Lee, S. H. Lee, H. Y. Kim, J. Park*, et al.* "Somatic Vhl Alteration and Its Impact on Prognosis in Patients with Clear Cell Renal Cell Carcinoma." *Oncol Rep* 13, no. 5 (May 2005): 859-64.

Kim, J. W., and C. V. Dang. "Multifaceted Roles of Glycolytic Enzymes." [In eng]. *Trends Biochem Sci* 30, no. 3 (Mar 2005): 142-50.

Kim, J. W., I. Tchernyshyov, G. L. Semenza, and C. V. Dang. "Hif-1-Mediated Expression of Pyruvate Dehydrogenase Kinase: A Metabolic Switch Required for Cellular Adaptation to Hypoxia." [In eng]. *Cell Metab* 3, no. 3 (Mar 2006): 177-85.

Kim, T. G., D. Byamba, W. H. Wu, and M. G. Lee. "Statins Inhibit Chemotactic Interaction between Ccl20 and Ccr6 in Vitro: Possible Relevance to Psoriasis Treatment." *Exp Dermatol* 20, no. 10 (Oct 2011): 855-7.

Kim, W. Y., and W. G. Kaelin. "Role of Vhl Gene Mutation in Human Cancer." *J Clin Oncol* 22, no. 24 (Dec 15 2004): 4991-5004.

Kimsey, T. F., A. S. Campbell, D. Albo, M. Wilson, and T. N. Wang. "Co-Localization of Macrophage Inflammatory Protein-3alpha (Mip-3alpha) and Its Receptor, Ccr6, Promotes Pancreatic Cancer Cell Invasion." *Cancer J* 10, no. 6 (Nov-Dec 2004): 374-80.

Kinnaird, A., P. Dromparis, B. Saleme, V. Gurtu, K. Watson, R. Paulin, S. Zervopoulos*, et al.* "Metabolic Modulation of Clear-Cell Renal Cell Carcinoma with Dichloroacetate, an Inhibitor of Pyruvate Dehydrogenase Kinase." *Eur Urol* 69, no. 4 (Apr 2016): 734-44.

Kinnaird, A., and E. D. Michelakis. "Metabolic Modulation of Cancer: A New Frontier with Great Translational Potential." *J Mol Med (Berl)* 93, no. 2 (Feb 2015): 127-42.

Kitagawa, Y., S. Kikuchi, Y. Arita, M. Nishimura, K. Mizuno, H. Ogasawara, T. Kawano*, et al.* "Inhibition of Ccl20 Increases Mortality in Models of Mouse Sepsis with Intestinal Apoptosis." *Surgery* 154, no. 1 (Jul 2013): 78-88.

Koishi, M., S. Yokota, T. Mae, Y. Nishimura, S. Kanamori, N. Horii, K. Shibuya, K. Sasai, and M. Hiraoka. "The Effects of Knk437, a Novel Inhibitor of Heat Shock Protein Synthesis, on the Acquisition of Thermotolerance in a Murine Transplantable Tumor in Vivo." [In eng]. *Clin Cancer Res* 7, no. 1 (Jan 2001): 215-9.

Kondo, K., M. Yao, M. Yoshida, T. Kishida, T. Shuin, T. Miura, M. Moriyama*, et al.* "Comprehensive Mutational Analysis of the Vhl Gene in Sporadic Renal Cell Carcinoma: Relationship to Clinicopathological Parameters." *Genes Chromosomes Cancer* 34, no. 1 (May 2002): 58-68.

Kong, X., R. Wang, Y. Xue, X. Liu, H. Zhang, Y. Chen, F. Fang, and Y. Chang. "Sirtuin 3, a New Target of Pgc-1alpha, Plays an Important Role in the Suppression of Ros and Mitochondrial Biogenesis." *PLoS One* 5, no. 7 (Jul 22 2010): e11707.

Krieg, M., R. Haas, H. Brauch, T. Acker, I. Flamme, and K. H. Plate. "Up-Regulation of Hypoxia-Inducible Factors Hif-1alpha and Hif-2alpha under Normoxic Conditions in Renal Carcinoma Cells by Von Hippel-Lindau Tumor Suppressor Gene Loss of Function." *Oncogene* 19, no. 48 (Nov 16 2000): 5435-43.

Kroeze, S. G., J. S. Vermaat, A. van Brussel, H. H. van Melick, E. E. Voest, T. G. Jonges, P. J. van Diest*, et al.* "Expression of Nuclear Fih Independently Predicts Overall Survival of Clear Cell Renal Cell Carcinoma Patients." *Eur J Cancer* 46, no. 18 (Dec 2010): 3375-82.

Kryukov, G. V., F. H. Wilson, J. R. Ruth, J. Paulk, A. Tsherniak, S. E. Marlow, F. Vazquez*, et al.* "Mtap Deletion Confers Enhanced Dependency on the Prmt5 Arginine Methyltransferase in Cancer Cells." *Science* 351, no. 6278 (Mar 11 2016): 1214-8.

Kumar, K., S. Wigfield, H. E. Gee, C. M. Devlin, D. Singleton, J. L. Li, F. Buffa*, et al.* "Dichloroacetate Reverses the Hypoxic Adaptation to Bevacizumab and Enhances Its Antitumor Effects in Mouse Xenografts." *J Mol Med (Berl)* 91, no. 6 (Jun 2013): 749-58.

Kuznetsova, A. V., J. Meller, P. O. Schnell, J. A. Nash, M. L. Ignacak, Y. Sanchez, J. W. Conaway, R. C. Conaway, and M. F. Czyzyk-Krzeska. "Von Hippel-Lindau Protein Binds Hyperphosphorylated Large Subunit of Rna Polymerase Ii through a Proline Hydroxylation Motif and Targets It for Ubiquitination." *Proc Natl Acad Sci U S A* 100, no. 5 (Mar 04 2003): 2706-11.

Lai, Y., M. Song, K. Hakala, S. T. Weintraub, and Y. Shiio. "Proteomic Dissection of the Von Hippel-Lindau (Vhl) Interactome." *J Proteome Res* 10, no. 11 (Nov 04 2011): 5175-82.

Latham, T., L. Mackay, D. Sproul, M. Karim, J. Culley, D. J. Harrison, L. Hayward*, et al.* "Lactate, a Product of Glycolytic Metabolism, Inhibits Histone Deacetylase Activity and Promotes Changes in Gene Expression." *Nucleic Acids Res* 40, no. 11 (Jun 2012): 4794-803.

Lee, J. V., A. Carrer, S. Shah, N. W. Snyder, S. Wei, S. Venneti, A. J. Worth*, et al.* "Akt-Dependent Metabolic Reprogramming Regulates Tumor Cell Histone Acetylation." *Cell Metab* 20, no. 2 (Aug 5 2014): 306-19.

Leong, H. S., N. F. Steinmetz, A. Ablack, G. Destito, A. Zijlstra, H. Stuhlmann, M. Manchester, and J. D. Lewis. "Intravital Imaging of Embryonic and Tumor Neovasculature Using Viral Nanoparticles." *Nat Protoc* 5, no. 8 (Aug 2010): 1406-17.

Lerin, C., J. T. Rodgers, D. E. Kalume, S. H. Kim, A. Pandey, and P. Puigserver. "Gcn5 Acetyltransferase Complex Controls Glucose Metabolism through Transcriptional Repression of Pgc-1alpha." *Cell Metab* 3, no. 6 (Jun 2006): 429-38.

Letouze, E., C. Martinelli, C. Loriot, N. Burnichon, N. Abermil, C. Ottolenghi, M. Janin*, et al.* "Sdh Mutations Establish a Hypermethylator Phenotype in Paraganglioma." *Cancer Cell* 23, no. 6 (Jun 10 2013): 739-52.

Li, J. J., H. Wang, J. A. Tino, J. A. Robl, T. F. Herpin, R. M. Lawrence, S. Biller*, et al.* "2-Hydroxy-N-Arylbenzenesulfonamides as Atp-Citrate Lyase Inhibitors." *Bioorg Med Chem Lett* 17, no. 11 (Jun 1 2007): 3208-11.

Li, L., L. Zhang, X. Zhang, Q. Yan, Y. A. Minamishima, A. F. Olumi, M. Mao, S. Bartz, and W. G. Kaelin, Jr. "Hypoxia-Inducible Factor Linked to Differential Kidney Cancer Risk Seen with Type 2a and Type 2b Vhl Mutations." *Mol Cell Biol* 27, no. 15 (Aug 2007): 5381-92.

Li, S., S. K. Swanson, M. Gogol, L. Florens, M. P. Washburn, J. L. Workman, and T. Suganuma. "Serine and Sam Responsive Complex Sesame Regulates Histone Modification Crosstalk by Sensing Cellular Metabolism." *Mol Cell* 60, no. 3 (Nov 5 2015): 408-21.

Li, T., M. Liu, X. Feng, Z. Wang, I. Das, Y. Xu, X. Zhou*, et al.* "Glyceraldehyde-3-Phosphate Dehydrogenase Is Activated by Lysine 254 Acetylation in Response to Glucose Signal." *J Biol Chem* 289, no. 6 (Feb 7 2014): 3775-85.

Lim, H. Y., Y. M. Yip, E. Chiong, H. Y. Tiong, B. Halliwell, K. Esuvaranathan, and K. P. Wong. "Metabolic Signatures of Renal Cell Carcinoma." *Biochem Biophys Res Commun* 460, no. 4 (May 15 2015): 938-43.

Lim, J. H., Y. M. Lee, Y. S. Chun, J. Chen, J. E. Kim, and J. W. Park. "Sirtuin 1 Modulates Cellular Responses to Hypoxia by Deacetylating Hypoxia-Inducible Factor 1alpha." *Mol Cell* 38, no. 6 (Jun 25 2010): 864-78.

Lim, U., and M. A. Song. "Dietary and Lifestyle Factors of DNA Methylation." *Methods Mol Biol* 863 (2012): 359-76.

Lin, R., R. Tao, X. Gao, T. Li, X. Zhou, K. L. Guan, Y. Xiong, and Q. Y. Lei. "Acetylation Stabilizes Atp-Citrate Lyase to Promote Lipid Biosynthesis and Tumor Growth." *Mol Cell* 51, no. 4 (Aug 22 2013): 506-18.

Liu, N., W. Y. Xia, S. S. Liu, H. Y. Chen, L. Sun, M. Y. Liu, L. F. Li*, et al.* "Microrna-101 Targets Von Hippel-Lindau Tumor Suppressor (Vhl) to Induce Hif1alpha Mediated Apoptosis and Cell Cycle Arrest in Normoxia Condition." *Sci Rep* 6 (Feb 04 2016): 20489.

Locasale, J. W. "Serine, Glycine and One-Carbon Units: Cancer Metabolism in Full Circle." *Nat Rev Cancer* 13, no. 8 (Aug 2013): 572-83.

Lodish, H., A. Berk, S.L. Zipursky, P. Matsudaira, D. Baltimore, and J. Darnell. "Section 11.4, Signal-Mediated Transport through Nuclear Pore Complexes." In *Molecular Cell Biology, 4th Edition*, edited by W.H. Freeman. New York: W.H. Freemand and Company, 2000.

Losman, J. A., and W. G. Kaelin, Jr. "What a Difference a Hydroxyl Makes: Mutant Idh, (R)-2-Hydroxyglutarate, and Cancer." *Genes Dev* 27, no. 8 (Apr 15 2013): 836-52.

Losman, J. A., R. E. Looper, P. Koivunen, S. Lee, R. K. Schneider, C. McMahon, G. S. Cowley*, et al.* "(R)-2-Hydroxyglutarate Is Sufficient to Promote Leukemogenesis and Its Effects Are Reversible." *Science* 339, no. 6127 (Mar 29 2013): 1621-5.

Lu, C., S. Venneti, A. Akalin, F. Fang, P. S. Ward, R. G. Dematteo, A. M. Intlekofer, *et al.* "Induction of Sarcomas by Mutant Idh2." *Genes Dev* 27, no. 18 (Sep 15 2013): 1986-98.
Lu, C., P. S. Ward, G. S. Kapoor, D. Rohle, S. Turcan, O. Abdel-Wahab, C. R. Edwards, *et al.* "Idh Mutation Impairs Histone Demethylation and Results in a Block to Cell Differentiation." *Nature* 483, no. 7390 (Mar 22 2012): 474-8.
Luo, W., H. Hu, R. Chang, J. Zhong, M. Knabel, R. O'Meally, R. N. Cole, A. Pandey, and G. L. Semenza. "Pyruvate Kinase M2 Is a Phd3-Stimulated Coactivator for Hypoxia-Inducible Factor 1." [In eng]. *Cell* 145, no. 5 (May 27 2011): 732-44.
Lv, L., Y. P. Xu, D. Zhao, F. L. Li, W. Wang, N. Sasaki, Y. Jiang, *et al.* "Mitogenic and Oncogenic Stimulation of K433 Acetylation Promotes Pkm2 Protein Kinase Activity and Nuclear Localization." *Mol Cell* 52, no. 3 (Nov 7 2013): 340-52.
Mack, F. A., J. H. Patel, M. P. Biju, V. H. Haase, and M. C. Simon. "Decreased Growth of Vhl-/- Fibrosarcomas Is Associated with Elevated Levels of Cyclin Kinase Inhibitors P21 and P27." *Mol Cell Biol* 25, no. 11 (Jun 2005): 4565-78.
Madeo, F., F. Pietrocola, T. Eisenberg, and G. Kroemer. "Caloric Restriction Mimetics: Towards a Molecular Definition." *Nat Rev Drug Discov* 13, no. 10 (Oct 2014): 727-40.
Manalo, D. J., A. Rowan, T. Lavoie, L. Natarajan, B. D. Kelly, S. Q. Ye, J. G. Garcia, and G. L. Semenza. "Transcriptional Regulation of Vascular Endothelial Cell Responses to Hypoxia by Hif-1." [In eng]. *Blood* 105, no. 2 (Jan 15 2005): 659-69.
Marino, G., F. Pietrocola, T. Eisenberg, Y. Kong, S. A. Malik, A. Andryushkova, S. Schroeder, *et al.* "Regulation of Autophagy by Cytosolic Acetyl-Coenzyme A." *Mol Cell* 53, no. 5 (Mar 6 2014): 710-25.
Marjon, K., M. J. Cameron, P. Quang, M. F. Clasquin, E. Mandley, K. Kunii, M. McVay, *et al.* "Mtap Deletions in Cancer Create Vulnerability to Targeting of the Mat2a/Prmt5/Riok1 Axis." *Cell Rep* 15, no. 3 (Apr 19 2016): 574-87.
Marsigliante, S., C. Vetrugno, and A. Muscella. "Ccl20 Induces Migration and Proliferation on Breast Epithelial Cells." *J Cell Physiol* 228, no. 9 (Sep 2013): 1873-83.
Martinez-Reyes, I., L. P. Diebold, H. Kong, M. Schieber, H. Huang, C. T. Hensley, M. M. Mehta, *et al.* "Tca Cycle and Mitochondrial Membrane Potential Are Necessary for Diverse Biological Functions." *Mol Cell* (Dec 23 2015).
Mashimo, T., K. Pichumani, V. Vemireddy, K. J. Hatanpaa, D. K. Singh, S. Sirasanagandla, S. Nannepaga, *et al.* "Acetate Is a Bioenergetic Substrate for Human Glioblastoma and Brain Metastases." *Cell* 159, no. 7 (Dec 18 2014): 1603-14.
Masui, K., K. Tanaka, S. Ikegami, G. R. Villa, H. Yang, W. H. Yong, T. F. Cloughesy, *et al.* "Glucose-Dependent Acetylation of Rictor Promotes Targeted Cancer Therapy Resistance." *Proc Natl Acad Sci U S A* 112, no. 30 (Jul 28 2015): 9406-11.
Matsuda, S., J. Adachi, M. Ihara, N. Tanuma, H. Shima, A. Kakizuka, M. Ikura, T. Ikura, and T. Matsuda. "Nuclear Pyruvate Kinase M2 Complex Serves as a Transcriptional Coactivator of Arylhydrocarbon Receptor." *Nucleic Acids Res* (Sep 23 2015).
Mavrakis, K. J., E. R. McDonald, 3rd, M. R. Schlabach, E. Billy, G. R. Hoffman, A. deWeck, D. A. Ruddy, *et al.* "Disordered Methionine Metabolism in Mtap/Cdkn2a-Deleted Cancers Leads to Dependence on Prmt5." *Science* 351, no. 6278 (Mar 11 2016): 1208-13.
Mayer, M. P., and B. Bukau. "Hsp70 Chaperones: Cellular Functions and Molecular Mechanism." [In eng]. *Cell Mol Life Sci* 62, no. 6 (Mar 2005): 670-84.

McBrian, M. A., I. S. Behbahan, R. Ferrari, T. Su, T. W. Huang, K. Li, C. S. Hong, *et al.* "Histone Acetylation Regulates Intracellular Ph." *Mol Cell* 49, no. 2 (Jan 24 2013): 310-21.

Meier, J. L. "Metabolic Mechanisms of Epigenetic Regulation." *ACS Chem Biol* 8, no. 12 (Dec 20 2013): 2607-21.

Mentch, S. J., M. Mehrmohamadi, L. Huang, X. Liu, D. Gupta, D. Mattocks, P. Gomez Padilla, *et al.* "Histone Methylation Dynamics and Gene Regulation Occur through the Sensing of One-Carbon Metabolism." *Cell Metab* (Sep 22 2015).

Metallo, C. M., P. A. Gameiro, E. L. Bell, K. R. Mattaini, J. Yang, K. Hiller, C. M. Jewell, *et al.* "Reductive Glutamine Metabolism by Idh1 Mediates Lipogenesis under Hypoxia." *Nature* 481, no. 7381 (Jan 19 2012): 380-4.

Michelakis, E. D., G. Sutendra, P. Dromparis, L. Webster, A. Haromy, E. Niven, C. Maguire, *et al.* "Metabolic Modulation of Glioblastoma with Dichloroacetate." *Sci Transl Med* 2, no. 31 (May 12 2010): 31ra34.

Middel, P., S. Brauneck, W. Meyer, and H. J. Radzun. "Chemokine-Mediated Distribution of Dendritic Cell Subsets in Renal Cell Carcinoma." *BMC Cancer* 10 (2010): 578.

Mihaylova, M. M., and R. J. Shaw. "The Ampk Signalling Pathway Coordinates Cell Growth, Autophagy and Metabolism." *Nat Cell Biol* 13, no. 9 (Sep 2011): 1016-23.

Milarski, K. L., and R. I. Morimoto. "Expression of Human Hsp70 During the Synthetic Phase of the Cell Cycle." [In eng]. *Proc Natl Acad Sci U S A* 83, no. 24 (Dec 1986): 9517-21.

Montgomery, D. C., A. W. Sorum, L. Guasch, M. C. Nicklaus, and J. L. Meier. "Metabolic Regulation of Histone Acetyltransferases by Endogenous Acyl-Coa Cofactors." *Chem Biol* 22, no. 8 (Aug 20 2015): 1030-9.

Moore, L. E., M. L. Nickerson, P. Brennan, J. R. Toro, E. Jaeger, J. Rinsky, S. S. Han, *et al.* "Von Hippel-Lindau (Vhl) Inactivation in Sporadic Clear Cell Renal Cancer: Associations with Germline Vhl Polymorphisms and Etiologic Risk Factors." *PLoS Genet* 7, no. 10 (Oct 2011): e1002312.

Morrish, F., N. Isern, M. Sadilek, M. Jeffrey, and D. M. Hockenbery. "C-Myc Activates Multiple Metabolic Networks to Generate Substrates for Cell-Cycle Entry." *Oncogene* 28, no. 27 (Jul 9 2009): 2485-91.

Morrish, F., J. Noonan, C. Perez-Olsen, P. R. Gafken, M. Fitzgibbon, J. Kelleher, M. VanGilst, and D. Hockenbery. "Myc-Dependent Mitochondrial Generation of Acetyl-Coa Contributes to Fatty Acid Biosynthesis and Histone Acetylation During Cell Cycle Entry." *J Biol Chem* 285, no. 47 (Nov 19 2010): 36267-74.

Mosashvilli, D., P. Kahl, C. Mertens, S. Holzapfel, S. Rogenhofer, S. Hauser, R. Buttner, *et al.* "Global Histone Acetylation Levels: Prognostic Relevance in Patients with Renal Cell Carcinoma." *Cancer Sci* 101, no. 12 (Dec 2010): 2664-9.

Motzer, R. J., B. Escudier, D. F. McDermott, S. George, H. J. Hammers, S. Srinivas, S. S. Tykodi, *et al.* "Nivolumab Versus Everolimus in Advanced Renal-Cell Carcinoma." *N Engl J Med* 373, no. 19 (Nov 05 2015): 1803-13.

Motzer, R. J., T. E. Hutson, P. Tomczak, M. D. Michaelson, R. M. Bukowski, O. Rixe, S. Oudard, *et al.* "Sunitinib Versus Interferon Alfa in Metastatic Renal-Cell Carcinoma." *N Engl J Med* 356, no. 2 (Jan 11 2007): 115-24.

Moussaieff, A., M. Rouleau, D. Kitsberg, M. Cohen, G. Levy, D. Barasch, A. Nemirovski, *et al.* "Glycolysis-Mediated Changes in Acetyl-Coa and Histone Acetylation Control the Early Differentiation of Embryonic Stem Cells." *Cell Metab* 21, no. 3 (Mar 3 2015): 392-402.

Mudd, S. H., and J. R. Poole. "Labile Methyl Balances for Normal Humans on Various Dietary Regimens." *Metabolism* 24, no. 6 (Jun 1975): 721-35.
Mukhopadhyay, D., B. Knebelmann, H. T. Cohen, S. Ananth, and V. P. Sukhatme. "The Von Hippel-Lindau Tumor Suppressor Gene Product Interacts with Sp1 to Repress Vascular Endothelial Growth Factor Promoter Activity." *Mol Cell Biol* 17, no. 9 (Sep 1997): 5629-39.
Mullen, A. R., W. W. Wheaton, E. S. Jin, P. H. Chen, L. B. Sullivan, T. Cheng, Y. Yang*, et al.* "Reductive Carboxylation Supports Growth in Tumour Cells with Defective Mitochondria." *Nature* 481, no. 7381 (Jan 19 2012): 385-8.
Mullen, P. "The Use of Matrigel to Facilitate the Establishment of Human Cancer Cell Lines as Xenografts." *Methods Mol Med* 88 (2004): 287-92.
Nandi, B., C. Pai, Q. Huang, R. H. Prabhala, N. C. Munshi, and J. S. Gold. "Ccr6, the Sole Receptor for the Chemokine Ccl20, Promotes Spontaneous Intestinal Tumorigenesis." *PLoS One* 9, no. 5 (2014): e97566.
Naya, F. J., B. L. Black, H. Wu, R. Bassel-Duby, J. A. Richardson, J. A. Hill, and E. N. Olson. "Mitochondrial Deficiency and Cardiac Sudden Death in Mice Lacking the Mef2a Transcription Factor." *Nat Med* 8, no. 11 (Nov 2002): 1303-9.
Nelson, D.L. and Cox M.M. *Principles of Biochemistry.* 6th Edition ed. New York, NY: W.H. Freeman and Company, 2013.
Oldham, K. A., G. Parsonage, R. I. Bhatt, D. M. Wallace, N. Deshmukh, S. Chaudhri, D. H. Adams, and S. P. Lee. "T Lymphocyte Recruitment into Renal Cell Carcinoma Tissue: A Role for Chemokine Receptors Cxcr3, Cxcr6, Ccr5, and Ccr6." *Eur Urol* 61, no. 2 (Feb 2012): 385-94.
Oldham, W. M., C. B. Clish, Y. Yang, and J. Loscalzo. "Hypoxia-Mediated Increases in L-2-Hydroxyglutarate Coordinate the Metabolic Response to Reductive Stress." *Cell Metab* 22, no. 2 (Aug 4 2015): 291-303.
Olia, A. S., K. Barker, C. E. McCullough, H. Y. Tang, D. W. Speicher, J. Qiu, J. LaBaer, and R. Marmorstein. "Nonenzymatic Protein Acetylation Detected by Nappa Protein Arrays." *ACS Chem Biol* 10, no. 9 (Sep 18 2015): 2034-47.
Onakpoya, I., S. K. Hung, R. Perry, B. Wider, and E. Ernst. "The Use of Garcinia Extract (Hydroxycitric Acid) as a Weight Loss Supplement: A Systematic Review and Meta-Analysis of Randomised Clinical Trials." *J Obes* 2011 (2011): 509038.
Palmer, T. D., J. Lewis, and A. Zijlstra. "Quantitative Analysis of Cancer Metastasis Using an Avian Embryo Model." *J Vis Exp*, no. 51 (2011).
Pante, N., and M. Kann. "Nuclear Pore Complex Is Able to Transport Macromolecules with Diameters of About 39 Nm." [In eng]. *Mol Biol Cell* 13, no. 2 (Feb 2002): 425-34.
Papandreou, I., R. A. Cairns, L. Fontana, A. L. Lim, and N. C. Denko. "Hif-1 Mediates Adaptation to Hypoxia by Actively Downregulating Mitochondrial Oxygen Consumption." *Cell Metab* 3, no. 3 (Mar 2006): 187-97.
Parsons, D. W., S. Jones, X. Zhang, J. C. Lin, R. J. Leary, P. Angenendt, P. Mankoo*, et al.* "An Integrated Genomic Analysis of Human Glioblastoma Multiforme." *Science* 321, no. 5897 (Sep 26 2008): 1807-12.
Patard, J. J., P. Fergelot, P. I. Karakiewicz, T. Klatte, Q. D. Trinh, N. Rioux-Leclercq, J. W. Said, A. S. Belldegrun, and A. J. Pantuck. "Low Caix Expression and Absence of Vhl Gene Mutation Are Associated with Tumor Aggressiveness and Poor Survival of Clear Cell Renal Cell Carcinoma." *Int J Cancer* 123, no. 2 (Jul 15 2008): 395-400.

Patel, J. H., Y. Du, P. G. Ard, C. Phillips, B. Carella, C. J. Chen, C. Rakowski*, et al.* "The C-Myc Oncoprotein Is a Substrate of the Acetyltransferases Hgcn5/Pcaf and Tip60." *Mol Cell Biol* 24, no. 24 (Dec 2004): 10826-34.

Paulin, R., P. Dromparis, G. Sutendra, V. Gurtu, S. Zervopoulos, L. Bowers, A. Haromy*, et al.* "Sirtuin 3 Deficiency Is Associated with Inhibited Mitochondrial Function and Pulmonary Arterial Hypertension in Rodents and Humans." *Cell Metab* 20, no. 5 (Nov 4 2014): 827-39.

Pearce, N. J., J. W. Yates, T. A. Berkhout, B. Jackson, D. Tew, H. Boyd, P. Camilleri*, et al.* "The Role of Atp Citrate-Lyase in the Metabolic Regulation of Plasma Lipids. Hypolipidaemic Effects of Sb-204990, a Lactone Prodrug of the Potent Atp Citrate-Lyase Inhibitor Sb-201076." *Biochem J* 334 (Pt 1) (Aug 15 1998): 113-9.

Peleg, S., C. Feller, I. Forne, E. Schiller, D. C. Sevin, T. Schauer, C. Regnard*, et al.* "Life Span Extension by Targeting a Link between Metabolism and Histone Acetylation in Drosophila." *EMBO Rep* (Jan 18 2016).

Peng, Y., M. Li, B. D. Clarkson, M. Pehar, P. J. Lao, A. T. Hillmer, T. E. Barnhart*, et al.* "Deficient Import of Acetyl-Coa into the Er Lumen Causes Neurodegeneration and Propensity to Infections, Inflammation, and Cancer." *J Neurosci* 34, no. 20 (May 14 2014): 6772-89.

Pietrocola, F., L. Galluzzi, J. M. Bravo-San Pedro, F. Madeo, and G. Kroemer. "Acetyl Coenzyme A: A Central Metabolite and Second Messenger." *Cell Metab* 21, no. 6 (Jun 2 2015): 805-21.

Pink, D. B., W. Schulte, M. H. Parseghian, A. Zijlstra, and J. D. Lewis. "Real-Time Visualization and Quantitation of Vascular Permeability in Vivo: Implications for Drug Delivery." *PLoS One* 7, no. 3 (2012): e33760.

Poirier, L. A., C. K. Wise, R. R. Delongchamp, and R. Sinha. "Blood Determinations of S-Adenosylmethionine, S-Adenosylhomocysteine, and Homocysteine: Correlations with Diet." *Cancer Epidemiol Biomarkers Prev* 10, no. 6 (Jun 2001): 649-55.

Polevoda, B., and F. Sherman. "Nalpha -Terminal Acetylation of Eukaryotic Proteins." *J Biol Chem* 275, no. 47 (Nov 24 2000): 36479-82.

Pon, J. R., and M. A. Marra. "Mef2 Transcription Factors: Developmental Regulators and Emerging Cancer Genes." *Oncotarget* 7, no. 3 (Jan 19 2016): 2297-312.

Potapova, I. A., M. R. El-Maghrabi, S. V. Doronin, and W. B. Benjamin. "Phosphorylation of Recombinant Human Atp:Citrate Lyase by Camp-Dependent Protein Kinase Abolishes Homotropic Allosteric Regulation of the Enzyme by Citrate and Increases the Enzyme Activity. Allosteric Activation of Atp:Citrate Lyase by Phosphorylated Sugars." *Biochemistry* 39, no. 5 (Feb 8 2000): 1169-79.

Pufulete, M., R. Al-Ghnaniem, A. Khushal, P. Appleby, N. Harris, S. Gout, P. W. Emery, and T. A. Sanders. "Effect of Folic Acid Supplementation on Genomic DNA Methylation in Patients with Colorectal Adenoma." *Gut* 54, no. 5 (May 2005): 648-53.

Quail, D. F., L. A. Walsh, G. Zhang, S. D. Findlay, J. Moreno, L. Fung, A. Ablack*, et al.* "Embryonic Protein Nodal Promotes Breast Cancer Vascularization." *Cancer Res* 72, no. 15 (Aug 1 2012): 3851-63.

Rini, B. I., and M. B. Atkins. "Resistance to Targeted Therapy in Renal-Cell Carcinoma." *Lancet Oncol* 10, no. 10 (Oct 2009): 992-1000.

Roberts, A. M., I. R. Watson, A. J. Evans, D. A. Foster, M. S. Irwin, and M. Ohh. "Suppression of Hypoxia-Inducible Factor 2alpha Restores P53 Activity Via Hdm2 and Reverses

Chemoresistance of Renal Carcinoma Cells." *Cancer Res* 69, no. 23 (Dec 1 2009): 9056-64.

Roche, T. E., Y. Hiromasa, A. Turkan, X. Gong, T. Peng, X. Yan, S. A. Kasten, H. Bao, and J. Dong. "Essential Roles of Lipoyl Domains in the Activated Function and Control of Pyruvate Dehydrogenase Kinases and Phosphatase Isoform 1." [In eng]. *Eur J Biochem* 270, no. 6 (Mar 2003): 1050-6.

Rodriguez, M. A., R. M. Garcia-Perez, L. Mendoza, T. Sanchez, N. Guillen, and E. Orozco. "The Pyruvate:Ferredoxin Oxidoreductase Enzyme Is Located in the Plasma Membrane and in a Cytoplasmic Structure in Entamoeba." [In eng]. *Microb Pathog* 25, no. 1 (Jul 1998): 1-10.

Roe, J. S., H. Kim, S. M. Lee, S. T. Kim, E. J. Cho, and H. D. Youn. "P53 Stabilization and Transactivation by a Von Hippel-Lindau Protein." *Mol Cell* 22, no. 3 (May 05 2006): 395-405.

Rohle, D., J. Popovici-Muller, N. Palaskas, S. Turcan, C. Grommes, C. Campos, J. Tsoi*, et al.* "An Inhibitor of Mutant Idh1 Delays Growth and Promotes Differentiation of Glioma Cells." *Science* 340, no. 6132 (May 3 2013): 626-30.

Rubie, C., V. O. Frick, P. Ghadjar, M. Wagner, H. Grimm, B. Vicinus, C. Justinger, S. Graeber, and M. K. Schilling. "Ccl20/Ccr6 Expression Profile in Pancreatic Cancer." *J Transl Med* 8 (2010): 45.

Sabari, B. R., Z. Tang, H. Huang, V. Yong-Gonzalez, H. Molina, H. E. Kong, L. Dai*, et al.* "Intracellular Crotonyl-Coa Stimulates Transcription through P300-Catalyzed Histone Crotonylation." *Mol Cell* 58, no. 2 (Apr 16 2015): 203-15.

Saha, S. K., C. A. Parachoniak, K. S. Ghanta, J. Fitamant, K. N. Ross, M. S. Najem, S. Gurumurthy*, et al.* "Mutant Idh Inhibits Hnf-4alpha to Block Hepatocyte Differentiation and Promote Biliary Cancer." *Nature* 513, no. 7516 (Sep 4 2014): 110-4.

Sahar, S., S. Masubuchi, K. Eckel-Mahan, S. Vollmer, L. Galla, N. Ceglia, S. Masri*, et al.* "Circadian Control of Fatty Acid Elongation by Sirt1 Protein-Mediated Deacetylation of Acetyl-Coenzyme a Synthetase 1." *J Biol Chem* 289, no. 9 (Feb 28 2014): 6091-7.

Schernhammer, E. S., E. Giovannucci, T. Kawasaki, B. Rosner, C. S. Fuchs, and S. Ogino. "Dietary Folate, Alcohol and B Vitamins in Relation to Line-1 Hypomethylation in Colon Cancer." *Gut* 59, no. 6 (Jun 2010): 794-9.

Scheuermann, T. H., Q. Li, H. W. Ma, J. Key, L. Zhang, R. Chen, J. A. Garcia*, et al.* "Allosteric Inhibition of Hypoxia Inducible Factor-2 with Small Molecules." *Nat Chem Biol* 9, no. 4 (Apr 2013): 271-6.

Schmid, T., J. Zhou, R. Kohl, and B. Brune. "P300 Relieves P53-Evoked Transcriptional Repression of Hypoxia-Inducible Factor-1 (Hif-1)." *Biochem J* 380, no. Pt 1 (May 15 2004): 289-95.

Schokrpur, S., J. Hu, D. L. Moughon, P. Liu, L. C. Lin, K. Hermann, S. Mangul*, et al.* "Crispr-Mediated Vhl Knockout Generates an Improved Model for Metastatic Renal Cell Carcinoma." *Sci Rep* 6 (Jun 30 2016): 29032.

Scholz, C., B. T. Weinert, S. A. Wagner, P. Beli, Y. Miyake, J. Qi, L. J. Jensen*, et al.* "Acetylation Site Specificities of Lysine Deacetylase Inhibitors in Human Cells." *Nat Biotechnol* 33, no. 4 (Apr 2015): 415-23.

Schraml, P., K. Struckmann, F. Hatz, S. Sonnet, C. Kully, T. Gasser, G. Sauter, M. J. Mihatsch, and H. Moch. "Vhl Mutations and Their Correlation with Tumour Cell Proliferation,

Microvessel Density, and Patient Prognosis in Clear Cell Renal Cell Carcinoma." *J Pathol* 196, no. 2 (Feb 2002): 186-93.
Schug, Z. T., B. Peck, D. T. Jones, Q. Zhang, S. Grosskurth, I. S. Alam, L. M. Goodwin*, et al.* "Acetyl-Coa Synthetase 2 Promotes Acetate Utilization and Maintains Cancer Cell Growth under Metabolic Stress." *Cancer Cell* 27, no. 1 (Jan 12 2015): 57-71.
Schutyser, E., S. Struyf, and J. Van Damme. "The Cc Chemokine Ccl20 and Its Receptor Ccr6." *Cytokine Growth Factor Rev* 14, no. 5 (Oct 2003): 409-26.
Seligson, D. B., S. Horvath, M. A. McBrian, V. Mah, H. Yu, S. Tze, Q. Wang*, et al.* "Global Levels of Histone Modifications Predict Prognosis in Different Cancers." *Am J Pathol* 174, no. 5 (May 2009): 1619-28.
Seligson, D. B., S. Horvath, T. Shi, H. Yu, S. Tze, M. Grunstein, and S. K. Kurdistani. "Global Histone Modification Patterns Predict Risk of Prostate Cancer Recurrence." *Nature* 435, no. 7046 (Jun 30 2005): 1262-6.
Semenza, G. L. "Defining the Role of Hypoxia-Inducible Factor 1 in Cancer Biology and Therapeutics." [In eng]. *Oncogene* 29, no. 5 (Feb 4 2010): 625-34.
Shan, C., S. Elf, Q. Ji, H. B. Kang, L. Zhou, T. Hitosugi, L. Jin*, et al.* "Lysine Acetylation Activates 6-Phosphogluconate Dehydrogenase to Promote Tumor Growth." *Mol Cell* 55, no. 4 (Aug 21 2014): 552-65.
Shan, C., H. B. Kang, S. Elf, J. Xie, T. L. Gu, M. Aguiar, S. Lonning*, et al.* "Tyr-94 Phosphorylation Inhibits Pyruvate Dehydrogenase Phosphatase 1 and Promotes Tumor Growth." *J Biol Chem* 289, no. 31 (Aug 1 2014): 21413-22.
Shen, Y. C., D. L. Ou, C. Hsu, K. L. Lin, C. Y. Chang, C. Y. Lin, S. H. Liu, and A. L. Cheng. "Activating Oxidative Phosphorylation by a Pyruvate Dehydrogenase Kinase Inhibitor Overcomes Sorafenib Resistance of Hepatocellular Carcinoma." *Br J Cancer* 108, no. 1 (Jan 15 2013): 72-81.
Shi, L., and B. P. Tu. "Acetyl-Coa Induces Transcription of the Key G1 Cyclin Cln3 to Promote Entry into the Cell Division Cycle in Saccharomyces Cerevisiae." *Proc Natl Acad Sci U S A* 110, no. 18 (Apr 30 2013): 7318-23.
Shi, Y., F. Lan, C. Matson, P. Mulligan, J. R. Whetstine, P. A. Cole, R. A. Casero, and Y. Shi. "Histone Demethylation Mediated by the Nuclear Amine Oxidase Homolog Lsd1." *Cell* 119, no. 7 (Dec 29 2004): 941-53.
Shi, Y., and J. O. Thomas. "The Transport of Proteins into the Nucleus Requires the 70-Kilodalton Heat Shock Protein or Its Cytosolic Cognate." [In eng]. *Mol Cell Biol* 12, no. 5 (May 1992): 2186-92.
Shimazu, T., M. D. Hirschey, J. Newman, W. He, K. Shirakawa, N. Le Moan, C. A. Grueter*, et al.* "Suppression of Oxidative Stress by Beta-Hydroxybutyrate, an Endogenous Histone Deacetylase Inhibitor." *Science* 339, no. 6116 (Jan 11 2013): 211-4.
Shiraki, N., Y. Shiraki, T. Tsuyama, F. Obata, M. Miura, G. Nagae, H. Aburatani*, et al.* "Methionine Metabolism Regulates Maintenance and Differentiation of Human Pluripotent Stem Cells." *Cell Metab* 19, no. 5 (May 6 2014): 780-94.
Shyh-Chang, N., J. W. Locasale, C. A. Lyssiotis, Y. Zheng, R. Y. Teo, S. Ratanasirintrawoot, J. Zhang*, et al.* "Influence of Threonine Metabolism on S-Adenosylmethionine and Histone Methylation." *Science* 339, no. 6116 (Jan 11 2013): 222-6.
Siebert, G., and G. B. Humphrey. "Enzymology of the Nucleus." [In eng]. *Adv Enzymol Relat Areas Mol Biol* 27 (1965): 239-88.

Soares, P., M. S. Gadd, J. Frost, C. Galdeano, L. Ellis, O. Epemolu, S. Rocha, K. D. Read, and A. Ciulli. "Group-Based Optimization of Potent and Cell-Active Inhibitors of the Von Hippel-Lindau (Vhl) E3 Ubiquitin Ligase: Structure-Activity Relationships Leading to the Chemical Probe (2s,4r)-1-((S)-2-(1-Cyanocyclopropanecarboxamido)-3,3-Dimethylbutanoyl)-4-Hydroxy -N-(4-(4-Methylthiazol-5-Yl)Benzyl)Pyrrolidine-2-Carboxamide (Vh298)." *J Med Chem* (Sep 18 2017).

Sperber, H., J. Mathieu, Y. Wang, A. Ferreccio, J. Hesson, Z. Xu, K. A. Fischer*, et al.* "The Metabolome Regulates the Epigenetic Landscape During Naive-to-Primed Human Embryonic Stem Cell Transition." *Nat Cell Biol* 17, no. 12 (Dec 2015): 1523-35.

Srinivasan, R., C. J. Ricketts, C. Sourbier, and W. M. Linehan. "New Strategies in Renal Cell Carcinoma: Targeting the Genetic and Metabolic Basis of Disease." *Clin Cancer Res* 21, no. 1 (Jan 1 2015): 10-7.

Stacpoole, P. W. "The Pharmacology of Dichloroacetate." *Metabolism* 38, no. 11 (Nov 1989): 1124-44.

Stacpoole, P. W., D. S. Kerr, C. Barnes, S. T. Bunch, P. R. Carney, E. M. Fennell, N. M. Felitsyn*, et al.* "Controlled Clinical Trial of Dichloroacetate for Treatment of Congenital Lactic Acidosis in Children." *Pediatrics* 117, no. 5 (May 2006): 1519-31.

Strahl, B. D., and C. D. Allis. "The Language of Covalent Histone Modifications." *Nature* 403, no. 6765 (Jan 6 2000): 41-5.

Sudarshan, S., J. A. Karam, J. Brugarolas, R. H. Thompson, R. Uzzo, B. Rini, V. Margulis*, et al.* "Metabolism of Kidney Cancer: From the Lab to Clinical Practice." *Eur Urol* 63, no. 2 (Feb 2013): 244-51.

Sumegi, B., Z. Liposits, L. Inman, W. K. Paull, and P. A. Srere. "Electron Microscopic Study on the Size of Pyruvate Dehydrogenase Complex in Situ." [In eng]. *Eur J Biochem* 169, no. 1 (Nov 16 1987): 223-30.

Sun, R. C., M. Fadia, J. E. Dahlstrom, C. R. Parish, P. G. Board, and A. C. Blackburn. "Reversal of the Glycolytic Phenotype by Dichloroacetate Inhibits Metastatic Breast Cancer Cell Growth in Vitro and in Vivo." *Breast Cancer Res Treat* 120, no. 1 (Feb 2010): 253-60.

Sutendra, G., P. Dromparis, A. Kinnaird, T. H. Stenson, A. Haromy, J. M. Parker, M. S. McMurtry, and E. D. Michelakis. "Mitochondrial Activation by Inhibition of Pdkii Suppresses Hif1a Signaling and Angiogenesis in Cancer." *Oncogene* 32, no. 13 (Mar 28 2013): 1638-50.

Sutendra, G., P. Dromparis, P. Wright, S. Bonnet, A. Haromy, Z. Hao, M. S. McMurtry*, et al.* "The Role of Nogo and the Mitochondria-Endoplasmic Reticulum Unit in Pulmonary Hypertension." [In eng]. *Sci Transl Med* 3, no. 88 (Jun 22 2011): 88ra55.

Sutendra, G., A. Kinnaird, P. Dromparis, R. Paulin, T. H. Stenson, A. Haromy, K. Hashimoto*, et al.* "A Nuclear Pyruvate Dehydrogenase Complex Is Important for the Generation of Acetyl-Coa and Histone Acetylation." *Cell* 158, no. 1 (Jul 03 2014): 84-97.

Sutendra, G., and E. D. Michelakis. "Pyruvate Dehydrogenase Kinase as a Novel Therapeutic Target in Oncology." *Front Oncol* 3 (2013): 38.

Takahashi, H., J. M. McCaffery, R. A. Irizarry, and J. D. Boeke. "Nucleocytosolic Acetyl-Coenzyme a Synthetase Is Required for Histone Acetylation and Global Transcription." *Mol Cell* 23, no. 2 (Jul 21 2006): 207-17.

Tao, R., M. C. Coleman, J. D. Pennington, O. Ozden, S. H. Park, H. Jiang, H. S. Kim*, et al.* "Sirt3-Mediated Deacetylation of Evolutionarily Conserved Lysine 122 Regulates Mnsod Activity in Response to Stress." *Mol Cell* 40, no. 6 (Dec 22 2010): 893-904.

Tsukada, Y., J. Fang, H. Erdjument-Bromage, M. E. Warren, C. H. Borchers, P. Tempst, and Y. Zhang. "Histone Demethylation by a Family of Jmjc Domain-Containing Proteins." *Nature* 439, no. 7078 (Feb 16 2006): 811-6.

Turcan, S., A. W. Fabius, A. Borodovsky, A. Pedraza, C. Brennan, J. Huse, A. Viale, G. J. Riggins, and T. A. Chan. "Efficient Induction of Differentiation and Growth Inhibition in Idh1 Mutant Glioma Cells by the Dnmt Inhibitor Decitabine." *Oncotarget* 4, no. 10 (Oct 2013): 1729-36.

Tzao, C., H. J. Tung, J. S. Jin, G. H. Sun, H. S. Hsu, B. H. Chen, C. P. Yu, and S. C. Lee. "Prognostic Significance of Global Histone Modifications in Resected Squamous Cell Carcinoma of the Esophagus." *Mod Pathol* 22, no. 2 (Feb 2009): 252-60.

Uhlen, M., C. Zhang, S. Lee, E. Sjostedt, L. Fagerberg, G. Bidkhori, R. Benfeitas*, et al.* "A Pathology Atlas of the Human Cancer Transcriptome." *Science* 357, no. 6352 (Aug 18 2017).

Vander Heiden, M. G., L. C. Cantley, and C. B. Thompson. "Understanding the Warburg Effect: The Metabolic Requirements of Cell Proliferation." *Science* 324, no. 5930 (May 22 2009): 1029-33.

Vander Heiden, M. G., J. W. Locasale, K. D. Swanson, H. Sharfi, G. J. Heffron, D. Amador-Noguez, H. R. Christofk*, et al.* "Evidence for an Alternative Glycolytic Pathway in Rapidly Proliferating Cells." [In eng]. *Science* 329, no. 5998 (Sep 17 2010): 1492-9.

Ventura, M., F. Mateo, J. Serratosa, I. Salaet, S. Carujo, O. Bachs, and M. J. Pujol. "Nuclear Translocation of Glyceraldehyde-3-Phosphate Dehydrogenase Is Regulated by Acetylation." *Int J Biochem Cell Biol* 42, no. 10 (Oct 2010): 1672-80.

Vervoorts, J., J. M. Luscher-Firzlaff, S. Rottmann, R. Lilischkis, G. Walsemann, K. Dohmann, M. Austen, and B. Luscher. "Stimulation of C-Myc Transcriptional Activity and Acetylation by Recruitment of the Cofactor Cbp." *EMBO Rep* 4, no. 5 (May 2003): 484-90.

Vogelauer, M., L. Rubbi, I. Lucas, B. J. Brewer, and M. Grunstein. "Histone Acetylation Regulates the Time of Replication Origin Firing." [In eng]. *Mol Cell* 10, no. 5 (Nov 2002): 1223-33.

Vousden, K. H., and K. M. Ryan. "P53 and Metabolism." *Nat Rev Cancer* 9, no. 10 (Oct 2009): 691-700.

Wagner, G. R., and M. D. Hirschey. "Nonenzymatic Protein Acylation as a Carbon Stress Regulated by Sirtuin Deacylases." *Mol Cell* 54, no. 1 (Apr 10 2014): 5-16.

Wagner, G. R., and R. M. Payne. "Widespread and Enzyme-Independent Nepsilon-Acetylation and Nepsilon-Succinylation of Proteins in the Chemical Conditions of the Mitochondrial Matrix." *J Biol Chem* 288, no. 40 (Oct 4 2013): 29036-45.

Wang, B., L. Shi, X. Sun, L. Wang, X. Wang, and C. Chen. "Production of Ccl20 from Lung Cancer Cells Induces the Cell Migration and Proliferation through Pi3k Pathway." *J Cell Mol Med* 20, no. 5 (May 2016): 920-9.

Wang, F., J. Travins, B. DeLaBarre, V. Penard-Lacronique, S. Schalm, E. Hansen, K. Straley*, et al.* "Targeted Inhibition of Mutant Idh2 in Leukemia Cells Induces Cellular Differentiation." *Science* 340, no. 6132 (May 3 2013): 622-6.

Wang, J., P. Alexander, L. Wu, R. Hammer, O. Cleaver, and S. L. McKnight. "Dependence of Mouse Embryonic Stem Cells on Threonine Catabolism." *Science* 325, no. 5939 (Jul 24 2009): 435-9.

Warburton, H. E., M. Brady, N. Vlatkovic, W. M. Linehan, K. Parsons, and M. T. Boyd. "P53 Regulation and Function in Renal Cell Carcinoma." *Cancer Res* 65, no. 15 (Aug 1 2005): 6498-503.

Ward, P. S., J. Patel, D. R. Wise, O. Abdel-Wahab, B. D. Bennett, H. A. Coller, J. R. Cross*, et al.* "The Common Feature of Leukemia-Associated Idh1 and Idh2 Mutations Is a Neomorphic Enzyme Activity Converting Alpha-Ketoglutarate to 2-Hydroxyglutarate." *Cancer Cell* 17, no. 3 (Mar 16 2010): 225-34.

Wellen, K. E., G. Hatzivassiliou, U. M. Sachdeva, T. V. Bui, J. R. Cross, and C. B. Thompson. "Atp-Citrate Lyase Links Cellular Metabolism to Histone Acetylation." *Science* 324, no. 5930 (May 22 2009): 1076-80.

Wellen, K. E., and C. B. Thompson. "A Two-Way Street: Reciprocal Regulation of Metabolism and Signalling." *Nat Rev Mol Cell Biol* 13, no. 4 (Apr 2012): 270-6.

West, A. C., and R. W. Johnstone. "New and Emerging Hdac Inhibitors for Cancer Treatment." *J Clin Invest* 124, no. 1 (Jan 2014): 30-9.

Whiteman, E. L., H. Cho, and M. J. Birnbaum. "Role of Akt/Protein Kinase B in Metabolism." *Trends Endocrinol Metab* 13, no. 10 (Dec 2002): 444-51.

Wise, D. R., P. S. Ward, J. E. Shay, J. R. Cross, J. J. Gruber, U. M. Sachdeva, J. M. Platt*, et al.* "Hypoxia Promotes Isocitrate Dehydrogenase-Dependent Carboxylation of Alpha-Ketoglutarate to Citrate to Support Cell Growth and Viability." *Proc Natl Acad Sci U S A* 108, no. 49 (Dec 6 2011): 19611-6.

Xiao, M., H. Yang, W. Xu, S. Ma, H. Lin, H. Zhu, L. Liu*, et al.* "Inhibition of Alpha-Kg-Dependent Histone and DNA Demethylases by Fumarate and Succinate That Are Accumulated in Mutations of Fh and Sdh Tumor Suppressors." *Genes Dev* 26, no. 12 (Jun 15 2012): 1326-38.

Xu, L., W. Xu, S. Qiu, and S. Xiong. "Enrichment of Ccr6+Foxp3+ Regulatory T Cells in the Tumor Mass Correlates with Impaired Cd8+ T Cell Function and Poor Prognosis of Breast Cancer." *Clin Immunol* 135, no. 3 (Jun 2010): 466-75.

Xu, M., J. S. Nagati, J. Xie, J. Li, H. Walters, Y. A. Moon, R. D. Gerard*, et al.* "An Acetate Switch Regulates Stress Erythropoiesis." *Nat Med* 20, no. 9 (Sep 2014): 1018-26.

Xu, W., H. Yang, Y. Liu, Y. Yang, P. Wang, S. H. Kim, S. Ito*, et al.* "Oncometabolite 2-Hydroxyglutarate Is a Competitive Inhibitor of Alpha-Ketoglutarate-Dependent Dioxygenases." *Cancer Cell* 19, no. 1 (Jan 18 2011): 17-30.

Yan, H., D. W. Parsons, G. Jin, R. McLendon, B. A. Rasheed, W. Yuan, I. Kos*, et al.* "Idh1 and Idh2 Mutations in Gliomas." *N Engl J Med* 360, no. 8 (Feb 19 2009): 765-73.

Yang, M., and K. H. Vousden. "Serine and One-Carbon Metabolism in Cancer." *Nat Rev Cancer* 16, no. 10 (Oct 2016): 650-62.

Yang, W., Y. Xia, D. Hawke, X. Li, J. Liang, D. Xing, K. Aldape*, et al.* "Pkm2 Phosphorylates Histone H3 and Promotes Gene Transcription and Tumorigenesis." [In eng]. *Cell* 150, no. 4 (Aug 17 2012): 685-96.

Yao, M., M. Yoshida, T. Kishida, N. Nakaigawa, M. Baba, K. Kobayashi, T. Miura*, et al.* "Vhl Tumor Suppressor Gene Alterations Associated with Good Prognosis in Sporadic Clear-Cell Renal Carcinoma." *J Natl Cancer Inst* 94, no. 20 (Oct 16 2002): 1569-75.

Yi, C. H., H. Pan, J. Seebacher, I. H. Jang, S. G. Hyberts, G. J. Heffron, M. G. Vander Heiden*, et al.* "Metabolic Regulation of Protein N-Alpha-Acetylation by Bcl-Xl Promotes Cell Survival." *Cell* 146, no. 4 (Aug 19 2011): 607-20.

Yi, Y., O. Mikhaylova, A. Mamedova, P. Bastola, J. Biesiada, E. Alshaikh, L. Levin*, et al.* "Von Hippel-Lindau-Dependent Patterns of Rna Polymerase Ii Hydroxylation in Human Renal Clear Cell Carcinomas." *Clin Cancer Res* 16, no. 21 (Nov 01 2010): 5142-52.

Yogev, O., E. Singer, E. Shaulian, M. Goldberg, T. D. Fox, and O. Pines. "Fumarase: A Mitochondrial Metabolic Enzyme and a Cytosolic/Nuclear Component of the DNA Damage Response." [In eng]. *PLoS Biol* 8, no. 3 (Mar 2010): e1000328.

Yu, W., K. E. Dittenhafer-Reed, and J. M. Denu. "Sirt3 Protein Deacetylates Isocitrate Dehydrogenase 2 (Idh2) and Regulates Mitochondrial Redox Status." *J Biol Chem* 287, no. 17 (Apr 20 2012): 14078-86.

Yu, W., C. Huang, Q. Wang, T. Huang, Y. Ding, C. Ma, H. Ma, and W. Chen. "Mef2 Transcription Factors Promotes Emt and Invasiveness of Hepatocellular Carcinoma through Tgf-Beta1 Autoregulation Circuitry." *Tumour Biol* 35, no. 11 (Nov 2014): 10943-51.

Yuan, Z. L., Y. J. Guan, D. Chatterjee, and Y. E. Chin. "Stat3 Dimerization Regulated by Reversible Acetylation of a Single Lysine Residue." *Science* 307, no. 5707 (Jan 14 2005): 269-73.

Zeng, L., and M. M. Zhou. "Bromodomain: An Acetyl-Lysine Binding Domain." *FEBS Lett* 513, no. 1 (Feb 20 2002): 124-8.

Zeng, W., H. Chang, M. Ma, and Y. Li. "Ccl20/Ccr6 Promotes the Invasion and Migration of Thyroid Cancer Cells Via Nf-Kappa B Signaling-Induced Mmp-3 Production." *Exp Mol Pathol* 97, no. 1 (Aug 2014): 184-90.

Zhao, Q., J. Wang, I. V. Levichkin, S. Stasinopoulos, M. T. Ryan, and N. J. Hoogenraad. "A Mitochondrial Specific Stress Response in Mammalian Cells." [In eng]. *EMBO J* 21, no. 17 (Sep 2 2002): 4411-9.

Zhou, Z. H., W. Liao, R. H. Cheng, J. E. Lawson, D. B. McCarthy, L. J. Reed, and J. K. Stoops. "Direct Evidence for the Size and Conformational Variability of the Pyruvate Dehydrogenase Complex Revealed by Three-Dimensional Electron Microscopy. The "Breathing" Core and Its Functional Relationship to Protein Dynamics." [In eng]. *J Biol Chem* 276, no. 24 (Jun 15 2001): 21704-13.

Zhou, Z. H., D. B. McCarthy, C. M. O'Connor, L. J. Reed, and J. K. Stoops. "The Remarkable Structural and Functional Organization of the Eukaryotic Pyruvate Dehydrogenase Complexes." [In eng]. *Proc Natl Acad Sci U S A* 98, no. 26 (Dec 18 2001): 14802-7.

Zimmer, M., B. L. Ebert, C. Neil, K. Brenner, I. Papaioannou, A. Melas, N. Tolliday*, et al.* "Small-Molecule Inhibitors of Hif-2a Translation Link Its 5'utr Iron-Responsive Element to Oxygen Sensing." *Mol Cell* 32, no. 6 (Dec 26 2008): 838-48.